IOWA STATE UNIVERSITY
Digital Repository

Graduate Theses and Dissertations

Iowa State University Capstones, Theses and Dissertations

2020

Synthesis and reactivity of rare earth and alkaline earth metal complexes

W Kasuni C. Boteju
Iowa State University

Follow this and additional works at: https://lib.dr.iastate.edu/etd

Recommended Citation

Boteju, W Kasuni C., "Synthesis and reactivity of rare earth and alkaline earth metal complexes" (2020). *Graduate Theses and Dissertations*. 17827.
https://lib.dr.iastate.edu/etd/17827

This Thesis is brought to you for free and open access by the Iowa State University Capstones, Theses and Dissertations at Iowa State University Digital Repository. It has been accepted for inclusion in Graduate Theses and Dissertations by an authorized administrator of Iowa State University Digital Repository. For more information, please contact digirep@iastate.edu.

www.manaraa.com

Synthesis and reactivity of rare earth and alkaline earth metal complexes

by

Walikadage Kasuni Boteju

A dissertation submitted to the graduate faculty

in partial fulfillment of the requirements for the degree of

DOCTOR OF PHILOSOPHY

Major: Inorganic Chemistry

Program of Study Committee:
Aaron D. Sadow, Major Professor
Wenyu Huang
Aaron Rossini
Igor Slowing
Theresa Windus

The student author, whose presentation of the scholarship herein was approved by the program of study committee, is solely responsible for the content of this dissertation. The Graduate College will ensure this dissertation is globally accessible and will not permit alterations after a degree is conferred.

Iowa State University

Ames, Iowa

2020

Copyright © Walikadage Kasuni Boteju, 2020. All rights reserved.

www.manaraa.com

To my dad whom I lost four years ago..

www.manaraa.com

TABLE OF CONTENTS

Page

www.manaraa.com

www.manaraa.com

ACKNOWLEDGMENTS

I would like to express my sincere gratitude to everyone who assisted me in many ways to successfully complete the PhD program.

First, I would like to thank my major professor, Dr. Aaron Sadow for the guidance and support throughout six years of the course of this research. Finally, I realized that "working hard to achieve research goals independently" not only benefited the research work but also it helped building a strong personality with a high tolerance mentality in myself. Thank you very much for driving me to success.

Next, I would like to thank my past and present committee members, Dr. Keith Woo, Dr. Sam Houk, Dr. Wenyu Huang, Dr. Igor Slowing, Dr. Theresa Windus, and Dr. Aaron Rossini, for your time and valuable suggestions. Furthermore, I would like to appreciate the support of CIF staff, Dr. Sarah Cady, Dr. Shu Xu, Dr. Steve Veysey and Rachel Hazzard for NMR and CHN analysis. A special thank goes to Dr. Arkady Ellern for his time to collect and solve all my crystal structures. Also, I would like to thank Trond Forre of the glass shop, Bruce Erickson and Bill Halterman of the machine shop for the help throughout.

In addition, I would like to thank present Sadow group members, Smita Patnaik, Abhranil Biswas, Yang Yun Chu, Kevin Basemann, Uddhav Kanbur, Austin Thompson and Akalanka Tennakoon for their enormous support. Thank you all for your help in and out of the lab. It was really fun working with all of you and I enjoyed it a lot. Further I need to thank Dr. Nicole Lampland for teaching me the lab techniques when I joined the group. Also, I would like to thank other past group members, Dr. Songchen Xu, Dr. Naresh Eedugurala, Dr. Aradhana Pindwal, Dr. Regina Reinig, Dr. Zak Weinstein, Jake Fleckenstein, Dr. Brad Schmidt, Megan Hovey, for your

www.manaraa.com

valuable suggestions. I want to offer my appreciation to colleagues, the department faculty and staff for making my time at Iowa State University a wonderful experience.

Further, I would like to thank my all Sri Lankan friends for the time we spent together including birthday celebrations, baby showers, cultural and religious events etc. Finally, I would like to thank my family for being patient with me throughout this long six years. Love you amma (mom), thaththa (dad), Dinuka (husband), Neyli (daughter), malli (brother) and my grandmother. I appreciate your tremendous support in many ways on my PhD journey. Thaththa, I wish you were here to see my accomplishment; I always miss you!

Again, without all of your support, this thesis would not have been possible. Thank you!

www.manaraa.com

ABSTRACT

One of the aspects of our research group is developing new ligands, for instance β-SiH containing alkyl, amide ligands and oxazoline based scorpionate type ligands for the synthesis of their rare earth metal, alkali earth metal and transition metal complexes which are used as catalyst precursors for organic transformation reactions.

Rare earth complexes of tris(dimethylsilyl)methyl ligand have been developed by our research group. In this thesis a new alkyl ligand is accessed by replacing one dimethylsilyl moiety with a phenyl group. The β-SiH functionalized benzyl ligand $HC(SiHMe_2)_2Ph$ is synthesized by reductive coupling of $HCBr_2Ph$ and $SiHMe_2Cl$ and the anion of the ligand $[C(SiHMe_2)_2Ph]^-$ is obtained by deprotonation of $HC(SiHMe_2)_2Ph$ with KCH_2Ph. An alternate route is introduced to obtain the same β-SiH functionalized benzyl anion $[C(SiHMe_2)_2Ph]^-$ by reaction of KO*t*Bu and $(Me_2HSi)_3CPh$ which reacts via C–Si cleavage. $LnI_3 \cdot THF_n$ and three equivalents of this carbanion combine to provide homoleptic tris(alkyl)lanthanide compounds $Ln\{C(SiHMe_2)_2Ph\}_3$ (Ln = La, Ce, Pr, Nd) containing secondary metal-ligand interactions.

Rare earth compounds of $–N(SiHMe_2)tBu$ ligand have been synthesized by our research group. A new amide ligand is accessed by introducing an aryl group to the tertbutyl position, and this ligand is the amide version of the new alkyl ligand reported in this thesis. Further, addition of substituents on the aryl group allows to vary the steric properties of the new ligand series. Three new hydridosilazido ligands, $–N(SiHMe_2)Aryl$ (Aryl = Ph, 2,6-$C_6Me_2H_3$ (dmp), 2,6-$C_6iPr_2H_3$ (dipp)) and their homoleptic rare earth complexes $Ln\{N(SiHMe_2)Aryl\}_3(THF)_n$ (Ln = Sc, Y, Lu; Aryl = Ph, n = 2; Aryl = dmp, n = 1; Aryl = dipp, n = 0) are synthesized. NMR, IR and X-ray diffraction studies of the complexes show that $Ln\{N(SiHMe_2)Ph\}_3(THF)_2$ contain only classical Si–H interactions with the metal center. $Y\{N(SiHMe_2)dmp\}_3THF$ and $Lu\{N(SiHMe_2)dmp\}_3THF$

www.manaraa.com

contain three and two bridging Si–H interactions respectively. Three secondary Ln←HSi interactions and one agostic CH bond per molecule are observed for planar Ln{N(SiHMe$_2$)dipp}$_3$ complexes. Further, the reaction of Ln{N(SiHMe$_2$)dipp}$_3$ with ketones provides the hydrosilylated product by inserting the C=O in bridging Ln←H-Si rather than inserting into the Y–N bond or enolate formation. The insertion reaction is postulated to occur via an associative mechanism.

Ln{N(SiHMe$_2$)dipp}$_3$ undergo β-SiH abstraction by Lewis acids, such as B(C$_6$F$_5$)$_3$. The reaction of Ln{N(SiHMe$_2$)dipp}$_3$ and one equivalent of B(C$_6$F$_5$)$_3$ provides the cationic species Ln{κ^2-N(dipp)SiMe$_2$N(SiHMe$_2$)dipp}{N(SiHMe$_2$)dipp}HB(C$_6$F$_5$)$_3$. The decomposition of that compound provides (Me$_2$Si–Ndipp)$_2$ and a rare earth adduct. A second order rate law is obtained for the decomposition of the cationic complex.

Tris(oxazolinyl)boratomagnesium alkyls (To^{M}MgR) have been developed by our research group and tested in various catalytic reactions for instance hydroboration and dehydrocoupling. In this thesis kinetic studies of the stoichiometric reaction between To^{M}MgR and HBpin are performed for comparison with other sigma bond metathesis type reactions. The reaction of To^{M}MgMe or To^{M}Mg^{n}Pr with HBpin was too fast even at –78 °C to measure using NMR and IR kinetics. In contrast, To^{M}MgBn reacts with HBpin or DBpin more slowly at room temperature, and kinetic studies revealed a bimolecular rate law. The activation parameters obtained for the reaction of To^{M}MgBn with HBpin and DBpin are $\Delta H^{\ddagger}$ = 13.08(0.02) kcal mol^{-1}, $\Delta S^{\ddagger}$ = –29.09(0.05) cal mol^{-1} K^{-1} and $\Delta H^{\ddagger}$ 11.86(0.05) kcal mol^{-1}, $\Delta S^{\ddagger}$ = –33.44(0.15) cal mol^{-1} K^{-1} respectively. This study shows a kinetic isotope effect of 1.35 at 55 °C and it appears to be increased with increasing the temperature. The mechanistic investigations show that B-H/B-D bond cleavage is involved in the rate-determining step.

www.manaraa.com

CHAPTER 1. GENERAL INTRODUCTION

Alkyl and amide rare earth compounds

Homoleptic rare earth alkyls and amides are useful precursors for heteroleptic compounds and catalytic applications. Lanthanide cations are highly Lewis acidic and have large coordination spheres (La^{3+} 1.03 Å, Lu^{3+} 0.86 Å), which are in the range of Ca^{2+} (1.00 Å) and Mg^{2+} (0.66 Å) radii.[1] Thus lanthanide alkyl complexes serve as efficient catalysts in hydroamination, ethylene polymerization, hydrophosphination and hydrosilylation reactions.[2-5] Lanthanide amide compounds have been used in catalytic reactions for instance hydrophosphination, hydroalkoxylation and aldehyde amidation etc.[4, 6, 7] Further, homoleptic lanthanide compounds contain equivalent ligand contributions to the metal center, therefore metal–ligand interactions of such complexes can be studied easily.

Attempts to synthesize homoleptic lanthanide alkyl complexes using Me, *t*Bu and $CH(SiMe_3)_2$ ligands provide a hexamethyl Li bound complex, an ate complex and a LiCl bound complex respectively due to lack of steric saturation.[8, 9] Also, the lanthanide compounds synthesized with $CH_2(SiMe_3)$ ligand (Ln = Lu, Yb, Er, Sm, Y) are unstable at room temperature and the compounds are limited only for smaller lanthanides.[10-12] Further, $C(SiMe_3)_3$ ligand is too bulky and is limited only for divalent complexes.[13] The reaction of $Ln\{O(2,6\text{-}t\text{BuPh})\}_3$ and $LiCH(SiMe_3)_2$ provided $Ln(CH(SiMe_3)_2)_3$ (Ln = Sc, Y, Lu, La, Ce) which is the first homoleptic lanthanide complex series.[14, 15] The $Ln(CH_2Ph)_3(THF)_3$ (Ln = Y, Ce, Pr, Nd, Sm, Gd, Dy, Er, La) complexes are stable at room temperature for about 2 h.[16] La and Nd benzyl complexes decompose via α elimination to $[PhCH_2La(H)OCH{=}CH_2\text{-}(THF)_2]$ and $[PhCH_2Nd{=}CHPh]$ respectively which are schrock carbene type products.[17] Further, ortho substituted $Ln(CH_2C_6H_4\text{-}o\text{-}NMe_2)_3$ (Ln = Y, La, Nd, Sm, Dy, Ho) and $Y(CH_2C_6H_4\text{-}o\text{-}SiMe_3)_3$ or para substituted $(La(CH_2C_6H_4\text{-}p\text{-}t\text{Bu})_3(THF)_3$,

www.manaraa.com

$La(CH_2C_6H_4\text{-}p\text{-}Me)_3(THF)_3$ lanthanide benzyl complexes are successfully synthesized.[3, 18] In addition, α carbon substituted series of complexes, $Ln(CH(NMe_2)Ph)_3$ (Ln = La, Ce, Nd, Pr, Sm, Gd, Y) are prepared recently.[19] In order to gain stable lanthanide complexes, chelating ligands or sterically demanding neutral ligands such as THF or TMEDA have been used in literature.

Homoleptic rare earth amides containing two bulky silyl groups are well known since decades $Ln[20]_3$ (Ln = Sc, Y, Lu).[21-24] However, the sterics of the ligand cannot be varied. The attempts to replace one $SiMe_3$ group in bistrimethyl silyl ligand with phenyl derivatives can be found in literature. The compounds known for those types of ligands are $Ln\{N(SiMe_3)(C_6H_5\}_3(THF)$ (Ln = Y, Lu), $[Y\{N(SiMe_3)(2,6\text{-}C_6H_3Et_2)\}_3Cl][Li(THF)_4]$, $Lu\{N(SiMe_3)(2,6\text{-}C_6H_3iPr_2)\}_2Cl(THF)$. Most of these compounds are ate or solvent coordinated complexes.[25, 26]

The manipulation of secondary interactions of alkyl and amide ligands is required for the synthesis of salt-free or solvent-free stable homoleptic rare earth alkyl and amide complexes which, are useful as precursors in catalytic transformations. A way of introducing the secondary interactions is, incorporating β-SiH containing ligands in such complexes. These compounds form bridging Ln←H-Si secondary interactions that increase the electron count as L-type donors and ligand bond number in these otherwise coordinatively unsaturated species.[27] Further, β-SiH provides a better spectroscopic handling in terms of characterizing the compounds. The ^1H NMR spectroscopy (chemical shift, low one-bond coupling constants ($^1J_{Si-H}$)) and IR stretching frequency of the SiH group (ν_{SiH} <2000 cm^{-1}) is distinct from other functional groups (e.g. CH, $SiMe_3$), facilitating tracking of the compounds.

The alkyl and amide ligands containing β-SiH moieties are reported in literature; for example, alkyl ligands $-C(SiHMe_2)(SiMe_3)_2$ and $-C(SiHMe_2)_3$ are synthesized by Eaborn and co-

www.manaraa.com

workers.[28] A series of homoleptic lanthanide complexes of the latter ligand Ln{C(SiHMe$_2$)$_3$}$_3$, (Ln = Y, La, Ce, Pr, Nd, Lu) is reported by Sadow group.[29, 30]

Furthermore, Anwander and co-workers have synthesized a series of lanthanide amide compounds Ln{N(SiHMe$_2$)$_2$}$_3$(THF)$_n$ Ln = Sc (n = 1), Y (n = 1 or 2), Lu (n = 2) using their –N(SiHMe$_2$)$_2$ ligand.[31] However, –N(SiHMe$_2$)$_2$ ligand is more acidic; therefore, the substitution chemistry is difficult. As a solution, one silyl group can be replaced with a R group –N(SiHMe$_2$)R which makes the ligand less acidic. In addition, variation of the R group helps to control the sterics of the ligand. The only known ligand which meets this requirement is –N(SiHMe$_2$)*t*Bu synthesized by Hoffman's group.[32] Schumann's and our group have reported solvent free homoleptic organolanthanides Ln{(N(SiHMe$_2$)*t*Bu}$_3$ Ln = Sc, Y, Er, Lu using that ligand.[33]

Typically, homoleptic lanthanide amides are trigonal pyramidal around the metal center except La{N(Si*t*BuMe$_2$)$_2$}$_3$ and Ln{N(SiMe$_3$)(Si*t*BuMe$_2$}$_3$ (Ln = La, Ce) compounds synthesized by Mills and co-workers.[34] Despite, the lanthanides of bulky alkyl ligand –C(SiHMe$_2$)$_3$ show trigonal planar geometry around the metal center.[30]

The reactivity of silazido complexes with Lewis acids and bases is known for tetramethyldisilazide N(SiHMe$_2$)$_2$ ligand containing compounds and explore the reactivity of β-SiHs is important in building new reaction mechanisms. Cp$_2$Zr{N(SiHMe$_2$)$_2$}H and B(C$_6$F$_5$)$_3$ provides cationic [Cp$_2$Zr{N(SiHMe$_2$)$_2$]$^+$ by abstracting the hydride. The reaction of Cp$_2$Zr{N(SiHMe$_2$)$_2$}R (R = Me, Et, *n*-C$_3$H$_7$, CH=CHSiMe$_3$) and B(C$_6$F$_5$)$_3$ gives a mixture of [Cp$_2$Zr{N(SiHMe$_2$)$_2$]$^+$ and [Cp$_2$ZrN(SiHMe$_2$)(SiRMe$_2$)]$^+$ indicating the abstraction of β-SiH and migration of R group to the β Si center. [Cp$_2$Zr{N(SiHMe$_2$)$_2$]$^+$ reacts with 4-(dimethylamino)-pyridine (dmap) to give [Cp$_2$Zr{N(SiHMe$_2$)(SiMe$_2$dmap)}H]$^+$ which contains only one β

www.manaraa.com

Si−H⇀Zr interaction and a new zirconium hydride. When $[Cp_2Zr\{N(SiHMe_2)_2]^+$ is reacted with 2 equivalents of acetone, it inserts between Si–H bond to provide the hydrosilylated product.[35]

This thesis contributes new alkyl and amide ligands featuring β-SiH groups and their homoleptic rare earth complexes. The reactivity of the SiH bond of the amide complexes is investigated through hydrosilation reactions with ketones and abstraction reactions with Lewis acids.

B–E (E = C, N, O) Bond formation type mechanisms

B–E formation involves M–E species interacting with H–B and it is important in catalytic hydroboarion reactions. Mechanistic understanding of B-E bond formation step or the activation step of a catalytic reaction is required when new selective catalytic sites are designed.

In literature, B–E bond formation type catalytic or stoichiometric reactions are postulated to involve concerted four-center transition states identified as σ-bond metathesis; for example, the hydroboration reactions of pyridine derivatives, aldehydes, ketones, aldemines and ketimines with HBpin using (^{Dipp}Nacnac)Mg*n*Bu (^{Dipp}Nacnac = [(2,6-diisopropyl-phenyl)NC-Me]$_2$CH) as the catalyst are proposed to occur through the concerted σ-bond metathesis mechanism by Hill's group.[36-38] Further, the same type of mechanism is proposed for the stoichiometric reactions of (^{Dipp}Nacnac)Mg*n*Bu and HBpin with benzophenone or PhHC=NPh to provide (^{Dipp}Nacnac)MgOCHPh$_2$ or [(^{Dipp}Nacnac)MgNPhCH$_2$Ph respectively.[36, 37]

In addition, B–E bond formation type catalytic or stoichiometric reactions are postulated to involve pathways avoiding σ-bond metathesis; for example, hydroboration of pyridine derivatives catalyzed by (^{Dipp}Nacnac)$_2$Mg$_2$H$_2$ and hydroboration of esters catalyzed by To^{M}MgMe are proposed to occur through a hydride transfer from borane to pyridine and a zwittorionic

www.manaraa.com

intermediate respectively.[39, 40] Further, the stoichiometric reaction between To^{M}MgNH*t*Bu and $PhMeSiH_2$ is proposed to occur through a nucleophilic attack by the magnesium amide.[41]

This thesis contributes the mechanistic studies of B–C bond formation reaction of magnesium alkyl complex with HBpin and identify parameters associated with σ-bond metathesis type reactions.

Thesis Organization

This thesis contains seven chapters composed of manuscripts in preparation for journal submission. Chapter one provides a general introduction of the motivation behind the development of homoleptic rare earth alkyl and amide complexes. Further, chapter one gives a background about importance of studying the reaction pathway of B–C bond formation. Chapter two through five are journal articles modified from manuscripts accepted in journal or in preparation for publication with in-depth discussion of the research conducted.

Chapter two contains the synthesis of the new bis(dimethylsilyl)benzyl ligand, –$C(SiHMe_2)_2Ph$ and its potassium salt. The synthesis of a series of new homoleptic lanthanide compounds, $Ln\{C(SiHMe_2)_2Ph\}_3$ (Ln = La, Ce, Pr, Nd) of that ligand is also described in the chapter. The compounds are characterized by NMR, IR and X-ray diffraction methods and the secondary metal-ligand interactions of the compounds are discussed.

Chapter three and four describes the synthesis of three new silazido ligands, –$N(SiHMe_2)Aryl$ (Aryl = Ph, 2,6-$C_6Me_2H_3$ (dmp), 2,6-$C_6iPr_2H_3$ (dipp)) and their lithium salts. The synthesis of their homoleptic rare earth complexes, $Ln\{N(SiHMe_2)Aryl\}_3(THF)_n$ (Ln = Sc, Y, Lu; Aryl = Ph, n = 2; Aryl = dmp, n = 1; Aryl = dipp, n = 0) is also described. The compounds are characterized by NMR, IR and X-ray diffraction techniques and explained the analysis in detail. The β-SiH groups in rare earth tris(silazido) dipp compounds are reacted with ketones cleanly to

www.manaraa.com

give hydrosilylated products. A postulated reaction pathway for the C=O insertion into SiH is mentioned in the chapter.

Chapter five describes the formation of cationic species, Ln{κ^2-N(dipp)$SiMe_2$N($SiHMe_2$)dipp}{N($SiHMe_2$)dipp}HB(C_6F_5)$_3$ (Ln = Y, Lu) of Ln{(N$SiHMe_2$)dipp}$_3$. The characterization of the compounds via NMR and IR techniques is discussed in the chapter. The rate law of the decomposition of the cationic species to give (Me_2Si–Ndipp)$_2$ and a lanthanide adduct is provided.

Chapter six describes the mechanistic investigations of B–C bond formation reaction using To^{M}MgBn and HBpin. The rate law, activation parameters, and the kinetic isotope effect are studied in the chapter to figure out the mechanism of the activation step in a hydroboration catalytic cycle. The kinetics of Si–C bond formation reaction using To^{M}MgMe and $PhSiH_3$ is published in Stevan Neal's thesis. Both B–C and Si–C formation kinetics studies will be published as one paper.

Iowa State University's crystallographer, Dr. Arkady Ellern, is credited with collecting data and solving all of the X-ray structures presented in this thesis.

References

1. Shannon, R. D., Revised effective ionic radii and systematic studies of interatomic distances in halides and chalcogenides. *Acta Crystallographica Section A* **1976,** *32* (5), 751-767.

2. Yuen, H. F.; Marks, T. J., *Organometallics* **2009,** *28* (8), 2423-2440.

3. Bambirra, S.; Meetsma, A.; Hessen, B., *Organometallics* **2006,** *25* (14), 3454-3462.

4. Kawaoka, A. M.; Douglass, M. R.; Marks, T. J., *Organometallics* **2003,** *22* (23), 4630-4632.

5. Ge, S.; Meetsma, A.; Hessen, B., *Organometallics* **2008,** *27* (20), 5339-5346.

6. Yu, X.; Seo, S.; Marks, T. J., *Journal of the American Chemical Society* **2007,** *129* (23), 7244-7245.

7. Seo, S.; Marks, T. J., *Organic Letters* **2008,** *10* (2), 317-319.

www.manaraa.com

8. Schumann, H.; Mueller, J.; Bruncks, N.; Lauke, H.; Pickardt, J.; Schwarz, H.; Eckart, K., *Organometallics* **1984,** *3* (1), 69-74.

9. Atwood, J. L.; Lappert, M. F.; Smith, R. G.; Zhang, H., *Journal of the Chemical Society, Chemical Communications* **1988,** (19), 1308-1309.

10. Lappert, M. F.; Pearce, R., *J. Chem. Soc., Chem. Commun.* **1973,** (4), 126.

11. Schumann, H.; Müller, J., *Journal of Organometallic Chemistry* **1978,** *146* (2), C5-C7.

12. Schumann, H.; Freckmann, D. M. M.; Dechert, S., *Zeitschrift für anorganische und allgemeine Chemie* **2002,** *628* (11), 2422-2426.

13. Qi, G.; Nitto, Y.; Saiki, A.; Tomohiro, T.; Nakayama, Y.; Yasuda, H., *Tetrahedron* **2003,** *59* (52), 10409-10418.

14. Hitchcock, P. B.; Lappert, M. F.; Smith, R. G.; Bartlett, R. A.; Power, P. P., *Journal of the Chemical Society, Chemical Communications* **1988,** (15), 1007-1009.

15. Avent, A. G.; Caro, C. F.; Hitchcock, P. B.; Lappert, M. F.; Li, Z.; Wei, X.-H., *Dalton Transactions* **2004,** (10), 1567-1577.

16. Wooles, A. J.; Mills, D. P.; Lewis, W.; Blake, A. J.; Liddle, S. T., *Dalton Transactions* **2010,** *39* (2), 500-510.

17. Thiele, K. H.; Unverhau, K.; Geitner, M.; Jacob, K., *Zeitschrift für anorganische und allgemeine Chemie* **1987,** *548* (5), 175-179.

18. Harder, S., *Organometallics* **2005,** *24* (3), 373-379.

19. Behrle, A. C.; Schmidt, J. A. R., *Organometallics* **2011,** *30* (15), 3915-3918.

20. Alyea, E. C.; Bradley, D. C.; Copperthwaite, R. G., *Journal of the Chemical Society, Dalton Transactions* **1972,** (14), 1580-1584.

21. Bradley, D. C.; Ghotra, J. S.; Hart, F. A., *Journal of the Chemical Society, Chemical Communications* **1972,** (6), 349-350.

22. Ghotra, J. S.; Hursthouse, M. B.; Welch, A. J., *Journal of the Chemical Society, Chemical Communications* **1973,** (18), 669-670.

23. Westerhausen, M.; Hartmann, M.; Pfitzner, A.; Schwarz, W., *Zeitschrift für anorganische und allgemeine Chemie* **1995,** *621* (5), 837-850.

24. Scarel, G.; Wiemer, C.; Fanciulli, M.; Fedushkin, I. L.; Fukin, G. K.; Domrachev, G. A.; Lebedinskii, Y.; Zenkevich, A.; Pavia, G., *Zeitschrift für anorganische und allgemeine Chemie* **2007,** *633* (11-12), 2097-2103.

www.manaraa.com

25. Schumann, H.; Winterfeld, J.; Rosenthal, E. C. E.; Hemling, H.; Esser, L., *Zeitschrift für anorganische und allgemeine Chemie* **1995,** *621* (1), 122-130.

26. Chao, Y. W.; Wexler, P. A.; Wigley, D. E., *Inorganic Chemistry* **1989,** *28* (20), 3860-3868.

27. Green, M. L. H., *Journal of Organometallic Chemistry* **1995,** *500* (1), 127-148.

28. Eaborn, C.; Hitchcock, P. B.; Lickiss, P. D., *Journal of Organometallic Chemistry* **1983,** *252* (3), 281-288.

29. Yan, K.; Pawlikowski, A. V.; Ebert, C.; Sadow, A. D., *Chemical Communications* **2009,** (6), 656-658.

30. Pindwal, A.; Yan, K.; Patnaik, S.; Schmidt, B. M.; Ellern, A.; Slowing, I. I.; Bae, C.; Sadow, A. D., *Journal of the American Chemical Society* **2017,** *139* (46), 16862-16874.

31. Anwander, R.; Runte, O.; Eppinger, J.; Gerstberger, G.; Herdtweck, E.; Spiegler, M., *Journal of the Chemical Society, Dalton Transactions* **1998,** (5), 847-858.

32. Kim, J.; Bott, S. G.; Hoffman, D. M., *Inorganic Chemistry* **1998,** *37* (15), 3835-3841.

33. Eedugurala, N.; Wang, Z.; Yan, K.; Boteju, K. C.; Chaudhary, U.; Kobayashi, T.; Ellern, A.; Slowing, I. I.; Pruski, M.; Sadow, A. D., *Organometallics* **2017,** *36* (6), 1142-1153.

34. Goodwin, C. A. P.; Joslin, K. C.; Lockyer, S. J.; Formanuik, A.; Morris, G. A.; Ortu, F.; Vitorica-Yrezabal, I. J.; Mills, D. P., *Organometallics* **2015,** *34* (11), 2314-2325.

35. Yan, K.; Duchimaza Heredia, J. J.; Ellern, A.; Gordon, M. S.; Sadow, A. D., *Journal of the American Chemical Society* **2013,** *135* (40), 15225-15237.

36. Arrowsmith, M.; Hill, M. S.; Kociok-Köhn, G., *Chemistry – A European Journal* **2013,** *19* (8), 2776-2783.

37. Arrowsmith, M.; Hadlington, T. J.; Hill, M. S.; Kociok-Köhn, G., *Chemical Communications* **2012,** *48* (38), 4567-4569.

38. Arrowsmith, M.; Hill, M. S.; Hadlington, T.; Kociok-Köhn, G.; Weetman, C., *Organometallics* **2011,** *30* (21), 5556-5559.

39. Intemann, J.; Lutz, M.; Harder, S., *Organometallics* **2014,** *33* (20), 5722-5729.

40. Mukherjee, D.; Ellern, A.; Sadow, A. D., *Chemical Science* **2014,** *5* (3), 959-964.

41. Dunne, J. F.; Neal, S. R.; Engelkemier, J.; Ellern, A.; Sadow, A. D., *Journal of the American Chemical Society* **2011,** *133* (42), 16782-16785.

www.manaraa.com

CHAPTER 2. HOMOLEPTIC ORGANOLANTHANIDE COMPOUNDS SUPPORTED BY THE BIS(DIMETHYLSILYL)BENZYL LIGAND

Kasuni C. Boteju, Arkady Ellern, Aaron D. Sadow*

US Department of Energy Ames Laboratory and Department of Chemistry, Iowa State University, Ames IA, 50011, USA

Modified from a manuscript published in Chemical Communications, 2017

Abstract

A β-SiH functionalized benzyl anion $[C(SiHMe_2)_2Ph]^-$ is obtained by deprotonation of $HC(SiHMe_2)_2Ph$ with KCH_2Ph or by reaction of KO*t*Bu and $(Me_2HSi)_3CPh$. $LnI_3 \cdot THF_n$ and three equivalents of this carbanion combine to provide homoleptic tris(alkyl)lanthanide compounds $Ln\{C(SiHMe_2)_2Ph\}_3$ (Ln = La, Ce, Pr, Nd) containing secondary metal-ligand interactions.

Introduction

Synthesis of homoleptic organolanthanide complexes, particularly those of the light trivalent lanthanides (La-Nd), is challenging due to these elements' large ionic radii, polar bonding, high charge, and high Lewis acidity.[1] Such homoleptic compounds should be valuable for synthesis of new catalysts and new materials,[2] yet solvent- or donor-group free, salt-free, and thermally robust organolanthanide compounds are not readily accessed for the larger metal centers. For example, the reaction of MeLi and $LaCl_3$ gives $Li_3[LaMe_6]$ as a TMEDA adduct.[3] Three THF molecules coordinate to the labile tris(benzyl)lanthanum allowing isolation of $LaBn_3THF_3$,[4], [5] however, even this adduct eliminates toluene at room temperature with a half-life of ca. 2 h. The persistence of related compounds may be enhanced by chelating benzylic ligands, for example $Ln(CH(NMe_2)Ph)_3$[6] or $Ln(CH_2C_6H_4\text{-}2\text{-}NMe_2)_3$.[7] An alternative approach combines bulky β-

www.manaraa.com

SiMe3 with benzyl groups in $C(SiMe_3)_2Ph$,[8] exemplified by a bis(alkyl)calcium compound possessing metal-aryl π-interactions. Coordinative unsaturation is important to reactivity of organolanthanides, and donors such as TMEDA or THF can diminish reactivity,[9] facilitate alkane elimination,[10] or react by C–O bond cleavage.[11] While donor-free lanthanum and cerium compounds such as $Ln\{CH(SiMe_3)_2\}_3$ are known, they are inconveniently accessed through multistep synthesis via $Ln\{O(2,6\text{-}C_6H_3tBu_2)\}_3$.[12, 13]

A strategy for stabilizing coordinatively unsaturated rare which form labile secondary interactions with the lanthanide center.[14] Furthermore, the SiH moiety provides a powerful signature in ^1H and ^{29}Si NMR and IR spectra. This β-SiH strategy may also be applied to alkyls, and the ligand $C(SiHMe_2)_3$ supports trivalent yttrium and divalent ytterbium and samarium homoleptic alkyls containing secondary Ln←H–Si interactions.[15, 16] Recently, we reported $Ce\{C(SiHMe_2)_3\}_3$ as a precursor to a zwitterionic hydrosilylation catalyst.[17] New chemistry might be accessed with alkyl ligand variations that include both β-SiH and benzylic functionalities, and these groups could compete to enhance the homoleptic compounds' resistance to undesired ligand elimination pathways. Both SiH and benzyl groups may have significant charge delocalization and secondary interactions that might stabilize homoleptic compounds. A single ligand containing both elements, namely $–C(SiHMe_2)_2Ph$, would test these ideas. Here we report the synthesis of alkane precursors, two routes to potassium alkyl reagents, and isolation and characterization of a series of homoleptic organolanthanide complexes.

Results and Discussion

Reductive coupling of $HCPhBr_2$ and $ClSiHMe_2$ affords $HC(SiHMe_2)_2Ph$ (**1**; eqn (1)) on preparative scale.

www.manaraa.com

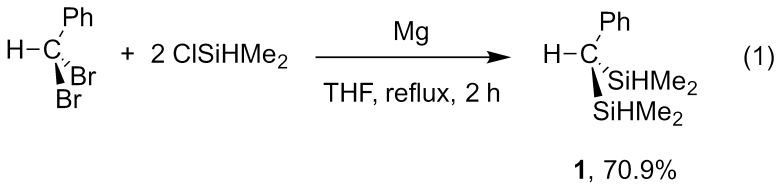

A diagnostic triplet in the ^{1}H NMR spectrum at 1.43 ppm ($^{3}J_{HH}$ = 4 Hz, 1 H) for the central H is coupled to a signal at 4.34 ppm assigned to the SiH (2 H, $^{1}J_{SiH}$ = 186 Hz). The two $SiHMe_2$ groups are magnetically inequivalent giving a virtual octet for the SiH resonance (a $M(AX_3Y_3)(AX_3Y_3)'$ spin system). Compound **1** is also characterized by an intense νSiH signal at 2115 cm^{-1} in its IR spectrum.

While $HC(SiHMe_2)_3$[18] reacts readily with lithium diisopropylamine,[19] deprotonation of $HC(SiHMe_2)_2Ph$ is more challenging. Attempts to synthesize $[C(SiHMe_2)_2Ph]–$ using $LiN(SiMe_3)_2$, *n*BuLi, KH, or $KC(SiHMe_2)_3$ as bases returned $HC(SiHMe_2)_2Ph$. Potassium benzyl (KBn) gives Me_2SiBn_2 as the major product in its reaction with 1 at room temperature. Fortunately, reactions with KBn performed at –78 °C yield a mixture now dominated by $KC(SiHMe_2)Ph$ (**2**), assigned to a doublet at 0.47 ppm in the ^{1}H NMR spectrum. This signal is affected by addition of TMEDA, which gives a new doublet at 0.57 ppm. In preparative scale reactions, the desired potassium alkyl is crystallized from pentane at –30 °C to provide $Ph(Me_2HSi)_2CK(TMEDA)$ (**2·TMEDA**) as dark red crystals (eqn (2)), albeit in low isolated yield.

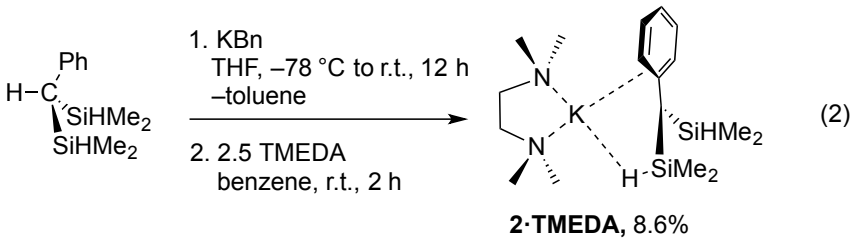

The ^{1}H NMR spectrum of isolated **2·TMEDA** contained a septet at 4.78 ppm ($^{1}J_{SiH}$ = 162 Hz). This one-bond coupling constant was reduced compared to $HC(SiHMe_2)_2Ph$ (186 Hz). In **2·TMEDA**, the $SiMe_2$ groups appeared as one doublet ($^{3}J_{HH}$ = 3.6 Hz), unlike the diastereotopic

www.manaraa.com

methyls in $HC(SiHMe_2)_2Ph$ noted above. In addition, the IR spectrum of **2·TMEDA** revealed two νSiH bands at 2115 and 1995 cm^{-1}.

A single-crystal X-ray diffraction study revealed a polymeric structure for **2·TMEDA**,‡ with each K cation interacting with two $C(SiHMe_2)_2Ph$ groups (Figure 1) through the H1s (2.82(4) Å), the C6 and C11 (from a phenyl group) of one ligand, and the C9 and C10 from a phenyl of the second. Notably, the K1–C1 distance (3.565(4) Å; i.e., to the presumed carbanionic center) is exceedingly long and outside expected bonding range. For comparison, the K–C distance (3.030(5) Å) is much shorter in dimeric $(Me_2HSi)_3CK(TMEDA)$ than in **2·TMEDA**.[16] SiH-free potassium alkyls $KC(Me_3Si)_2Ph$ (3.007(2) Å)[8] and $(Me_2PhSi)_2(Me_2HSi)CK$ (3.167(8) Å)[20] also have polymeric structures with π-coordinated arenes. While the central, carbanionic carbon adopts distorted, nearly planar geometries in these three examples ($\sum_{angles}$ = 358.8°, 357.4° and 356.5°),[8, 16, 20] C1 in **2·TMEDA** is perfectly planar ($\sum_{angles}$ = 360.0(5)°).

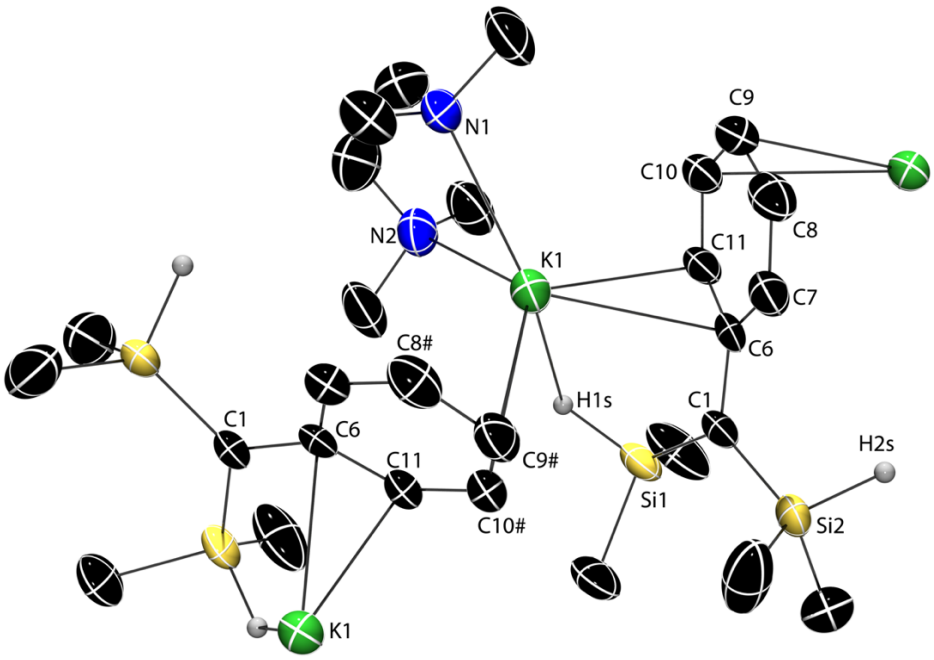

Figure 1. Thermal ellipsoid plot of $Ph(Me_2HSi)_2CK(TMEDA)$ (**2·TMEDA**) at 50% probability. H1s and H2s were located objectively in the Fourier difference map and refined. H atoms bonded

www.manaraa.com

to C are not illustrated for clarity. Selected interatomic distances (Å): K1–C1, 3.565(4); K1–H1s, 2.82(4); K1–Si1, 3.844(2); K1–C6, 3.049(4); K1–C7, 3.389(5); K1–C8#, 3.359(5); K1–C9#, 3.085(5); K1–C10#, 3.038(4); K1–C11, 3.091(5); C1–C6, 1.446(6); C6–C7, 1.434(7); C7–C8, 1.376(7); C8–C9, 1.392(7); C9–C10, 1.383(7); C10–C11, 1.374(6); C11–C6, 1.422(6). Selected interatomic angles (°): K1–H1s–Si1, 124(2); C6–C1–Si2, 119.8(3); Si2–C1–Si1, 121.6(2); Si1–C1–C6, 118.6(3).

The formation of Bn_2SiMe_2 in these reactions implies nucleophilic attack of KBn upon a $SiHMe_2$ group and suggests an alternative route to the desired $KC(SiHMe_2)_2Ph$ (**2**) via Si–C cleavage. A related Si–Si bond cleavage provides $MSi(SiMe_3)_3$ from $Si(SiMe_3)_4$ and LiMe or KO*t*Bu.[21] This idea was tested by the reaction of $(Me_2HSi)_3CPh$ and KO*t*Bu to give the desired $KC(SiHMe_2)_2Ph$ (**2**) in excellent yield (eqn (3)). The spectroscopic features of **2** and **2·TMEDA** were similar for the SiH, including the IR stretching frequency, the chemical shift, and the one-bond coupling constant.

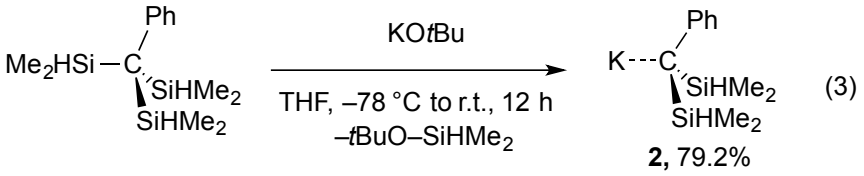

(3)

Reactions of three equiv. of **2** or **2·TMEDA** and LaI_3THF_4, CeI_3THF_4, PrI_3THF_3, or NdI_3THF_3 provide $Ln\{C(SiHMe_2)_2Ph\}_3$ (Ln = La (**3**), Ce (**4**), Pr (**5**), Nd (**6**) in excellent yields (eqn (4)).

www.manaraa.com

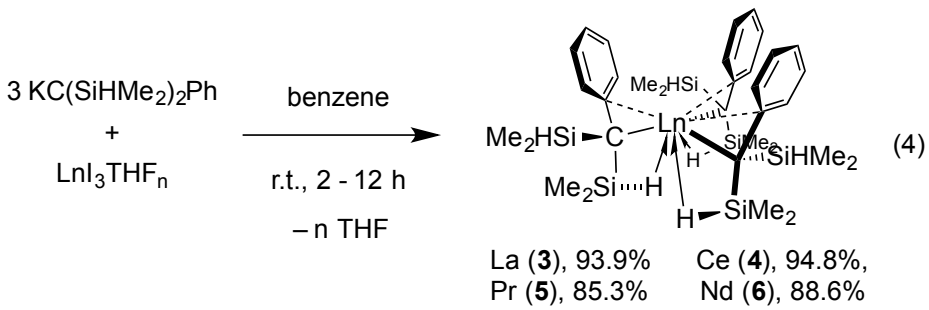

(4)

The series of compounds provide pale yellow, orange, yellow and green crystalline materials, respectively. IR spectra for **3**, **5**, and **6**, acquired as KBr pellets, each contained a sharp, higher energy ν_{SiH} band (2109±5 cm^{-1}) assigned to non-bridging SiH and a broad, lower energy band (1866±6 cm^{-1}) attributed to a ν_{SiH} of the Ln←H–Si. In contrast, the cerium compound **4** showed only one ν_{SiH} band, which appeared at 2115 cm^{-1}. The solution IR spectra similar showed two SiH signals for **3**, **5** and **6**. Although two ν_{SiH} signals were obtained for **4** in solution, the bands were low intensity and a number of the IR spectra were dominated by $HC(SiHMe_2)_2Ph$ signals. We attribute these observations to labile secondary Ln←H–Si interactions present both in solution and solid state.

The ^1H NMR spectrum of diamagnetic **3** revealed signals at 4.24, 0.43, and 0.32 ppm attributed to equivalent $SiHMe_2$ groups with diastereotopic methyl moieties. A doublet signal at 5.84 ppm, assigned to an *ortho*-C_6H_5, appeared upfield compared to its chemical shift in the alkane starting material (6.97 ppm), suggesting a multihapto benzyl-Ln coordination. Evidence for La←H–Si interactions were provided by the $^1J_{SiH}$ of 144 Hz. The equivalence of the $SiHMe_2$ in the room temperature NMR spectrum contrasts the two types of SiH groups observed in the IR spectra, suggesting fluxional process(es). A ^1H NMR spectrum collected at –73 °C in toluene-d_8 revealed that two $SiHMe_2$ groups were inequivalent: signals at 4.67 ($^1J_{SiH}$ ~ 180 Hz) and 3.82 ($^1J_{SiH}$ ~ 120 Hz) ppm were assigned to nonbridging SiH and bridging Ln←H–Si moieties, respectively. These resonances correlated in a COSY experiment to signals at 0.35 and 0.08 ppm (with the downfield

www.manaraa.com

SiH) and 0.77 and 0.67 ppm (with the upfield SiH) of the now inequivalent methyl groups. Notably, one of the ortho-C_6H_5, whose resonance appeared unusually upfield at 4.15 ppm, was even greater shielded than the nonbridging SiH. Moreover, all five H in the C_6H_5 were inequivalent. Thus, the low temperature solution-phase structure appears to contain equivalent alkyl ligands, each containing one La←H–Si and a π-coordinated aryl group.

Single crystal X-ray diffraction reveals that the molecular structure of **3** (P-3) contains three, crystallographically related $C(SiHMe_2)_2Ph$ ligands, each of which interacts with the lanthanum center through the central carbon (C1), through a benzylic-type coordination of the C6, and also through one La←H–Si (Figure 2).[§] The three ligands are arranged in a trigonal geometry around the lanthanum center ($\sum_{C1–La1–C1}$ = 357.15(6)°). This structure is consistent with the low temperature NMR and IR spectroscopic data. A few of the notable structural features include the longer Si1–H1s distance (1.44(4) Å) involved in the Ln←H–Si structure compared to that of the nonbridging Si2–H2s (1.36(4) Å), the nearly acute La1–C1–Si1 angle (93.1(1)°), short La1···Si1 and La1···H1s distances ((3.3141(9) and 2.69(4) Å), and an unusually long La1–C1 distance (2.674(3) Å). The corresponding La–C distances in six-coordinate tris(benzyl)lanthanum compounds, e.g., $La(CH_2Ph)_3THF_3$ (2.648(2) Å),[5] are shorter, and the distance in $La(CH(SiMe_3)_2)_3$ (2.515(9) Å) is much shorter.[12] These trends extend to the comparisons of structures of **4**-**6** to the analogous benzyllanthanide species. Moreover, the close contacts in the series (i.e, Ln–C, Ln···Si, and Ln···H) follow the expected trend based on ionic radius (La > Ce > Pr > Nd).

www.manaraa.com

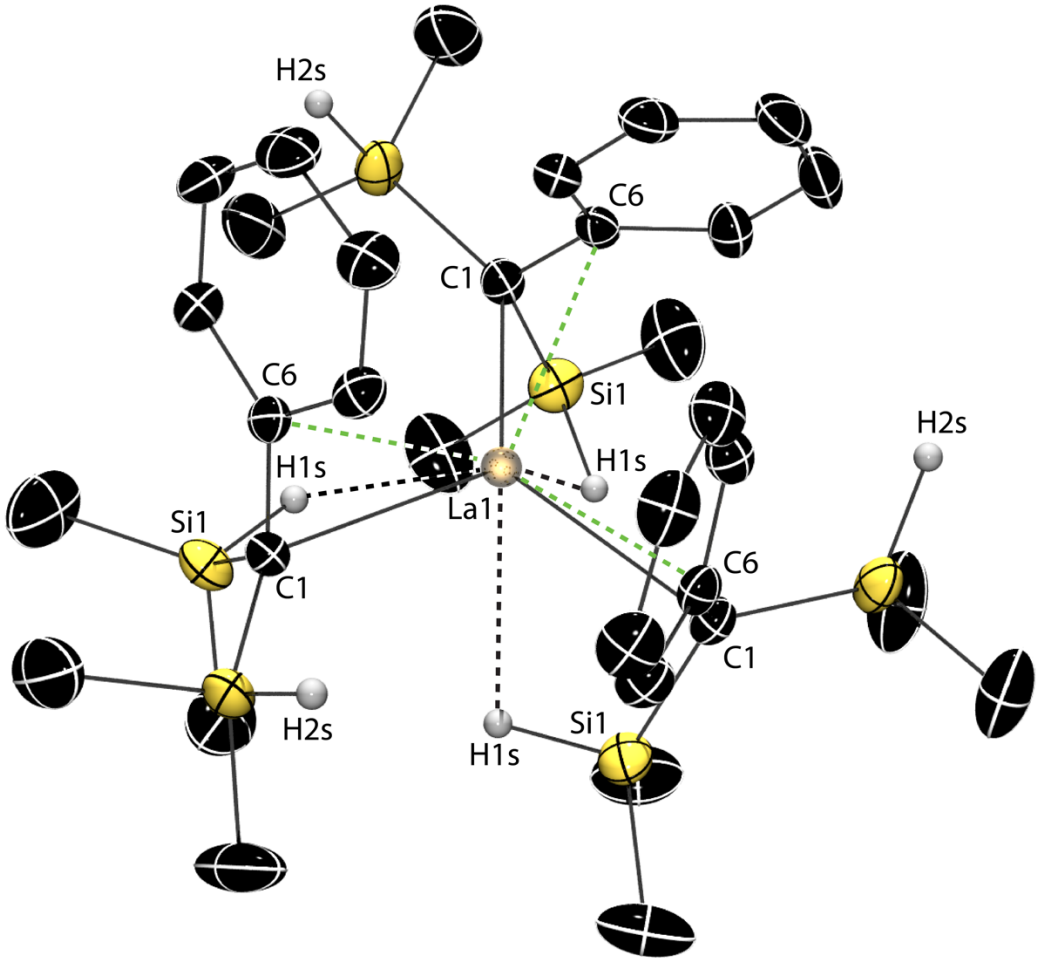

Figure 2. Thermal ellipsoid plot of $La(C(SiHMe_2)_2Ph)_3$ (**3**). H atoms bonded to Si were located in the Fourier difference map, refined anisotropically, and are illustrated. All other H atoms and a disordered pentane molecule (0.5) are not shown for clarity. Short La–C (green) and Ln←H–Si (black) distances are highlighted with dashed lines. Selected interatomic distances (Å): La1–C1, 2.674(3); La1–C6, 2.822(2); La1–Si1, 3.3141(9); La1–H1s, 2.69(4); C1–Si1, 1.821(3); Si1–H1s, 1.37(4); C1–Si2, 1.853(3); Si2–H2s, 1.45(4); C1–C6, 1.483(4); C6–C7, 1.415(5); C6–C11, 1.409(4). Selected interatomic angles (°):C1–La1–C1, 119.05(2); La1–C1–C6, 80.0(1); La1–C1–Si1, 93.0(1); La1–C1–Si1, 128.3(1).

www.manaraa.com

Interestingly, isomorphous cerium **4**, praseodymium **5** and neodymium **6** compounds' structures ($P2_1/c$) are inequivalent with that of La **3**. The two molecules in the unit cells for **4**, **5** and **6** have inequivalent configurations, with one molecule containing only two Ln←H–Si bridging moieties (Figure 3).[§§] The Ce–C distances for the five ligands that contain bridging Ce←H–Si interactions average 2.65 ± 0.02 Å, whereas the η^2-benzyl only ligand (Ce2–C56, 2.587(3) Å) distance is shorter. This distinction is also apparent in compounds **5** (Pr–C_{ave}, 2.63 ± 0.02; Pr2–C56, 2.556(5) Å) and **6** (Nd–C_{ave}, 2.61 ± 0.02; Nd–C56, 2.541(4) Å).

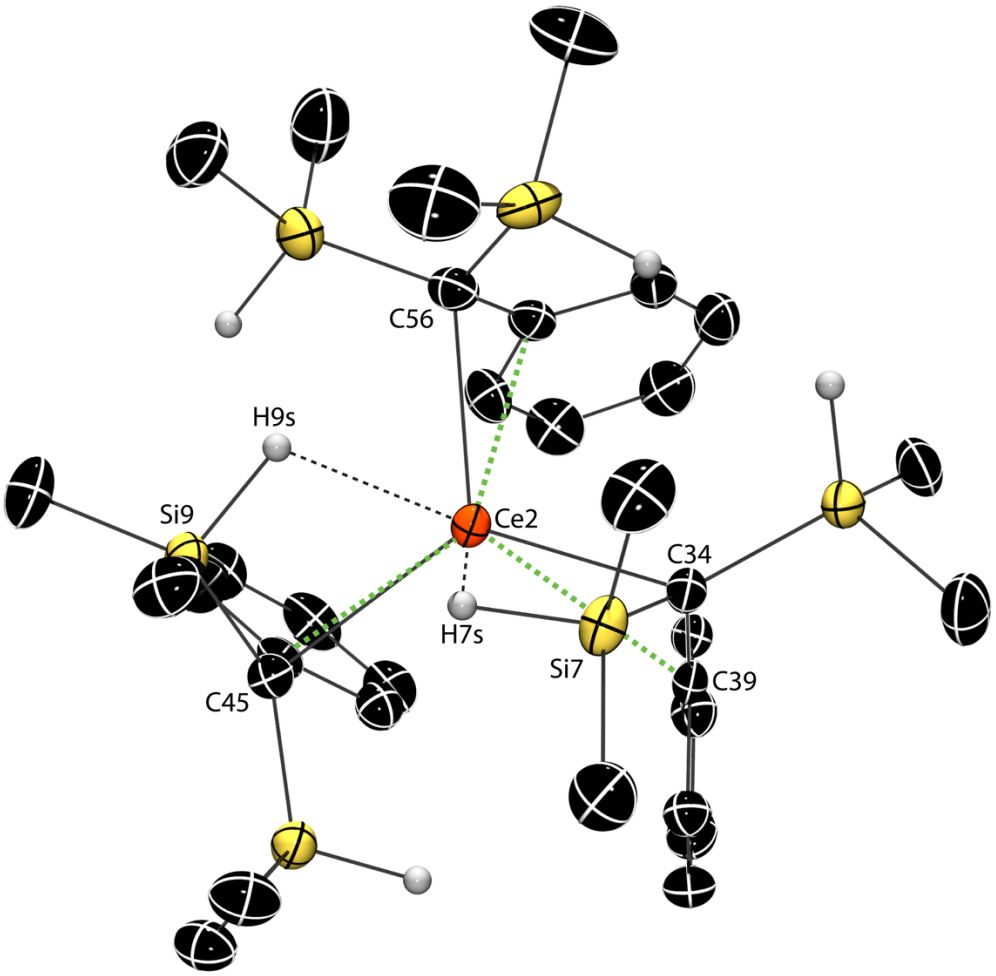

Figure 3. Thermal ellipsoid plot of one of two crystallographically distinct molecules of $Ce(C(SiHMe_2)_2Ph)_3$ (**4**). H atoms bonded to Si were located in the Fourier difference map, refined

www.manaraa.com

anisotropically, and are illustrated. All other H atoms are not shown for clarity. Short Ce–C (green) and Ln←H–Si (black) distances are highlighted with dashed lines. Selected interatomic distances (Å): Ce2–C34, 2.613(3); Ce2–C45, 2.671(2); Ce2–C56, 2.587(3); Ce2–Si7, 3.1947(9); Ce2–H7s, 2.47(2); C34–Si7, 1.829(2); Si7–H7s, 1.48(3); Ce2–Si9, 3.2379(9); Ce2–H9s, 2.46(3); C45–Si9, 1.829(3); Si9–H9s, 1.48(3); Selected interatomic angles (°): C34–Ce2–C45, 118.57(9); Ce2–C34–C39, 83.8(2); Ce2–C34–Si7, 90.1(1).

Conclusion

Thus, the idea that β-SiH groups support large, coordinatively unsaturated rare earth centers in homoleptic, solvent-free compounds has been extended to a new mixed benzyl dimethylsilyl ligand. A series of tris(alkyl) lanthanides $Ln\{C(SiHMe_2)_2Ph\}_3$ are synthesized in good yields, and the secondary interactions involving β-SiH and aryl moieties are likely important to the facile isolation of these compounds. The structural parameters (e.g., Ln–C, Si–H, Si–C distances) for moieties involved in secondary Ln←H–Si interactions are different than those with nonbridging SiH groups, and the Ln–C distances are also affected by the presence or lack of secondary Ln←H–Si interactions. The ligand itself is synthesized by deprotonation of the new alkane $HC(SiHMe_2)_2Ph$ with KBn, but Me_2SiBn_2 and other side products in reactions of $HC(SiHMe_2)_2Ph$ and KBn suggested a competing reaction involving nucleophilic attack on a Si center to cleave the C–Si bond. Therefore we developed an alternative route to $KC(SiHMe_2)_2Ph$ by reacting $PhC(SiHMe_2)_3$ with KO*t*Bu that affords the desired product in excellent yield. This straightforward two-step synthesis to homoleptic organolanthanides may allow their application in the preparation of heteroleptic lanthanide complexes and as precursors for new catalytic chemistry.

www.manaraa.com

Experimental

General. All manipulations were performed under a dry argon atmosphere using standard Schlenk techniques or under a nitrogen atmosphere in a glovebox unless otherwise indicated. Water and oxygen were removed from benzene, pentane, and THF solvents using an IT PureSolv system. Benzene-d_6 and toluene-d_8, were heated to reflux over Na/K alloy and chloroform-*d* was heated to reflux over CaH_2, and vacuum-transferred. LaI_3THF_4,[22, 23] CeI_3THF_4,[23] PrI_3THF_3,[24] and NdI_3THF_3[22, 23] were prepared by reaction of Ln with CI_2H_2 (La, Ce, Nd) and 1,2-$C_2I_2H_4$ according to the literature. α,α,α-Trichlorotoluene, α,α-dibromotoluene, and magnesium chips were purchased from Sigma-Aldrich, Alfa Aesar, and Strem Chemicals, respectively, and used as received. Dimethylchlorosilane was purchased from Gelest and distilled, and potassium tert-butoxide was purchased from Sigma-Aldrich and sublimed before use. Potassium benzyl was prepared according to the literature.[25] ^1H, $^{13}C\{^1H\}$, and $^{29}Si\{^1H\}$ HMBC NMR spectra were collected on a Bruker DRX-400 spectrometer or a Bruker Avance III-600 spectrometer. Infrared spectra were measured on a Bruker Vertex 80, using KBr pellet (transmission mode) or Pike Miracle ATR (solution measurements). Elemental analyses were performed using a Perkin-Elmer 2400 Series II CHN/S. X-ray diffraction data was collected on a Bruker APEX II diffractometer.

$HC(SiHMe_2)_2Ph$ (1). An oven-dried three-neck flask equipped with an addition funnel and a condenser was allowed to cool under vacuum. Mg turnings (6.00 g, 0.247 mol) were added to the flask under an Ar purge, and then THF (96 mL) was added. Me_2HSiCl (27.3 mL, 0.246 mol) was added to the flask through the addition funnel, which was subsequently rinsed with THF (36 mL). A THF solution of $PhCHBr_2$ (20.4 mL, 0.123 mol) was added in a dropwise fashion to initiate the reaction. Once the addition was complete, the reaction mixture was heated at reflux for 2.5 h. The solution was filtered in air to remove salt byproducts, the filtrate was washed with water (3 ×

www.manaraa.com

200 mL), and the salt residue was further extracted with pentane. The filtrate and pentane extracts were combined and dried over $MgSO_4$. The filtrate was concentrated under vacuum, and the resulting yellow liquid was distilled at 50 °C (3 mmHg) to yield $HC(SiHMe_2)_2Ph$ as a colorless product (18.2 g, 0.0874 mol, 70.9%) which contained only one peak in the chromatogram of a GC-MS with a m/z of 208.1. ^1H NMR (benzene-d_6, 600 MHz, 25 °C): δ 7.12 (t, 2 H, $^3J_{HH}$ = 7.7 Hz, *m*-C_6H_5), 6.96 (d, 2 H, *o*-C_6H_5 and t, 1 H, *p*-C_6H_5 overlapped), 4.34 (v octet, 2 H, $^1J_{SiH}$ = 186 Hz, Si*H*Me$_2$), 1.43 (t, 1 H, $^3J_{HH}$ = 4.0 Hz, *H*C(SiHMe$_2$)$_2$Ph), 0.085 (d, 6 H, $^3J_{HH}$ = 4.0 Hz, SiH*Me*$_2$), 0.035 (d, 6 H, $^3J_{HH}$ = 4.0 Hz, SiH*Me*$_2$). $^{13}C\{^1H\}$ NMR (benzene-d_6, 150 MHz, 25 °C): δ 142.42 (*ipso*-C_6H_5), 129.21 (*m*-C_6H_5), 129.15 (*p*-C_6H_5), 124.58 (*o*-C_6H_5), 24.68 (*C*(SiHMe$_2$)$_2$), –3.10 (SiH*Me*$_2$), –3.62 (SiH*Me*$_2$). $^{29}Si\{^1H\}$ NMR (benzene-d_6, 119.3 MHz, 25 °C): δ –12.9. IR (KBr, cm^{-1}): 3078 m, 3022 m, 2959 s, 2901 m, 2847 w, 2115 s (SiH), 1702 w, 1597 s, 1450 s, 1419 m, 1252 s, 1206 s, 1070 m, 1032 s, 896 s br, 836 s, 785 m, 699 s, 645 m, 537 m.

(TMEDA)KC(SiHMe$_2$)$_2$Ph. THF solutions of $HC(SiHMe_2)_2Ph$ (1.32 g, 6.32 mmol, 5 mL) and KBn (0.823 g, 6.32 mmol, 15 mL) were cooled to –78 °C. The KBn solution was added to the cold, vigorously stirred $HC(SiHMe_2)_2Ph$ solution in a dropwise fashion to give a dark green solution. The reaction mixture was slowly warmed to room temperature and then was stirred for 17 h. The solvent was removed under vacuum, and the residue was washed with pentane (5 × 3 mL) and dried under vacuum overnight to yield $K(SiHMe_2)_2Ph$ as a dark brown oily THF adduct. TMEDA (2.3 mL, 15.3 mmol) was added, and the mixture was stirred in benzene (8 mL) for 2 h at room temperature. The solvent was evaporated under reduced pressure, and the residue was extracted with pentane (6 × 5 mL). The extracts were combined, concentrated in vacuo, and cooled at –30 °C to yield X-ray quality crystals (0.189 g, 0.521 mmol, 8.60%). ^1H NMR (benzene-d_6, 400

www.manaraa.com

MHz, 25 °C): δ 6.92 (t, 2 H, $^{3}J_{HH}$ = 7.0 Hz, *m*-C_6H_5), 6.85 (d, 2 H, $^{3}J_{HH}$ = 8.0 Hz, *o*-C_6H_5), 6.25 (t, 1 H, $^{3}J_{HH}$ = 7.0 Hz, *p*-C_6H_5), 4.78 (m, 2 H, $^{3}J_{HH}$ = 3.6 Hz, $^{1}J_{SiH}$ = 162 Hz, Si*H*Me_2), 1.96 (s, 4 H, NC*H*$_2$), 1.88 (s, 12 H N*Me*), 0.56 (d, 12 H, $^{3}J_{HH}$ = 3.6 Hz, SiH*Me*$_2$). $^{13}C\{^{1}H\}$ NMR (benzene-d_6, 150 MHz, 25 °C): δ 158.58 (*ipso*-C_6H_5), 130.16 (*m*-C_6H_5), 121.19 (*o*-C_6H_5), 109.31 (*p*-C_6H_5), 57.82 (N*C*H_2), 45.95 (*C*(SiHMe_2)$_2$), 45.40 (N*Me*), 1.54 (SiH*Me*$_2$). $^{29}Si\{^{1}H\}$ NMR (benzene-d_6, 119.3 MHz, 25 °C): δ –27.30. $^{15}N\{^{1}H\}$ NMR (benzene-d_6, 61 MHz, 25 °C): δ –361.9. IR (KBr, cm^{-1}): 3055 m, 2948 s, 2890 m, 2115 m (SiH), 1995 s (SiH), 1579 s, 1470 s, 1262 s br, 1187 m, 1150 m, 1080 m, 1026 m, 894 s br, 826 s, 756 s, 700 s, 632 m, 527 m. Anal. Calcd for $C_{17}H_{35}KN_2Si_2$: C, 56.29; H, 9.73; N, 7.72. Found: C, 56.18; H, 9.87; N, 7.26. mp 54 - 56 °C.

PhC(SiHMe$_2$)$_3$. This compound was previously synthesized from α,α,α-tribromotoluene, and its NMR spectra were previously reported in chloroform-d_1.[26] We synthesized the compound starting from α,α,α-trichlorotoluene. An oven-dried three-neck flask equipped with a condenser and an addition funnel was cooled under vacuum. Mg turnings (12.0 g, 0.494 mol) were added to the flask. THF (180 mL) was added, and Me_2HSiCl (54.8 mL, 0.494 mol) was added through the addition funnel, which was then rinsed with THF (60 mL). $PhCCl_3$ (23.3 mL, 0.165 mol) was added to the flask in a dropwise fashion. The reaction mixture was heated at refluxed for 4 h. Once the reflux was complete, the reaction mixture was cooled to room temperature and filtered in air to remove the salt byproducts. The filtrate was washed with water, and the salts were extracted with pentane. The filtrate and the pentane extracts were combined and dried over $MgSO_4$ for 15 min. The solution was filtered and concentrated under vacuum. The oily residue distilled at 87 °C under dynamic vacuum to yield the product as a colorless liquid (17.0 g, 0.0636 mol, 38.7%). GC-MS analysis revealed a single peak in the chromatograph corresponding to a m/z of 266.1

www.manaraa.com

(expected 266.6). ^{1}H NMR (chloroform-d_1, 150 MHz, 25 °C): δ 7.29 (d, 2 H, $^{3}J_{HH}$ = 7.7 Hz, *o*-C_6H_5), 7.24 (t, 2 H, $^{3}J_{HH}$ = 7.6 Hz, *m*-C_6H_5), 7.08 (t, 1 H, $^{3}J_{HH}$ = 7.3 Hz, *p*-C_6H_5), 4.33 (sept, 3 H, $^{3}J_{HH}$ = 3.8 Hz, $^{1}J_{SiH}$ = 188 Hz, Si*H*Me$_2$), 0.20 (d, 18 H, $^{3}J_{HH}$ = 3.6 Hz, SiH*Me*$_2$). ^{1}H NMR (benzene-d_6, 400 MHz, 25 °C): δ 7.39 (d, 2 H, $^{3}J_{HH}$ = 7.8 Hz, *o*-C_6H_5), 7.12 (t, 2 H, $^{3}J_{HH}$ = 7.4 Hz, *m*-C_6H_5), 6.95 (t, 1 H, $^{3}J_{HH}$ = 7.4 Hz, *p*-C_6H_5), 4.56 (sept, 3 H, $^{3}J_{HH}$ = 3.7 Hz, $^{1}J_{SiH}$ = 188 Hz, Si*H*Me$_2$), 0.22 (d, 18 H, $^{3}J_{HH}$ = 3.6 Hz, SiH*Me*$_2$). ^{13}C{^{1}H} NMR (benzene-d_6, 150 MHz, 25 °C): δ 142.78 (*ipso*-C_6H_5), 130.92 (*o*-C_6H_5), 129.08 (*m*-C_6H_5), 124.77 (*p*-C_6H_5), 15.47 (*C*(SiHMe$_2$)$_2$), –2.05 (SiH*Me*$_2$). ^{29}Si{^{1}H} NMR (benzene-d_6, 119.3 MHz, 25 °C): δ –13.08. IR (KBr, cm^{-1}): 3084 w, 3058 w, 2959 m, 2904 m, 2120 s (SiH), 1592 m, 1495 m, 1441 w, 1419 w, 1255 s, 1166 m, 1083 w, 1038 m, 916 s br, 882 s br, 844 s br, 756 w, 699 s, 644 m. m/z for $C_{13}H_{26}Si_3$: Calcd 266.61, Found 266.1.

KC(SiHMe$_2$)$_2$Ph (2). A THF solution of PhC(SiHMe$_2$)$_3$ (1.28 g, 4.79 mmol, 5 mL) was cooled to –78 °C. In a separate vessel, KO^{t}Bu (0.510 g, 4.55 mmol) was dissolved in THF (15 mL) and cooled to –78 °C. This solution was slowly added to PhC(SiHMe$_2$)$_3$. The reaction mixture was stirred for 30 min at –78 °C and then slowly warmed to room temperature and stirred overnight. The solvent was removed under vacuum, and the residue was washed with pentane (3 × 3 mL). The residual pentane was removed under vacuum to yield the product as a brownish yellow powder (0.792 g, 3.21 mmol, 79.2%). ^{1}H NMR (benzene-d_6, 400 MHz, 25 °C): δ 6.75 (t, 2 H, $^{3}J_{HH}$ = 7.6 Hz, *m*-C_6H_5), 6.58 (d, 2 H, $^{3}J_{HH}$ = 8.0 Hz, *o*-C_6H_5), 6.08 (t, 1 H, $^{3}J_{HH}$ = 6.9 Hz, *p*-C_6H_5), 4.57 (sept, 2 H, $^{3}J_{HH}$ = 3.6 Hz, $^{1}J_{SiH}$ = 163 Hz, Si*H*Me$_2$), 0.42 (d, 12 H, $^{3}J_{HH}$ = 3.6 Hz, SiH*Me*$_2$). ^{13}C{^{1}H} NMR (benzene-d_6, 150 MHz, 25 °C): δ 157.90 (*ipso*-C_6H_5), 130.66 (*m*-C_6H_5), 120.51 (*o*-C_6H_5), 109.64 (*p*-C_6H_5), 45.97 (*C*(SiHMe$_2$)$_2$), 1.28 (SiH*Me*$_2$). ^{29}Si{^{1}H} NMR (benzene-d_6, 119.3 MHz, 25 °C): δ –27.53. IR (KBr, cm^{-1}): 3055 m, 2940 s, 2889 m, 2493 w, 2118 m (SiH), 1995 s (SiH),

www.manaraa.com

1583 s, 1532 m, 1472 s, 1263 s, 1252 s, 1187 m, 1081 w, 1010 s br, 898 s, 828 m, 800 m, 757 s, 700 s, 679 m, 630 m. Anal. Calcd for $C_{11}H_{19}KSi_2$: C, 53.59; H, 7.77. Found: C, 53.36; H, 8.00. mp 126 - 128 °C.

La{C(SiHMe$_2$)$_2$Ph}$_3$ (3). Method A. $LaI_3(THF)_4$ (0.0603 g, 0.0746 mmol) and (TMEDA)KC(SiHMe$_2$)$_2$Ph (0.0812 g, 0.224 mmol) were stirred in a mixture of pentane (2.5 mL) and benzene (2.5 mL) for 2 h at room temperature. The solvents were evaporated, and the solid residue was extracted with pentane (3 × 3 mL). The pentane was removed under vacuum to provide an analytically pure yellow sticky solid (0.0545 g, 0.0716 mmol, 95.9%). Recrystallization from pentane at –30 °C provided X-ray quality crystals. **Method B.** $LaI_3(THF)_4$ (0.219 g, 0.270 mmol) and KC(SiHMe$_2$)$_2$Ph (0.200 g, 0.811 mmol) were stirred in benzene (8 mL) for 2 h at room temperature. La{C(SiHMe$_2$)$_2$Ph}$_3$ was isolated following the workup procedure described in Method A to obtain a yellow solid in high yield (0.193 g, 0.254 mmol, 93.9%). ^{1}H NMR (benzene-d_6, 600 MHz, 25 °C): δ 7.10 (t, 6 H, $^3J_{HH}$ = 8.1 Hz, *m*-C_6H_5), 6.81 (t, 3 H, $^3J_{HH}$ = 7.4 Hz, *p*-C_6H_5), 5.84 (d, 6 H, $^3J_{HH}$ = 7.5 Hz, *o*-C_6H_5), 4.24 (septet, 6 H, $^1J_{SiH}$ = 144 Hz, Si*H*Me$_2$), 0.43 (d, 18 H, $^3J_{HH}$ = 3.2 Hz, SiH*Me*$_2$), 0.32 (d, 18 H, $^3J_{SiH}$ = 3.5 Hz, SiH*Me*$_2$). ^{1}H NMR (toluene-d_8, 125 MHz, –73 °C): δ 7.27 (3 H, *o*-C_6H_5, 3 H *m*-C_6H_5), 6.80 (3 H, *p*-C_6H_5, 3 H, *m*-C_6H_5), 4.68 (s br, 3 H, Si*H*Me$_2$), 4.15 (3 H, *o*-C_6H_5), 3.81 (s br, 3 H, Si*H*Me$_2$), 0.78, 0.68, (s br, 18 H La←HSi*Me*$_2$) 0.35, 0.08 (s br, 18 H, SiH*Me*$_2$). ^{13}C{^{1}H} NMR (benzene-d_6, 150 MHz, 25 °C): δ 149.66 (*ipso*-C_6H_5), 134.61 (*m*-C_6H_5), 129.96 (*o*-C_6H_5), 122.59 (*p*-C_6H_5), 56.29 (*C*(SiHMe$_2$)$_2$), 1.89 (SiH*Me*$_2$), 1.29 (SiH*Me*$_2$). ^{13}C{^{1}H} NMR (toluene-d_8, 150 MHz, –73 °C): δ 148.27 (*ipso*-C_6H_5), *m*-C_6H_5 and *o*-C_6H_5 overlap with toluene-d_8, 122.26 (*p*-C_6H_5), 53.48 (*C*(SiHMe$_2$)$_2$), 2.33 (SiH*Me*$_2$), 1.47 (La←HSi*Me*$_2$), 0.89 (La←HSi*Me*$_2$), 0.41 (SiH*Me*$_2$). ^{29}Si{^{1}H} NMR (benzene-d_6, 119.3 MHz, 25

www.manaraa.com

°C): δ –18.0 (*Si*HMe$_2$).^{29}Si{^{1}H} NMR (toluene-d_8, 119.3 MHz, –73 °C): δ 1.80 (*Si*HMe$_2$), –12.97 (La←H*Si*Me$_2$). IR (KBr, cm^{-1}): 2954 m, 2111 m (SiH), 1859 m br (SiH), 1583 m, 1473 m, 1253 s, 1207 m, 1071 m, 888 s, 834 s, 767 m, 703 m, 462 m br. IR (ATR, pentane, cm^{-1}): 2106 m br (SiH), 1859 m br (SiH), 1585 m, 1474 m, 1256 m, 1248 m, 1209 s, 1033 m br, 930 s, 890 s, 834 s, 767 s, 708 m. Anal. Calcd for $C_{33}H_{57}LaSi_6$: C, 52.07; H, 7.55. Found: C, 52.48; H, 7.67. mp 119 °C.

Ce(C(SiHMe$_2$)$_2$Ph)$_3$ (4). **Method A.** $CeI_3(THF)_4$ (0.0682 g, 0.0843 mmol) and (TMEDA)KC(SiHMe$_2$)$_2$Ph (0.0917 g, 0.253 mmol) were stirred in a mixture of pentane (2.5 mL) and benzene (2.5 mL) for 5 h at room temperature. The color changed from dark red to orange. The solvents were evaporated, and the residue was extracted with pentane (3 × 3 mL). The pentane was removed under vacuum to yield an orange sticky solid (0.0599 g, 0.0786 mmol, 93.2%). Recrystallization from pentane at –30 °C afforded X-ray quality crystals. **Method B.** $CeI_3(THF)_4$ (0.0750 g, 0.0928 mmol) and KC(SiHMe$_2$)$_2$Ph (0.0686 g, 0.278 mmol) were stirred in benzene (5 mL) for 5 h at room temperature. Ce{C(SiHMe$_2$)$_2$Ph}$_3$ was isolated following the workup procedure described in Method A to yield the product as an orange solid (0.0670 g, 0.0928 mmol, 94.8%). IR (KBr, cm^{-1}): 3024 s, 2959 s, 29254 s, 2853 s, 2115 m (SiH), 1648 m, 1598 m, 1493 m, 1459 m, 1398 br, 1256 s, 1206 m, 1155 m, 1092 m, 1028 s, 891 s, 837 s, 798 s. IR (ATR, pentane, cm^{-1}): 2958 s, 2923 s, 2874 s, 2115 w (SiH), 1865 w (SiH), 1461 m, 1380 m, 1248 w, 1208 w, 890 s br, 836 m, 766 m, 728 m. Anal. Calcd for $C_{33}H_{57}CeSi_6$: C, 51.99; H, 7.54. Found: C, 51.82 ; H, 7.45 . mp 118 °C.

www.manaraa.com

$Pr(C(SiHMe_2)_2Ph)_3$ (5). Method A. $PrI_3(THF)_3$ (0.0657 g, 0.0890 mmol) and $(TMEDA)KC(SiHMe_2)_2Ph$ (0.0969 g, 0.267 mmol) were stirred in a mixture of pentane (2.5 mL) and benzene (2.5 mL) overnight at room temperature. The color changed from dark red to greenish yellow. The solvents were removed under vacuum, and the residue was extracted with pentane (3 × 3 mL). The pentane was removed under vacuum to yield a yellow sticky solid (0.0510 g, 0.0668 mmol, 75.1%). X-ray quality yellow crystals were obtained from recrystallization from a pentane solution cooled at –30 °C. **Method B.** $PrI_3(THF)_3$ (0.0750 g, 0.102 mmol) and $KC(SiHMe_2)_2Ph$ (0.0751 g, 0.305 mmol) were stirred in benzene (5 mL) overnight at room temperature. $Pr\{C(SiHMe_2)_2Ph\}_3$ was isolated following the workup procedure described in Method A to yield the product as a yellow solid (0.0662 g, 0.0867 mmol, 85.3%). IR (KBr, cm^{-1}): 2955 s, 2926 s, 2854 s, 2113 s (SiH), 1868 br (SiH), 1595 m, 1492 m, 1473 m, 1415 br, 1251 s, 1207 s, 1030 s. IR (ATR, pentane, cm^{-1}): 2950 w, 2898 w, 2114 w br (SiH), 1870 w br (SiH), 1585 w, 1475 m, 1248 m, 1207 m, 1033 m br, 930 s, 888 s, 834 s, 768 s, 708 m, 677 w. Anal. Calcd for $C_{33}H_{57}PrSi_6$: C, 51.92; H, 7.54. Found: C, 51.81; H, 7.72. mp 123 °C.

$Nd(C(SiHMe_2)_2Ph)_3$. (6) Method A. $NdI_3(THF)_3$ (0.0563 g, 0.0759 mmol) and $(TMEDA)KC(SiHMe_2)_2Ph$ (0.0827 g, 0.228 mmol) were stirred in a mixture of pentane (2.5 mL) and benzene (2.5 mL) overnight at room temperature. The color changed from dark red to green. The solvents were removed under vacuum, and the residue was extracted with pentane (3 × 3 mL). The pentane was removed under vacuum to yield a green sticky solid (0.0519 g, 0.0677 mmol, 89.1%). Green, X-ray quality crystals were obtained after recrystallization from pentane at –30 °C. **Method B.** $NdI_3(THF)_3$ (0.0744 g, 0.100 mmol) and $KC(SiHMe_2)_2Ph$ (0.0742 g, 0.301 mmol) were stirred in benzene (5 mL) overnight at room temperature. The above procedure for isolation

www.manaraa.com

of $Nd\{C(SiHMe_2)_2Ph\}_3$ was followed to yield the product as a green solid (0.0681 g, 0.0888 mmol, 88.6%). ^1H NMR (benzene-d_6, 600 MHz, 25 °C): δ 4.89, 1.36, –1.76, –2.22. IR (KBr, cm^{-1}): 2952 m, 2104 m (SiH), 1871 m br (SiH), 1583 m, 1473 m, 1252 s, 1209 m, 1071 m, 1032 m, 888 s, 832 s, 763 m, 704 m, 456 m br. IR (ATR, pentane, cm^{-1}): 2951 w, 2898 w, 2116 w br (SiH), 1869 m br (SiH), 1586 w, 1474 m, 1255 m, 1207 m, 1033 m br, 888 s, 834 s, 767 m, 708 m. Anal. Calcd for $C_{33}H_{57}NdSi_6$: C, 51.71; H, 7.50. Found: C, 51.96; H, 7.60. mp 121 °C.

References

1. M. Zimmermann and R. Anwander, *Chem. Rev.*, 2010, **110**, 6194-6259.

2. A. M. Kawaoka, M. R. Douglass and T. J. Marks, *Organometallics*, 2003, **22**, 4630-4632; H. F. Yuen and T. J. Marks, *Organometallics*, 2008, **27**, 155-158; H. F. Yuen and T. J. Marks, *Organometallics*, 2009, **28**, 2423-2440; M. P. Conley, G. Lapadula, K. Sanders, D. Gajan, A. Lesage, I. del Rosal, L. Maron, W. W. Lukens, C. Copéret and R. A. Andersen, *J. Am. Chem. Soc.*, 2016, **138**, 3831-3843; M. Zimmermann, K. W. Törnroos and R. Anwander, *Organometallics*, 2006, **25**, 3593-3598; H. Martin Dietrich, G. Raudaschl-Sieber and R. Anwander, *Angew. Chem. Int. Ed.*, 2005, **44**, 5303-5306; R. Taube, S. Maiwald and J. Sieler, *J. Organomet. Chem.*, 2001, **621**, 327-336; S. R. Daly, D. Y. Kim, Y. Yang, J. R. Abelson and G. S. Girolami, *J. Am. Chem. Soc.*, 2010, **132**, 2106-2107.

3. H. Schumann, J. Muller, N. Bruncks, H. Lauke, J. Pickardt, H. Schwarz and K. Eckart, *Organometallics*, 1984, **3**, 69-74.

4. A. J. Wooles, D. P. Mills, W. Lewis, A. J. Blake and S. T. Liddle, *Dalton Trans.*, 2010, **39**, 500-510.

5. S. Bambirra, A. Meetsma and B. Hessen, *Organometallics*, 2006, **25**, 3454-3462.

6. A. C. Behrle and J. A. R. Schmidt, *Organometallics*, 2011, **30**, 3915-3918.

7. S. Harder, *Organometallics*, 2005, **24**, 373-379.

8. F. Feil and S. Harder, *Organometallics*, 2000, **19**, 5010-5015.

9. P. L. Watson, *J. Am. Chem. Soc.*, 1982, **104**, 337-339.

10. H. Van der Heijden, C. J. Schaverien and A. G. Orpen, *Organometallics*, 1989, **8**, 255-258.

11. P. L. Watson, *J. Chem. Soc., Chem. Commun.*, 1983, 276-277.

www.manaraa.com

12. P. B. Hitchcock, M. F. Lappert, R. G. Smith, R. A. Bartlett and P. P. Power, *J. Chem. Soc., Chem. Commun.*, 1988, 1007-1009.

13. A. G. Avent, C. F. Caro, P. B. Hitchcock, M. F. Lappert, Z. N. Li and X. H. Wei, *J. Chem. Soc., Dalton Trans.*, 2004, 1567-1577.

14. W. A. Herrmann, J. Eppinger, M. Spiegler, O. Runte and R. Anwander, *Organometallics*, 1997, **16**, 1813-1815; J. William S. Rees, O. Just, H. Schumann and R. Weimann, *Angew. Chem. Int. Ed.*, 1996, **35**, 419-422.

15. K. Yan, A. V. Pawlikowski, C. Ebert and A. D. Sadow, *Chem. Commun.*, 2009, 656-658; K. Yan, B. M. Upton, A. Ellern and A. D. Sadow, *J. Am. Chem. Soc.*, 2009, **131**, 15110-15111; A. Pindwal, A. Ellern and A. D. Sadow, *Organometallics*, 2016, **35**, 1674-1683.

16. K. Yan, G. Schoendorff, B. M. Upton, A. Ellern, T. L. Windus and A. D. Sadow, *Organometallics*, 2013, **32**, 1300-1316.

17. A. Pindwal, S. Patnaik, W. C. Everett, A. Ellern, T. L. Windus and A. D. Sadow, *Angew. Chem. Int. Ed.*, 2017, **56**, 628-631.

18. C. Eaborn, P. B. Hitchcock and P. D. Lickiss, *J. Organomet. Chem.*, 1983, **252**, 281-288.

19. E. J. Hawrelak, F. T. Ladipo, D. Sata and J. Braddock-Wilking, *Organometallics*, 1999, **18**, 1804-1807.

20. A. Asadi, A. G. Avent, M. P. Coles, C. Eaborn, P. B. Hitchcock and J. D. Smith, *J. Organomet. Chem.*, 2004, **689**, 1238-1248.

21. C. Marschner, *Eur. J. Inorg. Chem.*, 1998, 221-226; G. Gutekunst and A. G. Brook, *J. Organomet. Chem.*, 1982, **225**, 1-3.

22. G. B. Deacon, T. Feng, P. C. Junk, G. Meyer, N. M. Scott, B. W. Skelton and A. H. White, *Aust. J. Chem.*, 2000, **53**, 853-865.

23. P. N. Hazin, J. C. Huffman and J. W. Bruno, *Organometallics*, 1987, **6**, 23-27.

24. D. G. Karraker, *Inorg. Chim. Acta*, 1987, **139**, 189-191.

25. M. Schlosser and J. Hartmann, *Angew. Chem. Int. Ed.*, 1973, **12**, 508-509.

26. L. H. Gade, C. Becker and J. W. Lauher, *Inorg. Chem.*, 1993, **32**, 2308-2314.

www.manaraa.com

CHAPTER 3. RARE EARTH ARYLSILAZIDO COMPOUNDS WITH INEQUIVALENT SECONDARY INTERACTIONS

Kasuni C. Boteju,[a] Suchen Wan,[b] Amrit Venkatesh,[a] Arkady Ellern,[c] Aaron J. Rossini[a], Aaron D. Sadow* [a]

[a] US Department of Energy Ames Laboratory and Department of Chemistry, Iowa State University, Ames IA, 50011, USA, [b] College of Chemistry, Beijing Normal University, No. 19, XinJieKouWai St., HaiDian District, Beijing 100875, P. R. China, [c] Department of Chemistry, Iowa State University, Ames IA, 50011, USA

Modified from a manuscript published in Chemical Communications, 2018

Abstract

A new bulky silazido ligand, –N(SiHMe$_2$)Dipp (Dipp = C$_6$H$_3$-2,6-*i*Pr$_2$) supports planar, three-coordinate homoleptic rare earth complexes Ln{N(SiHMe$_2$)Dipp}$_3$ (Ln = Sc, Y, Lu) that each contain three secondary Ln←HSi interactions and one agostic CH bond. Y{N(SiHMe$_2$)Dipp}$_3$ and acetophenone react via hydrosilylation, rather than insertion into the Y–N bond or enolate formation.

Introduction

The hexamethyl disilazido group's use as a ligand in homoleptic and heteroleptic complexes, which find myriad synthetic applications, spans the periodic table.[1] This ligand is particularly useful in early metal and lanthanide chemistry because its steric properties lead to monomeric, reactive species. Interestingly, solid-state structures of trivalent lanthanide compounds Ln{N(SiMe$_3$)$_2$}$_3$ are pyramidalized ($\sum_{NLnN}$ = 339–353°),[2] whereas smaller M{N(SiMe$_3$)$_2$}$_3$ (M = Ti, V, Cr, Fe, Al, Ga, In) are planar.[3] The scandium compound Sc{N(SiMe$_3$)$_2$}$_3$ is planar in the gas-phase[4] but pyramidal in the solid state. These compounds, as

www.manaraa.com

well as those supported by the less hindered tetramethyldisilazido, contain secondary interactions of the type Ln←RSi (R = Me, H) with groups beta to the metal center;[5, 6, 7] however, these interactions are not sufficient to prevent additional solvent coordination or dimerization in homoleptic tetramethyldisilazido rare earth compounds.[5, 8] Indirect, but compelling, evidence for the existence of Ln←HSi interactions is provided by distorted ligand conformations in X-ray diffraction studies, reduced one-bond coupling constants ($^1J_{SiH}$) in NMR spectra, or low energy Si-H stretching modes (ν_{SiH}) in infrared spectra.[5, 6] Bulkier disilazido ligands N(Si*t*BuMe$_2$)SiMe$_3$ or N(Si*t*BuMe$_2$)$_2$ form planar homoleptic lanthanide compounds.[9]

The bulky silazido ligand N(SiMe$_3$)Dipp (Dipp = 2,6-diisopropylphenyl) supports homoleptic divalent first row metal centers[10] and heteroleptic rare earth species, such as LuCl{N(SiMe$_3$)Dipp}$_2$THF.[11] Less bulky aryl substitution also gives THF-coordinated or "ate"-type rare earth compounds, including Ln{N(SiMe$_3$)Ph}$_3$THF (Ln = Y, Lu),[11] and [YCl{N(SiMe$_3$)2,6-C$_6$H$_3$Et$_2$}$_3$][Li(THF)$_4$].[12] Alternatively, a combination of the large *t*Bu and the small, β-SiH-containing SiHMe$_2$ substituents in a silazido provides homoleptic Ln{N(SiHMe$_2$)*t*Bu}$_3$ (Ln = Sc, Y, Lu, Er).[13, 14] Ln{N(SiHMe$_2$)*t*Bu}$_3$ form pyramidal structures akin to Ln{N(SiMe$_3$)$_2$}$_3$, contain three bridging Ln←HSi in a C_3-symmetric structure, and will coordinate THF or Et$_2$O. The SiH group in N(SiHMe$_2$)*t*Bu is reactive. For example, Cp$_2$Zr{N(SiHMe$_2$)*t*Bu}X compounds react by H abstraction of the silicon hydride.[15] The combination of an even larger substituent than *t*Bu with the small SiHMe$_2$ could result in further SiH bond activation by pushing the smaller group closer to the metal center. To explore this idea, we constructed N(SiHMe$_2$)Dipp as a sterically off-balanced ligand.

www.manaraa.com

Results and Discussion

The synthesis of HN(SiHMe$_2$)Dipp is modified from the preparation of HN(SiMe$_3$)Dipp.[16] Deprotonation of H$_2$NDipp by *n*BuLi in pentane generates LiN(H)Dipp as a white precipitate. This crude material and Me$_2$HSiCl react in diethyl ether to provide HN(SiHMe$_2$)Dipp (**1**; eqn (1)), which is isolated in good yield by distillation.

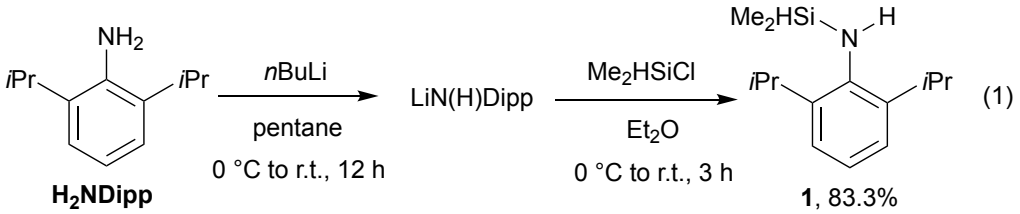

(1)

Deprotonation of **1** with *n*BuLi in pentane gives the desired lithium silazido LiN(SiHMe$_2$)Dipp (**2**; eqn (2)) as a white solid. Recrystallization from a saturated pentane solution at –30 °C provides analytically pure crystalline material. The ^{1}H NMR spectra of **1** and **2** contained resonances at 4.89 ppm ($^1J_{SiH}$ = 199 Hz) and 5.09 ppm ($^1J_{SiH}$ = 177 Hz), respectively, assigned to the SiH groups. The higher frequency chemical shift (δ_{SiH}) of **2**, with respect to silazane **1**, contrasts the lower δ_{SiH} in LiN(SiHMe$_2$)$_2$ and LiN(SiHMe$_2$)*t*Bu compared to their silazanes (Table 1). The IR spectra for **1** and **2** revealed signals at 2112 cm^{-1} and 2022 cm^{-1}, respectively, that were assigned to ν_{SiH}.

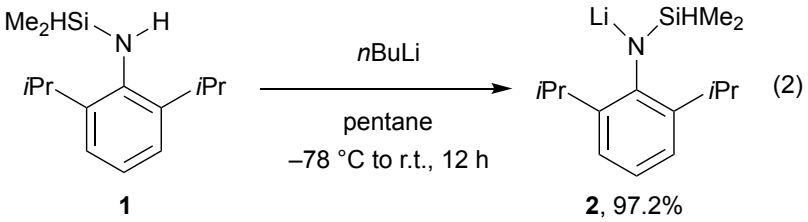

(2)

www.manaraa.com

Table 1. Room temperature ^{1}H NMR (in benzene-d_6) and IR spectroscopic properties of SiH groups in silazanes, disilazanes, lithium silazido, and rare earth silazido compounds.

Compound	δ_{SiH} (ppm)	$^1J_{SiH}$ (Hz)	ν_{SiH} (cm^{-1})
HN(SiHMe$_2$)Dipp (1)	4.89	199	2112
LiN(SiHMe$_2$)Dipp (2)	5.09	177	2022
HN(SiHMe$_2$)$_2$[a]	4.82	170	2120
LiN(SiHMe$_2$)$_2$[a]	4.49	168	1990
HN(SiHMe$_2$)*t*Bu[b]	4.82	192	2135 and 2104
LiN(SiHMe$_2$)*t*Bu[b]	4.49	168	2052
Sc{N(SiHMe$_2$)Dipp}$_3$ (3)	5.43	143	2105, 2046, 1908
Y{N(SiHMe$_2$)Dipp}$_3$ (4)	5.17	129	2107, 1934, 1883
Lu{N(SiHMe$_2$)Dipp}$_3$ (5)	5.43	128	2108, 1942, 1877

[a]See reference 5; [b]See references 14, 17.

Salt metathesis reactions of $LnCl_3THF_n$ and **2** (3 equiv.) provide the homoleptic tris(silazido) rare earth compounds Ln{N(SiHMe$_2$)Dipp}$_3$ (Ln = Sc (**3**), Y (**4**), Lu (**5**); eqn (3)).

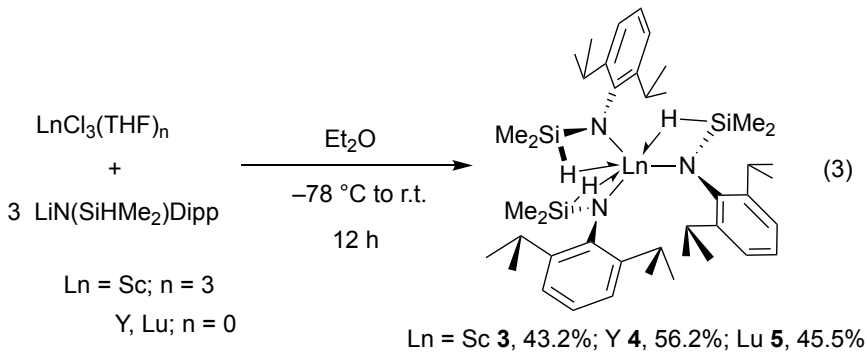

The reactions proceed in diethyl ether at low temperature, and the products are isolated as donor-free and salt-free crystalline materials after extraction and crystallization from pentane.

www.manaraa.com

Their ^{1}H NMR spectra, measured at room temperature in benzene-d_6, revealed one set of N(SiHMe$_2$)Dipp resonances. The isopropyl groups appeared as a well-resolved doublet and a septet in each spectrum of **3** – **5**, indicating that the Dipp group rapidly rotates around the N–C bond at room temperature. The SiH signal appeared as a broad singlet in **3**, but the spectra of **4** and **5** contained the expected septet splitting pattern.

The room temperature δ_{SiH} for **3** – **5** were even higher than the corresponding values in the lithium silazido starting material **2** (Table 1), and $^{1}J_{SiH}$ values were also significantly reduced (143 – 128). We noticed, however, that the $^{1}J_{SiH}$ values in **3** – **5** were larger than those in the related series Ln{N(SiHMe$_2$)*t*Bu}$_3$ (Ln = Sc, 125 Hz; Y, 124 Hz; Lu 121 Hz). The chemical shifts and coupling constants of the latter compounds' three bridging Ln⇽HSi groups are temperature independent to 200 K.[14]

In contrast to Ln{N(SiHMe$_2$)*t*Bu}$_3$, **3** – **5** are fluxional; moreover, the low temperature NMR spectra suggest a low symmetry structure with three unique N(SiHMe$_2$)Dipp ligands. For example, the ^{1}H NMR spectrum of **4** at 205 K in toluene-d_8 (Figure 1) contained δ_{SiH} at 5.41 ppm ($^{1}J_{SiH}$ = 132 Hz), 5.26 ppm ($^{1}J_{SiH}$ = 141 Hz) and 4.89 ppm ($^{1}J_{SiH}$ = 116 Hz). In addition, the Dipp signals in the ^{1}H NMR spectra indicated that their rotation slowed at low temperature. The ^{1}H NMR spectrum of **4** at 205 K in toluene-d_8 contained six well-resolved resonances from 4.17 ppm to 2.34 ppm (1 H each) and twelve, partly overlapping resonances (1.63 ppm – 0.65 ppm) assigned to the methine and methyl moieties in the three distinct Dipp groups.

A 2D ^{1}H-^{89}Y HSQC spectrum (Figure 2A), acquired at 205 K in toluene-d_8, showed correlations between the three SiH signals and the ^{89}Y NMR signal at 378.5 ppm. The cross-peaks reveal inequivalent through-bond interactions between yttrium and the three bridging SiH moieties. The intensity of the cross-peaks is directly proportional to the strength of the ^{1}H-^{89}Y *J*-

www.manaraa.com

coupling, thus the most upfield ^{1}H NMR signal with the lowest $^{1}J_{SiH}$ value most strongly couples with the yttrium center. Note that although the ^{1}H T_2 also affects HSQC peak intensity, the three SiH groups have similar T_2 values.

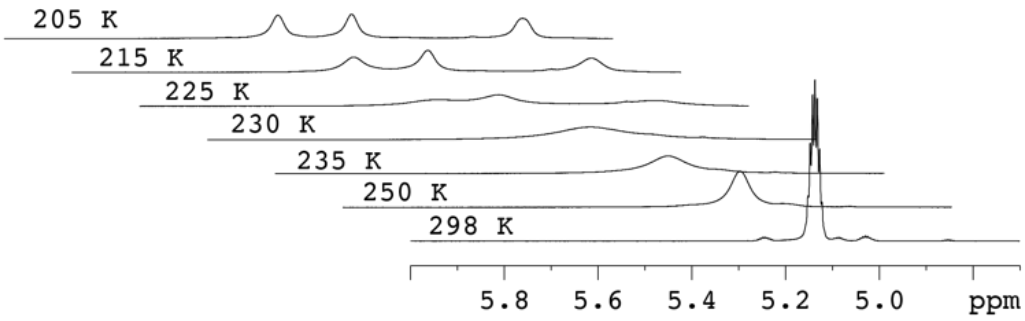

Figure 1. SiH region of ^{1}H NMR spectra of **4** acquired in toluene-d_8 from 298 to 205 K.

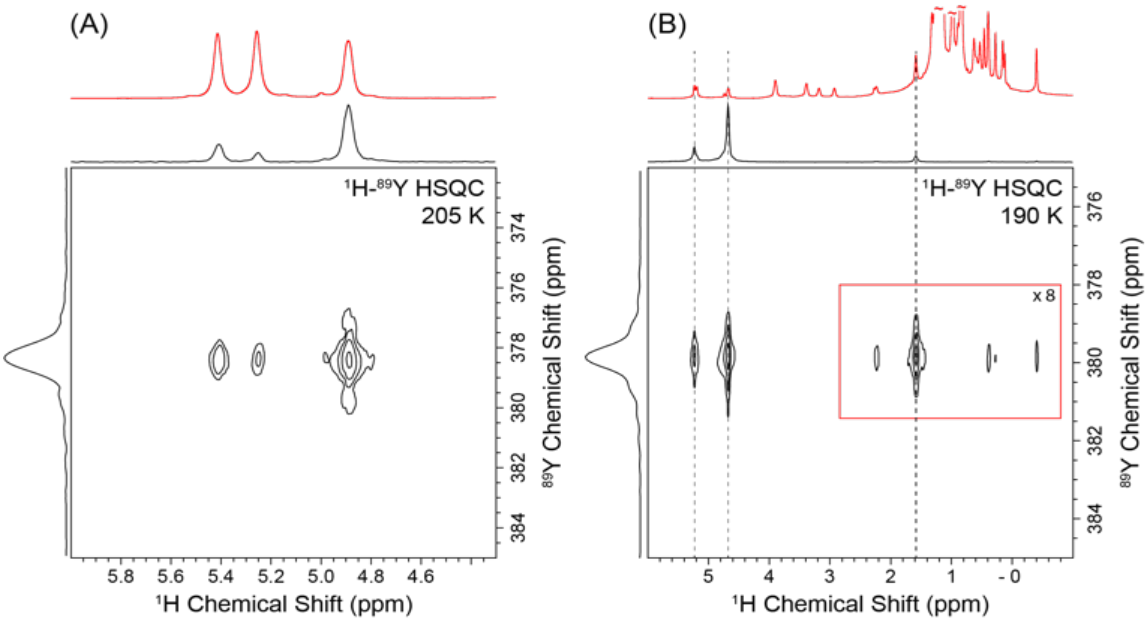

Figure 2. ^{1}H-^{89}Y HSQC NMR spectra of **4** acquired at (A) 205 K in toluene-d_8 and (B) 190 K in pentane-d_{12}. 1D ^{1}H NMR spectra (red) are overlaid above the ^{1}H projections of the 2D spectra.

The ^{29}Si NMR signal for **4** at room temperature appeared at –28.2 ppm (measured by a ^{1}H-^{29}Si HMBC experiment), and this signal split at 205 K into three cross-peaks that ranged from only

www.manaraa.com

–29.4 to –30.2 ppm. In addition, the most upfield ^{1}H NMR signal at 4.89 ppm correlated to the middle ^{29}Si NMR signal at –29.6 ppm. These data suggest that the differences in Ln←HSi between the three N(SiHMe$_2$)Dipp ligands have minimal effect on the silicon centers.

Three bands in the IR spectra of **3**, **4** and **5** in the ν_{SiH} region (KBr pellet; Table 1) indicate that the three N(SiHMe$_2$)Dipp ligands are also inequivalent in the solid state. This result is consistent with the solution phase structures measured by NMR spectroscopy at low temperature. Interestingly, the lowest frequency band in each compound is sharpest.

Recrystallization of **3** – **5** from pentane provides X-ray quality crystals. All three compounds crystallize in the same space group ($P2_1/c$) with similar unit cell parameters (a ~12 Å, b ~20 Å, c ~ 36 Å) and two independent molecules per unit cell. There are a number of interesting crystallographic features of these similarly structured molecules, including trigonal planar LnN_3 cores, low symmetry, and short Ln–H interatomic distances. First, the six molecules have similar trigonal planar LnN_3 coordination geometry (See Figure 3 and ESI), in contrast to the pyramidal geometries of Ln{N(SiMe$_3$)$_2$}$_3$[2] and Ln{N(SiHMe$_2$)*t*Bu}$_3$.[13, 14] We have recently described solid state structures of alkyl compounds containing SiHMe$_2$ moieties and aryl groups, and these also give planar LnC_3 coordination geometries.[18]

Second, the three diisopropylphenylsilazido ligands are not related by crystallographic- or pseudo-symmetry elements in Ln{N(SiHMe$_2$)Dipp}$_3$. Two of the Dipp groups are disposed syn and located on one side of the LnN_3 plane, whereas the third Dipp is on the other side of the LnN_3 plane. In contrast, Ln{N(SiHMe$_2$)*t*Bu}$_3$ and Ln{N(SiMe$_2$*t*Bu)SiMe$_3$}$_3$ form pseudo-C_3 symmetrical molecular propellers.[9, 13, 14] The inequivalence of the N(SiHMe$_2$)Dipp ligands extends to their interactions with the metal center. In **3** for example, the Sc1–N3 distance (2.124(2) Å) is significantly longer than Sc1–N1 and Sc1–N2 (2.089(2) and 2.098(2) Å). The non-classsical

www.manaraa.com

Sc←HSi interactions, as characterized by the Sc–H interatomic distances (H atoms bonded to Si are located objectively in the electron difference map and are included in the refinement) and ∠Sc-N-Si (94 – 105°), and Sc–N–Si–H torsion angles (2.6 – 9.8°) are all consistent with Sc←HSi interactions and also are all inequivalent. In particular, the Sc1–H3s distance of 2.05(2) Å is considerably shorter than the Sc1–H1s and Sc1–H2s distances (2.47(2) and 2.56(2) Å, respectively). Interestingly, the ligand with the shortest Sc–H distance is also the one with the longest Sc–N distance.

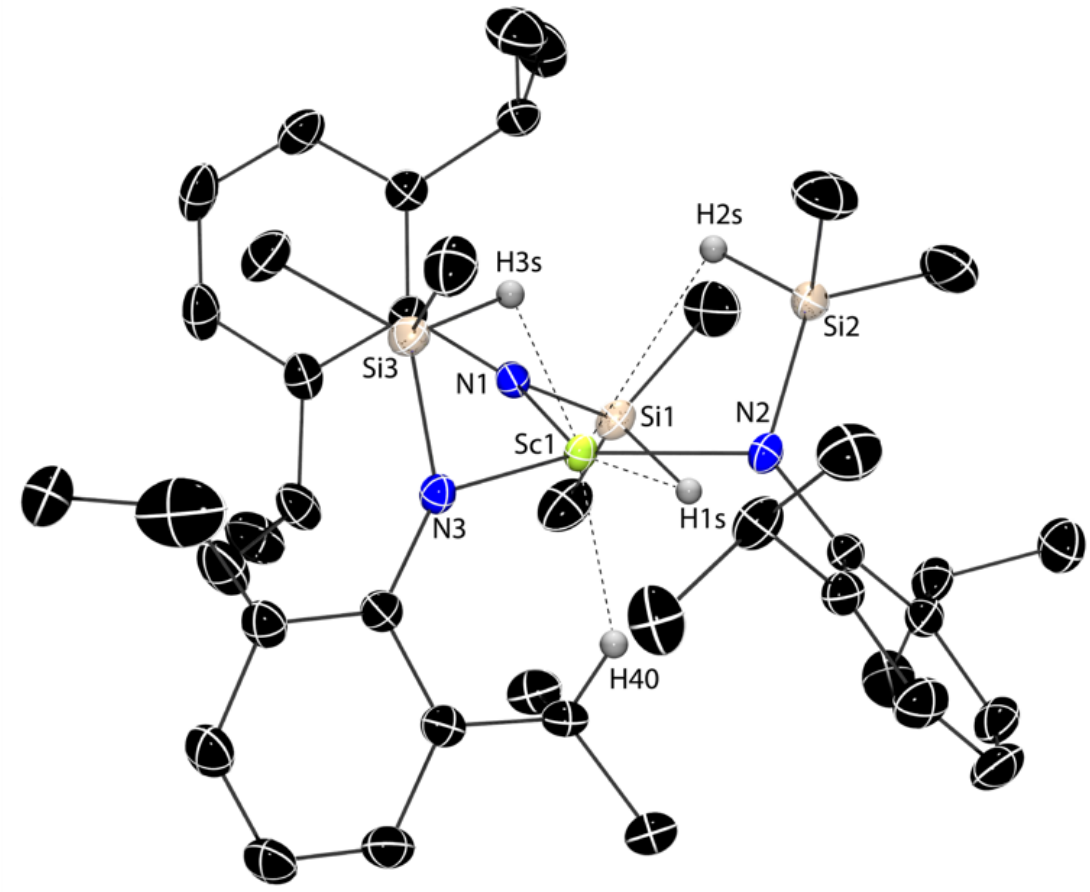

Figure 3. Rendered thermal ellipsoid plot of Sc{N(SiHMe$_2$)Dipp}$_3$ (**3**) with ellipsoids represented at 50% probability. One of two crystallographically independent molecules is illustrated (see ESI), and the H atoms included in the image are <3 Å from the Sc1 center, are located objectively and included in the refinement. Selected interatomic distances (Å): Sc1-N1, 2.089(2); Sc1-N2,

www.manaraa.com

2.098(2); Sc1-N3, 2.124(2); Sc1-H1s, 2.47(2); Sc1-H2s, 2.56(2); Sc1-H3s, 2.05(2); Sc1-H40, 2.34(3). Selected interatomic angles (°): N1–Sc1–N2, 129.55(7); N2–Sc1–N3, 115.05(7); N3–Sc1–N1, 113.32(7).

Remarkably, H40, which is bonded to the methine carbon of one of the isopropyl groups, also approaches the scandium center with a very short distance (Sc1-H40, 2.34(3) Å) and suggests an agostic Sc←HC interaction. At this point, we re-examined the ^{1}H-^{89}Y HSQC spectrum to look for additional correlations; however, at 205 K, no cross-peaks were observed. Instead, the ^{1}H-^{89}Y HSQC NMR spectrum acquired at 190 K in pentane showed weak correlations between ^{89}Y and the methine and methyl signals at 2.24 and 1.59 ppm, respectively (Figure 2B).

The reaction of **4** and one equiv. of acetophenone in benzene-d_6 instantaneously provides the product Y{N(SiMe$_2$OCHMePh)Dipp}{N(SiHMe$_2$)Dipp}$_2$ (**6**) resulting from hydrosilylation of the ketone by one of the SiH groups (eqn (4)).

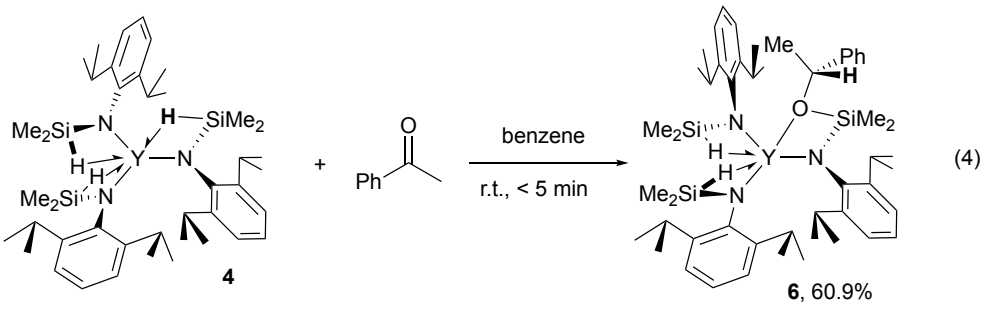

(4)

The reaction in benzene on a synthetic scale, followed by extraction with pentane and crystallization at –30 °C provides **6** as a crystalline material. The ^{1}H NMR spectrum of **6** at room temperature showed one peak at 5.33 ppm (2 H, $^{1}J_{SiH}$ = 136 Hz). This coupling constant is higher than the value observed for the starting material **4** (129 Hz). A new quartet and doublet at 5.0 and 1.42 ppm, which correlated in a COSY experiment, were assigned to the CHMe that resulted from acetophenone insertion into one of the SiH in **4**. These signals also correlated in ^{1}H-^{13}C HMQC and HMBC experiments with a ^{13}C NMR signal at 77.5 ppm assigned to the carbon bonded to

www.manaraa.com

oxygen. A ^{1}H NMR spectrum of **6** acquired at 205 K contained two resonances at 5.55 ppm ($^{1}J_{SiH}$ = 133 Hz) and 5.11 ppm ($^{1}J_{SiH}$ = 124 Hz) assigned to the SiH in inequivalent N(SiHMe$_2$)Dipp ligands. These coupling constant values indicate that two non-classical interactions Y←HSi are present in compound **6**. The IR data also showed bands at 1997 cm^{-1} and 1891 cm^{-1} assigned to two SiH moieties.

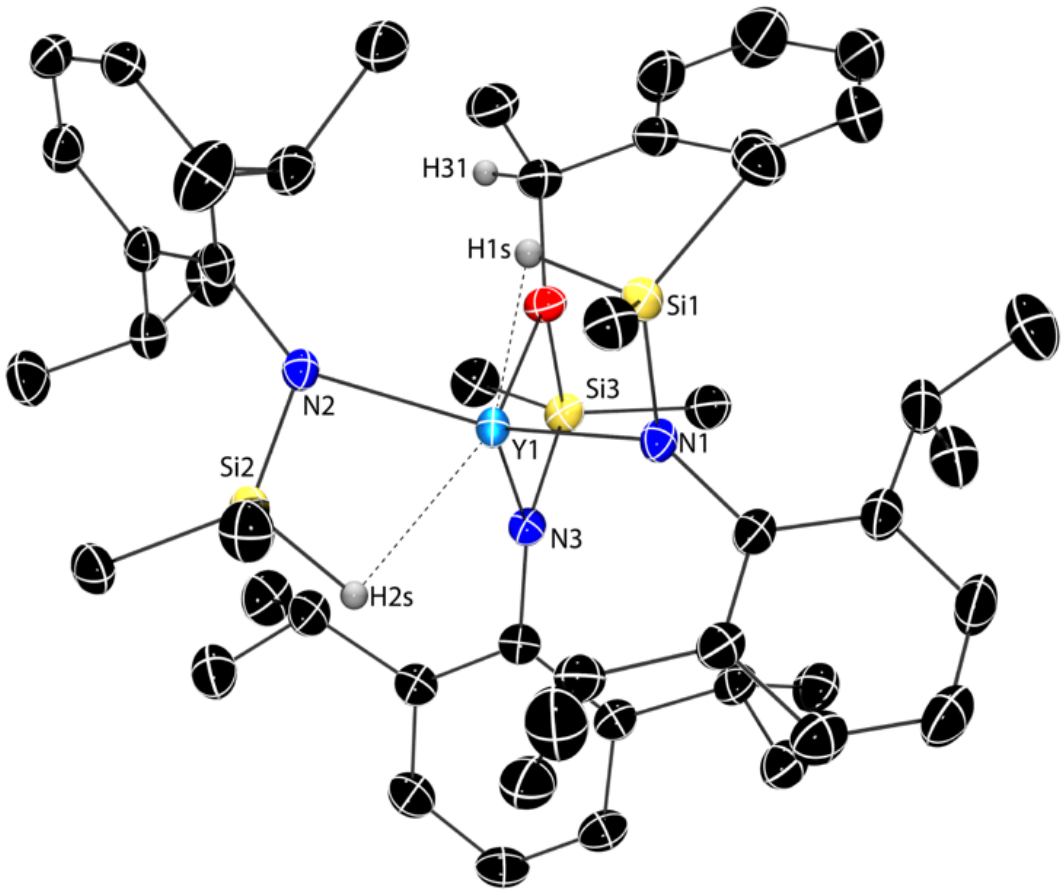

Figure 4. Thermal ellipsoid plot of Y{N(SiMe$_2$OCHMePh)Dipp}{N(SiHMe$_2$)Dipp}$_2$ (**6**). H atoms bonded to Si were located in the Fourier difference map, refined, and are included in the illustration. H31, which was placed in a calculated position, is included in the image. All other H atoms, a second crystallographically independent but structurally similar molecule of **6**, and co-crystallized pentane molecules are not shown for clarity. Selected interatomic distances (Å): Y1–N1, 2.251(2); Y1–N2, 2.293(2); Y1–N3, 2.276(2); Y1–Si1, 3.0659(9); Y1–Si2, 3.0977(9); Y1–

www.manaraa.com

Si3, 3.0799(8); Y1–H1s, 2.43(3); Y1–H2s, 2.48(3); Y1–O1, 2.319(2); Si1–H1s, 1.46(3); Si2–H2s, 1.54(3). Selected interatomic angles (°): N1–Y1–N2, 121.76(8); N2–Y1–N3, 124.52(8); N3–Y1–N1, 111.15(8).

An X-ray single crystal diffraction study on **6** confirms that acetophenone has inserted into one of the SiH groups (Figure 4). In addition, the study reveals similar features for **6** as **4**, including a planar YN_3 core and short Ln–H distances (2.43(3) and 2.48(3) Å) indicative of two Y←HSi interactions. All three Y–N distances are similar, with Y1–N3 distance (2.276 Å) of the transformed ligand falling in between the other two.

In contrast, mixtures of the silazane $HN(SiHMe_2)Dipp$ and acetophenone contain only starting materials after 1.5 d at room temperature in benzene-d_6. The observed reactivity of **4** is also distinct from the lithium silazido, which reacts with acetophenone in benzene-d_6 to provide $HN(SiHMe_2)Dipp$ and the lithium enolate. Related reactions of $[Cp_2ZrN(SiHMe_2)_2]^+$ and formaldehyde or acetone afford double addition products $[Cp_2ZrN(SiMe_2OR)_2]^+$ (R = Me, iC_3H_7).[19] In the present case, attempts to add more than one equivalent of acetophenone to **4** provided multiple, unidentified products.

Conclusion

Thus, one of three Y←HSi secondary interactions reacts inequivalently from the two others. Here, we note that the Y←HSi moiety with the lowest δ_{SiH} and smallest $^1J_{SiH}$ also shows the greatest ^1H-^{89}Y HSQC peak intensity. The latter measurement probes through-bond interactions (*J*) and it is tempting to assign this group as the most activated and reactive toward hydrosilylation; however, the covalent contribution may be a small component to the overall

www.manaraa.com

bonding in Ln←HE interactions. In this context, we are currently studying the reactions of **3** – **5** with other electrophiles, including more hindered ketones, to identify which SiH group reacts.

Experimental

General. All manipulations were performed under a dry argon atmosphere using standard Schlenk techniques or under a nitrogen atmosphere in a glovebox unless otherwise indicated. Water and oxygen were removed from benzene, pentane, and ether solvents using an IT PureSolv system. Benzene-d_6 and toluene-d_8, were heated to reflux over Na/K alloy and vacuum-transferred. $ScCl_3THF_3$ was prepared by reaction of Sc_2O_3 with conc. HCl followed by dehydration with $SOCl_2$ according to the literature.[20, 21, 22] YCl_3 and $LuCl_3$ were purchased from Strem Chemicals and used as received. Diisopropylaniline and Dimethylchlorosilane were purchased from Sigma-Aldrich and Gelest respectively and distilled, and *n*BuLi was purchased from Sigma-Aldrich and used as received. ^{1}H, $^{13}C\{^{1}H\}$, and $^{29}Si\{^{1}H\}$ HMBC NMR spectra were collected on a Bruker DRX-400 spectrometer or a Bruker Avance III-600 spectrometer. Infrared spectra were measured on a Bruker Vertex 80, using KBr pellet (transmission mode). Elemental analyses were performed using a Perkin-Elmer 2400 Series II CHN/S. X-ray diffraction data was collected on a Bruker APEX II diffractometer.

HN(SiHMe$_2$)Dipp (1). *n*BuLi (21.2 mL, 0.0530 mol) was added dropwise to a solution of H_2NDipp (10.0 mL, 0.0530 mol) in pentane (300 mL) cooled to 0 °C. A white precipitate was observed immediately. The reaction mixture was warmed to room temperature and stirred overnight. The white precipitate was isolated by filtration, and then it was dissolved in ether (500 mL). The solution was cooled to 0 °C and $ClSiHMe_2$ (5.89 mL, 0.0530 mol) was added slowly to the solution. The reaction was warmed to room temperature and stirred for 3 h. The solution was

www.manaraa.com

filtered, and the filtrate was evaporated under vacuum to remove the volatile materials. The resulting yellowish solution distilled under dynamic vacuum at 104 °C to obtain the desired dimethylsilazane as a colorless product (9.88 g, 0.0420 mol, 83.3%). ^{1}H NMR (benzene-d_6, 600 MHz, 25 °C): δ 7.12 – 7.08 (3 H, *m*-C_6H_5 and *p*-C_6H_5 overlap), 4.89 (virtual octet, 1 H, $^{1}J_{SiH}$ = 199.2 Hz, Si*H*Me$_2$), 3.44 (septet, 2 H, $^{3}J_{HH}$ = 6.9 Hz, C*H*Me$_2$), 2.19 (s, 1 H, N*H*), 1.21 (d, 12 H, $^{3}J_{HH}$ = 6.9 Hz, CH*Me$_2$*), 0.09 (d, 6 H, $^{3}J_{HH}$ = 3.0 Hz, SiH*Me$_2$*). ^{13}C{^{1}H} NMR (benzene-d_6, 150 MHz, 25 °C): δ 144.15 (*o*-C_6H_5), 139.74 (*ipso*-C_6H_5), 124.48 (*p*-C_6H_5), 123.87 (*m*-C_6H_5), 28.88 (*C*HMe$_2$), 24.27 (CH*Me$_2$*), –1.14 (SiH*Me$_2$*). ^{15}N {^{1}H} NMR (benzene-d_6, 60.8 MHz, 25 °C): δ –343.6. ^{29}Si{^{1}H} NMR (benzene-d_6, 119.3 MHz, 25 °C): *δ* –9.9. IR (KBr, cm^{-1}): 3392 w (NH), 3066 w, 2963 s, 2870 m, 2112 m (SiH), 1462 m, 1441 m, 1326 m, 1253 s, 1196 w, 1108 w, 1056 w, 1044 w, 912 s, 831 m, 789 m, 747 m, 665 w.

LiN(SiHMe$_2$)Dipp (**2**). A solution of HN(SiHMe$_2$)Dipp (2.51 g, 0.0107 mol) in pentane (40 mL total volume) was cooled to –78 °C. *n*BuLi (4.26 mL, 0.0107 mol) was added to the solution, which was then stirred for 20 min at –78 °C. The reaction mixture became milky white, and then it was warmed to room temperature and stirred overnight. The solvent was evaporated for 2 h to directly provide the product as a white, highly air-sensitive solid (2.48 g, 0.0103 mol, 97.2%). ^{1}H NMR (benzene-d_6, 600 MHz, 25 °C): δ 7.03 (d, 2 H, $^{3}J_{HH}$ = 7.6 Hz, *m*-C_6H_5) 6.90 (t, 1 H, $^{3}J_{HH}$ = 7.6 Hz, *p*-C_6H_5), 5.09 (br m, 1 H, $^{1}J_{SiH}$ = 177 Hz, Si*H*Me$_2$), 3.54 (septet, 2 H, $^{3}J_{HH}$ = 6.7 Hz, C*H*Me$_2$), 1.13 (br d, 12 H, $^{3}J_{HH}$ = ~6 Hz, CH*Me$_2$*), 0.07 (d, 6 H, $^{3}J_{HH}$ = 2.7 Hz, SiH*Me$_2$*). ^{13}C{^{1}H} NMR (benzene-d_6, 150 MHz, 25 °C): δ 149.09 (*ipso*-C_6H_5), 142.71 (*o*-C_6H_5), 124.97 (*m*-C_6H_5), 120.67 (*p*-C_6H_5), 27.66 (*C*HMe$_2$), 25.28 (CH*Me$_2$*), 0.79 (SiH*Me$_2$*). ^{29}Si{^{1}H} NMR (benzene-d_6, 119.3 MHz, 25 °C): δ –20.21 (*Si*HMe$_2$). ^{7}Li{^{1}H} NMR (benzene-d_6, MHz, 25 °C): *δ*

www.manaraa.com

0.99 (*Li*N). IR (KBr, cm^{-1}, small amounts of silazane are formed during measurement): 3390 w (silazane NH), 3050 w, 2961 s, 2868 m, 2108 w (silazane SiH), 2022 s (SiH), 1663 w, 1588 w, 1460 s, 1422 s, 1384 w, 1364 w, 1313 s, 1249 s, 1194 s, 1105 m, 1041 m, 936 s, 905 s, 821 m, 782 s, 751 s, 664 w 640 w. Anal. Calcd for $C_{14}H_{24}LiNSi$: C, 69.66; H, 10.02; N, 5.80. Found: C, 69.67; H, 10.21; N, 5.71. mp 139 - 141 °C.

Sc{N(SiHMe$_2$)Dipp}$_3$ (3). A solid mixture of $ScCl_3(THF)_3$ (0.100 g, 0.272 mmol) and LiN(SiHMe$_2$)Dipp (0.197 g, 0.816 mmol) was cooled to –78 °C for 30 min. Ether (7 mL) was cooled to –78 °C for 30 min in a separate vial. The solvent was added to the solid mixture and stirred at –78 °C for 1 h. The reaction vial was warmed to room temperature and stirred overnight. Ether was evaporated under vacuum and the remaining white solid was extracted with pentane (3 X 5 mL). The pentane extracts were combined and pumped down to obtain a sticky solid. The mentioned solid was extracted with pentane, concentrated and kept at –30 °C for 36 h. The pentane was decanted and the vial was dried under vacuum to obtain the desired product as a white crystalline solid (0.0879 g, 0.117 mmol, 43.2%). ^{1}H NMR (benzene-d_6, 600 MHz, 25 °C): δ 7.05 (d, 6 H, $^3J_{HH}$ = 7.6 Hz, *m*-C_6H_5) 6.96 (t, 3 H, $^3J_{HH}$ = 7.5 Hz, *p*-C_6H_5), 5.43 (br s, 3 H, $^1J_{SiH}$ = 142.6 Hz, Si*H*Me$_2$), 3.38 (septet, 6 H, $^3J_{HH}$ = 4.9 Hz, C*H*Me$_2$), 1.18 (d, 36 H, $^3J_{HH}$ = 6.6 Hz, CH*Me$_2$*), 0.27 (broad, 18 H, SiH*Me$_2$*). ^{13}C{^{1}H} NMR (benzene-d_6, 150 MHz, 25 °C): δ 148.81 (*ipso*-C_6H_5), 141.03 (*o*-C_6H_5), 124.64 (*m*-C_6H_5), 122.09 (*p*-C_6H_5), 29.22 (*C*HMe$_2$), 25.28 (CH*Me$_2$*), 1.77 (SiH*Me$_2$*). ^{15}N {^{1}H} NMR (benzene-d_6, 60.8 MHz, 25 °C): δ –221.0. ^{29}Si{^{1}H} NMR (benzene-d_6, 119.3 MHz, 25 °C): δ –28.08. IR (KBr, cm^{-1}): 3061 m, 3046 m, 2963 s, 2865 m, 2105 m (SiH), 2046 m (SiH), 1908 s (SiH), 1587 m, 1457 s, 1427 s, 1360 m, 1326 m, 1309 s, 1251 s, 1194 s, 1118 m, 1047 m, 1001 m, 950 s, 903 s, 878 s, 834 s, 812 s, 782 s, 760 s, 683 m, 670 m, 635 m.

www.manaraa.com

Anal. Calcd for $C_{42}H_{72}ScN_3Si_3$: C, 67.42; H, 9.70; N, 5.62. Found: C, 66.93; H, 9.54; N, 5.43. mp 186 - 188 °C.

Y{N(SiHMe$_2$)Dipp}$_3$ (4). A solid mixture of YCl_3 (0.0836 g, 0.428 mmol) and LiN(SiHMe$_2$)Dipp (0.310 g, 1.28 mmol) was cooled to –78 °C for 30 min. Ether (7 mL) was cooled to –78 °C for 30 min in a separate vial. The solvent was added to the solid mixture and stirred at –78 °C for 1 h. The reaction vial was warmed to room temperature and stirred overnight. Ether was evaporated under vacuum and the remaining white solid was extracted with pentane (3 X 5 mL). The pentane extracts were combined and pumped down to obtain a sticky solid. The mentioned solid was extracted with pentane, concentrated and kept at –30 °C for 36 h. The pentane was decanted and the vial was dried under vacuum to obtain the desired product as a white crystalline solid (0.190 g, 0.240 mmol, 56.2%). ^{1}H NMR (benzene-d_6, 600 MHz, 25 °C): δ 7.04 (d, 6 H, $^3J_{HH}$ = 7.7 Hz, *m*-C_6H_5) 6.93 (t, 3 H, $^3J_{HH}$ = 7.6 Hz, *p*-C_6H_5), 5.17 (br pentet, 3 H, $^1J_{SiH}$ = 129.2 Hz, Si*H*Me$_2$), 3.42 (septet, 6 H, $^3J_{HH}$ = 6.5 Hz, C*H*Me$_2$), 1.16 (d, 36 H, $^3J_{HH}$ = 6.8 Hz, CH*Me$_2$*), 0.33 (d, 18 H, $^3J_{HH}$ = 2.7 Hz, SiH*Me$_2$*). ^{1}H NMR (toluene-d_8, 600 MHz, –68.15 °C): δ 7.26 – 6.76 (9 H, aromatic region), 5.42 (br s, 1 H, $^1J_{SiH}$ = 131.9 Hz, Si*H*Me$_2$), 5.26 (br s, 1 H, $^1J_{SiH}$ = 140.7 Hz, Si*H*Me$_2$), 4.89 (br s, 1 H, $^1J_{SiH}$ = 115.8 Hz, Si*H*Me$_2$), 4.18 (br s, 1 H, C*H*Me$_2$), 4.06 (br s, 1 H, C*H*Me$_2$), 3.59 (br s, 1 H, C*H*Me$_2$), 3.30 (br s, 1 H, C*H*Me$_2$), 3.00 (br s, 1 H, C*H*Me$_2$), 2.34 (br s, 1 H, C*H*Me$_2$), 1.63 (br s, 3 H, CH*Me$_2$*), 1.46 (br s, 3 H, CH*Me$_2$*), 1.43 (br s, 3 H, CH*Me$_2$*), 1.40 (br s, 3 H, CH*Me$_2$*), 1.21 (br s, 3 H, CH*Me$_2$*), 1.18 (br s, 3 H, CH*Me$_2$*), 1.11 (br s, 9 H, CH*Me$_2$*), 0.84 (br s, 3 H, CH*Me$_2$*), 0.77 (br s, 3 H, CH*Me$_2$*), 0.66 (br s, 3 H, CH*Me$_2$*), 0.57 (br s, 3 H, SiH*Me$_2$*), 0.54 (br s, 3 H, SiH*Me$_2$*), 0.42 (br s, 3 H, SiH*Me$_2$*), 0.37 (br s, 3 H, SiH*Me$_2$*), 0.22 (br s, 3 H, SiH*Me$_2$*), –0.06 (br s, 3 H, SiH*Me$_2$*). ^{13}C{^{1}H} NMR (benzene-d_6, 150 MHz, 25 °C): δ 147.82 (*ipso*-

www.manaraa.com

C_6H_5), 140.75 (*o*-C_6H_5), 124.45 (*m*-C_6H_5), 121.14 (*p*-C_6H_5), 28.93 (*C*HMe$_2$), 25.16 (CH*Me$_2$*), 1.96 (SiH*Me$_2$*). ^{15}N {^{1}H} NMR (benzene-d_6, 60.8 MHz, 25 °C): δ –239.61. ^{29}Si{^{1}H} NMR (benzene-d_6, 119.3 MHz, 25 °C): δ –28.18. IR (KBr, cm^{-1}): 3062 m, 3045 m, 2962 s, 2865 m, 2107 w (SiH), 1934 s (SiH), 1883 s (SiH), 1588 m, 1458 m, 1383 s, 1359 m, 1327 m, 1296 s, 1250 s, 1177 s, 1143 s, 1116 s, 1044 s, 1017 s, 951 s, 873 s, 833 s, 779 s, 758 s, 672 m, 626 m. Anal. Calcd for $C_{42}H_{72}YN_3Si_3$: C, 63.68; H, 9.16; N, 5.30. Found: C, 63.55; H, 9.55; N, 5.20. mp 193 - 195 °C.

Lu{N(SiHMe$_2$)Dipp}$_3$ (5). A solid mixture of $LuCl_3$ (0.235 g, 0.834 mmol) and LiN(SiHMe$_2$)Dipp (0.604 g, 2.50 mmol) was cooled to –78 °C for 30 min. Ether (7 mL) was cooled to –78 °C for 30 min in a separate vial. The solvent was added to the solid mixture and stirred at –78 °C for 1 h. The reaction vial was warmed to room temperature and stirred overnight. Ether was evaporated under vacuum and the remaining white solid was extracted with pentane (3 X 5 mL). The pentane extracts were combined and pumped down to obtain a sticky solid. The mentioned solid was extracted with pentane, concentrated and kept at –30 °C for 36 h. The pentane was decanted and the vial was dried under vacuum to obtain the desired product as a white crystalline solid (0.334 g, 0.380 mmol, 45.5%). ^{1}H NMR (benzene-d_6, 600 MHz, 25 °C): δ 7.04 (d, 6 H, $^3J_{HH}$ = 7.5 Hz, *m*-C_6H_5) 6.92 (t, 3 H, $^3J_{HH}$ = 7.6 Hz, *m*-C_6H_5), 5.43 (br t, 3 H, $^1J_{SiH}$ = 127.6 Hz, Si*H*Me$_2$), 3.46 (septet, 6 H, $^3J_{HH}$ = 5.2 Hz, C*H*Me$_2$), 1.17 (d, 36 H, $^3J_{HH}$ = 6.7 Hz, CH*Me$_2$*), 0.35 (d, 18 H, $^3J_{HH}$ = 1.7 Hz, SiH*Me$_2$*). ^{1}H NMR (toluene-d_8, 600 MHz, –68.15 °C): δ 7.26 – 6.75 (9 H, aromatic region), 5.59 (br s, 1 H, $^1J_{SiH}$ = 132.1 Hz, Si*H*Me$_2$), 5.35 (br s, 2 H, $^1J_{SiH}$ = 151.5 Hz, Si*H*Me$_2$), 4.18 (br s, 1 H, C*H*Me$_2$), 4.07 (br s, 1 H, C*H*Me$_2$), 3.64 (br s, 1 H, C*H*Me$_2$), 3.31 (br s, 1 H, C*H*Me$_2$), 2.96 (br s, 1 H, C*H*Me$_2$), 2.51 (br s, 1 H, C*H*Me$_2$), 1.60 (br s, 3 H, CH*Me$_2$*), 1.45 (br s, 3 H, CH*Me$_2$*), 1.42 (br s, 3 H, CH*Me$_2$*), 1.40 (br s, 3 H, CH*Me$_2$*), 1.21 (br s, 6 H, CH*Me$_2$*), 1.17 (br

www.manaraa.com

s, 3 H, CH*Me*$_2$), 1.11 (br s, 6 H, CH*Me*$_2$), 0.80 (br s, 3 H, CH*Me*$_2$), 0.76 (br s, 3 H, CH*Me*$_2$), 0.69 (br s, 3 H, CH*Me*$_2$), 0.59 (br s, 3 H, SiH*Me*$_2$), 0.55 (br s, 3 H, SiH*Me*$_2$), 0.48 (br s, 3 H, SiH*Me*$_2$), 0.39 (br s, 3 H, SiH*Me*$_2$), 0.24 (br s, 3 H, SiH*Me*$_2$), –0.08 (br s, 3 H, SiH*Me*$_2$). ^{13}C{^{1}H} NMR (benzene-d_6, 150 MHz, 25 °C): δ 148.17 (*ipso*-C_6H_5), 141.23 (*o*-C_6H_5), 124.46 (*m*-C_6H_5), 121.28 (*p*-C_6H_5), 28.89 (*C*HMe$_2$), 25.11 (CH*Me*$_2$), 1.84 (SiH*Me*$_2$). ^{15}N {^{1}H} NMR (benzene-d_6, 60.8 MHz, 25 °C): δ –241.64. ^{29}Si{^{1}H} NMR (benzene-d_6, 119.3 MHz, 25 °C): δ –27.62. IR (KBr, cm^{-1}): 3062 m, 3045 m, 2962 s, 2864 s, 2108 w (SiH), 1942 s (SiH), 1877 s (SiH), 1587 m, 1457 s, 1428 s, 1383 m, 1360 m, 1311 s, 1250 s, 1199 s, 1105 m, 1046 s, 951 s, 874 s, 833 s, 780 s, 758 s, 671 m, 628 m. Anal. Calcd for $C_{42}H_{72}LuN_3Si_3$: C, 57.44; H, 8.26; N, 4.78. Found: C, 57.41; H, 8.28; N, 4.72. mp 189 - 191 °C.

Y{N(SiMe$_2$OCHMePh)Dipp}{N(SiHMe$_2$)Dipp}$_2$ (6). Y{N(SiHMe$_2$)Dipp} (0.101 g, 0.127 mmol) was dissolved in benzene (3 mL), and acetophenone (14.9 μL, 0.127 mmol) was added to the solution. The reaction mixture was stirred for 15 min., and the solvent was evaporated under vacuum. The resulting oily residue was extracted with pentane (3 × 5 mL), concentrated, and cooled to –30 °C to provide the desired product as a white crystalline solid (0.0761 g, 0.0774 mmol, 60.9%). ^{1}H NMR (benzene-d_6, 600 MHz, 25 °C): δ 7.17 – 6.96 (14 H, aromatic region), 5.33 (br s, 2 H, $^1J_{SiH}$ = 135.5 Hz, Si*H*Me$_2$), 5.00 (q, 1 H, $^3J_{HH}$ = 6.5 Hz, OC*H*MePh), 3.79 (br vt, 4 H, $^3J_{HH}$ = 5.2 Hz, C*H*Me$_2$), 3.66 (v pentet, 2 H, $^3J_{HH}$ = 6.6 Hz, C*H*Me$_2$), 1.42 (d, 3 H, $^3J_{HH}$ = 6.4 Hz, OCH*Me*Ph), 1.32 (d, 12 H, $^3J_{HH}$ = 6.0 Hz, CH*Me*$_2$), 1.26 (br, 12 H, CH*Me*$_2$), 1.18 (d, 6 H, $^3J_{HH}$ = 6.4 Hz, CH*Me*$_2$), 1.02 (d, 6 H, $^3J_{HH}$ = 5.2 Hz, CH*Me*$_2$), 0.37 (br s, 12 H, SiH*Me*$_2$), 0.22 (s, 3 H, Si*Me*$_2$), –0.24 (s, 3 H, Si*Me*$_2$). ^{13}C{^{1}H} NMR (benzene-d_6, 150 MHz, 25 °C): δ 147.99, 145.01, 144.05, 142.89, 141.97, 129.36, 128.68, 127.07, 124.82, 124.28, 122.22, 122.16 (aromatic region),

www.manaraa.com

77.46 (OCHMePh), 28.01(*C*HMe$_2$), 27.80 (*C*HMe$_2$), 26.80 (CH*Me*$_2$), 26.57 (OCH*Me*Ph), 26.10 (CH*Me*$_2$), 25.55 (CH*Me*$_2$), 4.08 (Si*Me*$_2$), 2.57 (SiH*Me*$_2$), 2.35 (Si*Me*$_2$). ^{29}Si{^{1}H} NMR (benzene-d_6, 119.3 MHz, 40 °C): δ –23.4 (*Si*HMe$_2$), 3.94 (*Si*Me$_2$). IR (KBr, cm^{-1}): 3388 w, 3052 m, 2962 s, 2869 s, 2110 w (SiH, from hydrolysis), 1997 w (SiH), 1891 m (SiH), 1588 w, 1459 s, 1426 s, 1382 m, 1361 w, 1309 s, 1245 s, 1189 s, 1148 w, 1109 s, 1041 s, 918 s, 866 s, 836 s, 811 s, 779 s, 702 s, 675 w, 634 w. Anal. Calcd for $C_{55}H_{91}N_3OSi_3Y$ (with pentane): C, 67.17; H, 9.33; N, 4.27. Found: C, 67.07; H, 9.40; N, 4.17. mp 181 - 183 °C.

References

1. M. Lappert, A. Protchenko, P. Power and A. Seeber, *Metal Amide Chemistry*, John Wiley, New York, 2008.

2. R. Anwander, in *Organolanthoid Chemistry: Synthesis, Structure, Catalysis*, Springer Berlin Heidelberg, Berlin, Heidelberg, 1996, pp. 33-112.

3. P. G. Eller, D. C. Bradley, M. B. Hursthouse and D. W. Meek, *Coord. Chem. Rev.*, 1977, **24**, 1-95.

4. T. Fjeldberg and R. A. Andersen, *J. Mol. Struct.*, 1985, **128**, 49-57.

5. R. Anwander, O. Runte, J. Eppinger, G. Gerstberger, E. Herdtweck and M. Spiegler, *J. Chem. Soc. Dalton Trans.*, 1998, 847-858.

6. M. P. Conley, G. Lapadula, K. Sanders, D. Gajan, A. Lesage, I. del Rosal, L. Maron, W. W. Lukens, C. Copéret and R. A. Andersen, *J. Am. Chem. Soc.*, 2016, **138**, 3831-3843; J. Eppinger, M. Spiegler, W. Hieringer, W. A. Herrmann and R. Anwander, *J. Am. Chem. Soc.*, 2000, **122**, 3080-3096; T. D. Tilley, R. A. Andersen and A. Zalkin, *Inorg. Chem.*, 1984, **23**, 2271-2276.

7. W. A. Herrmann, R. Anwander, F. C. Munck, W. Scherer, V. Dufaud, N. W. Huber and G. R. J. Artus, *Z. Naturforsch., B: Chem. Sci.*, 1994, **49**, 1789-1797.

8. H. F. Yuen and T. J. Marks, *Organometallics*, 2009, **28**, 2423-2440.

9. C. A. P. Goodwin, K. C. Joslin, S. J. Lockyer, A. Formanuik, G. A. Morris, F. Ortu, I. J. Vitorica-Yrezabal and D. P. Mills, *Organometallics*, 2015, **34**, 2314-2325.

10. C.-Y. Lin, J.-D. Guo, J. C. Fettinger, S. Nagase, F. Grandjean, G. J. Long, N. F. Chilton and P. P. Power, *Inorg. Chem.*, 2013, **52**, 13584-13593; I. C. Cai, M. I. Lipschutz and T. D. Tilley, *Chem. Commun.*, 2014, **50**, 13062-13065.

www.manaraa.com

11. H. Schumann, J. Winterfeld, E. C. E. Rosenthal, H. Hemling and L. Esser, *Z. Anorg. Allg. Chem.*, 1995, **621**, 122-130.

12. S.-w. Wang, H.-m. Qian, W. Yao, L.-j. Zhang, S.-l. Zhou, G.-s. Yang, X.-c. Zhu, J.-x. Fan, Y.-y. Liu, G.-d. Chen and H.-b. Song, *Polyhedron*, 2008, **27**, 2757-2764.

13. W. S. J. Rees, O. Just, H. Schumann and R. Weimann, *Angew. Chem. Int. Ed. Engl.*, 1996, **35**, 419-422.

14. N. Eedugurala, Z. Wang, K. Yan, K. C. Boteju, U. Chaudhary, T. Kobayashi, A. Ellern, I. I. Slowing, M. Pruski and A. D. Sadow, *Organometallics*, 2017, **36**, 1142-1153.

15. L. J. Procopio, P. J. Carroll and D. H. Berry, *J. Am. Chem. Soc.*, 1991, **113**, 1870-1872; L. J. Procopio, P. J. Carroll and D. H. Berry, *J. Am. Chem. Soc.*, 1994, **116**, 177-185.

16. Y. W. Chao, P. A. Wexler and D. E. Wigley, *Inorg. Chem.*, 1989, **28**, 3860-3868.

17. G. H. Wiseman, D. R. Wheeler and D. Seyferth, *Organometallics*, 1986, **5**, 146-152.

18. K. C. Boteju, A. Ellern and A. D. Sadow, *Chem. Commun.*, 2017, **53**, 716-719; A. Pindwal, K. Yan, S. Patnaik, B. M. Schmidt, A. Ellern, I. I. Slowing, C. Bae and A. D. Sadow, *J. Am. Chem. Soc.*, 2017, **139**, 16862-16874.

19. K. Yan, J. J. D. Heredia, A. Ellern, M. S. Gordon and A. D. Sadow, *J. Am. Chem. Soc.*, 2013, **135**, 15225-15237.

20. Freeman, J. H.; Smith, M. L. *J. Inorg. Nucl. Chem*. 1958, **7,** 224

21. Burton, N. C.; Cloke, F. G. N.; Hitchcock, P. B.; Lemos, H. C. D.; Sameh, A. A. *J. Chem. Soc., Chem. Commun.* 1989, 1462

22. Burton, N. C. *D. Phil. Thesis*, University of Sussex, (1991)

www.manaraa.com

CHAPTER 4. SYNTHESIS AND REACTIVITY OF ARYLSILAZIDO RARE EARTH COMPOUNDS

Kasuni C. Boteju,[a] Suchen Wan,[b] Amrit Venkatesh,[a] Arkady Ellern,[c] Aaron J. Rossini[a], Aaron D. Sadow* [a]

[a] US Department of Energy Ames Laboratory and Department of Chemistry, Iowa State University, Ames IA, 50011, USA, [b] College of Chemistry, Beijing Normal University, No. 19, XinJieKouWai St., HaiDian District, Beijing 100875, P. R. China, [c] Department of Chemistry, Iowa State University, Ames IA, 50011, USA

Modified from a manuscript to be submitted to Dalton Transactions

Abstract

Three new hydridosilazido ligands, –N(SiHMe$_2$)Aryl (Aryl = Ph, 2,6-C$_6$Me$_2$H$_3$ (dmp), 2,6-C$_6$*i*Pr$_2$H$_3$ (dipp)) and their homoleptic rare earth complexes Ln{N(SiHMe$_2$)Aryl}$_3$(THF)$_n$ (Ln = Sc, Y, Lu; Aryl = Ph, n = 2; Aryl = dmp, n = 1; Aryl = dipp, n = 0) were synthesized to study the relationships between ligand steric properties, secondary Ln←H-Si bonding, and the reactivity of amide and SiH groups. In these compounds, the steric properties of the aryl group were systematically increased from phenyl to 2,6-dimethylphenyl to 2,6-diisopropyl. NMR, IR and X-ray diffraction studies of the complexes characterize the presence of secondary interactions and additional THF ligands coordinated to the rare earth centers. The complexes with the phenylsilazido ligands, Ln{N(SiHMe$_2$)Ph}$_3$(THF)$_2$, contain features associated with non-bridging 2c-2e Si–H. Characterization of Ln{N(SiHMe$_2$)dmp}$_3$THF reveals three and two Ln←H-Si interactions for yttrium and lutetium analogs respectively and one coordinated THF per complex. Ln{N(SiHMe$_2$)dipp}$_3$ is formed THF-free, and all three ligands adopt Ln←H-Si bonding modes. The reaction between Ln{N(SiHMe$_2$)dipp}$_3$ and ketones provides the hydrosilylated product via

www.manaraa.com

insertion of C=O in bridging Ln←H-Si. The ketone insertion reaction is proposed to occur through an associative mechanism.

Introduction

Homoleptic rare earth compounds often contain secondary interactions and bulky ligands, which together stabilize low-coordinate and low-electron count metal centers.[1] These features can be included in rational design of new low-coordinate electrophilic pseudo-organometallic compounds which have a range of uses in synthesis and catalysis, and for their potential derived from unique electronic and magnetic properties; however, the relative contributions of secondary interactions and sterics in stabilization of solvent-free and salt-free highly electrophilic organometallic and pseudo-organometallic compounds has not been systematically established. Moreover, the relationship between reactivity of the Ln←H-Si motif and the spectroscopic and structural features of the compounds is also not established.

A few disilazido ligands have been used to support rare earth metal centers with low coordination geometries, including hexamethyldisilazide $N(SiMe_3)_2$,[2] the smaller tetramethyldisilazide $N(SiHMe_2)_2$,[3] pentamethyl-tert-butyldisilazide $N(SiMe_3)(SiMe_2tBu)$, and the bulkiest tetramethyldi-tert-butyldisilazide $N(SiMe_2tBu)_2$.[4] The $N(SiMe_2)_3$ ligand and its rare earth compounds have been used extensively as starting materials, catalysts, and species for grafting onto surfaces.[1] These species have interesting structural features, including trigonal pyramidal geometries even though the species are typically $f^n d^0$ and secondary Ln←C–Si interactions.[1, 5] In contrast, the sterically hindered ligands give trigonal planar structures, while the smallest ligand, $N(SiHMe_2)_2$, typically provides solvent-coordinated compounds or N-bridged dimeric species.

www.manaraa.com

For example, the compounds Ln{N(SiHMe$_2$)$_2$}$_3$(THF)$_n$ (Ln = Sc (n = 1), Y (n = 1 or 2), Lu (n = 2)) are prepared by salt metathesis reactions of LiN(SiHMe$_2$)$_2$ and LnX$_3$.[6] Alternatively, the acidic HN(SiHMe$_2$)$_2$ (pKa = 22.8)[7] reacts with La{N(SiMe$_3$)$_2$}$_3$ to give THF-free, dimeric [La{N(SiHMe$_2$)$_2$}$_3$]$_2$.[8] These compounds form bridging M←H-Si secondary interactions that increase the electron count as L-type donors and ligand bond number in these otherwise coordinatively unsaturated species.[9, 10] The ^{1}H NMR spectroscopy (chemical shift, one-bond coupling constants) and IR stretching frequency of the SiH group is distinct from other functional groups (e.g. CH, SiMe$_3$), facilitating tracking of the compounds. These features are also responsive to the presence, and possibly the strength of, Ln←H–Si interactions. The disilazido ligands are relatively acidic (e.g., HN(SiMe$_3$)$_2$ pKa = 25.8)[7] from the two silyl substitutents. This electronic property, and the limited steric variation of these disilazido ligands create opportunity for other amide ligands in homoleptic compounds as synthetic precursors to catalysts and materials.

A larger number of silazido ligands of the type N(SiMe$_3$)Aryl (Aryl = Ph, 2,6-C$_6$Et$_2$H$_3$, and 2-C$_6$H$_4$OPh, and C$_6$(*i*C$_3$H$_7$)$_2$H$_3$) suggest rich, yet underexplored chemistry comes from variation of these ligands' steric and electronic features. The bulkiest ligand containing the ortho-diisopropylaryl moiety, can support the two-coordinate iron compound Fe{N(SiMe$_3$)(2,6-C$_6$H$_3$*i*Pr$_2$)}$_2$,[11, 12] while rare earth compounds such as Ln{N(SiMe$_3$)C$_6$H$_5$}$_3$THF (Ln = Y, Lu), [Y{N(SiMe$_3$)(2,6-C$_6$H$_3$Et$_2$)}$_3$Cl][Li(THF)$_4$], and Lu{N(SiMe$_3$)(2,6-C$_6$H$_3$*i*Pr$_2$)}$_2$Cl(THF) typically are solvent coordinated or form "ate" compounds.[13, 14] Donor groups included in the silazido ligand, such as in Y{N(SiMe$_3$)(2-C$_6$H$_4$OPh)}$_3$, coordinate to the exclusion of THF and LiCl.[15]

The silazido ligand N(SiHMe$_2$)*t*Bu also supports solvent-free homoleptic organolanthanides Ln{N(SiHMe$_2$)*t*Bu}$_3$ (Ln = Sc, Y, Er, Lu).[16, 17] Bonding of these lanthanide-silazidos includes secondary Ln←H–Si interactions, which are assigned by low $^1J_{Si–H}$ in ^{1}H NMR

www.manaraa.com

spectra, low frequencies ν_{SiH} (<2000 cm^{-1}) in the IR spectra, and from single crystal X-ray diffraction studies. The structures are trigonal pyramidal around the metal center. $Y\{N(SiHMe_2)tBu\}_3$ grafted on MSN performs catalytic reactivity on hydroamination of aminodialkenes. In addition, a set of solvent-coordinated homoleptic rare earth compounds of the same ligand is reported $Ln\{N(SiHMe_2)tBu\}_3L$ {(Ln = Y, Lu), (L = THF, Et_2O)}. The values of $^1J_{Si-H}$ and ν_{SiH} of $Ln\{N(SiHMe_2)tBu\}_3THF$ (Ln = Y, Lu) are higher than that of solvent-free compounds.

Exploring the reactivity of β SiHs in catalyst precursors is important to build new reaction mechanisms for catalytic conversions. Interestingly $[Cp_2Zr\{N(SiHMe_2)_2]^+$ reacts with one equivalent of 4-(dimethylamino)-pyridine (dmap) where dmap coordinated to a silicon center to give a new zirconium hydride $[Cp_2Zr\{N(SiHMe_2)(SiMe_2dmap)\}H]^+$. When $[Cp_2Zr\{N(SiHMe_2)_2]^+$ is reacted with 2 equivalents of acetone, it inserts between Si–H bond to provide the hydrosilylated product.[18]

In this paper, we have designed a new set of silazido ligands which combines a β SiH moiety and an aryl group with systematically varied steric properties by changing the substitution on ortho position. The new ligands reported here are $–N(SiHMe_2)Aryl$ (Aryl = Ph, 2,6-$C_6Me_2H_3$ (dmp), 2,6-$C_6iPr_2H_3$ (dipp)). A set of rare earth (Ln = Sc, Y, Lu) compounds of the particular ligands are synthesized as well. We try to study how the substitution on the aryl group of the ligands affect the coordination number, geometry and solvent coordination of new silazido compounds. In addition, we have explored how the β SiH is activated and reacted with ketones.

www.manaraa.com

Results

Synthesis of dimethylsilyl anilides

The reaction of aniline derivatives H_2NAryl (Aryl = Ph, dmp, dipp) with *n*BuLi, followed by the reaction with $ClSiHMe_2$ provides $HN(SiHMe_2)Aryl$ (Aryl = Ph, dmp, dipp; eq 1) based on a modification of procedures for preparation of $HN(SiMe_3)$dipp.[19] A mixture of $HN(SiHMe_2)$Ph (**1a**) and the disilylaniline $N(SiHMe_2)_2$Ph was obtained as a 10.5:1 ratio with the parent aniline. Further separation of this mixture is not necessary because its reaction with nBuLi provides pure $LiN(SiHMe_2)$Ph in the subsequent step (see below). Pure $HN(SiHMe_2)$dmp (**1b**) and $HN(SiHMe_2)$dipp **1c** are obtained after distillation without any issue. Throughout this paper, compounds of $N(SiHMe_2)$Aryl are labelled on the basis of the substitution of the aryl group by (**a**) for phenyl, (**b**) for 2,6-dimethylphenyl, and (**c**) for 2,6-diisopropylphenyl dimethylsilazido.

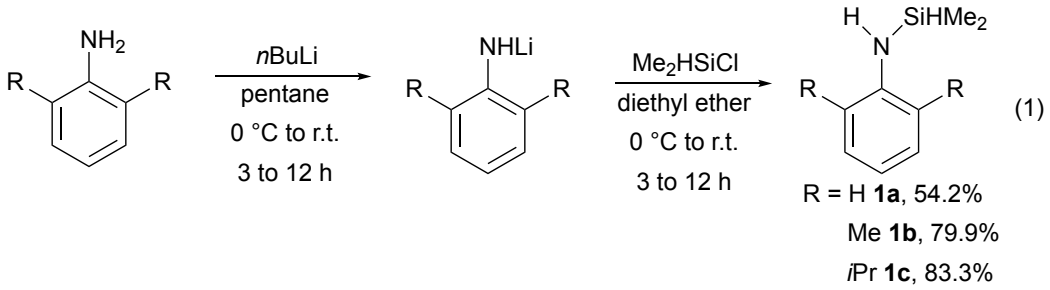

(1)

Because the NMR (chemical shift and one-bond silicon-hydrogen coupling constant) and IR (SiH stretching frequency) spectroscopic features of the SiH group are important for characterizing the bridging M←H-Si bonding described below, these data for the (nonbridging) silazane starting materials are briefly reported here. The ^{1}H NMR signals for **1a** at 4.82 ($^1J_{SiH}$ = 200.1 Hz), **1b** at 4.87 ($^1J_{SiH}$ = 201.5 Hz), and **1c** at 4.89 ppm ($^1J_{SiH}$ = 199.2 Hz) are assigned to the SiH groups on the basis of chemical shift and coupling constant, which are typical of silazanes. These coupling constants are similar to other SiH-substituted silazanes $HN(SiHMe_2)$*t*Bu ($^1J_{SiH}$ = 192 Hz)[20] and disilazane $HN(SiHMe_2)_2$ ($^1J_{SiH}$ = 170 Hz).[6] The anilines **1a**, **1b**, and **1c** contain IR

www.manaraa.com

frequencies at 2129, 2126, and 2112 cm^{-1} for Si–H stretching in each compound respectively. Interestingly $HN(SiHMe_2)tBu$ contains two IR bands at 2135 and 2104 cm^{-1} while $HN(SiHMe_2)_2$ shows one band at 2120 cm^{-1} or Si–H stretching similar to **1a**, **1b**, and **1c**.[6, 17]

The deprotonation of **1a-c** with *n*BuLi gives the desired lithium silazido compounds $LiN(SiHMe_2)$Aryl (**2a-c**; eq 2) in good yields. **2a** is purified by washing the solid product with pentane, while **2b** and **2c** are recrystallized from pentane to obtain analytically pure products.

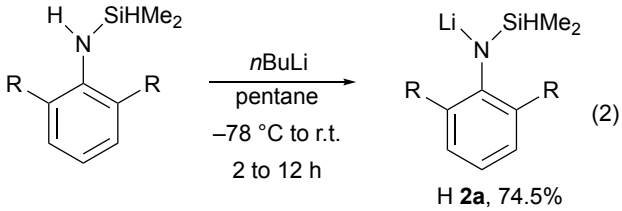

(2)

H **2a**, 74.5%
R = Me **2b**, 83.3%
*i*Pr **2c**, 97.2%

The ^1H NMR chemical shifts for the resonances assigned to the SiH moiety in **2a**, **2b**, and **2c** were 4.72 ppm ($^1J_{SiH}$ = 177 Hz), 5.10 ppm ($^1J_{SiH}$ = 165 Hz), and 5.09 ppm ($^1J_{SiH}$ = 177 Hz) ppm, respectively. Note that the signal in the phenylsilazido **2a** appeared at lower frequency than its silazane precursor, whereas the chemical shifts for **2b** and **2c** were higher than the corresponding silazanes. The latter observation is atypical. For example, deprotonation of $HN(SiHMe_2)tBu$ to form $LiN(SiHMe_2)tBu$ (δ_{SiH} = 4.49 ppm)[20] or $HN(SiHMe_2)_2$ to give $LiN(SiHMe_2)_2$ (δ_{SiH} = 4.49 ppm)[6] provides lower ^1H NMR chemical shifts than the silazanes. The coupling constants ($^1J_{SiH}$) are all smaller for the lithium silazido **2** than for the corresponding arylsilazanes **1**. The IR spectra of these compounds (KBr) contained signals at 2069 cm^{-1} (**2a**), 2056 cm^{-1} (**2b**) and 1981 cm^{-1} and 2022 cm^{-1} (**2c**) assigned to the ν_{SiH}.

Salt metathesis reactions of the rare earth chlorides and $LiN(SiHMe_2)Ph$ in THF afford the series of new $Ln\{N(SiHMe_2)Ph\}_3(THF)_2$ (Ln = Sc, **3a**; Y, **4a**; Lu, **5a**; eq 3) in moderate yields after extraction with benzene. Two THF molecules are coordinated to the rare earth center in all

www.manaraa.com

three complexes. Attempts to prepare THF-free species by reactions of THF-free lanthanide salts in benzene, toluene, or diethyl ether did not provide isolable products.

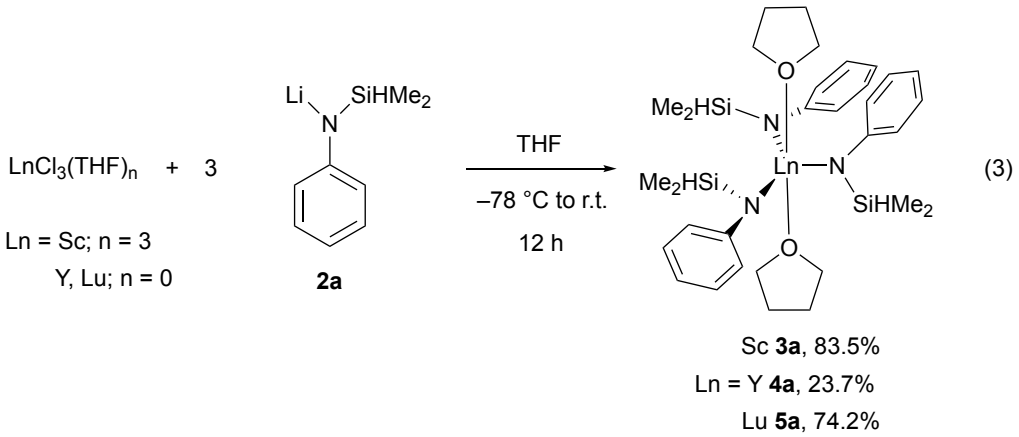

(3)

The ^{1}H NMR spectra of **3a**-**5a** revealed equivalent silazido ligands and equivalent THF ligands, present in a 3:2 ratio. The ^{1}H NMR resonances assigned to the Si–H moieties appeared at 5.24 ppm (**3a**, $^1J_{SiH}$ = 175.9 Hz), 4.95 ppm (**4a**, $^1J_{SiH}$ = 173.2 Hz), and 4.90 ppm (**5a**, $^1J_{SiH}$ = 173.6 Hz). The high $^1J_{SiH}$ values indicate that the compounds contain only classical, 2-center-2-electron (2c-2e) Si-H groups. The apparent equivalence of the silazido ligands was maintained in an ^{1}H NMR spectrum of **4a** acquired at 194 K in toluene-d_8, which contained only one Si–H resonance at 5.11 ppm. Each compound's IR spectrum (KBr) gives a result at odds with this picture of highly symmetric molecules. Two high frequency modes (>2000 cm^{-1}) were observed at 2113 and 2064 cm^{-1} for **3a**, at 2117 and 2075 cm^{-1} for **4a**, and at 2123 and 2081 cm^{-1} for **5a**.

X-ray quality crystals for all three compounds were obtained from pentane at –30 °C. Compound **3a** crystallizes as two independent molecules, and **4a** and **5a** crystallize with one molecule per unit cell. Nonetheless, the molecular structures of **3a**, **4a**, and **5a** adopt similarly distorted trigonal bipyramidal geometries with two pseudo-axial THF and three equatorial silazido ligands. For example, the ScN_3 core is planar ($\sum_{NScN}$ = 360°) and the axial THF give O1-Sc1-O2 of 170.59(8)° in **3a** (Figure 1). None of the structures contains close contacts between the

www.manaraa.com

lanthanide center and the SiH moiety (i.e., structural features typically attributed to Ln←H-Si are not observed), which is consistent with the NMR and IR spectroscopic data. All the silazido ligands are planar (e.g., sum of angles around N is 360 ± 0.1°), but their orientations are not equivalent. Two of the silazido ligands are approximately coplanar with the LnN_3 plane of the trigonal bipyramidal molecules, whereas the plane of the third ligand is orthogonal.

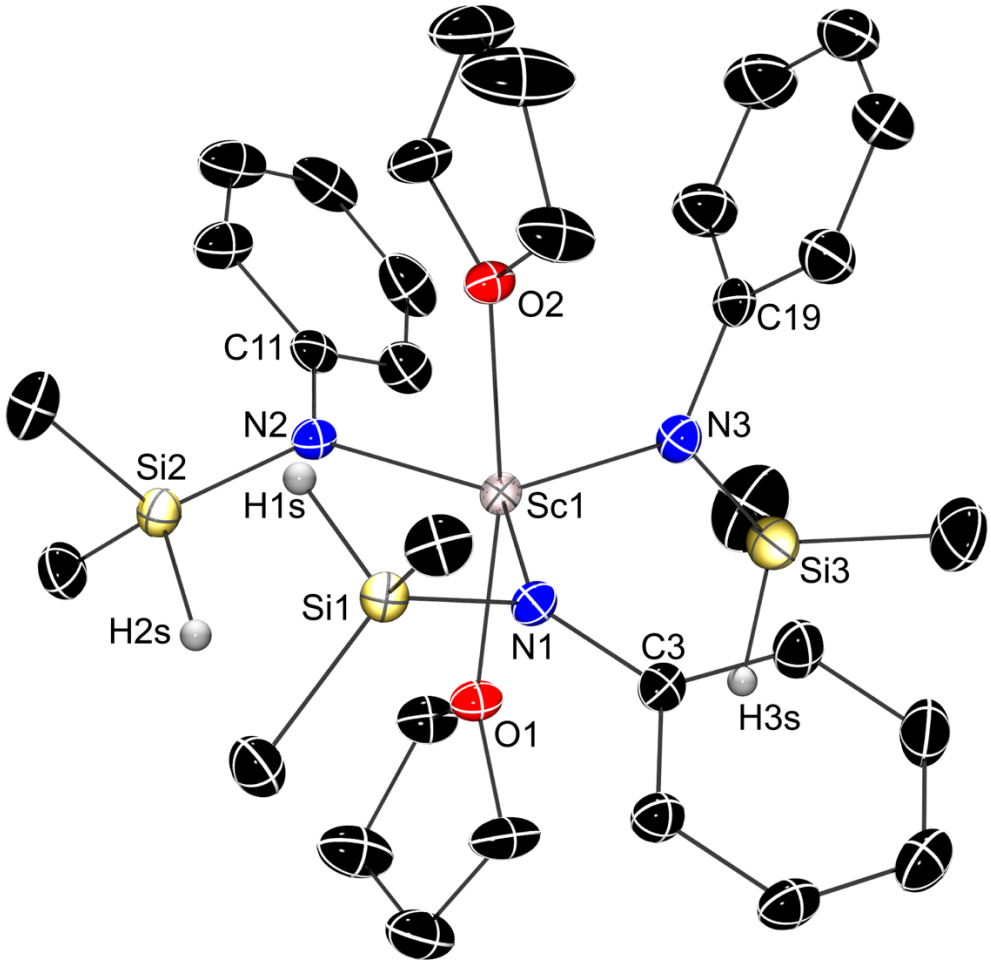

Figure 1. Thermal ellipsoid plot of $Sc\{N(SiHMe_2)Ph\}_3(THF)_2$ (**3a**). Only one of two independent molecules is included in the image. The only H atoms shown are those bonded to silicon centers, which were found objectively and refined using a riding model. Selected interatomic distances (Å): Sc1–N1, 2.142(2); Sc1–N2, 2.137(2); Sc1–N3, 2.077(2); Sc1–Si1, 3.250(1); Sc1–Si2,

www.manaraa.com

3.320(1); Sc1–Si3, 3.400(1); Sc1–H1s, 2.99(3); Sc1–H2s, 3.19(3); Sc1–H3s, 3.46(3); Si1–H1s, 1.42(3); Si2–H2s, 1.44(3); Si3–H3s, 1.44(3); Selected interatomic angles (°): N1–Sc1–N2, 129.86(9); N2–Sc1–N3, 114.86(9); N3–Sc1–N1, 115.27(9); O1–Sc1–O2, 170.59(8); Sc1–N1–Si1, 114.5(1); Sc1–N2–Si2, 118.5(1); Sc1–N3–Si3, 126.6(1).

In **3a** for example, the first two silazido planes (defined by the points at N1,Si1,C3 or N2,Si2,C11) and the scandium plane (defined by Sc1,N2,N3) intersect with angles of 13.9° or 22.9°, while the intersection with the third silazido plane (defined by N3,Si3,C19) is 81.6°. The structural parameters of N1- and N2-based silazido ligands are also distinct from those of the N3 ligand. The Sc1-N1 and Sc1-N2 distances (2.142(2) and 2.137(2) Å) are longer than the Sc1-N3 distance (2.077(2) Å) of the orthogonally-oriented ligand. The Si1-N1-C3 and Si2-N2-C11 angles (119.4(2) and 118.4(2)°, respectively) of the coplanar-oriented ligands are larger than the Si3-N3-C19 angle (112.0(2)°). These features extend to the other independent scandium molecule in the unit cell of **3a**, and yttrium **4a** and lutetium **5a** analogues.

Salt metathesis reactions of the yttrium and lutetium chloride and 3 equiv. of LiN(SiHMe$_2$)dmp (**2b**) provide Ln{N(SiHMe$_2$)dmp}$_3$THF (Ln = Y, **4b**; Lu, **5b**; eq 4) in good yields. Unfortunately, the synthesis of the scandium analogue was not successful, and instead the reaction afforded the free amine.

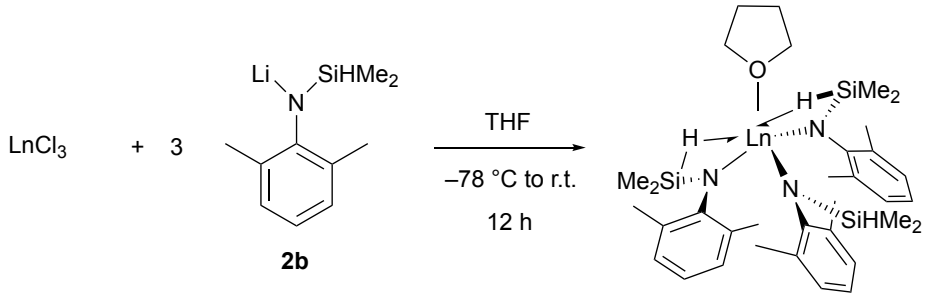

(4)

www.manaraa.com

These yttrium (**4b**) and lutetium (**5b**) compounds are only formed in THF, as was observed for phenyl-based ligands above. Integration of the ^{1}H NMR spectra of **4b** and **5b** revealed that only one molecule of THF coordinates to the metal center, likely a result of the more sterically hindered 2,6-dimethylphenyl-substituted silazido ligands compared to the phenyl substituted **3a**, **4a**, and **5a**. The ^{1}H NMR spectra suggest that **4b** and **5b** also contain three equivalent silazido ligands. The signals assigned to SiH groups in the ^{1}H NMR spectra, acquired at room temperature, showed reduced coupling constants for **4b** (5.20 ppm, $^{1}J_{SiH}$ = 151.3 Hz) and **5b** (5.20 ppm, $^{1}J_{SiH}$ = 155.8 Hz). These compounds are likely fluxional, but the exchange was not resolved in ^{1}H NMR spectra of **4b** and **5b** acquired at 191.5 K, which showed a flat region and a broad, very low intensity signal, respectively, in the region expected for the SiH resonance. Infrared spectra (KBr) contained one moderate and one weak intensity IR signals in the ν_{Si-H} region of **4b** at (2057 and 1966 cm^{-1}) and **5b** (2071 and 1902 cm^{-1}) for non-bridging and bridging interactions in solid state respectively. Together, these data suggest that the Si–H moieties form bridging interactions with the metal center, and weakly and strongly interacting SiH groups undergo fast exchange on the NMR timescale to give an averaged signal with a moderate coupling constant at room temperature.

Both **4b** and **5b** complexes form X-ray quality crystals from pentane solutions cooled at –30 °C. Although both compounds contain four-coordinate Ln{N(SiHMe$_2$)dmp}$_3$THF species, the solid-state structures have different conformations. The yttrium **4b** contains three, similarly bonded ligands, with each exhibiting a bridging Y←H–Si (Figure 2), whereas the lutetium compound contains only two Lu←H–Si (Figure 3). In particular, the Y–N interatomic distances (2.233 Å) are equivalent within error, and the N–Y–N angles and N–Y–O (110±1°) are close to those of an ideal tetrahedron. Two of the ligands (N1 and N2) have metrics associated with slightly shorter Y←H–Si than the third (N3) including Y–H distances (cf. Y1–H1s, 2.62(3); Y1–H2s,

www.manaraa.com

2.69(3) vs. Y1–H3s, 2.89(4) Å; H atoms bonded to Si were located on the difference Fourier map), Y–Si (cf. Y1–Si1, 3.1423(9); Y1–Si2, 3.1596(9) vs Y1–Si3, 3.256(1) Å) and Y–N–Si angles (Y1–N1–Si1, 104.9(1); Y1–N2–Si2, 105.6(1) vs Y1–N3–Si3, 110.9(1)Å). Despite these small differences, the three ligands are related by approximate C_3 symmetry (ignoring the conformation of the THF), with the $SiHMe_2$ groups all pointing counter-clockwise when the molecule is viewed along O1–Y1 vector. In addition, the SiH groups are also directed toward the THF ligand, while the aryl groups point away from the THF ligand.

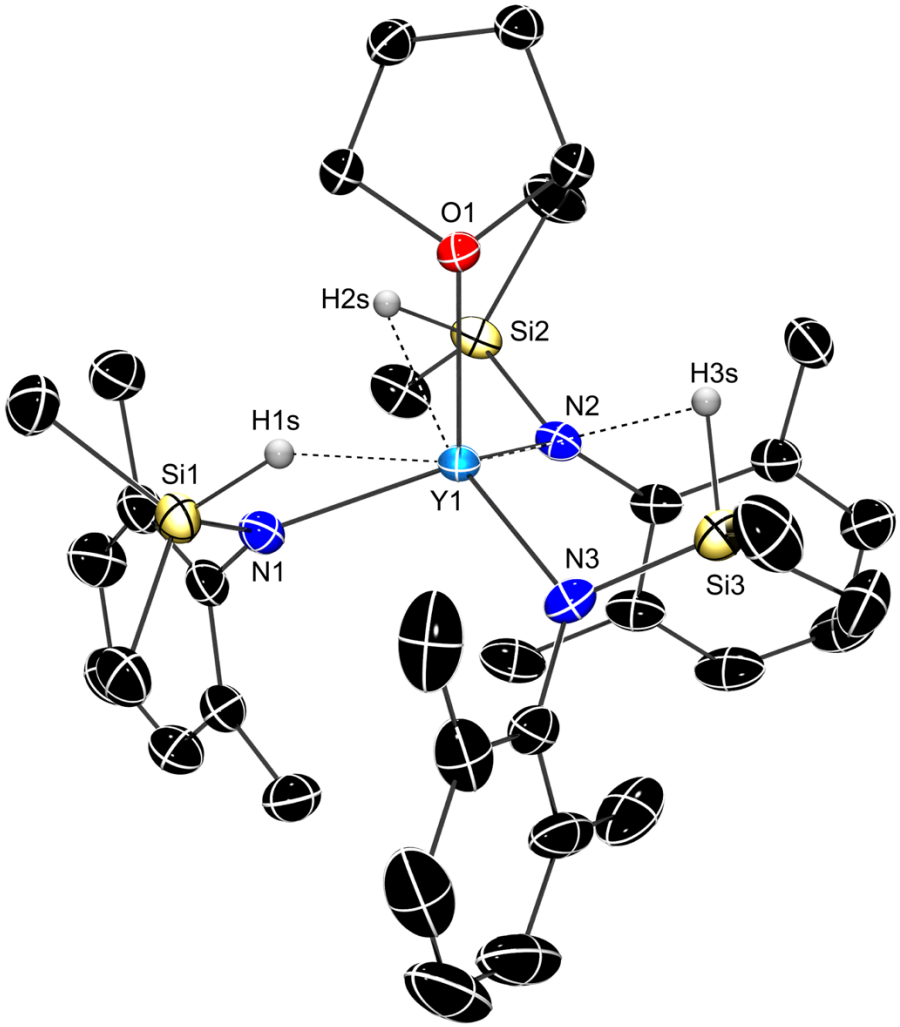

Figure 2. Thermal ellipsoid plot of $Y\{N(SiHMe_2)dmp\}_3THF$ (**4b**). H atoms bonded to Si were located in the Fourier difference map, refined anisotropically, and were included in the illustration.

www.manaraa.com

All other H atoms were placed in calculated positions and are not shown for clarity. Selected interatomic distances (Å): Y1–N1, 2.233(2); Y1–N2, 2.235(2); Y1–N3, 2.235(3); Y1–Si1, 3.1423(9); Y1–Si2, 3.1596(9); Y1–Si3, 3.256(1); Y1–H1s, 2.62(3); Y1–H2s, 2.69(3); Y1–H3s, 2.89(4); Si1–H1s, 1.45(3); Si2–H2s, 1.39(2); Si3–H3s, 1.45(4); Selected interatomic angles (°): N1–Y1–N2, 110.74(9); N2–Y1–N3, 109.81(9); N3–Y1–N1, 111.01(9); O1–Y1–N1, 111.12(8).

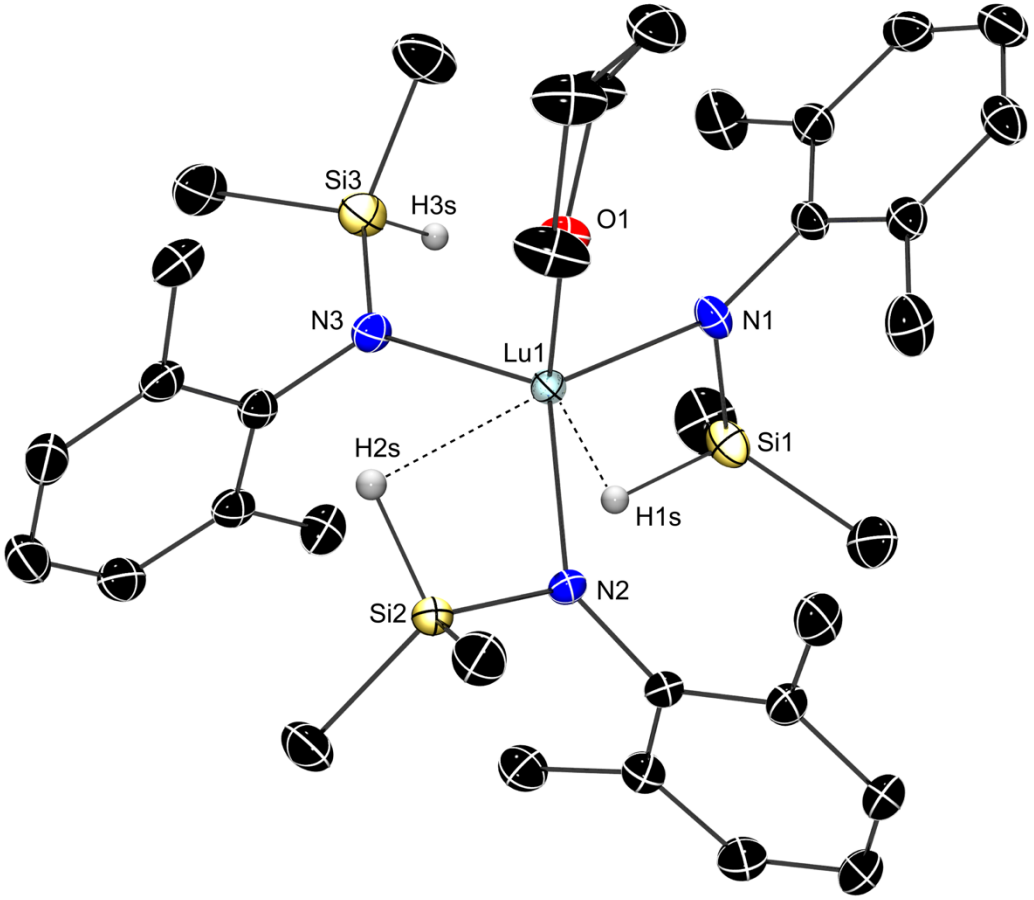

Figure 3. Thermal ellipsoid plot of Lu{N(SiHMe$_2$)dmp}$_3$THF (**5b**). (Å): Lu1–N1, 2.202(3); Lu1–N2, 2.194(3); Lu1–N3, 2.179(3); Lu1–Si1, 2.997(1); Lu1–Si2, 3.180(1); Lu1–Si3, 3.480(1); Lu1–H1s, 2.32(5); Lu1–H2s, 2.73(4); Lu1–H3s, 3.95(4); Si1–H1s, 1.40(2); Si2–H2s, 1.400(7); Si3–H3s, 1.40(3); Selected interatomic angles (°): N1–Lu1–N2, 116.9(1); N2–Lu1–N3, 120.1(1); N3–Lu1–N1, 108.8(1); O1–Lu1–N1, 98.0(1).

www.manaraa.com

The lutetium analogue **5b** (Figure 3), in contrast, contains three inequivalently bonded silazido ligands with long (Lu1–N1, 2.202(3) Å), medium (Lu1–N2, 2.193(3) Å) and short (Lu1–N3, 2.179(3) Å) metal-nitrogen distances. Moreover, the ligand with the shortest distance between Lu and Si atoms (i.e., Lu1–Si1, 2.997(1) Å) and the smallest angle to silicon (Lu1–N1–Si1, 99.2(1)°) is the one with the longest Lu–N distance. The N2 silazido forms a bridging Lu⬸H–Si with relative long Lu1–Si2 (3.180(1) Å) and moderate Lu1–N2–Si2 angle (108.6(10°), suggestive of a weak interaction. The N–Lu–N angles vary considerably from those of an ideal tetrahedron (N1–Lu1–N2, 116.9(1); N1–Lu1–N3, 108.8(1); N2–Lu1–N3, 120.1(1)°), but the LuN_3 core is also not planar ($\sum_{NLuN}$ = 345.8°). In fact, instead of approximate C_3 symmetry, the N1 silazido ligand is oriented with its bridging Lu⬸H–Si pseudo-*trans* to the THF ligand, and its aryl group points toward the THF. Thus, **4b** and **5b**, which appear very similar in spectroscopic features, crystallize with distinct structures.

Salt metathesis reactions of rare earth chlorides and $LiN(SiHMe_2)dipp$ provide solvent-free homoleptic organolanthanides in moderate yields; $Ln\{N(SiHMe_2)dipp\}_3$ (Ln = Sc, **3c**; Y, **4c**; Lu, **5c**; eq 5).

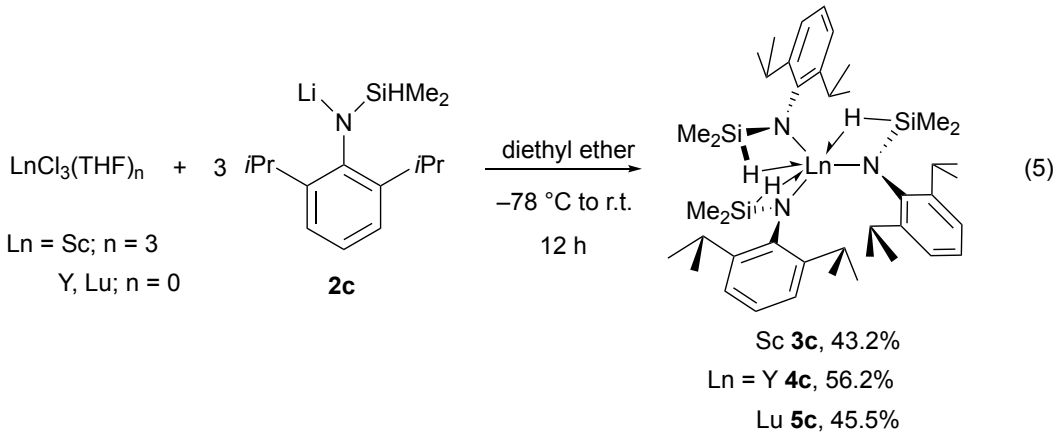

Fortunately, and in contrast to the THF solvent required for syntheses of **3-5a** and **3-5b**, the salt metathesis reactions of **2c** proceed in diethyl ether at low temperature. The crude products

www.manaraa.com

were re-crystallized in pentane to provide analytically pure **3-5c**. Integration and the chemical resonances of the ^{1}H NMR spectra revealed that the rare earth amides **3-5c** contained one set of signals for the silazido ligand, which suggested that the compounds contain three equivalent ligands in solution at room temperature. Similarly, ^{1}H-^{15}N HMBC experiments contained one crosspeak, with ^{15}N NMR chemical shifts of 160.90 (**3c**), 142.29 ppm (**4c**), and 140.26 ppm (**5c**) which correlated with the proton signal of SiMe group.

The ^{1}H NMR resonances assigned to the Si–H groups appeared at 5.43 ppm ($^{1}J_{SiH}$ = 142.6 Hz), 5.17 ppm ($^{1}J_{SiH}$ = 129.2 Hz), and 5.43 ppm ($^{1}J_{SiH}$ = 127.6 Hz) for **3c**, **4c**, and **5c** at room temperature respectively. The reduced $^{1}J_{SiH}$ value provide the first data suggesting that these compounds contain Ln←H–Si bridging interactions. Most significantly, the Si–H signal of **4c** at 5.17 ppm correlated with the yttrium chemical resonance at 378.5 ppm in a ^{1}H-^{89}Y HSQC experiment (measured at room temperature) which, also provides the evidence of non-classical interactions between SiHs and the metal center.

The ^{1}H NMR spectrum of **3c**, acquired at 213 K, contained three resonances at 5.55 ppm, 5.44 ppm, and 5.24 ppm assigned to three inequivalent Si–H groups (Figure 4). Similarly, the spectrum of **4c** obtained at 205 K contained three signals at 5.41 ppm ($^{1}J_{SiH}$ = 131.9 Hz), 5.26 ppm ($^{1}J_{SiH}$ = 140.7 Hz) and 4.89 ppm ($^{1}J_{SiH}$ = 115.8 Hz) assigned to the Si–H moieties. In addition, six multiplets were assigned to methine protons of Dipp groups. The low temperature ^{1}H NMR spectrum of **5c** acquired at 215 K contained only two resonances at 5.58 ppm (1 H) and 5.33 ppm (2 H), with the latter signal assigned to coincident SiH ^{1}H NMR chemical shifts (Figure 5). A ^{1}H-^{29}Si HMQC spectrum of **5c**, acquired at 215 K (decoupling off), contained three signals at –29.73 ppm, –29.07 ppm and –26.60 ppm in silicon dimension that correlated with signals at 5.58 ppm

www.manaraa.com

($^1J_{SiH}$ = 133.1 Hz), 5.33 ppm ($^1J_{SiH}$ = 138.5 Hz), and 5.33 ppm ($^1J_{SiH}$ = 111.8 Hz) respectively (Figure 6). These observations indicate that the three ligands of **3-5c** are inequivalent in solution.

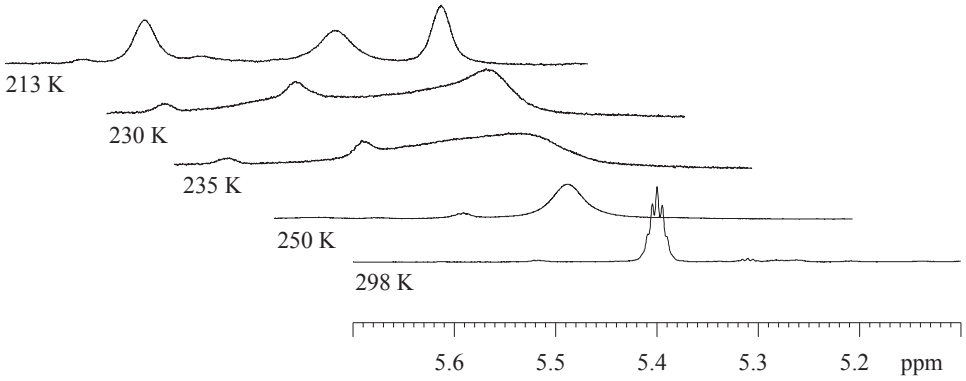

Figure 4. ^{1}H NMR variable temperature stack plot of **3c** in toluene-d_8

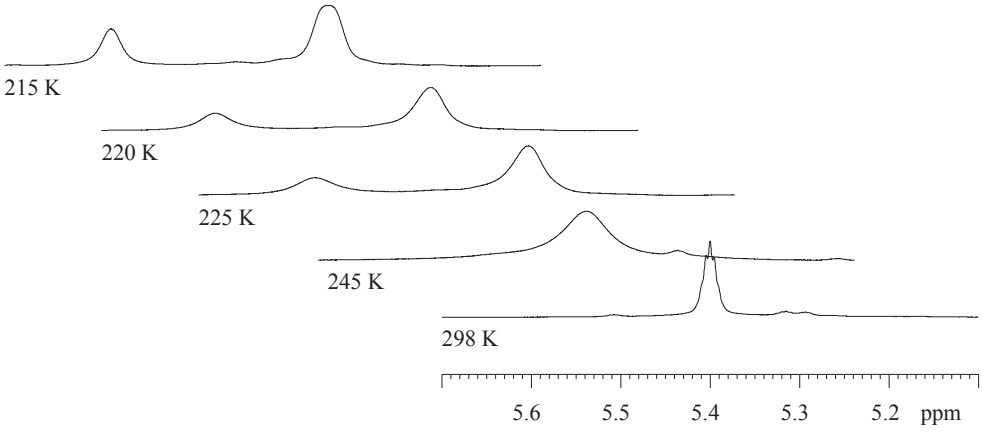

Figure 5. ^{1}H NMR variable temperature stack plot of **5c** in toluene-d_8

When the room temperature and low temperature ^{1}H NMR data is considered, the SiH moieties of **3-5c** undergo fast exchange on NMR time scale at room temperature to give one signal assigned to SiH moiety while the exchange process slows down at low temperature to give resolved signals assigned to SiH groups on NMR time scale. The EXSY experiments of **4c** performed at 205 K further confirms that the SiHs exchange with each other (Figure 7).

www.manaraa.com

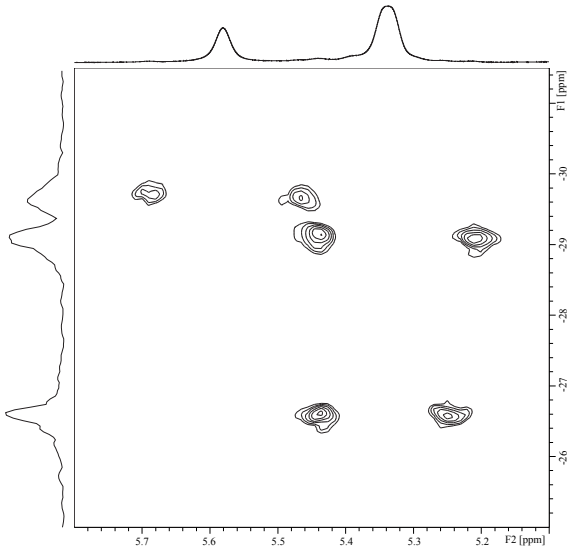

Figure 6. ^{1}H-^{29}Si HMQC NMR of **5c** at 215 K in toluene-d_8

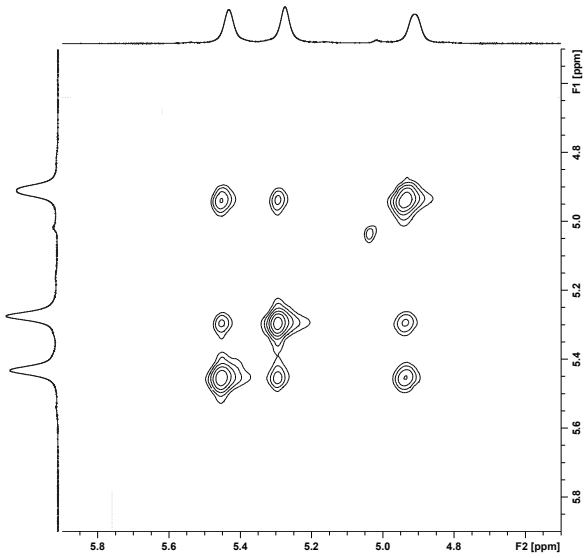

Figure 7. EXSY NMR spectrum of **4c** obtained at 205 K in toluene-d_8

The IR spectrum contained bands in the ν_{Si-H} region at 2046 and 1908 cm^{-1} for **3c**, 1934 and 1883 cm^{-1} for **4c**, and 1942 and 1877 cm^{-1} for **5c**. The lower energy signal is more intense than the higher energy band, suggesting that the bridging moieties with (relatively) strong metal-hydrogen are most prevalent in the structure.

www.manaraa.com

X-ray quality crystals of **3**-**5c** were obtained from pentane at –30 °C. All three compounds crystallize as two independent molecules per unit cell. The solid-state structures of **3**-**5c** adopt trigonal planner geometries ($\sum_{NLnN}$ ~360°). Two of the dipp groups are located above the LnN_3 plane, while the third is located below the LnN_3 plane. This conformation, as well as the metrical parameters (Ln–N distances, Ln–H distances, and ∠Ln-N-Si) highlight the inequivalence of ligands in **3-5c**. For example, one ligand (N2) in **4c** (Figure 8) contains longer Y–N distance, shorter Y–H distance and smaller Y–N–Si angle than in other two ligands (N1 and N3); Y–N distances (cf. Y1–N2, 2.293(3) vs. Y1–N1, 2.247(3); Y1–N3, 2.251(3) Å), Y–H distances (cf. Y1–H2s, 2.24(4) vs. Y1–H1s, 2.50(5); Y1–H3s, 2.43(4) Å) and Y–N–Si angles (Y2–N2–Si2, 94.2(2) vs. Y1–N1–Si1, 102.4(1); Y3–N3–Si3, 101.4(1)°). Similarly to the yttrium analogue, the lutetium compound **5c** also contains inequivalent ligands, one with longer Lu1–N3 distance (2.235(4) Å), shorter Lu1–H3s distance (1.94(6) Å) and smaller Lu–N–Si angle (Lu1–N3–Si3, 95.0(2)°) than in other two ligands. Despite the inequivalent nature of the ligands, these interatomic distances and bond angles of **4c** and **5c** provide the evidence of Ln←H–Si interactions. Interestingly, the distance between the rare earth center and one of the methine CHs in yttrium and lutetium analogs are Y1–H27A, 2.37(4) Å and Lu1–H40A, 2.34(6) Å respectively suggesting agostic interactions Ln←H–C.

www.manaraa.com

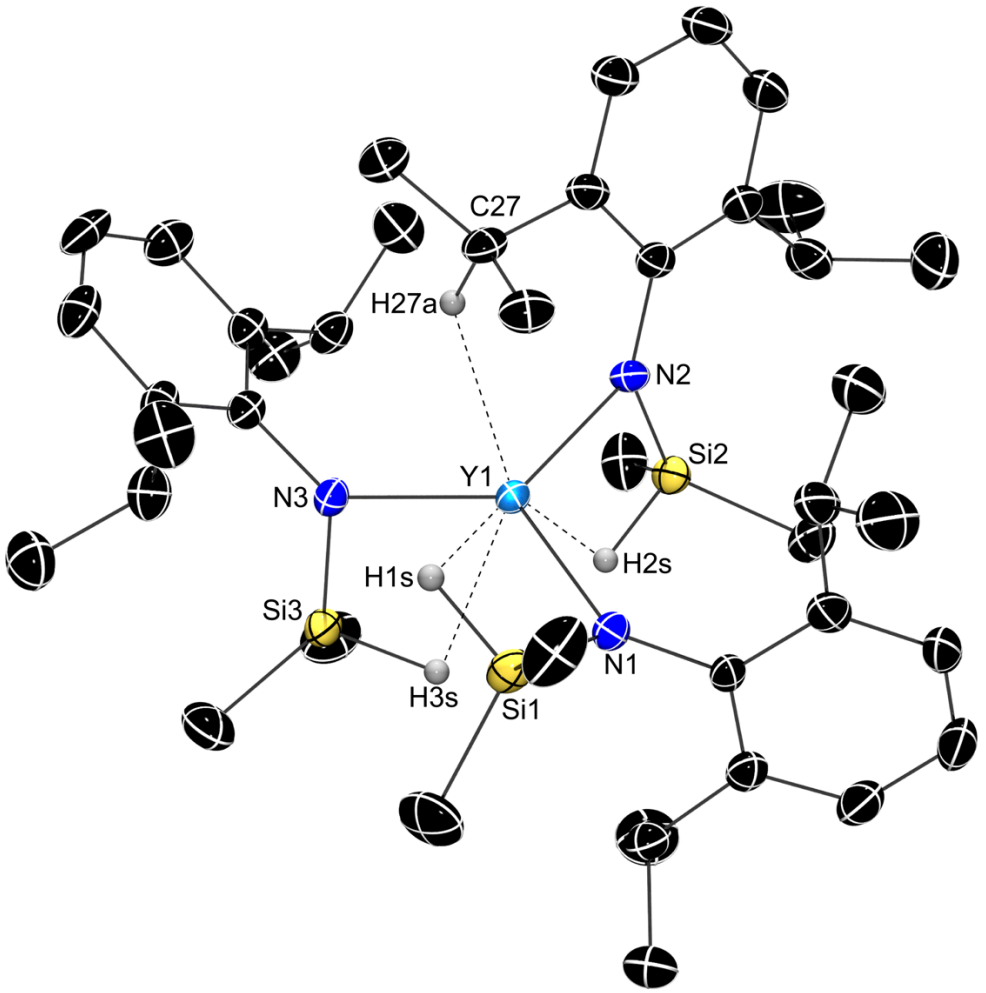

Figure 8. Thermal ellipsoid plot of Y{N(SiHMe$_2$)dipp}$_3$ (**4c**). H atoms bonded to Si are located in the Fourier difference map, refined anisotropically, and are included in the illustration. All other H atoms are not shown for clarity. Selected interatomic distances (Å): Y1–N1, 2.247(3); Y1–N2, 2.293(3); Y1–N3, 2.251(3); Y1–Si1, 3.090(1); Y1–Si2, 2.974(1); Y1–Si3, 3.073(1); Y1–H1s, 2.50(5); Y1–H2s, 2.24(4); Y1–H3s, 2.43(4); Si1–H1s, 1.37(6); Si2–H2s, 1.38(4); Si3–H3s, 1.53(4); Selected interatomic angles (°): N1–Y1–N2, 113.4(1); N2–Y1–N3, 114.2(1); N3–Y1–N1, 130.0(1).

www.manaraa.com

Addition of one equivalent of pyridine to **4c** in benzene provides **4c·py** (eq 6), which was re-crystallized in pentane. The ^{1}H NMR spectrum of **4c·py** contained two signals assigned to methyl groups of dipp moiety, whereas the dipp methyls of **4c** appeared as a single doublet. **4c** and **4c·py** each contained only one set of signals for the silazido ligand.

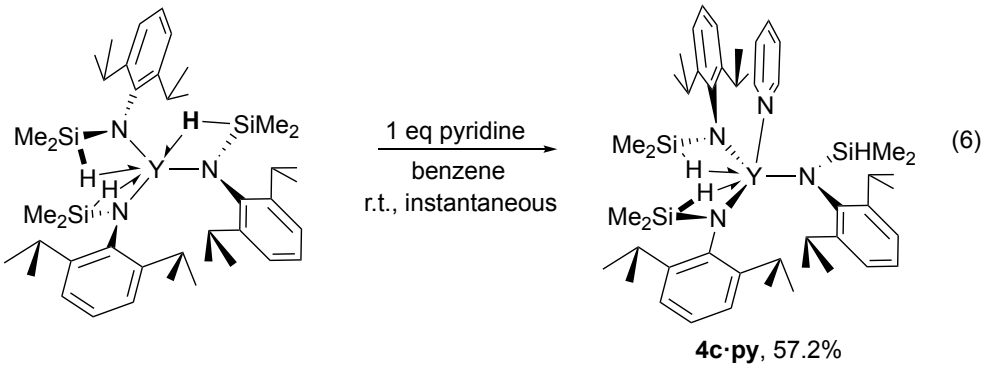

(6)

The ^{1}H NMR resonances assigned to the Si–H groups of **4c·py** appeared at 5.33 ppm ($^1J_{SiH}$ = 150.5 Hz), at room temperature. The $^1J_{SiH}$ value of **4c·py** is larger than that of **4c** suggesting that the coordination of pyridine affected the Ln←H–Si bridging interactions. Likewise, the IR spectrum of **4c·py** contained two bands in the ν_{Si-H} region at 2103 and 1959 cm^{-1}, indicating the presence of both classical and non-classical SiH interactions with the metal center.

X-ray quality crystals of **4c·py** were obtained from pentane at –30 °C. The X-ray diffraction studies confirmed that pyridine molecule of **4c·py** is coordinated to the yttrium center (Figure 9). The solid-state structure of **4c·py** ($\sum_{NLnN}$ ~ 349°) is deviated from planarity around the yttrium center compared to **4c** ($\sum_{NLnN}$ ~ 358°). The Y–H interatomic distances (Y1–H1s, 2.64(3) Å and Y1–H2s, 2.47(4) Å) and Y–N–Si bond angles (Y1–N1–Si1, 104.1(1)° and Y1–N2–Si2, 99.2(1)°) of two ligands provide the evidence of Y←H–Si interactions. The silazido ligand associated with N3 does not show parameters associated with a Y←H–Si secondary interaction (i.e., Y1–H3s (3.85(5) Å and ∠Y1–N3–Si3 (128.1(1)°), confirming the IR assignment above. Interestingly, the interatomic bond distance of Y1–N3 (2.261(2) Å) is in between Y1–N2 (2.286(3)

www.manaraa.com

Å) and Y1–N1 (2.249(2) Å), both of which have parameters indicative of secondary interactions. These structural parameters indicate that, as in **4c**, the silazido ligands are inequivalent in **4c·py**.

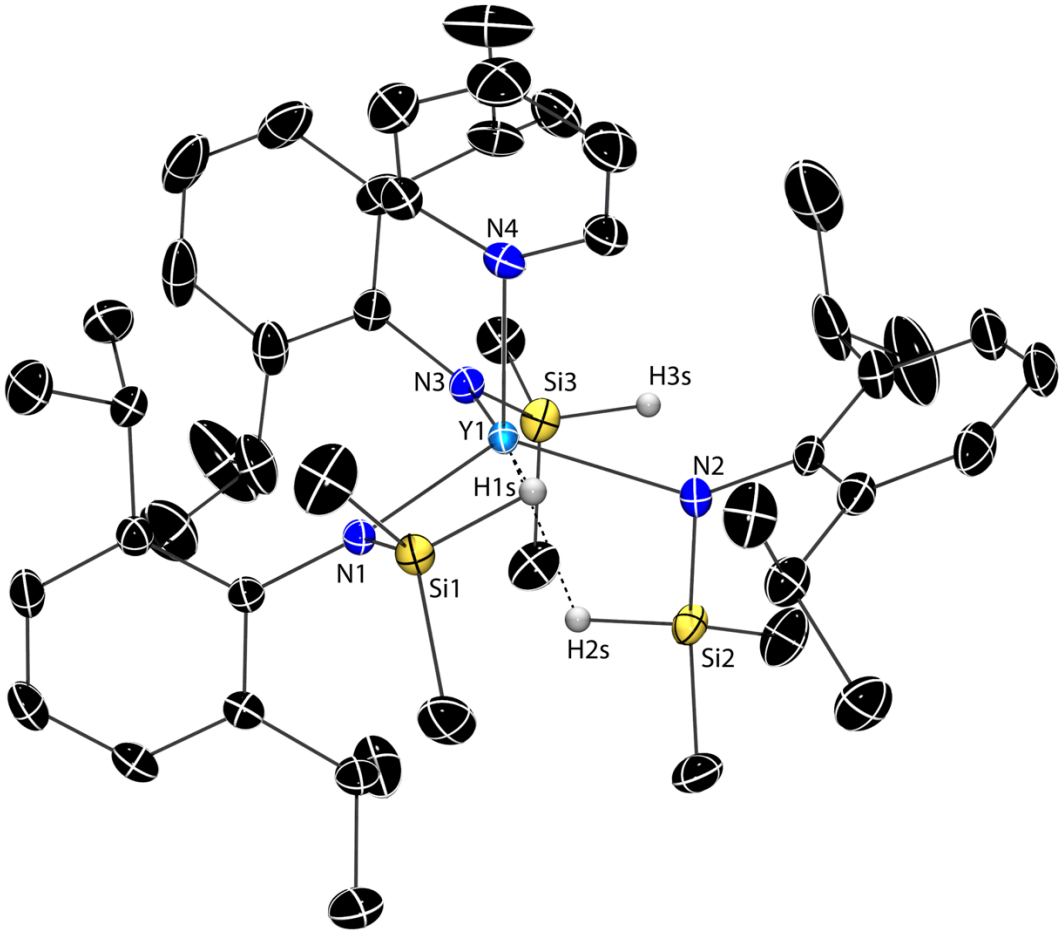

Figure 9. Thermal ellipsoid plot of Y{N(SiHMe$_2$)dipp}$_3$.pyridine (**4c·py**). H atoms bonded to Si are located in the Fourier difference map, refined anisotropically, and are included in the illustration. All other H atoms are not shown for clarity. Selected interatomic distances (Å): Y1–N1, 2.249(2); Y1–N2, 2.286(3); Y1–N3, 2.261(2); Y1–Si1, 3.146(1); Y1–Si2, 3.061(1); Y1–Si3, 3.594(1); Y1–H1s, 2.64(3); Y1–H2s, 2.47(4); Y1–H3s, 3.85(5); Si1–H1s, 1.43(4); Si2–H2s, 1.36(4); Si3–H3s, 1.33(5); Selected interatomic angles (°): N1–Y1–N2, 116.53(8); N2–Y1–N3, 113.91(9); N3–Y1–N1, 118.65(8).

www.manaraa.com

Spectroscopic and structural comparison of silazido compounds

Here we compare series of three-coordinate tris(silazido) compounds, four-coordinate tris(silazido) ether compounds, and five coordinate tris(silazido) bis(ether) compounds, examining the relationship between coordination number, geometry, and spectroscopic and structural features associated with bridging Ln←H–Si groups. We note that many of these coordination environments are accessible with a few of the commonly studied silazido ligands for instance, –$N(SiHMe_2)_2$, and –$N(SiHMe_2)$*t*Bu., as well as the new ligands described here.

Three coordinate compounds. Ln{$N(SiHMe_2)$dipp}$_3$ and Ln{$N(SiHMe_2)$*t*Bu}$_3$ (Ln = Sc, Y, Lu) contain three silazido ligands, and each silazido ligand contains a bridging Ln←H-Si moiety.[17] The comparison is somewhat limited because these are the only two series of 3-coordinate silazido or disilazido compounds containing β-SiH moieties; however, the comparisons are systematic for scandium, yttrium, and lutetium compounds. The spectroscopic and structural features of Ln{$N(SiHMe_2)$*t*Bu}$_3$ suggest their SiH are more activated compared to Ln{$N(SiHMe_2)$dipp}$_3$. For example, the Ln{$N(SiHMe_2)$*t*Bu}$_3$ compounds contain lower $^1J_{SiH}$ and lower ν_{SiH} compared to the diisopropylsilazido-supported compounds. X-ray diffraction studies also indicated that the average Ln···Si distance in **3c**-**5c** is longer compared to the distances in corresponding Ln{$N(SiHMe_2)$*t*Bu}$_3$ compounds (Sc: 2.9303 vs 2.8501 Å); Y: 3.046 vs 3.0195 Å; Lu: 3.005 vs 2.9581 Å). The $\sum_{NLnN}$ of **3c**-**5c** were 357.92(7)°, 357.7(1)° and 357.8(2)° respectively indicating that the compounds contain planar geometry around the rare earth center. In contrast, $\sum_{NLnN}$ of Ln{$N(SiHMe_2)$*t*Bu}$_3$ were 348.63(4)°, 351.29(6)° and 348.97(8)° for Sc, Y, Lu analogs respectively indicating the compounds show pyramidal geometry.

Four coordinate compounds. Ln{(N(SiHMe$_2$)dmp}$_3$(THF) and Ln{(N(SiHMe$_2$)*t*Bu}$_3$(THF) (Ln = Y, Lu) contain three silazido ligands and one coordinated

www.manaraa.com

THF, and each silazido ligand contains a bridging Ln←H-Si moiety except in Lu{(N(SiHMe$_2$)dmp}$_3$(THF).[17] Y{(N(SiHMe$_2$)dipp}$_3$(pyridine) contains three silazido ligands and one coordinated pyridine molecule, and only two bridging Ln←H-Si interactions are observed similarly to **5b**. The $^1J_{SiH}$ values of Y{(N(SiHMe$_2$)*t*Bu}$_3$(THF), **4b** and **4c·py** were 142.9 Hz, 151.3 Hz and 150.5 Hz respectively indicating that former compound show stronger Ln←H–Si interactions than latter two compounds. Lutetium analogs of –N(SiHMe$_2$)*t*Bu}$_3$ and –N(SiHMe$_2$)dmp also show the same trend as above. According to IR spectroscopy data (ν_{Si-H}) **4b** (2095, 2057, 1966 cm^{-1}), **5b** (2071, 1902 cm^{-1}), **4c·py** (2103, 1959 cm^{-1}) and Y{(N(SiHMe$_2$)*t*Bu}$_3$(THF) (2019, 1967 cm^{-1}) contain both stronger and weaker interacting SiH moieties with the metal center, while Lu{(N(SiHMe$_2$)*t*Bu}$_3$(THF) contains only one band at 1989 cm^{-1}assigned to stronger interacting SiH groups. The solid state structures of Y{(N(SiHMe$_2$)*t*Bu}$_3$(THF) **(**2.255 Å) contains longer Ln–N$_{(avg)}$ than in **4b** (2.234 Å). In addition, former compound contains shorter Ln–Si$_{(avg)}$ than that of **4b** (3.117 Å, 3.1860 Å respectively). The trend is observed for Lu{(N(SiHMe$_2$)*t*Bu}$_3$(THF) and **5b**. These observations further confirm that SiH are more activated in Ln{(N(SiHMe$_2$)*t*Bu}$_3$(THF) than in Ln{(N(SiHMe$_2$)dmp}$_3$(THF). However, **4c·py** contains the longest Ln–N$_{(avg)}$ (2.265(2) Å) and the longest Ln–Si$_{(avg)}$ (3.267(1) Å) which is not consistent with the trend above. The reason could be that –N(SiHMe$_2$)dipp ligand is larger and the solid state structure of **4c·py** cannot be compared with other four coordinated yttrium compounds described here. $\sum_{NLnN}$ of **4b, 5b**, **4c·py** and Ln{(N(SiHMe$_2$)*t*Bu}$_3$(THF) (Ln = Y, Lu) were in the range of 331 – 349 ° indicating that the solid state structures are deviated from planarity around the metal center.

Five coordinate compounds. Ln{N(SiHMe$_2$)Ph}$_3$(THF)$_2$ (Ln = Sc, Y, Lu) and Ln{N(SiHMe$_2$)$_2$}$_3$(THF)$_2$ (Ln = Y, Lu) contain three silazido and disilazido ligands respectively

www.manaraa.com

with two coordinated THF molecules.[6] The compounds **3a**, **4a** and **5a** is comparable with $Y\{N(SiHMe_2)_2\}_3(THF)_2$ and $Lu\{N(SiHMe_2)_2\}_3(THF)_2$ as all five compounds contain larger $^1J_{SiH}$ values in a range of 165 – 176 Hz and IR stretching frequencies >2000 cm^{-1} for the Si–H band. These observations suggest that these compounds contain only classical β Si–H interactions with the rare earth center. The X-ray diffraction studies showed that the average inter atomic distances $Y–Si_{(avg)}$ of **4a** (3.4307 Å) and $Y\{N(SiHMe_2)_2\}_3(THF)_2$ (3.4 Å) are equivalent with in error while $Lu–Si_{(avg)}$ of **5a** (3.435(4) Å) is longer than that of $Lu\{N(SiHMe_2)_2\}_3(THF)_2$ (3.374(1) Å)**.** The compounds **3a** – **5a**, and $Ln\{N(SiHMe_2)_2\}_3(THF)_2$ showed distorted trigonal bipyramidal geometry around the metal center though $\sum_{NLnN}$ is ~ 360°.

Reactions of dimethylsilyl anilides and carbonyls: reactivity of the SiH

The attempts to react $Ln\{N(SiHMe_2)Ph\}_3(THF)_2$ or $Ln\{N(SiHMe_2)dmp\}_3THF$ with ketones did not provide any clean isolable products.

The diisopropylaniline-substituted silazido compounds **4c** and **5c** rapidly react with acetophenone and benzophenone to give silylether-containing heteroleptic silazido compounds of the type $Ln\{\kappa^2\text{-}N(SiMe_2OCHRR')dipp\}\{N(SiHMe_2)dipp\}_2$ {eq. 7; R,R' = Ph,Me (Ln = Y, **4d**; Ln = Lu, **5d**); Ph,Ph (Ln = Y, **4e**; Ln = Lu, **5e**)}. These reactions are remarkably rapid, and even reactions performed at –78 °C in toluene-d_8, and measured by ^{1}H NMR at that temperature, react within 3 mins. to give the product quantitatively. These products also form in reactions performed at room temperature.

www.manaraa.com

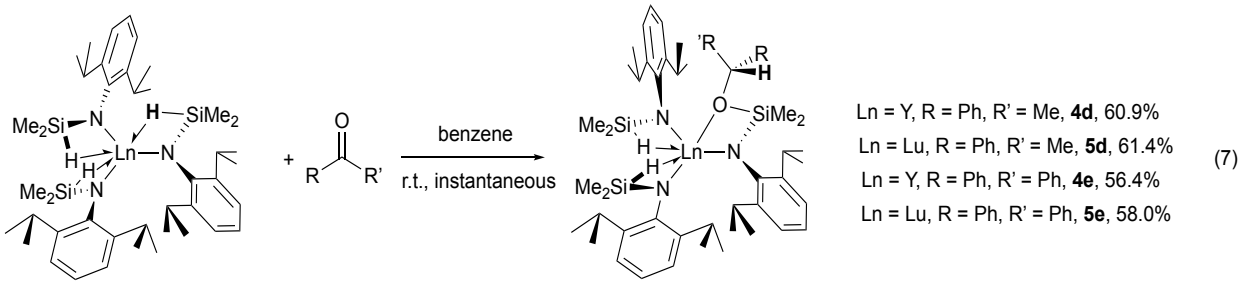

A ratio of 2:1 was observed for the integrals of SiH to new CH formed in the ^{1}H NMR spectrum. The signal assigned to that CH appeared as a multiplet in acetophenone inserted compounds (**4d**, **5d**) while it appeared as a broad singlet in benzophenone inserted compounds (**4e**, **5e**) which indicates that the hydride of one SiH group was transferred to the carbonyl carbon. Further, ^{1}H-^{13}C HMQC spectrum also provides the evidence for the formation of a new CH bond as a correlation was observed between the silyl ether carbon and the proton. The ^{29}Si NMR resonance assigned to the reacted ligand of inserted compounds showed a downfield chemical shift compared to the precursor (Table 1). Together these observations suggest the insertion of C=O into Si–H via C–H and Si–O bond formation.

Table 1. Chemical shifts, coupling constants and IR bands of **4d**, **5d**, **4e** and **5e**

Compound	^{13}C δ_{CH} (ppm)	^{1}H δ_{CH} (ppm)	^{29}Si δ_{SiO} (ppm)	^{1}H δ_{SiH} (ppm)	$^{1}J_{SiH}$ (Hz)	IR (cm^{-1})
4d (acetophenone inserted in to **4c**)	77.46	5.00	3.94	5.33	135.5	1997, 1891
5d (acetophenone inserted in to **5c**)	78.09	5.06	3.46	5.57	135.3	2001, 1881
4e (benzophenone inserted in to **4c**)	84.42	6.53	4.84	5.01	131.9	1965, 1886
5e (benzophenone inserted in to **5c**)	83.58	6.62	–4.10	5.29	133.1	1957 br
4c (Y{N(SiHMe$_2$)dipp}$_3$)	NA	NA	–28.18	5.17	129.2	1934, 1883
5c (Lu{N(SiHMe$_2$)dipp}$_3$)	NA	NA	–27.62	5.43	127.6	1942, 1877

www.manaraa.com

^{1}H NMR spectra contained one set of signals assigned for -N(SiHMe$_2$)dipp moieties which indicates that these two ligands are equivalent in solution at room temperature. The chemical shift of SiH observed in ^{1}H NMR for the acetophenone inserted compounds (**4d**, **5d**) are higher and the benzophenone inserted compounds (**4e**, **5e**) are lower than that of the starting materials. The reduced $^1J_{SiH}$ values of **4d**, **5d**, **4e** and **5e** suggest that the compounds contain bridging interactions between β-SiH and the metal center. The $^1J_{SiH}$ coupling constants are higher in all four complexes than that of precursors, which indicates that the precursors contain stronger non-classical Ln←H–Si interactions than inserted compounds.

The IR spectra of **4d**, **5d** and **4e** contained two bands while **5e** contained one band assigned to Si–H groups which indicates that -N(SiHMe$_2$)dipp moieties are inequivalent in solid state at room temperature except in the last compound. Similarly, to the precursors, the IR frequencies of all four compounds assigned to the Si–H region (ν_{Si-H}) appeared at < 2000 cm^{-1} which confirms the presence of non-classical Ln←H–Si interactions.

All compounds formed X-ray quality crystals from saturated pentane solutions cooled to –30 °C. The acetophenone-inserted compounds **4d** and **5d** crystallized as two independent molecules while the other two contained only one molecule in the unit cell. In all the complexes two dipp groups are located above the NLnN plane and one dipp group is located below the plane (Figure 10). The inserted ketone is located below the plane in all the compounds and the dipp group of that reacted ligand is one of the dipp groups located above the LnN3 plane. Although the oxygen atom is coordinated to the metal center to give tetra-coordinated compounds (Ln–O, 2.258 – 2.363 Å), planarity is retained around the rare earth center as $\sum_{NLnN}$ is 356.14 - 357.43° in all four complexes. Interestingly, Ln–N bond distances of three ligands in each complex are equivalent within error though a ketone is inserted into one ligand, for example the Ln–N bond

www.manaraa.com

distances of **4e** are; Y1–N1, 2.282(2) Å, Y1–N2, 2.268(2) Å, Y1–N3, 2.267(2) Å. The shorter interatomic distance of Ln–H (2.35 - 2.48 Å) and smaller angles of ∠Ln-N-Si, (98.1 - 101.2°) of the compounds provide the evidence of Ln⇜H–Si interactions.

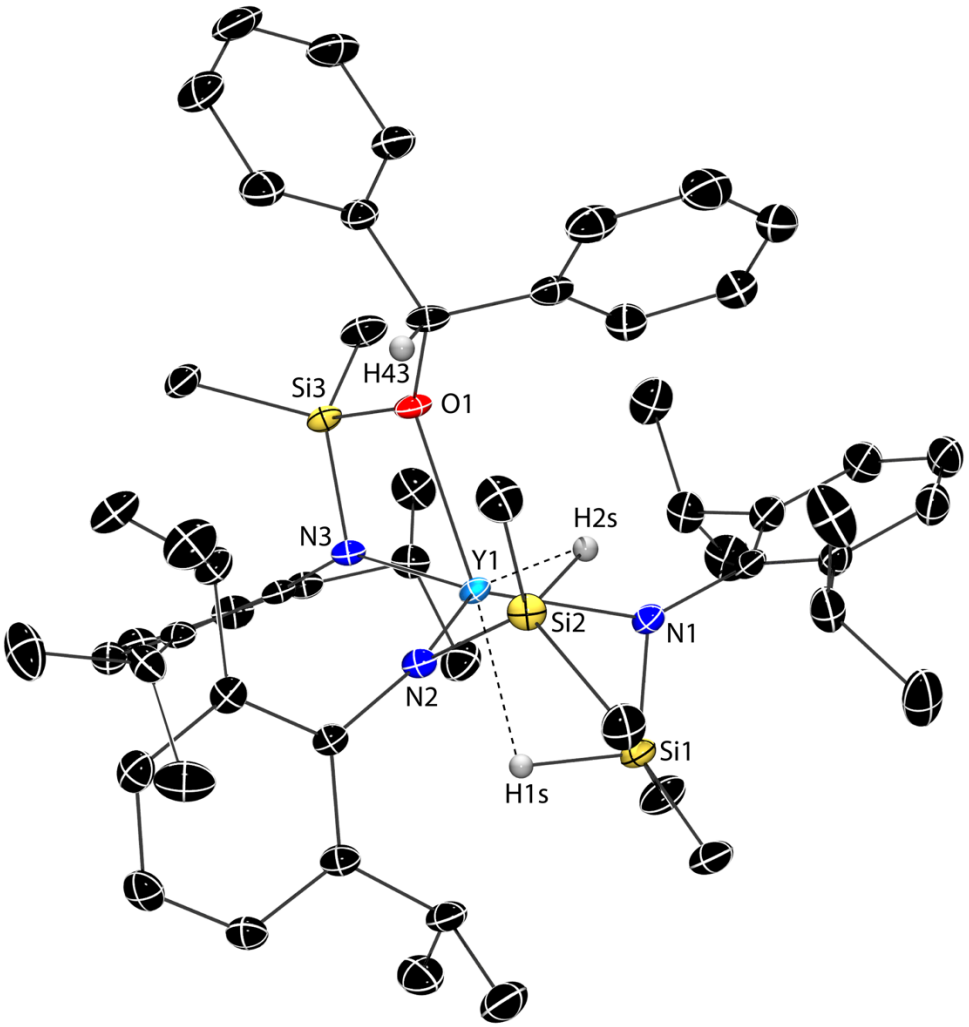

Figure 10. Thermal ellipsoid plot of Y{N(SiMe$_2$OCHPh$_2$)dipp}{N(SiHMe$_2$)dipp}$_2$ (**4e**). H atoms bonded to Si are located in the Fourier difference map, refined anisotropically, and are illustrated. All other H atoms are not shown for clarity. Selected interatomic distances (Å): Y1–N1, 2.282(2); Y1–N2, 2.268(2); Y1–N3, 2.267(2); Y1–Si1, 3.052(1); Y1–Si2, 3.071(1); Y1–Si3, 3.097(1); Y1–O1, 2.363(2); Y1–H1s, 2.42(3); Y1–H2s, 2.38(2); Si1–H1s, 1.47(2); Si2–H2s, 1.47(3); Selected interatomic angles (°): N1–Y1–N2, 119.21(8); N2–Y1–N3, 118.96(8); N3–Y1–N1, 117.97(8).

www.manaraa.com

Similarly, to the insertion reaction of ketones with **4c**, **4c·py** complex also reacts instantaneously with acetophenone to give the hydrosilylated product **4d** and free pyridine.

Attempts to add multiple acetophenone molecules across the Si–H of the complexes **4c** and **5c** was not successful. The reaction of three equiv. of acetophenone with **4c** or **5c** provides multiple unknown products and free amine. In contrast, 3 equiv. of benzophenone reacts with **4c** and **5c** to **4e** and **5e** respectively leaving excess benzophenone.

As acetone is the least sterically hindered ketone, it was reacted with **4c** in order to insert multiple ketones. The reactions of 2 – 5 equivalents of acetone and **4c** at room temperature in benzene provide mixtures of 2 and 3 acetone inserted products (3 acetone inserted product is tentatively assigned and failed to isolate it). Addition of 2.2 equivalents of acetone to **4c** at –78 °C in toluene also provides the same as above. The 2 equivalents of acetone inserted product into **4c** Y{κ^2-N(SiMe$_2$OCHMe$_2$)dipp}$_2${N(SiHMe$_2$)dipp} **4f** was isolated (eq 8), after removing the 3 equivalents acetone inserted product with pentane.

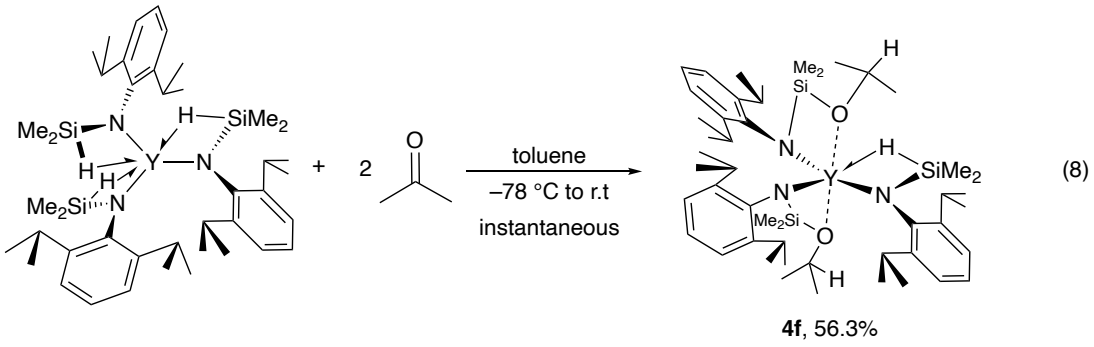

4f, 56.3% (8)

The ^{1}H NMR spectrum of **4f** showed an integration ratio of 1:2 for the Si–H to two new CHs (3.71 ppm 1H, 3.54 ppm 1H) formed which indicates that two hydrides from SiH groups were transferred to carbonyl carbons. Similarly, to **4d, 5d, 4e** and **5e**, ^{1}H-^{13}C HMQC spectrum of **4f** also showed correlations between the silyl ether carbons and the protons which transferred from SiH

www.manaraa.com

groups. The ^{29}Si NMR resonances assigned to the reacted ligands of **4f** appeared deshielded at 0.23 ppm and 0.25 ppm which indicates the formation of Si–O bonds.

The ^{1}H NMR spectrum of **4f** contained three sets of signals assigned to three ligands indicating the inequivalent nature of the ligands in solution, for example the chemical shifts for the resonances assigned to methine peaks were at 4.17 ppm, 3.98 ppm and 3.71 ppm. The Si–H signal of **4f** showed at 5.57 ppm in the ^{1}H NMR with a reduced one bond coupling constant ($^{1}J_{SiH}$ = 138.1 Hz) suggesting the presence of non-classical interactions between β Si–H and the yttrium center. The IR spectroscopy data contained a stretching frequency at 1991 cm^{-1} assigned for the SiH group and this value confirms the existence of Y←H–Si interactions in **4f**.

X-ray quality crystals of **4f** were obtained at –30 °C in pentane. The shorter Y–O interatomic distances ~ 2.3 Å indicate that **4f** is a five-coordinate compound including three nitrogen and two oxygen atoms coordinated to the metal center (Figure 11). In the solid-state structure of **4f**, one acetone molecule is located above the LnN_3 plane while the other acetone is located below the plane. The dipp groups of the inserted ligands are positioned inversely from the ketone direction. Similarly to other hydrosilylated compounds, **4f** also contains a planar geometry around yttrium center ($\sum_{NLnN}$ = 359.91(6)°). The shorter interatomic bond distance of Y–H3s 2.30(3) Å shows the existence of bridging interactions with the yttrium center. In addition, the smaller angles of ∠Y-N-Si (97.2° -101.4°) confirms the Y←H–Si interactions.

www.manaraa.com

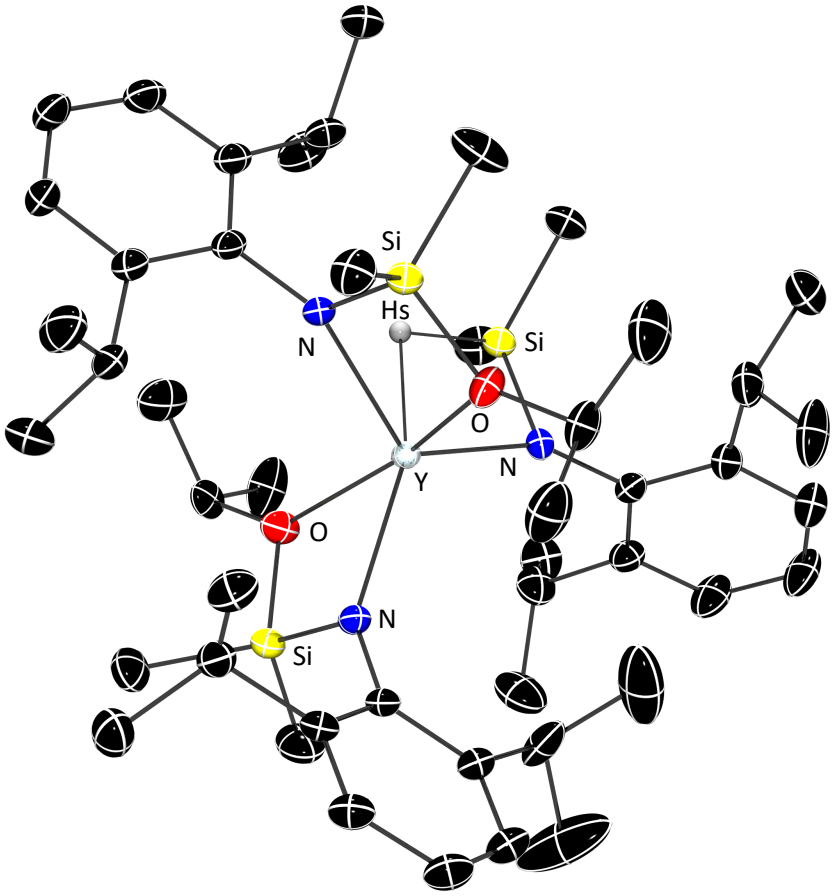

Figure 11. Thermal ellipsoid plot of Y{N(SiMe$_2$OCHMe$_2$)dipp}$_2${N(SiHMe$_2$)dipp}(**4f**). H atoms bonded to Si are located in the Fourier difference map, refined anisotropically, and are illustrated. All other H atoms are not shown for clarity. Selected interatomic distances (Å): Y1–N1, 2.294(2); Y1–N2, 2.345(2); Y1–N3, 2.319(2); Y1–Si1, 3.1112(8); Y1–Si2, 3.1194(7); Y1–Si3, 3.0443(8); Y1–O1, 2.344(2); Y1–O2, 2.358(2); Y1–H3s, 2.30(3); Si3–H3s, 1.52(2); Selected interatomic angles (°): N1–Y1–N2, 117.59(6); N2–Y1–N3, 125.42(6); N3–Y1–N1, 116.90(6).

The attempts to monitor the insertion reaction between **4c** or **4c·py** and ketone failed in NMR time scale as the reaction is instantaneous even at –80 °C. Further, above reaction takes place the same way in the presence of excess pyridine (5 eq) too. As the pyridine coordinated

www.manaraa.com

compound reacts similarly to **4c**, we were curious if the reaction pathway of insertion of carbonyl in to SiH of LnDipp complexes is an associative or a dissociative mechanism. To study the reaction pathway, EXSY NMR experiments were performed with **4c** in the presence of excess pyridine (1.5 eq). The mixing times were changed from 0.05 – 0.4 seconds to obtain the rate constant of exchange at a particular temperature. The data was acquired at four different temperatures (4.6 to –24.9 °C) in order to obtain the activation parameters (Figure 12). The results showed that coordinated pyridine exchanges with **4c** associatively. ($\Delta S = -19.7$ calmol^{-1}K^{-1}).

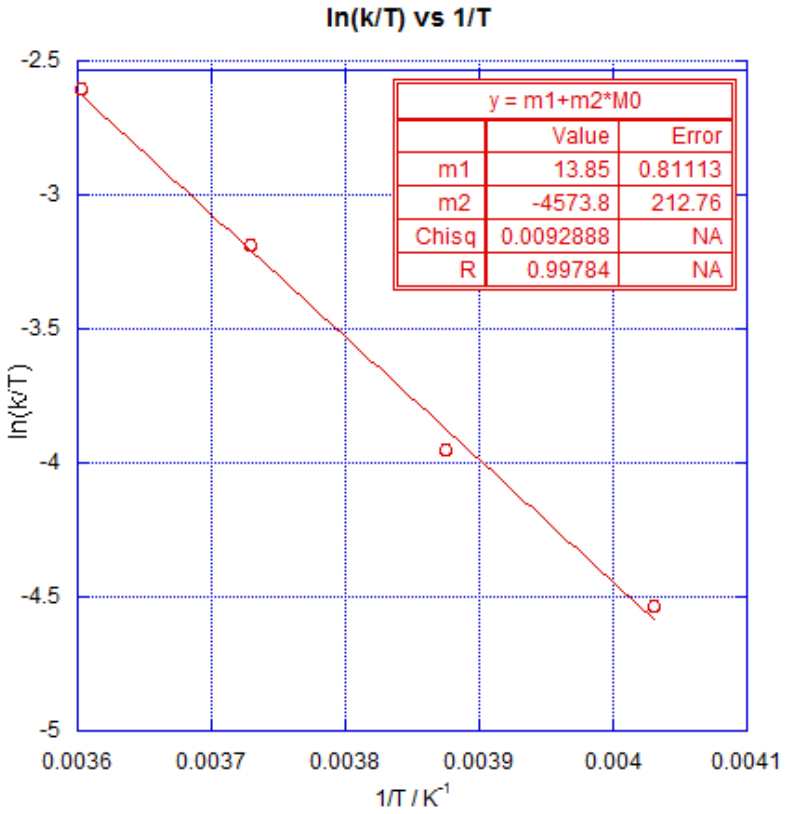

Figure 12. The Eyring plot of pyridine exchange on **4c**

Two mechanisms are proposed for the reaction of ketone insertion in to **4c** or **4c·py** (Figure 13). The ketone coordinates to the metal center first in **4c** or **4c·py** as mentioned in reaction

www.manaraa.com

pathway A. Pyridine molecule can be either dissociated prior to oxygen atom attacks the silicon center while the hydride transferrers to the carbonyl carbon to give the product or it can stay coordinated until the above step is completed. Then pyridine molecule can be dissociated from the metal center to provide the desired product.

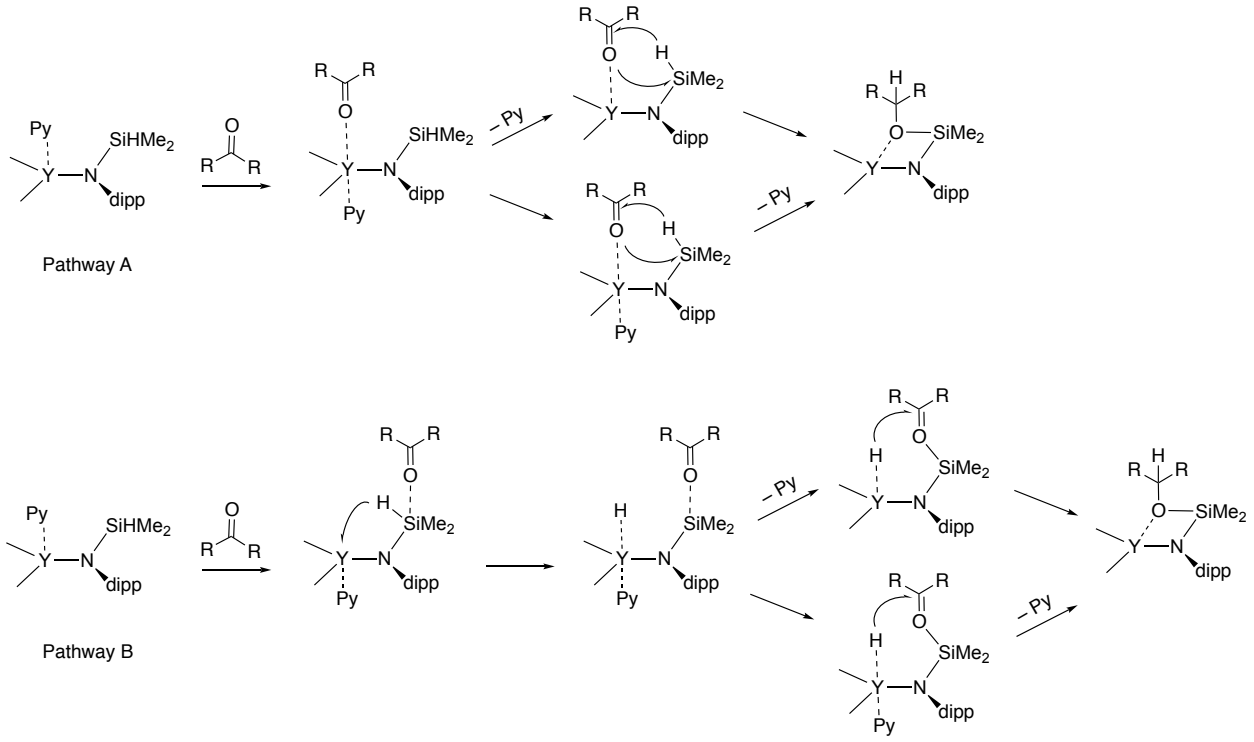

Figure 13. Proposed ketone insertion mechanisms in to SiH of **4c** or **4c·py**

The other proposed mechanism (pathway B) is that the ketone coordinates to the silicon center rather than to the yttrium center followed by a hydride transfer to provide the metal hydride. The hydride can be then transferred on to carbonyl carbon to give the inserted product. The EXSY NMR results, showed that the reaction pathway occurs through an associative mechanism. Therefore, pathway B is ruled out and pathway A is accepted for the ketone insertion reaction.

www.manaraa.com

Conclusion

A new series of homoleptic rare earth amide complexes are synthesized $Ln\{N(SiHMe_2)Aryl\}_3(THF)_n$ {Ln = Sc, Y, Lu (Aryl = Ph, n = 2) (Aryl = dmp, n = 1) (Aryl = dipp, n = 0)} in moderate yields. The number of solvent molecules coordinated to the metal center is varies based on the steric properties of the ligand. A greater number of bridging interactions between β SiH and the metal center are observed for the complexes with fewer number of coordinated solvent molecules. The overall symmetry of the complexes is affected by the symmetry of the ligands. Rare earth dipp silazido complexes and ketones react via hydrosilylation, rather than insertion into the Ln–N bond or formation of an enolate. The ketone insertion into SiH is proposed to occur through coordination of the carbonyl oxygen to the rare earth center. The attempts to catalyze the hydrosilylation reaction of ketone and $HN(SiHMe_2)$dipp failed in the presence of $Y\{N(SiHMe_2)dipp\}_3$ as the pre catalyst. The reason for the failure could be that the substrates may not be able to access the pre catalyst due to sterically hindered dipp ligand.

Experimental

General. All manipulations were performed under a dry argon atmosphere using standard Schlenk techniques or under a nitrogen atmosphere in a glovebox unless otherwise indicated. Water and oxygen were removed from benzene, pentane, and ether solvents using an IT PureSolv system. Benzene-d_6, tetrahydrofuran-d_8, and toluene-d_8 were heated to reflux over Na/K alloy and vacuum-transferred. $ScCl_3THF_3$ was prepared by reaction of Sc_2O_3 with conc. HCl followed by dehydration with $SOCl_2$ according to the literature.[25, 26, 27] YCl_3 and $LuCl_3$ were purchased from Strem Chemicals and used as received. Aniline, 2,6-dimethylaniline, and 2,6-diisopropylaniline and were purchased from Sigma-Aldrich (aniline compounds) and dimethylchlorosilane was purchased from Gelest and distilled before use. *n*BuLi was purchased from Sigma-Aldrich and

www.manaraa.com

used as received. ^{1}H, $^{13}C\{^{1}H\}$, and $^{29}Si\{^{1}H\}$ HMBC NMR spectra were collected on a Bruker DRX-400 spectrometer or a Bruker Avance III-600 spectrometer. Infrared spectra were measured on a Bruker Vertex 80, using KBr pellet (transmission mode). Elemental analyses were performed using a Perkin-Elmer 2400 Series II CHN/S. X-ray diffraction data was collected on a Bruker APEX II diffractometer.

HN(SiHMe$_2$)Ph (**1a**). A mixture of aniline (4.83 mL, 0.0530 mol) and pentane (300 mL) was cooled to 0 °C, and *n*BuLi (21.2 mL, 0.0530 mol) was added in a dropwise fashion. The reaction mixture was warmed to room temperature and stirred overnight. A pale-yellow solid precipitated, which was isolated by filtration. The solid was dissolved in diethyl ether (500 mL), and the solution was cooled to 0 °C. Then, ClSiHMe$_2$ (5.89 mL, 0.0530 mol) was added slowly, and the reaction mixture was allowed to warm to room temperature and stir overnight. The solution was filtered to remove the salts (presumably LiCl), and the filtrate was concentrated under vacuum. The resulting red liquid was distilled under full vacuum (34 °C) to obtain a colorless solution. The solution was a mixture of the desired HN(SiHMe$_2$)Ph (4.34 g, 0.0287 mol, 54.2%) and the disilylaniline N(SiHMe$_2$)$_2$Ph in a ratio 10.5:1 ratio. This mixture was used directly in the synthesis of LiN(SiHMe$_2$)Ph described below. ^{1}H NMR (benzene-d_6, 600 MHz, 25 °C): δ 7.13 (t, 2 H, $^{3}J_{HH}$ = 7.6 Hz, *m*-C_6H_5), 6.77 (t, 1 H, $^{3}J_{HH}$ = 7.8 Hz, *p*-C_6H_5), 6.61 (d, 2 H, $^{3}J_{HH}$ = 8.4 Hz, *o*-C_6H_5), 4.82 (virtual octet, 1 H, $^{1}J_{SiH}$ = 200.1 Hz, Si*H*Me$_2$), 2.93 (s, 1 H, N*H*), 0.07 (d, 6 H, $^{3}J_{HH}$ = 3.2 Hz, SiH*Me*$_2$). $^{13}C\{^{1}H\}$ NMR (benzene-d_6, 150 MHz, 25 °C): δ 147.84 (*ipso*-C_6H_5), 129.96 (*m*-C_6H_5), 118.79 (*p*-C_6H_5), 116.73 (*o*-C_6H_5), –1.92 (SiH*Me*$_2$). $^{15}N\{^{1}H\}$ NMR (benzene-d_6, 60.8 MHz, 25 °C): δ –320.81 (*N*H). $^{29}Si\{^{1}H\}$ NMR (benzene-d_6, 119.3 MHz, 25 °C): δ –14.22 (*Si*HMe$_2$). IR (KBr, cm^{-1}): 3471 w, 3383 m, 3212 w, 3074 w, 3040 m, 2962 m, 2902 w, 2129 s (SiH), 1923 w,

www.manaraa.com

1602 s, 1499 s, 1422 s, 1294 s, 1253 s, 1177 m, 1154 w, 1077 m, 1029 m, 997 m, 904 s, 834 m, 802 w, 752 s, 718 w, 692 s, 650 w, 632 w.

HN(SiHMe$_2$)dmp (1b). A mixture of H_2Ndmp (9.20 mL, 0.0747 mol; dmp = 2,6-dimethylphenyl) and pentane (300 mL) was cooled to 0 °C, and *n*BuLi (30.0 mL, 0.0747 mol) was slowly added in a dropwise manner. The reaction mixture was warmed to room temperature and stirred for 3 h, forming a white precipitate. The solid was isolated by filtration. The precipitate was dissolved in diethyl ether (500 mL) to give a solution that was cooled to 0 °C. ClSiHMe$_2$ (8.40 mL, 0.0747 mol) was then added in a dropwise fashion. The reaction mixture was warmed to room temperature and stirred for 3 h. The solution was filtered, and the volatile materials were evaporated under vacuum. The resulting yellow liquid was distilled under dynamic vacuum at 56 °C to obtain the product as a colorless liquid (10.7 g, 0.0597 mol, 79.9%). ^{1}H NMR (benzene-d_6, 600 MHz, 25 °C): δ 7.00 (d, 2 H, $^3J_{HH}$ = 7.6 Hz, *m*-C$_6$Me$_2$H$_3$), 6.86 (t, 1 H, $^3J_{HH}$ = 7.5 Hz, , *p*-C$_6$Me$_2$H$_3$), 4.87 (virtual octet, 1 H, $^1J_{SiH}$ = 201.5 Hz, Si*H*Me$_2$), 2.18 (s, 6 H, C$_6$*Me*$_2$H$_3$), 1.89 (s, 1 H, N*H*), 0.05 (d, 6 H, $^3J_{HH}$ = 3.1 Hz, SiH*Me*$_2$). ^{13}C{^{1}H} NMR (benzene-d_6, 150 MHz, 25 °C): δ 143.66 (*ipso*-C$_6$Me$_2$H$_3$), 131.08 (*o*-C$_6$Me$_2$H$_3$), 129.20 (*m*-C$_6$Me$_2$H$_3$), 122.38 (*p*-C$_6$Me$_2$H$_3$), 19.98 (C$_6$*Me*$_2$H$_3$), –0.89 (SiH*Me*$_2$). ^{15}N{^{1}H} NMR (benzene-d_6, 60.8 MHz, 25 °C): δ –333.5. ^{29}Si{^{1}H} NMR (benzene-d_6, 119.3 MHz, 25 °C): δ –10.4. IR (KBr, cm^{-1}): 3485 w, 3379 m (NH), 3074 w, 3026 w, 2960 s, 2920 m, 2855 m, 2732 w, 2126 s (SiH), 1912 w, 1842 w, 1781 w, 1724 w, 1626 m, 1596 m, 1475 s, 1432 s, 1373 s, 1318 w, 1254 s, 1219 s, 1163 w, 1098 s, 1031 w, 988 w, 910 s, 833 s, 804 w, 734 s, 700 w, 662 m, 633 w.

www.manaraa.com

LiN(SiHMe$_2$)Ph (**2a**). The mixture (2.00 g) of silylaniline HN(SiHMe$_2$)Ph (1.77 g, 0.0117 mol) and disilylaniline was added to pentane (40 mL) and cooled to –78 °C. *n*BuLi (4.68 mL, 0.0117 mol) was added in a dropwise manner, and a white precipitate formed as the addition occurred. The reaction mixture was warmed to room temperature and stirred overnight. The precipitate was isolated by filtration followed by pentane washings (2 × 20 mL). The white residue was dried under vacuum for 2.5 h to obtain the desired product as a white solid (1.37 g, 0.00872 mol, 74.5%). ^{1}H NMR (THF-d_8, 600 MHz, 25 °C): δ 6.71 (t, 2 H, $^{3}J_{HH}$ = 7.7 Hz, *m*-C$_6$H$_5$), 6.42 (d, 2 H, $^{3}J_{HH}$ = 8.3 Hz, *o*-C$_6$H$_5$), 6.05 (t, 1 H, $^{3}J_{HH}$ = 8.3 Hz, *p*-C$_6$H$_5$), 4.72 (d, br, 1 H, $^{1}J_{SiH}$ = 176.9 Hz, Si*H*Me$_2$), 0.09 (d, br, 6 H, $^{3}J_{HH}$ = 16.9 Hz, SiH*Me*$_2$). ^{13}C{^{1}H} NMR (thf-d_8, 150 MHz, 25 °C): δ 163.64 (*ipso*-C$_6$H$_5$), 128.73 (*m*-C$_6$H$_5$), 122.31 (*o*-C$_6$H$_5$), 111.00 (*p*-C$_6$H$_5$), 1.26 (SiH*Me*$_2$). ^{15}N{^{1}H} NMR (thf-d_8, 60.8 MHz, 25 °C): δ –280.79. ^{29}Si{^{1}H} NMR (THF-d_8, 119.3 MHz, 25 °C): δ –29.19 (*Si*HMe$_2$). ^{7}Li{^{1}H} NMR (THF-d_8, MHz, 25 °C): δ 0.51(s). IR (KBr, cm^{-1}): 3384 m, 3065 w, 3051 w, 3014 m, 2898 w, 2525 w, 2069 s (SiH), 1926 w, 1585 s, 1546 m, 1479 s, 1384 w, 1293 s, 1244 s, 1179 m, 1151 w, 1075 m, 1027 m, 993 m, 931 s, 904 s, 885 s, 826 s, 767 s, 753 s, 699 s, 634 w. Anal. Calcd for C$_8$H$_{12}$LiNSi: C, 61.12; H, 7.69; N, 8.91. Found: C, 61.06; H, 7.71; N, 8.71. mp 238 - 240 °C.

LiN(SiHMe$_2$)dmp (**2b**). HN(SiHMe$_2$)dmp (2.00 g, 0.0112 mol) in pentane (40 ml) was cooled to –78 °C, and *n*BuLi (4.47 mL, 0.0112 mol) was added dropwise. The reaction was warmed to room temperature and stirred overnight. The solvent was evaporated under vacuum for 2 h to obtain the product as a white solid (1.73 g, 0.00933 mol, 83.3%). ^{1}H NMR (benzene-d_6, 600 MHz, 25 °C): δ 6.93 (d, 2 H, $^{3}J_{HH}$ = 7.3 Hz, *m*-C$_6$Me$_2$H$_3$) 6.70 (br t, 1 H, *p*-C$_6$Me$_2$H$_3$), 5.10 (br s, 1 H, $^{1}J_{SiH}$ = 164.8 Hz, Si*H*Me$_2$), 1.98 (s, 6 H, C$_6$*Me*$_2$H$_3$), 0.16 (br d, 6 H, SiH*Me*$_2$). ^{13}C{^{1}H} NMR

www.manaraa.com

(benzene-d_6, 150 MHz, 25 °C): δ 154.01 (*ipso*-$C_6Me_2H_3$), 131.56 (*o*-$C_6Me_2H_3$), 129.96 (*m*-$C_6Me_2H_3$), 120.00 (*p*-$C_6Me_2H_3$), 21.13 ($C_6Me_2H_3$), 1.14 (SiHMe_2). $^{15}N\{^1H\}$ NMR (benzene-d_6, 60.8 MHz, 25 °C): δ –305.4. $^{29}Si\{^1H\}$ NMR (benzene-d_6, 119.3 MHz, 25 °C): *δ* –21.3. $^{7}Li\{^1H\}$ NMR (benzene-d_6, MHz, 25 °C): δ 1.97 (s). IR (KBr, cm^{-1}): 3374 w (NH), 3059 w, 3010 w, 2955 s, 2898 s, 2843 m, 2731 w, 2704 w, 2122 w (SiH), 2056 m (SiH), 1981 s (SiH), 1839 w, 1782 w, 1712 w, 1661 w, 1590 s, 1469 s, 1417 s, 1377 s, 1251 s, 1219 s, 1161 w, 1097 s, 935 s, 889 s, 827 s, 787 s, 759 s, 661 m, 638 m. Anal. Calcd for $C_{10}H_{16}LiNSi$: C, 64.83; H, 8.71; N, 7.56. Found: C, 64.85; H, 8.42; N, 7.24. mp 86 - 88 °C.

$Sc\{N(SiHMe_2)Ph\}_3(THF)_2$ (3a). A solid mixture of $ScCl_3(THF)_3$ (0.0779 g, 0.212 mmol) and $LiN(SiHMe_2)Ph$ (0.100 g, 0.636 mmol) was cooled to –78 °C. THF (7 mL) was cooled to –78 °C in a separate vessel. The cold THF was added to the solid mixture, and the reaction mixture was maintained at –78 °C for 1 h. The reaction mixture was allowed to warm to room temperature and stir overnight. The solvent was removed under vacuum, and the residue was extracted with pentane (3 × 5 mL). The pentane extracts were combined, and the solvent was evaporated to obtain the desired product as a white sticky solid (0.113 g, 0.177 mmol, 83.5%). ^1H NMR (benzene-d_6, 600 MHz, 25 °C): δ 7.19 (t, 6 H, $^3J_{HH}$ = 7.3 Hz, *m*-C_6H_5), 7.08 (d, 6 H, $^3J_{HH}$ = 7.8 Hz, *o*-C_6H_5), 6.87 (t, 3 H, $^3J_{HH}$ = 7.0 Hz, *p*-C_6H_5), 5.24 (br, 3 H, $^1J_{SiH}$ = 175.9 Hz, Si*H*Me_2), 3.39 (s, br, 4 H, OC$H_2$$CH_2$), 0.89 (s, br, 4 H, OCH_2CH_2), 0.28 (d, 18 H, $^3J_{HH}$ = 3.1 Hz, SiHMe_2). $^{13}C\{^1H\}$ NMR (benzene-d_6, 150 MHz, 25 °C): δ 153.33 (*ipso*-C_6H_5), 129.71 (*m*-C_6H_5), 126.06 (*o*-C_6H_5), 121.20 (*p*-C_6H_5), 72.46 (OCH_2CH_2), 25.23 (OCH_2CH_2), 0.10 (SiHMe_2). $^{15}N\{^1H\}$ NMR (benzene-d_6, 60.8 MHz, 25 °C): δ –214.05. $^{29}Si\{^1H\}$ NMR (benzene-d_6, 119.3 MHz, 25 °C): δ –21.94. IR (KBr, cm^{-1}): 3381 w, 3068 w, 2957 m, 2897 w, 2531 w, 2113 m (SiH), 2064 m (SiH), 1932 w, 1586 s, 1475

www.manaraa.com

s, 1384 w, 1242 s, 1167 m, 1069 m, 999 m, 898 s, 832 s, 805 s, 753 s, 696 s. Anal. Calcd for $C_{28}H_{44}N_3OScSi_3$(1THF): C, 59.22; H, 7.81; N, 7.40. Found: C, 58.90; H, 7.70; N, 7.08. mp 110 - 112 °C.

$Y\{N(SiHMe_2)Ph\}_3(THF)_2$ (4a). A solid mixture of YCl_3 (0.120 g, 0.614 mmol) and $LiN(SiHMe_2)Ph$ (0.290 g, 1.84 mmol) was cooled to –78 °C. THF (7 mL) was cooled to –78 °C in a separate vessel. The cold THF was added to the solid mixture. The reaction mixture was maintained at –78 °C for 1 h, then it was allowed to warm to room temperature and stir overnight. The solvent was removed under vacuum, and the residue was extracted with pentane (3 × 5 mL). The pentane extracts were combined, and the solvent was evaporated to obtain the desired product as a white sticky solid (0.0995 g, 0.145 mmol, 23.7%). ^{1}H NMR (benzene-d_6, 600 MHz, 25 °C): δ 7.22 (t, 6 H, $^3J_{HH}$ = 7.7 Hz, *m*-C_6H_5), 7.07 (d, 6 H, $^3J_{HH}$ = 8.6 Hz, *o*-C_6H_5), 6.83 (t, 3 H, $^3J_{HH}$ = 7.4 Hz, *p*-C_6H_5), 4.95 (septet, 3 H, $^3J_{HH}$ = 3.1 Hz, $^1J_{SiH}$ = 173.2 Hz, Si*H*Me_2), 3.68 (s, 8 H, OC*H*$_2$$CH_2$), 1.11 (s, 8 H, OCH_2C*H*$_2$), 0.39 (d, 18 H, $^3J_{HH}$ = 3.3 Hz, SiH*Me*$_2$). ^{13}C{^{1}H} NMR (benzene-d_6, 150 MHz, 25 °C): δ 155.33 (*ipso*-C_6H_5), 129.82 (*m*-C_6H_5), 124.89 (*o*-C_6H_5), 119.17 (*p*-C_6H_5), 71.53 (O*C*$H_2$$CH_2$), 25.48 ($OCH_2$*C*$H_2$), 0.59 (SiH*Me*$_2$). ^{15}N{^{1}H} NMR (benzene-d_6, 60.8 MHz, 25 °C): δ –234.97. ^{29}Si{^{1}H} NMR (benzene-d_6, 119.3 MHz, 25 °C): δ –24.66 (*Si*HMe_2). IR (KBr, cm^{-1}): 3383 w, 3067 w, 3047 w, 2958 m, 2896 w, 2531 w, 2117 m (SiH), 2075 m (SiH), 1588 s, 1481 s, 1384 w, 1293 m, 1256 s, 1244 s, 1219 s, 1181 w, 1076 w, 1019 m, 995 m, 919 s, 876 s, 831 m, 791 m, 697 s, 646 w, 630 w. Anal. Calcd for $C_{32}H_{52}N_3O_2Si_3Y$: C, 56.20; H, 7.66; N, 6.14. Found: C, 56.23; H, 7.67; N, 6.13. mp 114 - 116 °C.

www.manaraa.com

Lu{N(SiHMe$_2$)Ph}$_3$(THF)$_2$ (5a). A solid mixture of $LuCl_3$ (0.145 g, 0.515 mmol) and LiN(SiHMe$_2$)Ph (0.243 g, 1.54 mmol) was cooled to –78 °C. THF (7 mL) was cooled to –78 °C in a separate vessel. The cold THF was added to the solid mixture, and the reaction mixture was allowed to stand for 1 h at –78 °C. The mixture was warmed to room temperature and stirred overnight. The solvent was removed under vacuum and the residue was extracted with pentane (3 × 5 mL). The pentane extracts were combined, and the solvent was evaporated to obtain the desired product as a white sticky solid (0.0984 g, 0.128 mmol, 24.8%). ^{1}H NMR (benzene-d_6, 600 MHz, 25 °C): δ 7.22 (t, 6 H, $^3J_{HH}$ = 7.5 Hz, *m*-C_6H_5), 7.12 (d, 6 H, $^3J_{HH}$ = 7.5 Hz, *o*-C_6H_5), 6.83 (t, 3 H, $^3J_{HH}$ = 7.1 Hz, *p*-C_6H_5), 4.90 (septet, 3 H, $^3J_{HH}$ = 3.1 Hz, $^1J_{SiH}$ = 173.6 Hz, Si*H*Me$_2$), 3.66 (s, 8 H, OC*H*$_2$CH$_2$), 1.09 (s, 8 H, OCH$_2$C*H*$_2$), 0.40 (d, 18 H, $^3J_{HH}$ = 3.2 Hz, SiH*Me*$_2$). ^{13}C{^{1}H} NMR (benzene-d_6, 150 MHz, 25 °C): δ 155.21 (*ipso*-C_6H_5), 129.76 (*m*-C_6H_5), 125.30 (*o*-C_6H_5), 119.47 (*p*-C_6H_5), 71.68 (O*C*H$_2$CH$_2$), 25.50 (OCH$_2$*C*H$_2$), 0.53 (SiH*Me*$_2$). ^{15}N{^{1}H} NMR (benzene-d_6, 60.8 MHz, 25 °C): δ –233.56. ^{29}Si{^{1}H} NMR (benzene-d_6, 119.3 MHz, 25 °C): δ –22.97. IR (KBr, cm^{-1}): 3380 w, 3069 w, 3046 w, 2958 m, 2896 w, 2532 w, 2123 m (SiH), 2081 m (SiH), 1932 w, 1589 s, 1480 s, 1384 w,1243 s, 1213 s, 1180 w, 1076 w, 1016 m, 995 m, 918 s, 884 s, 831 m, 793 m, 754 s, 698 s, 646 w, 630 w. Anal. Calcd for $C_{32}H_{52}LuN_3O_2Si_3$: C, 49.92; H, 6.81; N, 5.46. Found: C, 50.38; H, 6.67; N, 5.55. mp 118 - 120 °C.

Y{N(SiHMe$_2$)dmp}$_3$(THF) (4b). A solid mixture of YCl_3 (0.104 g, 0.531 mmol) and LiN(SiHMe$_2$)dmp (0.295 g, 1.59 mmol) was cooled to –78 °C. THF (7 mL) was cooled to –78 °C separately and added to the solid mixture. The reaction vial was stirred at –78 °C for 1 h and warmed to room temperature and stirred overnight. The solvent was evaporated under vacuum and the solid was extracted with pentane (3 X 5 mL). The pentane extract was dried under vacuum to

www.manaraa.com

obtain the product as a sticky solid (0.265 g, 0.381 mmol, 71.7%). ^{1}H NMR (benzene-d_6, 600 MHz, 25 °C): δ 7.10 (d, 6 H, $^{3}J_{HH}$ = 7.4 Hz, *m*-$C_6Me_2H_3$), 6.84 (t, 3 H, $^{3}J_{HH}$ = 7.4 Hz, *p*-$C_6Me_2H_3$), 5.20 (s, broad, 3 H, $^{1}J_{SiH}$ = 151.3 Hz, Si*H*Me_2), 3.45 (s, broad, 4 H, OC*H*$_2$CH$_2$), 2.36 (s, 18 H, C_6*Me*$_2H_3$), 0.94 (s, broad, 4 H, OCH$_2$C*H*$_2$), 0.15 (broad, 18 H, SiH*Me*$_2$). ^{13}C{^{1}H} NMR (benzene-d_6, 150 MHz, 25 °C): δ 151.02 (*ipso*-$C_6Me_2H_3$), 132.86 (*o*-$C_6Me_2H_3$), 129.01 (*m*-$C_6Me_2H_3$), 120.95 (*p*-$C_6Me_2H_3$), 72.24 (O*C*H$_2$CH$_2$), 25.06 (OCH$_2$*C*H$_2$), 21.72 (C_6*Me*$_2H_3$), 2.19 (SiH*Me*$_2$). ^{15}N{^{1}H} NMR (benzene-d_6, 60.8 MHz, 25 °C): δ –234.6. ^{29}Si{^{1}H} NMR (benzene-d_6, 119.3 MHz, 25 °C): δ –25.28. IR (KBr, cm^{-1}): 3059 w, 2948 m, 2095 m, 2057 m (SiH), 1966 w (SiH), 1590 m, 1468 s, 1420 s, 1370 w, 1252 s, 1218 s, 1098 m, 1006 m, 927 s, 882 s, 834 s, 796 s, 762 s, 661 w, 635 w. Anal. Calcd for $C_{34}H_{56}N_3OSi_3Y$: C, 58.67; H, 8.11; N, 6.04. Found: C, 58.52; H, 8.19; N, 5.97. mp 142 - 144 °C.

Lu{N(SiHMe$_2$)dmp}$_3$(THF) (5b). A solid mixture of $LuCl_3$ (0.468 g, 1.66 mmol) and LiN(SiHMe$_2$)dmp (0.924 g, 4.99 mmol) was cooled to –78 °C. THF (7 mL) was cooled to –78 °C separately and added to the solid mixture. The reaction vial was stirred at –78 °C for 1 h and warmed to room temperature and stirred overnight. The solvent was evaporated under vacuum and the solid was extracted with benzene (3 X 5 mL). The benzene extract was dried under vacuum to obtain the product as a white solid (1.02 g, 1.31 mmol, 78.6%). ^{1}H NMR (benzene-d_6, 600 MHz, 25 °C): δ 7.11 (d, 6 H, $^{3}J_{HH}$ = 7.3 Hz, *m*-$C_6Me_2H_3$) 6.85 (t, 3 H, $^{3}J_{HH}$ = 7.4 Hz, *p*-$C_6Me_2H_3$), 5.20 (septet, 3 H, $^{1}J_{SiH}$ = 155.8 Hz, Si*H*Me_2), 3.57 (s, broad, 4 H, OC*H*$_2$CH$_2$), 3.56 (s, broad, 8 H, residual THF), 2.39 (s, 18 H, C_6*Me*$_2H_3$), 1.41 (s, broad, 8 H, residual THF), 0.97 (s, broad, 4 H, OCH$_2$C*H*$_2$), 0.13 (d, 18 H, $^{3}J_{HH}$ = 3.0 Hz, SiH*Me*$_2$). ^{13}C{^{1}H} NMR (benzene-d_6, 150 MHz, 25 °C): δ 151.17 (*ipso*-$C_6Me_2H_3$), 133.53 (*o*-$C_6Me_2H_3$), 128.99 (*m*-$C_6Me_2H_3$), 121.23 (*p*-$C_6Me_2H_3$), 73.06 (O*C*H$_2$CH$_2$), 68.28 (residual THF), 26.08 (residual THF), 25.10 (OCH$_2$*C*H$_2$), 21.77 (C_6*Me*$_2H_3$),

www.manaraa.com

2.00 (SiH*Me*$_2$). ^{15}N{^{1}H} NMR (benzene-d_6, 60.8 MHz, 25 °C): δ –235.2. ^{29}Si{^{1}H} NMR (benzene-d_6, 119.3 MHz, 25 °C): δ –23.72. IR (KBr, cm^{-1}): 3057 m, 3031 m, 2970 s, 2945 s, 2886 s, 2071 s (SiH), 1902 w (SiH), 1832 w, 1764 w, 1589 s, 1464 s, 1417 s, 1370 m, 1254 s, 1216 s, 1098 s, 1045 s, 936 s, 873 s, 831 s, 798 s, 758 s, 733 s, 674 m, 659 m, 634 m. Anal. Calcd for $C_{34}H_{56}LuN_3OSi_3$: C, 52.22; H, 7.22; N, 5.37. Found: C, 52.49; H, 7.38; N, 5.09. mp 130 - 132 °C.

Lu{N(SiMe$_2$OCHMePh)dipp}{N(SiHMe$_2$)dipp}$_2$ (5d). Lu{N(SiHMe$_2$)dipp}$_3$ (0.1781 g, 0.203 mmol) was dissolved in benzene (3 mL), and acetophenone (23.6 μL, 0.203 mmol) was added to the solution. The reaction mixture was stirred for 15 min., and the solvent was evaporated under vacuum. The resulting oily residue was extracted with pentane (3 × 5 mL), concentrated, and cooled to –30 °C to provide the desired product as a white crystalline solid (0.133 g, 0.125 mmol, 61.4%). ^{1}H NMR (benzene-d_6, 600 MHz, 25 °C): δ 7.19 – 6.95 (14 H, aromatic region), 5.57 (br s, 2 H, $^1J_{SiH}$ = 135.3 Hz, Si*H*Me$_2$), 5.06 (q, 1 H, $^3J_{HH}$ = 6.5 Hz, OC*H*MePh), 3.85 (br vt, 4 H, C*H*Me$_2$), 3.66 (v pentet, 2 H, $^3J_{HH}$ = 5.7 Hz, C*H*Me$_2$), 1.39 (d, 3 H, $^3J_{HH}$ = 6.5 Hz, OCH*Me*Ph), 1.32 (br, 12 H, CH*Me*$_2$), 1.26 (br, 12 H, CH*Me*$_2$), 1.19 (d, 6 H, $^3J_{HH}$ = 6.6 Hz, CH*Me*$_2$), 1.00 (br s, 6 H, CH*Me*$_2$), 0.40 (br s, 12 H, SiH*Me*$_2$), 0.21 (s, 3 H, Si*Me*$_2$), –0.24 (s, 3 H, Si*Me*$_2$). ^{13}C{^{1}H} NMR (benzene-d_6, 150 MHz, 25 °C): δ 148.25, 145.07, 144.60, 143.62, 143.42, 141.81, 129.40, 129.30, 128.68, 127.22, 124.83, 124.28, 122.46, 122.35 (aromatic region), 78.09 (O*C*HMePh), 27.95 (*C*HMe$_2$), 27.71 (*C*HMe$_2$), 27.30 (CH*Me*$_2$), 27.09 (CH*Me*$_2$), 26.48 (OCH*Me*Ph), 26.19 (CH*Me*$_2$), 24.23 (CH*Me*$_2$), 4.23 (Si*Me*$_2$), 3.91 (SiH*Me*$_2$), 2.57 (Si*Me*$_2$). ^{29}Si{^{1}H} NMR (benzene-d_6, 119.3 MHz, 40 °C): δ 3.46 (*Si*Me$_2$). IR (KBr, cm^{-1}): 3388 w, 3051 w, 2962 s, 2929 m, 2868 m, 2109 w (SiH, from hydrolysis), 2001 w (SiH), 1881 m (SiH), 1621 w, 1588 w, 1494 w, 1460 s, 1427 s, 1382 w, 1361 w, 1307 m, 1251 s, 1238 s, 1190 s, 1148 w, 1110 s, 1060 m, 1038 s, 1009

www.manaraa.com

w, 996 w, 951 m, 922 s, 910 s, 859 m, 838 s, 812 m, 781 s, 763 m, 748 m, 702 m, 676 w, 637 w, 606 w. Anal. Calcd for $C_{55}H_{91}N_3OSi_3Lu$ (with pentane): C, 61.76; H, 8.58; N, 3.93. Found: C, 61.85; H, 8.65; N, 3.75. mp 184 - 186 °C.

Y{N(SiMe$_2$OCHPh$_2$)dipp}{N(SiHMe$_2$)dipp}$_2$ (4e). Y{N(SiHMe$_2$)dipp}$_3$ (0.0614 g, 0.0775 mmol) was dissolved in benzene (3 mL), and benzophenone (0.0141 g, 0.0775 mmol) was added to the solution. The reaction mixture was stirred for 15 min., and the solvent was evaporated under vacuum. The resulting oily residue was extracted with pentane (3 × 5 mL), concentrated, and cooled to –30 °C to provide the desired product as a white crystalline solid (0.0426 g, 0.0437 mmol, 56.4%). ^{1}H NMR (benzene-d_6, 600 MHz, 25 °C): δ 7.29 – 6.88 (19 H, aromatic region), 6.53 (s, 1 H, OC*H*Ph$_2$), 5.01 (br s, 2 H, $^1J_{SiH}$ = 131.9 Hz, Si*H*Me$_2$), 3.71 (v pentet, 2 H, $^3J_{HH}$ = 6.5 Hz, C*H*Me$_2$), 3.65 (br, 4 H C*H*Me$_2$), 1.26 (br, 24 H, CH*Me$_2$*), 1.13 (br, 12 H CH*Me$_2$*), 0.21 (br s, 12 H, SiH*Me$_2$*), 0.05 (s, 6 H, Si*Me$_2$*). ^{13}C{^{1}H} NMR (benzene-d_6, 150 MHz, 25 °C): δ 148.59, 146.13, 144.30, 142.60, 140.94, 129.64, 129.30, 124.85, 124.42, 122.31, 121.87 (aromatic region), 83.42 (O*C*HPh$_2$), 28.19(*C*HMe$_2$), 27.94 (*C*HMe$_2$), 26.68 (CH*Me$_2$*), 26.56 (CH*Me$_2$*), 4.33 (Si*Me$_2$*), 3.10 (SiH*Me$_2$*). ^{29}Si{^{1}H} NMR (benzene-d_6, 119.3 MHz, 40 °C): δ –24.1 (*Si*HMe$_2$), 4.84 (*Si*Me$_2$). IR (KBr, cm^{-1}): 3387 w, 3062 w, 2962 s, 2929 s, 2869 m, 2108 w (SiH, from hydrolysis), 1965 w (SiH), 1886 w (SiH), 1620 w, 1588 w, 1459 s, 1425 s, 1382 w, 1360 w, 1306 s, 1251 s, 1235 s, 1187 s, 1148 w, 1110 m, 1056 m, 1040 m, 998 s, 933 s, 914 s, 861 m, 837 s, 814 m, 782 s, 745 s, 702 s, 678 w, 632 w. Anal. Calcd for $C_{55}H_{82}N_3OSi_3Y$: C, 67.79; H, 8.48; N, 4.31. Found: C, 68.24; H, 7.94; N, 3.95. mp 187 - 189 °C.

www.manaraa.com

Lu{N(SiMe$_2$OCHPh$_2$)dipp}{N(SiHMe$_2$)dipp}$_2$ (5e). Lu{N(SiHMe$_2$)dipp}$_3$ (0.0533 g, 0.0607 mmol) was dissolved in benzene (3 mL), and benzophenone (0.0110 g, 0.0609 mmol) was added to the solution. The reaction mixture was stirred for 15 min., and the solvent was evaporated under vacuum. The resulting oily residue was extracted with pentane (3 × 5 mL), concentrated, and cooled to –30 °C to provide the desired product as a white crystalline solid (0.0375 g, 0.0352 mmol, 58.0%). ^{1}H NMR (benzene-d_6, 600 MHz, 25 °C): δ 7.24 – 6.87 (19 H, aromatic region), 6.62 (s, 1 H, OC*H*Ph$_2$), 5.29 (br s, 2 H, $^1J_{SiH}$ = 133.1 Hz, Si*H*Me$_2$), 3.72 (br s, 6 H, C*H*Me$_2$), 1.26 (br, 24 H, CH*Me*$_2$), 1.12 (br, 12 H CH*Me*$_2$), 0.26 (br s, 12 H, SiH*Me*$_2$), 0.05 (s, 6 H, Si*Me*$_2$). ^{13}C{^{1}H} NMR (benzene-d_6, 150 MHz, 25 °C): δ 148.69, 146.15, 144.94, 143.15, 141.11, 129.41, 129.14, 124.95, 124.31, 122.54, 122.09 (aromatic region), 83.58 (O*C*HPh$_2$), 28.24(*C*HMe$_2$), 27.79 (*C*HMe$_2$), 26.80 (CH*Me*$_2$), 26.65 (CH*Me*$_2$), 4.49 (Si*Me*$_2$), 3.12 (SiH*Me*$_2$). ^{29}Si{^{1}H} NMR (benzene-d_6, 119.3 MHz, 40 °C): δ –21.79 (*Si*HMe$_2$), –4.10 (*Si*Me$_2$). IR (KBr, cm^{-1}): 3387 w, 3059 w, 3046 w, 3008 s, 2963 s, 2869 m, 2110 w (SiH, from hydrolysis), 1957 m (SiH), 1619 w, 1587 w, 1497 w, 1458 s, 1425 s, 1382 m, 1360 w, 1317 m, 1305 s, 1248 s, 1235 s, 1188 s, 1147 w, 1098 m, 1059 m, 1040 m, 994 s, 935 s, 910 s, 875 m, 834 s, 804 m, 781 s, 749 m, 738 m, 702 s, 681 w, 655 w, 628 w Anal. Calcd for $C_{55}H_{82}N_3OSi_3Lu$: C, 62.29; H, 7.79; N, 3.96. Found: C, 62.35; H, 8.16; N, 3.85. mp 190 - 192 °C.

Y{N(SiMe$_2$OCHMe$_2$)dipp}$_2${N(SiHMe$_2$)dipp} (4f).

Y{N(SiHMe$_2$)dipp}$_3$ (0.105 g, 0.132 mmol) was dissolved in toluene (3 mL), and cooled to –78 °C. Acetone (0.0215 mL, 0.291 mmol) was added to the cold solution, and the reaction mixture was stirred for 10 min. The solvent was evaporated under vacuum. The resulting oily residue was washed with pentane (3 × 5 mL) and dried under vacuum to provide the desired

www.manaraa.com

product as a white solid (0.0678 g, 0.0746 mmol, 56.3%). Further recrystallization with pentane at –30 °C gave the X-ray quality crystals. ^{1}H NMR (benzene-d_6, 600 MHz, 25 °C): δ 7.24 – 7.03 (9 H, aromatic region), 5.57 (br s, 1 H, $^{1}J_{SiH}$ = 138.7 Hz, Si*H*Me$_2$), 4.17 (v pentet, 2 H, $^{3}J_{HH}$ = 6.5 Hz, OC*H*Me$_2$), 3.98 (v pentet, 2 H, $^{3}J_{HH}$ = 6.5 Hz, C*H*Me$_2$), 3.71 (br, 3 H, C*H*Me$_2$), 3.54 (v triplet, 1 H, $^{3}J_{HH}$ = 6.5 Hz, C*H*Me$_2$), 1.52 (d, 6 H, $^{3}J_{HH}$ = 7.2 Hz CH*Me*$_2$), 1.48 (d, 3 H, $^{3}J_{HH}$ = 6.6 Hz, CH*Me*$_2$), 1.42 (d, 6 H, $^{3}J_{HH}$ = 6.6 Hz CH*Me*$_2$), 1.29 (v triplet, 6 H, $^{3}J_{HH}$ = 5.5 Hz, CH*Me*$_2$), 1.23 (d, 6 H, $^{3}J_{HH}$ = 6.4 Hz CH*Me*$_2$), 1.19 (d, 3 H, $^{3}J_{HH}$ = 6.7 Hz, CH*Me*$_2$), 0.93 (br s, 6 H, CH*Me*$_2$), 0.88 (d, 6 H, $^{3}J_{HH}$ = 6.1 Hz OCH*Me*$_2$), 0.84 (d, 6 H, $^{3}J_{HH}$ = 6.1 Hz OCH*Me*$_2$), 0.49 (d, 3 H, $^{3}J_{HH}$ = 2.2 Hz SiH*Me*$_2$), 0.34 (d, 3 H, $^{3}J_{HH}$ = 2.4 Hz SiH*Me*$_2$), 0.32 (s, 6 H, Si*Me*$_2$), 0.23 (s, 6 H, Si*Me*$_2$). ^{13}C{^{1}H} NMR (benzene-d_6, 150 MHz, 25 °C): δ 150.03, 147.24, 144.35, 144.09, 143.55, 143.12, 124.85, 124.72, 124.60, 121.79 (aromatic region), 71.33 (O*C*HMe$_2$), 28.38 (CH*Me*$_2$), 28.28 (CH*Me*$_2$), 28.09 (CH*Me*$_2$), 27.95 (CH*Me*$_2$), 27.40 (*C*HMe$_2$), 27.35 (*C*HMe$_2$), 27.29 (*C*HMe$_2$), 26.87 (CH*Me*$_2$), 26.70 (CH*Me*$_2$), 26.37 (CH*Me*$_2$), 25.59 (OCH*Me*$_2$), 24.91(OCH*Me*$_2$), 5.21 (SiH*Me*$_2$), 4.99 (Si*Me*$_2$), 4.12 (Si*Me*$_2$), 3.55 (SiH*Me*$_2$). ^{29}Si{^{1}H} NMR (benzene-d_6, 119.3 MHz, 40 °C): –25.36 (*Si*HMe$_2$), 0.23 (*Si*Me$_2$), 0.25 (*Si*Me$_2$). IR (KBr, cm^{-1}): 3050 w, 2964 s, 2870 m, 1991 w (SiH), 1622 w, 1588 w, 1462 s, 1423 s, 1381 m, 1361 w, 1306 s, 1251 s, 1229 s, 1181 s, 1143 w, 1109 s, 1039 w, 960 s, 937 s, 873 w, 859 w, 836 s, 812 m, 779 s, 745 w, 701 w, 680 w, 629 w. Anal. Calcd for $C_{48}H_{84}N_3O2Si_3Y$: C, 63.47; H, 9.32; N, 4.63. Found: C, 63.02; H, 9.34; N, 4.50. mp 215 - 217 °C.

Y{N(SiHMe$_2$)dipp}$_3${pyridine} (4c·py). Y{N(SiHMe$_2$)dipp}$_3$ (0.142 g, 0.179 mmol) was dissolved in benzene (3 mL), and pyridine (0.0144 mL, 0.179 mmol) was added to the solution. The reaction mixture was stirred for 10 min and the solvent was evaporated under vacuum. The

www.manaraa.com

resulting oily residue was extracted with pentane (3 × 5 mL), concentrated, and cooled to –30 °C to provide the desired product as a white crystalline solid (0.0893 g, 0.102 mmol, 57.2%). ^{1}H NMR (benzene-d_6, 600 MHz, 25 °C): δ 8.07 (br s, 2 H, *o*-NC_5H_5), 7.15 (br s, 6 H, *m*-C_6H_5), 7.05 (t, 3 H, $^{3}J_{HH}$ = 7.3 Hz, *p*-C_6H_5), 6.60 (br s, 1 H, *p*-NC_5H_5), 6.35 (br s, 2 H, *m*-NC_5H_5), 5.33 (br s, 3 H, $^{1}J_{SiH}$ = 150.5 Hz, Si*H*Me_2), 3.64 (br s, 6 H, C*H*Me_2), 1.24 (br s, 18 H, CH*Me*$_2$), 1.00 (br s, 18 H, CH*Me*$_2$), 0.21 (br s, 18 H, SiH*Me*$_2$). ^{13}C{^{1}H} NMR (benzene-d_6, 150 MHz, 25 °C): δ 149.51 (*o*-NC_5H_5), 148.78 (*ipso*-C_6H_5), 143.50 (*o*-C_6H_5), 140.24 (*p*-NC_5H_5), 124.89 (*m*-NC_5H_5), 124.53 (*m*-C_6H_5), 121.91 (*p*-C_6H_5), 27.92 (*C*HMe_2), 26.84 (CH*Me*$_2$), 25.67 (CH*Me*$_2$), 2.45 (SiH*Me*$_2$). ^{29}Si{^{1}H} NMR (benzene-d_6, 119.3 MHz, 25 °C): δ –26.54. IR (KBr, cm^{-1}): 3067 w, 3049 w, 2963 s, 2869 m, 2103 m (SiH), 1959 w (SiH), 1623 w, 1604 m, 1588 w, 1462 s, 1444 m, 1425 s, 1383 w, 1361 w, 1309 m, 1259 s, 1188 s, 1156 w, 1144 w, 1107 s, 1055 s, 1040 s, 1011 s, 933 s, 912 s, 864 w, 786 s, 756 s, 704 m, 675 w, 631 w. Anal. Calcd for $C_{47}H_{77}N_4Si_3Y$: C, 64.79; H, 8.91; N, 6.43. Found: C, 64.66; H, 8.83; N, 6.43. mp 156 - 158 °C

References

1. Anwander, R., Lanthanide amides. In *Organolanthoid Chemistry: Synthesis, Structure, Catalysis*, Springer Berlin Heidelberg: Berlin, Heidelberg, 1996; pp 33-112.

2. Bradley, D. C.; Ghotra, J. S.; Hart, F. A., *Journal of the Chemical Society, Chemical Communications* **1972,** (6), 349-350.

3. Mainz, V. V.; Andersen, R. A., *Inorg. Chem.* **1980,** *19* (7), 2165-9.

4. Goodwin, C. A. P.; Joslin, K. C.; Lockyer, S. J.; Formanuik, A.; Morris, G. A.; Ortu, F.; Vitorica-Yrezabal, I. J.; Mills, D. P., *Organometallics* **2015,** *34* (11), 2314-2325.

5. Fjeldberg, T.; Andersen, R. A., *J. Mol. Struct.* **1985,** *128* (1), 49-57.

6. Anwander, R.; Runte, O.; Eppinger, J.; Gerstberger, G.; Herdtweck, E.; Spiegler, M., *J. Chem. Soc. Dalton Trans.* **1998,** (5), 847-858.

www.manaraa.com

7. Eppinger, J.; Spiegler, M.; Hieringer, W.; Herrmann, W. A.; Anwander, R., *J. Am. Chem. Soc.* **2000,** *122* (13), 3080-3096.

8. Yuen, H. F.; Marks, T. J., *Organometallics* **2009,** *28* (8), 2423-2440.

9. Parkin, G., Classification of Organotransition Metal Compounds. In *Comprehensive Organometallic Chemistry III*, Mingos, D. M. P.; Crabtree, R. H., Eds. Elsevier: Oxford, 2007; pp 1-57.

10. Green, M. L. H., *J. Organomet. Chem.* **1995,** *500* (1-2), 127-148.

11. Lin, C.-Y.; Guo, J.-D.; Fettinger, J. C.; Nagase, S.; Grandjean, F.; Long, G. J.; Chilton, N. F.; Power, P. P., *Inorg. Chem.* **2013,** *52* (23), 13584-13593.

12. Lin, C.-Y.; Fettinger, J. C.; Grandjean, F.; Long, G. J.; Power, P. P., *Inorg. Chem.* **2014,** *53* (17), 9400-9406.

13. Schumann, H.; Winterfeld, J.; Rosenthal, E. C. E.; Hemling, H.; Esser, L., *Zeitschrift für anorganische und allgemeine Chemie* **1995,** *621* (1), 122-130.

14. Wang, S.-w.; Qian, H.-m.; Yao, W.; Zhang, L.-j.; Zhou, S.-l.; Yang, G.-s.; Zhu, X.-c.; Fan, J.-x.; Liu, Y.-y.; Chen, G.-d.; Song, H.-b., *Polyhedron* **2008,** *27* (13), 2757-2764.

15. Deacon, Glen B.; Forsyth, Craig M.; Scott, Natalie M., *European Journal of Inorganic Chemistry* **2002,** *2002* (6), 1425-1438.

16. Rees, W. S. J.; Just, O.; Schumann, H.; Weimann, R., *Angew. Chem. Int. Ed. Engl.* **1996,** *35* (4), 419-422.

17. Eedugurala, N.; Wang, Z.; Yan, K.; Boteju, K. C.; Chaudhary, U.; Kobayashi, T.; Ellern, A.; Slowing, I. I.; Pruski, M.; Sadow, A. D., *Organometallics* **2017,** *36* (6), 1142-1153.

18. Yan, K.; Duchimaza Heredia, J. J.; Ellern, A.; Gordon, M. S.; Sadow, A. D., *Journal of the American Chemical Society* **2013,** *135* (40), 15225-15237.

19. Chao, Y. W.; Wexler, P. A.; Wigley, D. E., *Inorganic Chemistry* **1989,** *28* (20), 3860-3868.

20. Wiseman, G. H.; Wheeler, D. R.; Seyferth, D., *Organometallics* **1986,** *5* (1), 146-152.

21. Guzei, I. A.; Wendt, M., Program Solid-G. *UW-Madison, WI, USA* **2004**.

22. Guzei, I. A.; Wendt, M., *Dalton Trans.* **2006,** (33), 3991-3999.

23. Smith, J. M.; Taverner, B. C.; Coville, N. J., *J. Organomet. Chem.* **1997,** *530* (1-2), 131-140.

24. White, D.; Coville, N. J., In *Adv. Organomet. Chem.*, Academic Press: New York, 1994; Vol. 36, pp 95-158.

25. Freeman, J. H.; Smith, M. L. *J. Inorg. Nucl. Chem*. **1958**, *7*, 224

www.manaraa.com

26. Burton, N. C.; Cloke, F. G. N.; Hitchcock, P. B.; Lemos, H. C. D.; Sameh, A. A. *J. Chem. Soc., Chem. Commun.* **1989**, 1462

27. Burton, N. C. *D. Phil. Thesis*, University of Sussex, (1991)

Appendix

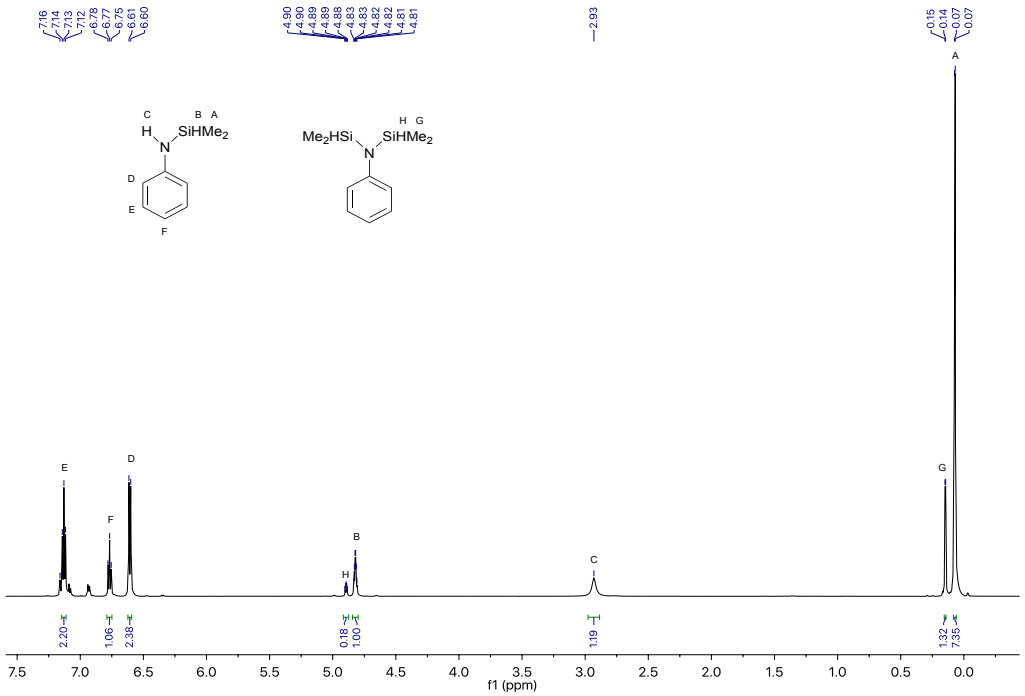

Figure S1. ^{1}H NMR spectrum of HN(SiHMe$_2$)Ph (**1a**) acquired in benzene-d_6 at room temperature. The disilazane impurity is removed during the subsequent deprotonation step.

www.manaraa.com

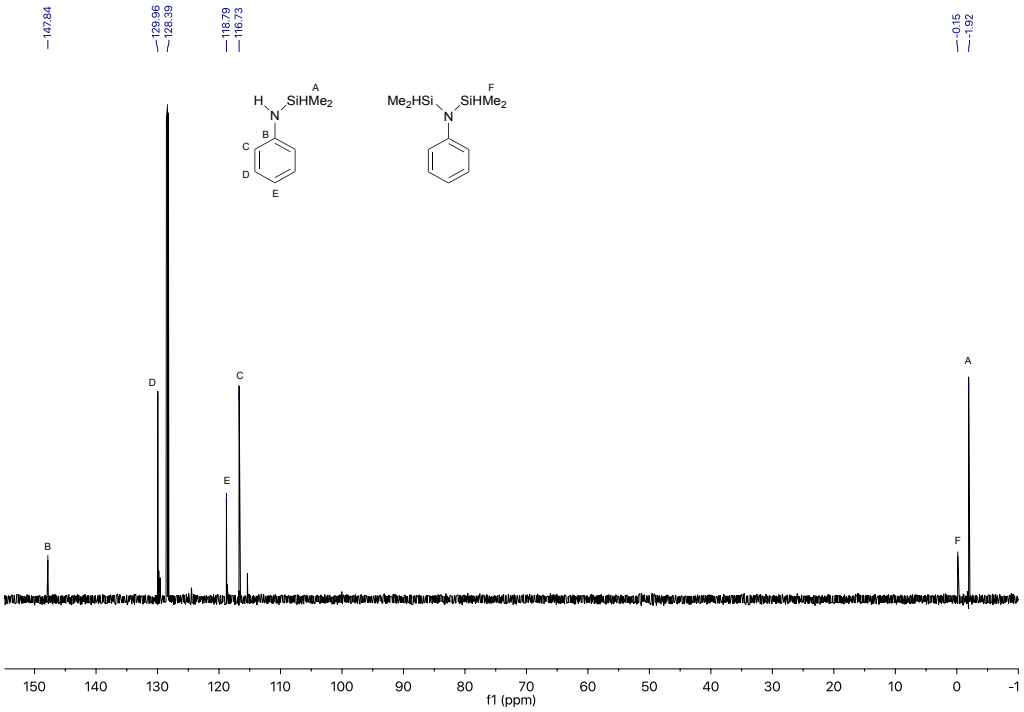

Figure S2. $^{13}C\{^{1}H\}$ NMR spectrum of HN(SiHMe$_2$)Ph (**1a**) acquired in benzene-d_6 at room temperature. The disilazane impurity is removed during the subsequent deprotonation step.

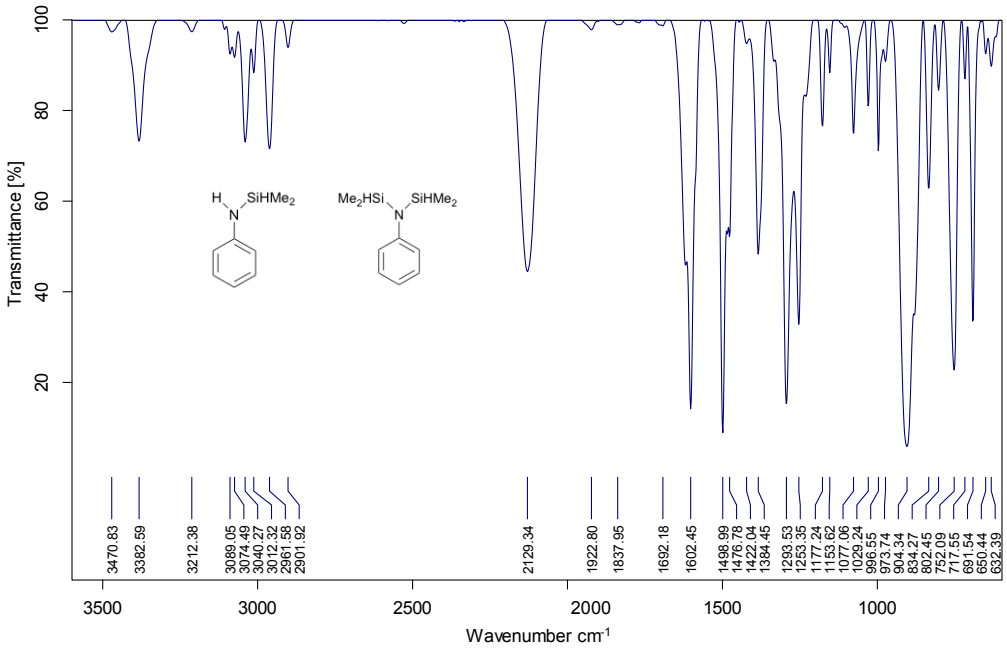

Figure S3. Infrared spectrum of HN(SiHMe$_2$)Ph (**1a**) (KBr pellet).

www.manaraa.com

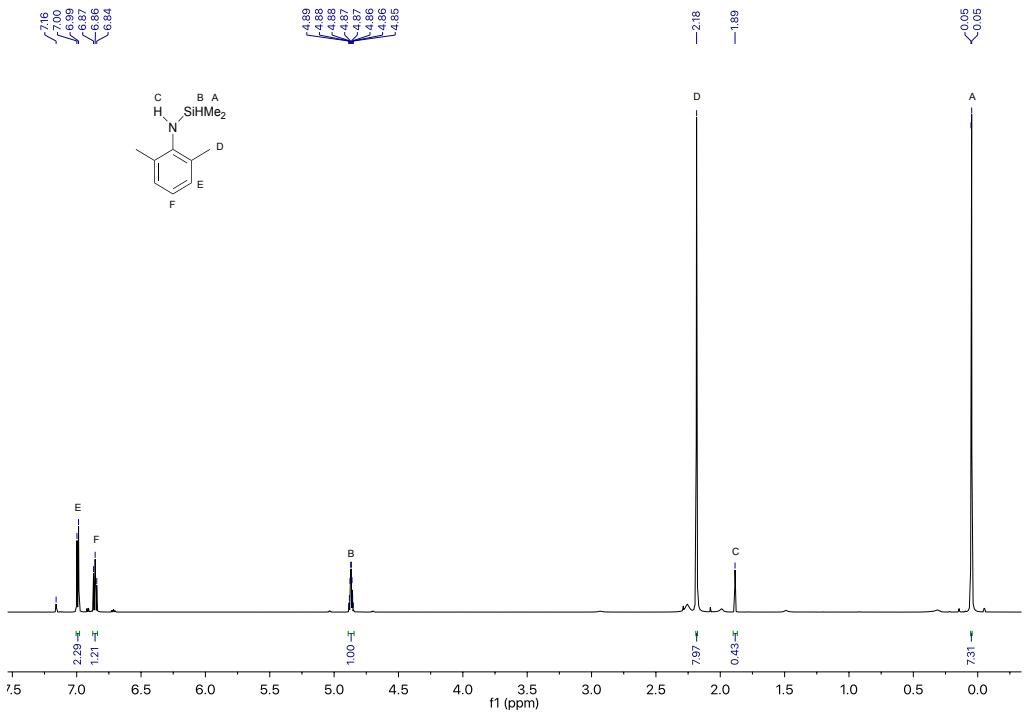

Figure S4. ^{1}H NMR spectrum of HN(SiHMe$_2$)dmp (**1b**) acquired in benzene-d_6 at room temperature.

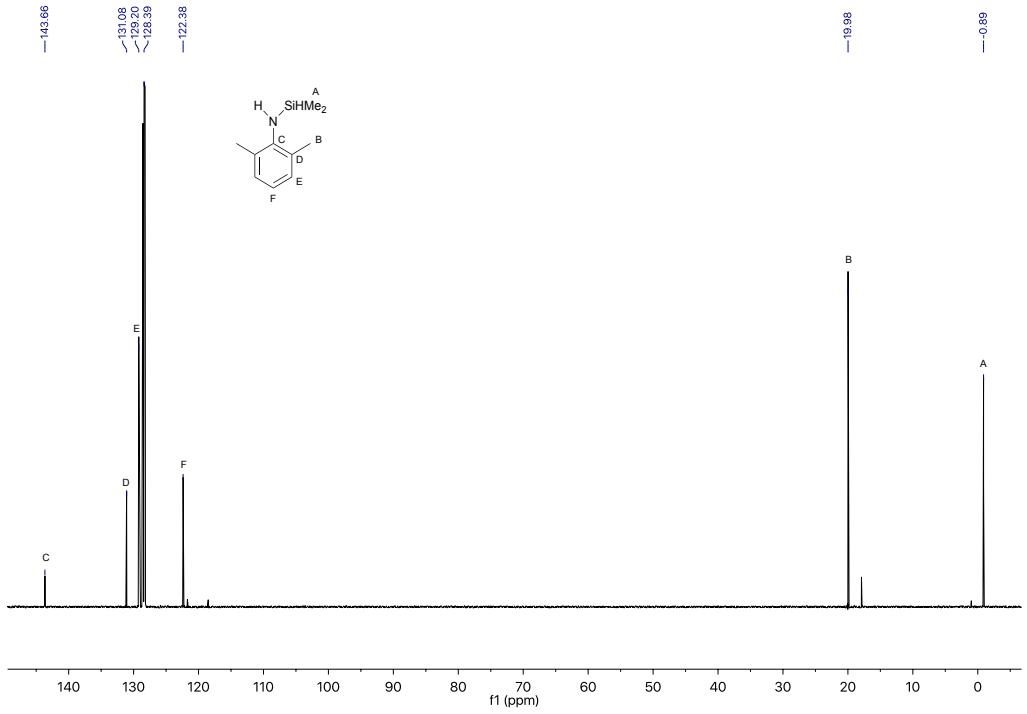

Figure S5. ^{13}C{^{1}H} NMR spectrum of HN(SiHMe$_2$)dmp (**1b**) acquired in benzene-d_6 at room temperature.

www.manaraa.com

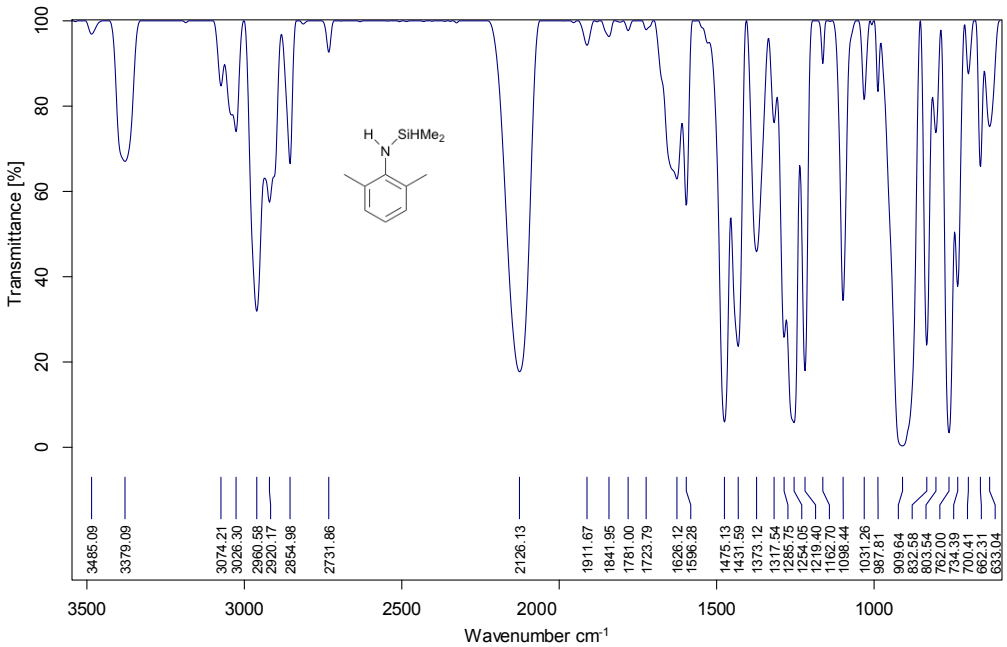

Figure S6. Infrared spectrum of HN(SiHMe$_2$)dmp (**1b**) (KBr pellet).

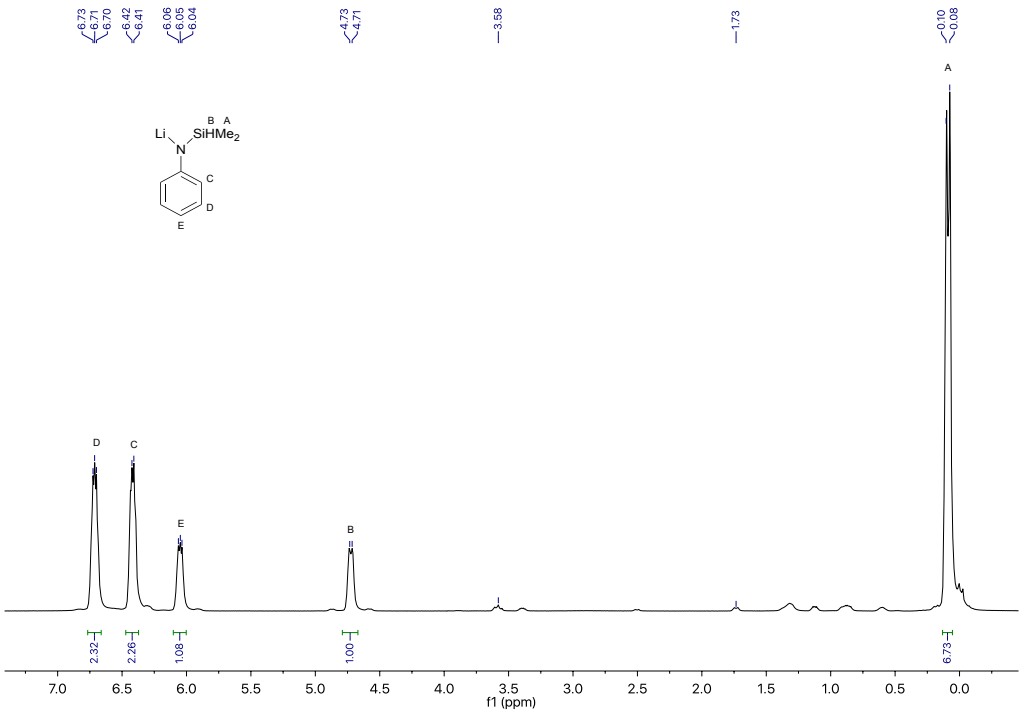

Figure S7. ^{1}H NMR spectrum of LiN(SiHMe$_2$)Ph (**2a**) acquired in tetrahydrofuran-d_8 at room temperature.

www.manaraa.com

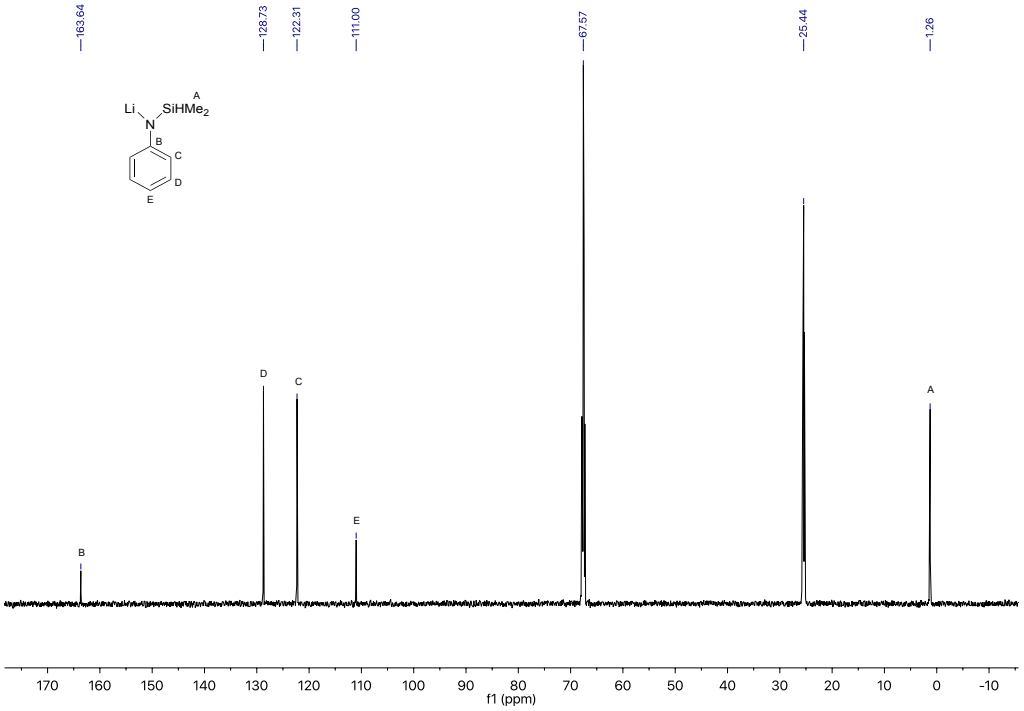

Figure S8. $^{13}C\{^{1}H\}$ NMR spectrum of LiN(SiHMe$_2$)Ph (**2a**) acquired in thf-d_8 at room temperature.

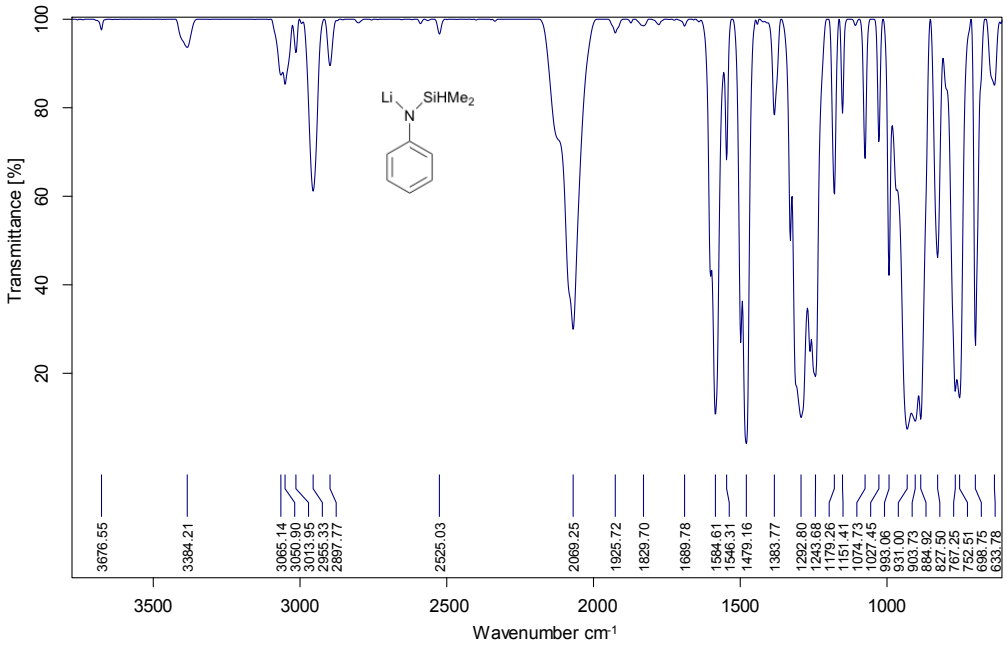

Figure S9. Infrared spectrum of LiN(SiHMe$_2$)Ph (**2a**) (KBr pellet).

www.manaraa.com

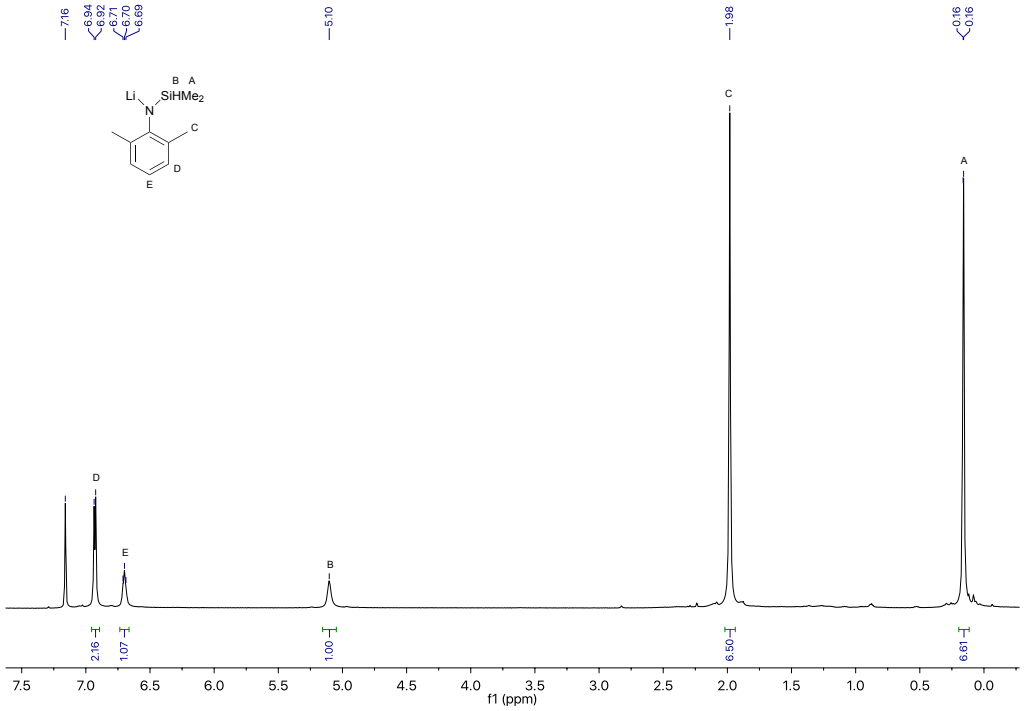

Figure S10. ^{1}H NMR spectrum of LiN(SiHMe$_2$)dmp (**2b**) acquired in benzene-d_6 at room temperature.

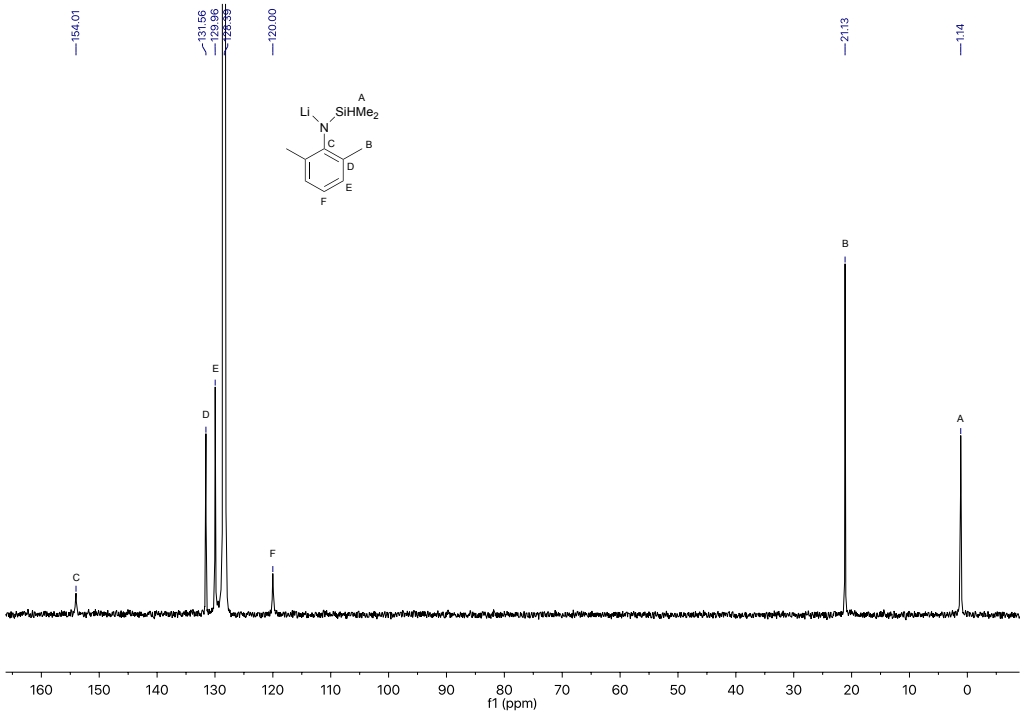

Figure S11. ^{13}C{^{1}H} NMR spectrum of LiN(SiHMe$_2$)dmp (**2b**) acquired in benzene-d_6 at room temperature.

www.manaraa.com

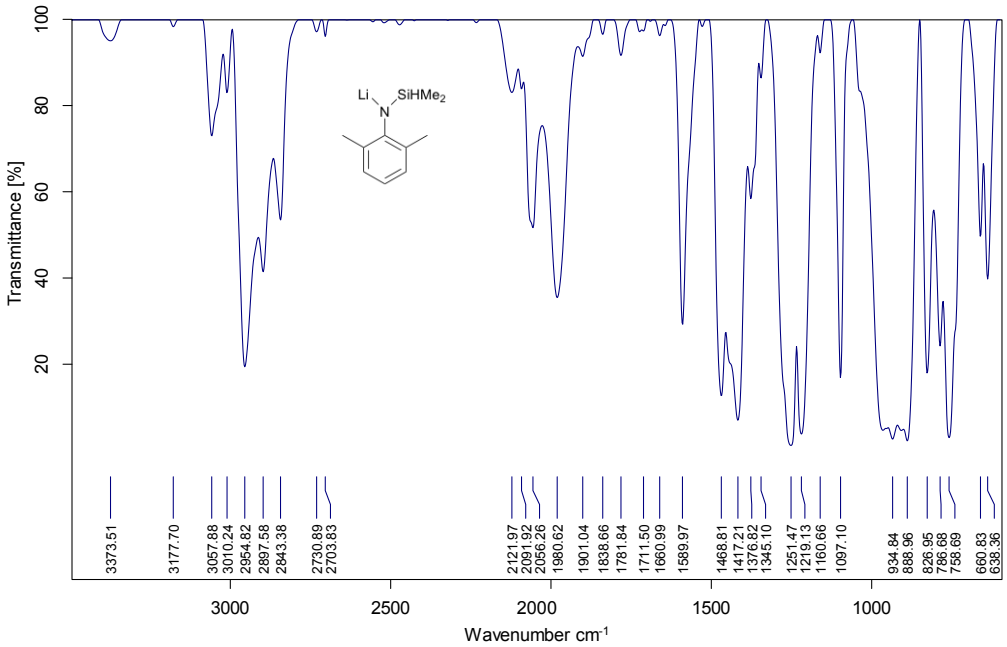

Figure S12. Infrared spectrum of LiN(SiHMe$_2$)dmp (**2b**) (KBr pellet).

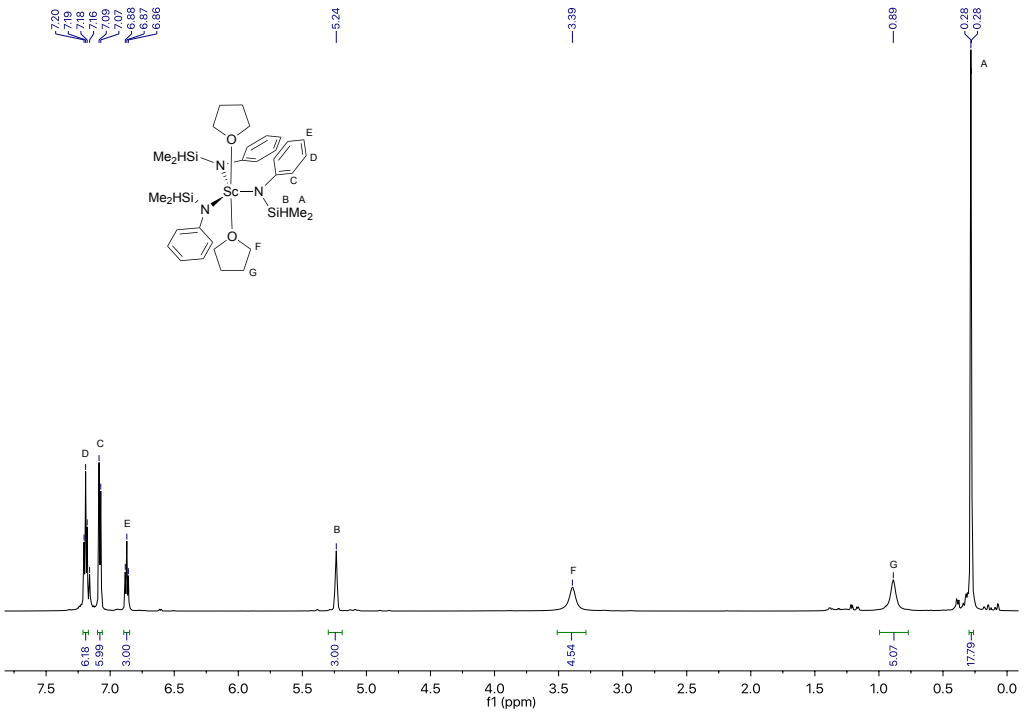

Figure S13. ^{1}H NMR spectrum of Sc{N(SiHMe$_2$)Ph}$_3$(THF)$_2$ (**3a**) acquired in benzene-d_6 at room temperature.

www.manaraa.com

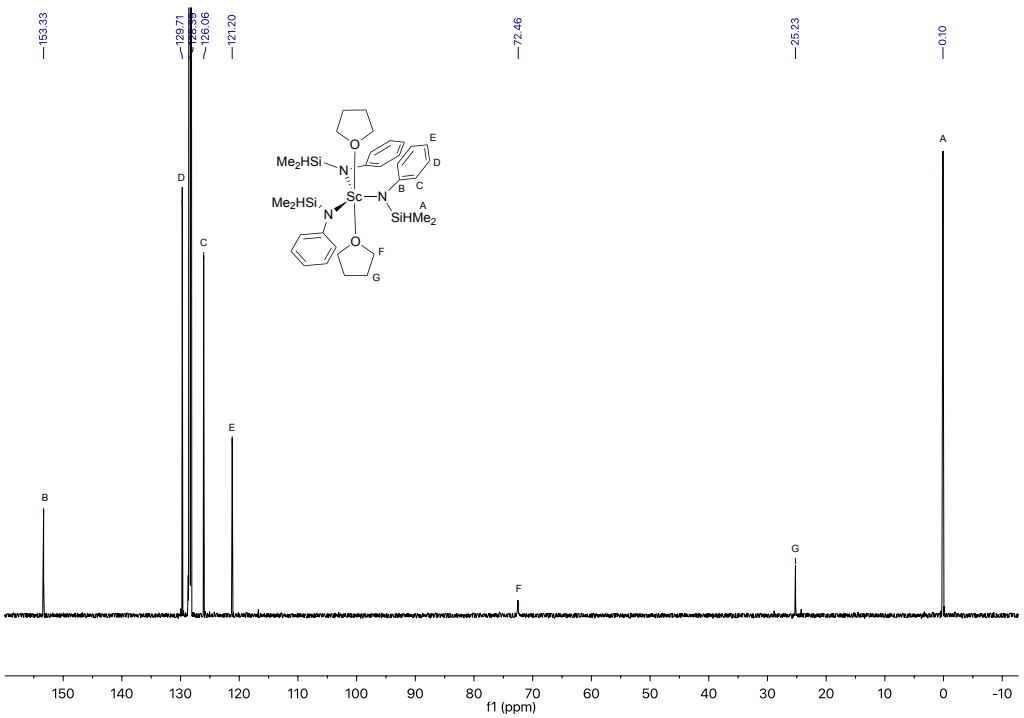

Figure S14. $^{13}C\{^{1}H\}$ NMR spectrum of $Sc\{N(SiHMe_2)Ph\}_3(THF)_2$ (**3a**) acquired in benzene-d_6 at room temperature.

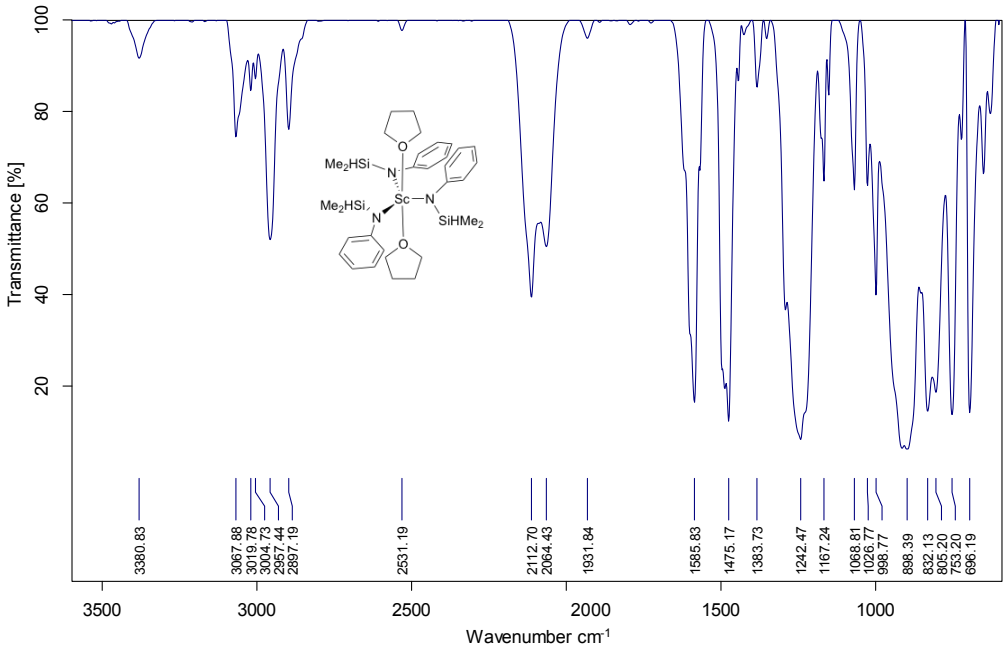

Figure S15. Infrared spectrum of $Sc\{N(SiHMe_2)Ph\}_3(THF)_2$ (**3a**) (KBr pellet).

www.manaraa.com

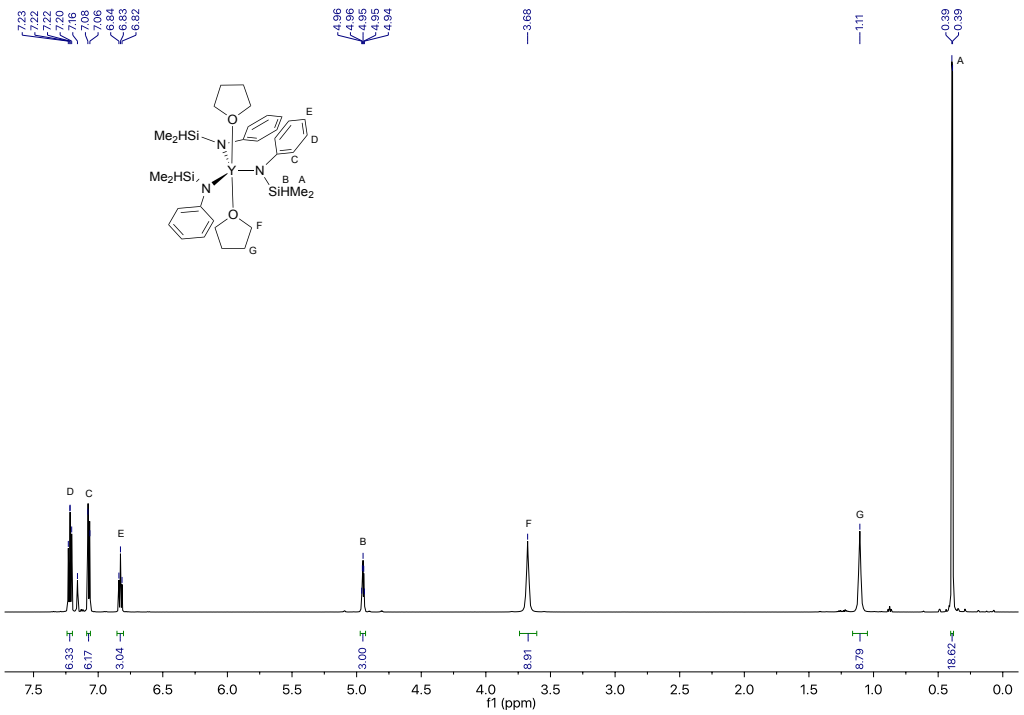

Figure S16. ^{1}H NMR spectrum of Y{N(SiHMe$_2$)Ph}$_3$(THF)$_2$ (**4a**) acquired in benzene-d_6 at room temperature.

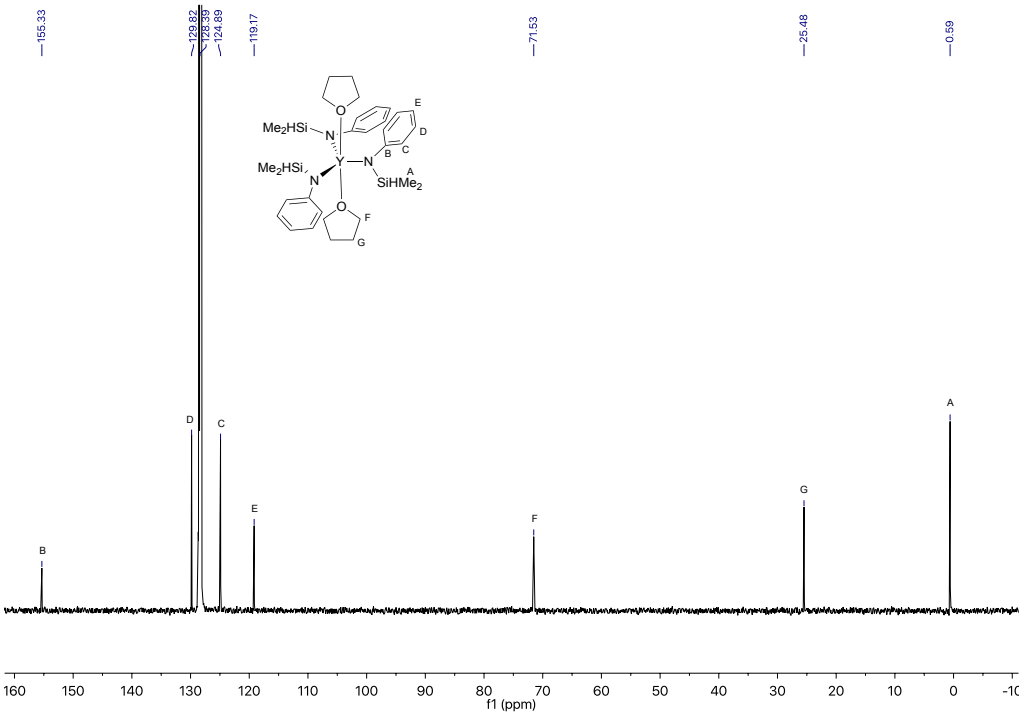

Figure S17. ^{13}C{^{1}H} NMR spectrum of Y{N(SiHMe$_2$)Ph}$_3$(THF)$_2$ (**4a**) acquired in benzene-d_6 at room temperature.

www.manaraa.com

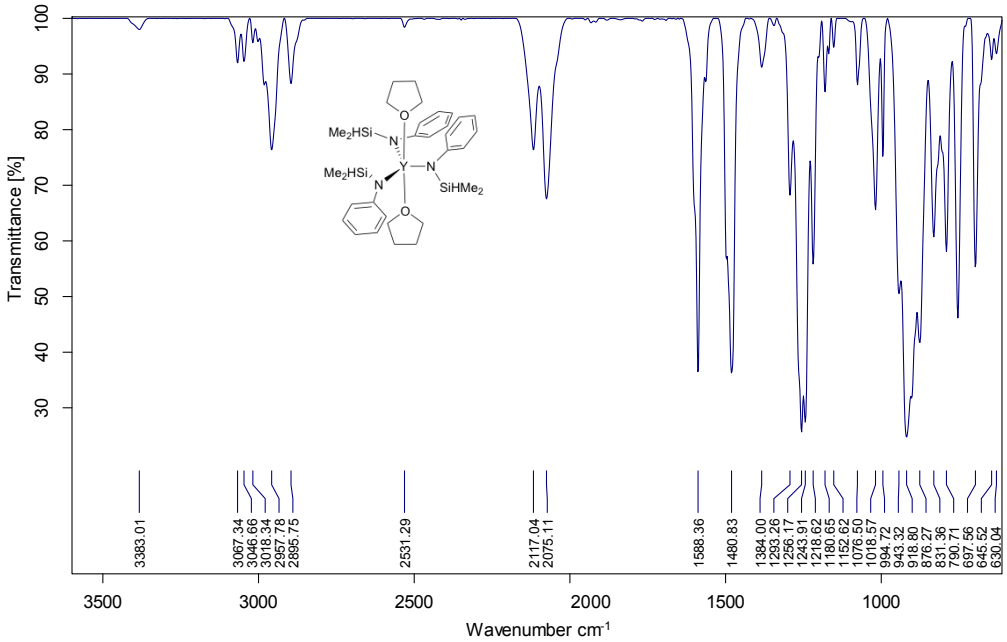

Figure S18. Infrared spectrum of $Y\{N(SiHMe_2)Ph\}_3(THF)_2$ (**4a**) (KBr pellet).

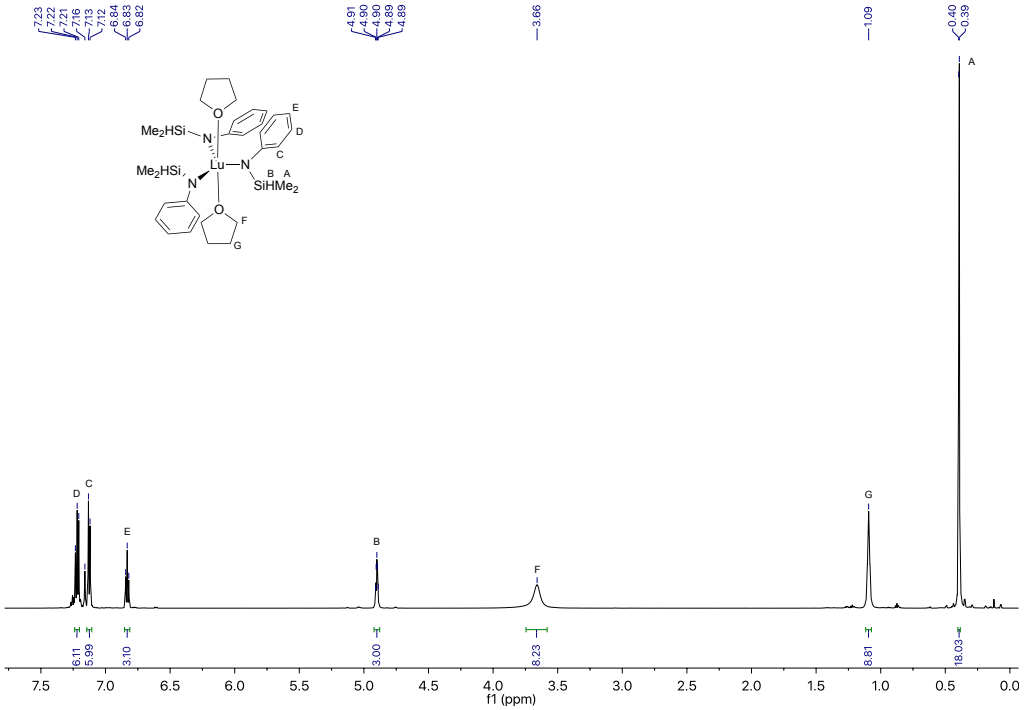

Figure S19. ^1H NMR spectrum of $Lu\{N(SiHMe_2)Ph\}_3(THF)_2$ (**5a**) acquired in benzene-d_6 at room temperature.

www.manaraa.com

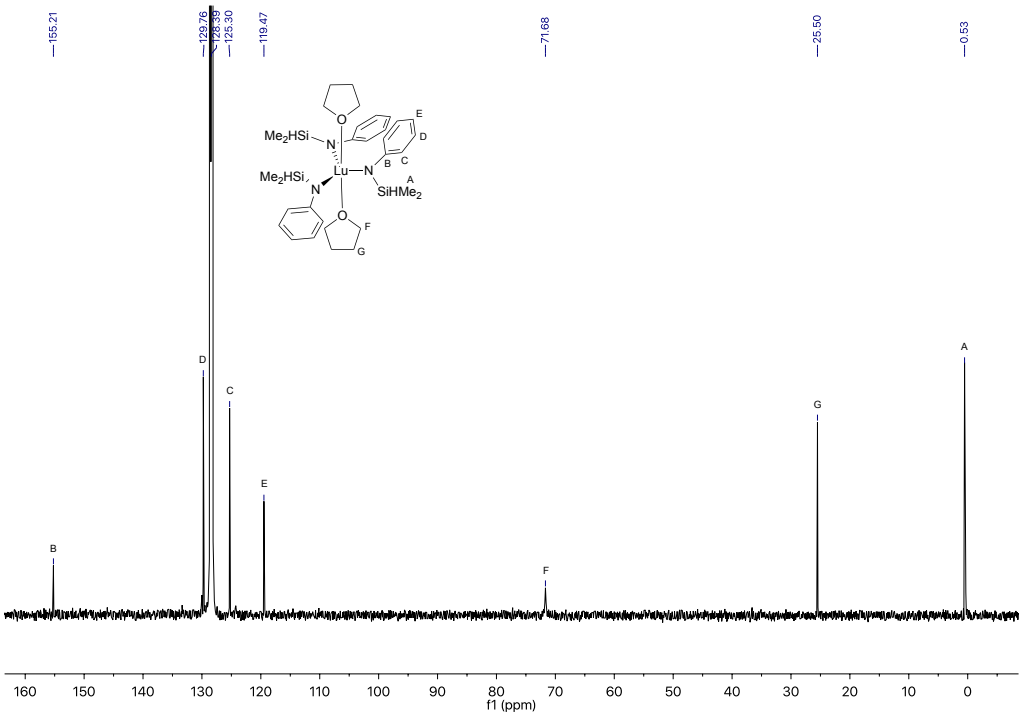

Figure S20. $^{13}C\{^{1}H\}$ NMR spectrum of Lu{N(SiHMe$_2$)Ph}$_3$(THF)$_2$ (**5a**) acquired in benzene-d_6 at room temperature.

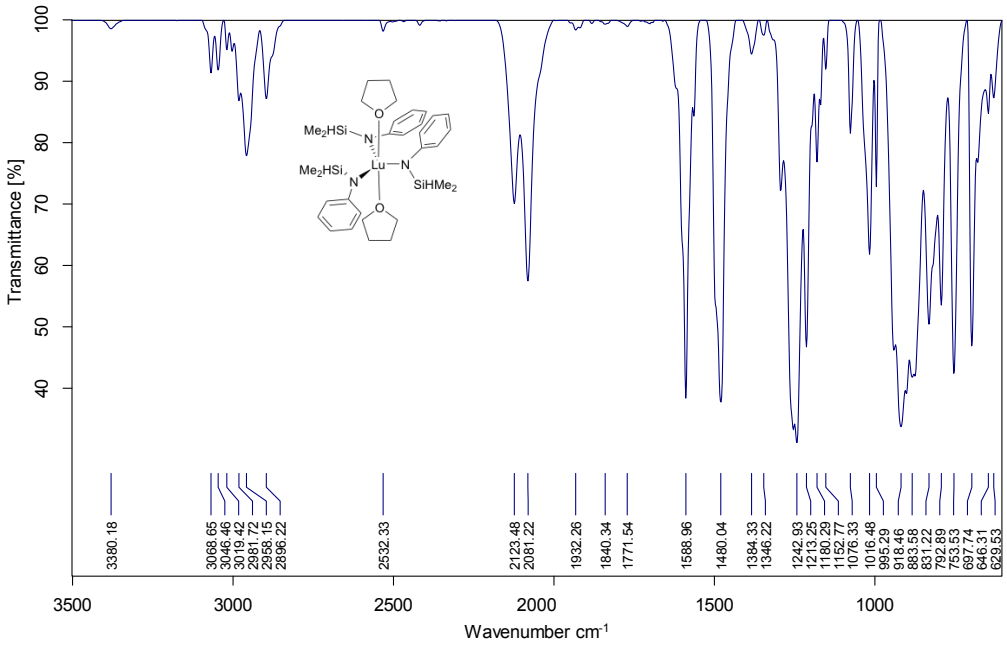

Figure S21. Infrared spectrum of Lu{N(SiHMe$_2$)Ph}$_3$(THF)$_2$ (**5a**) (KBr pellet).

www.manaraa.com

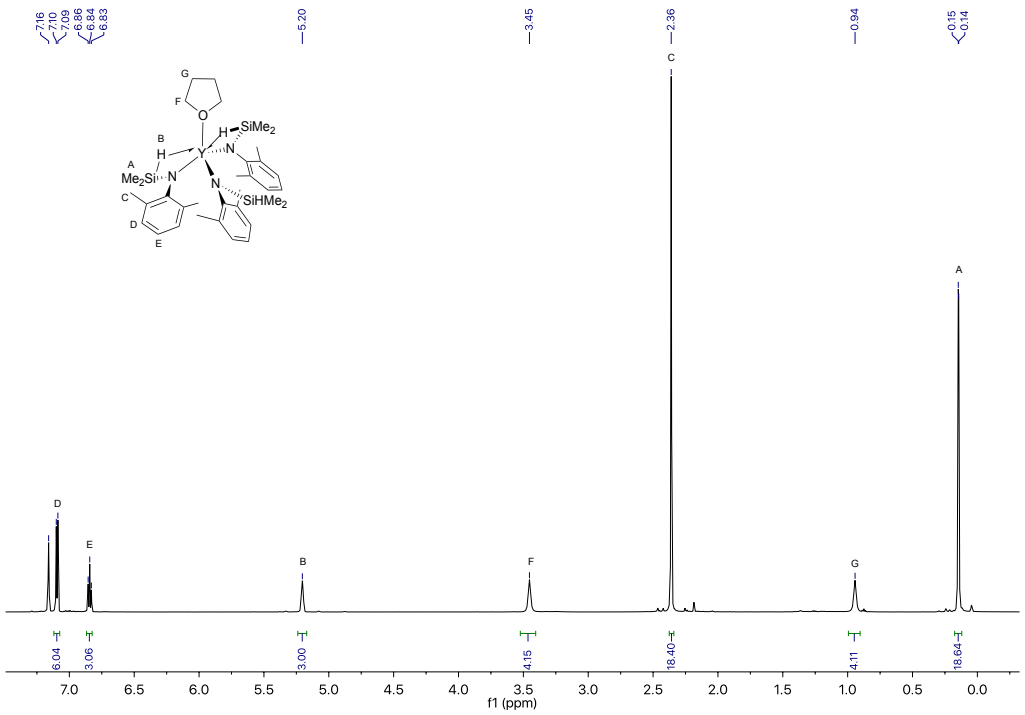

Figure S22. ^{1}H NMR spectrum of Y{N(SiHMe$_2$)dmp}$_3$(THF) (**4b**) acquired in benzene-d_6 at room temperature.

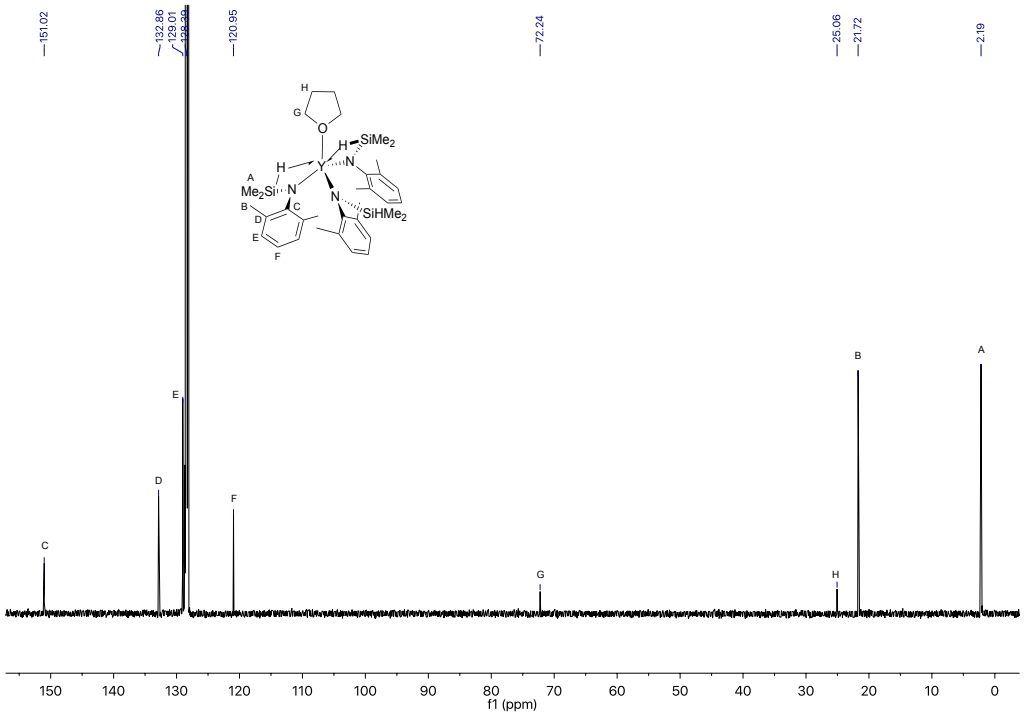

Figure S23. ^{13}C{^{1}H} NMR spectrum of Y{N(SiHMe$_2$)dmp}$_3$(THF) (**4b**) acquired in benzene-d_6 at room temperature.

www.manaraa.com

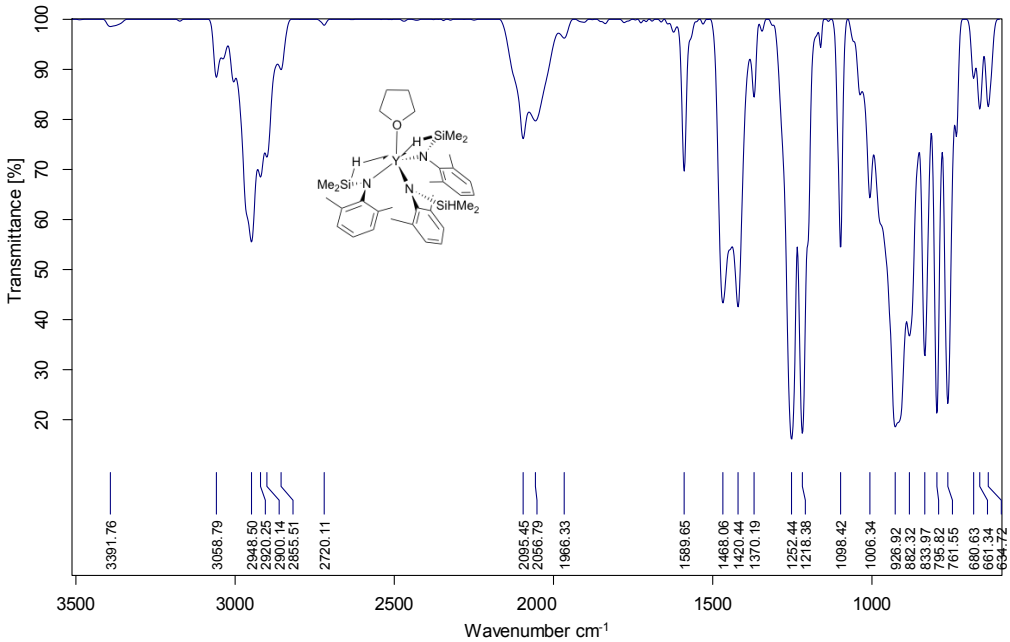

Figure S24. Infrared spectrum of Y{N(SiHMe$_2$)dmp}$_3$(THF) (**4b**) (KBr pellet).

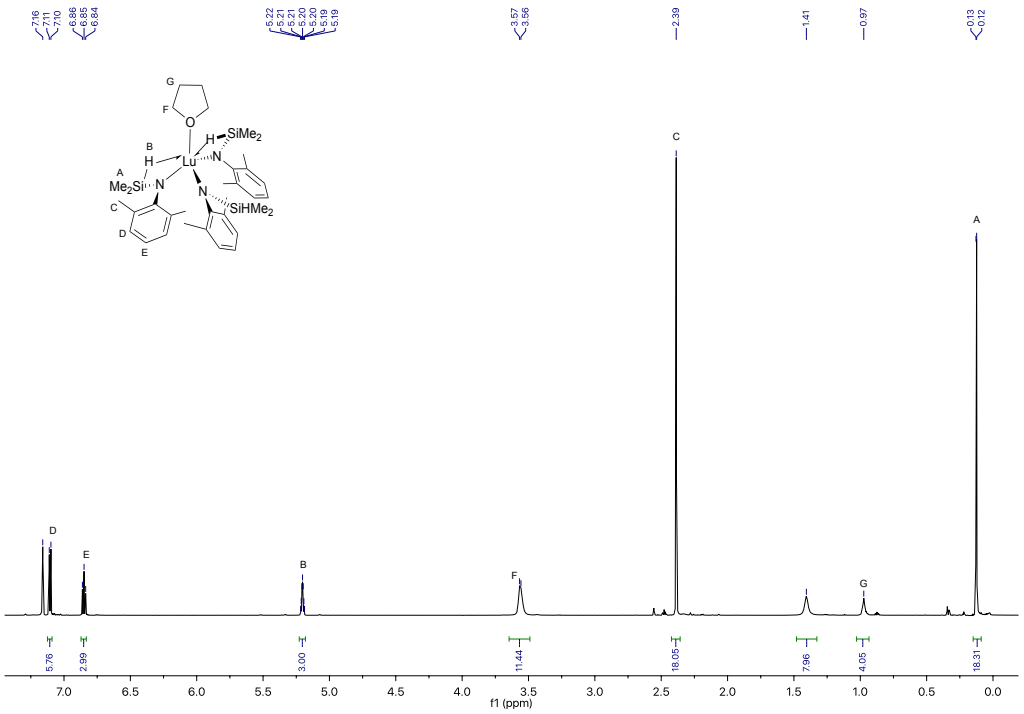

Figure S25. ^{1}H NMR spectrum of Lu{N(SiHMe$_2$)dmp}$_3$(THF) (**5b**) acquired in benzene-d_6 at room temperature.

www.manaraa.com

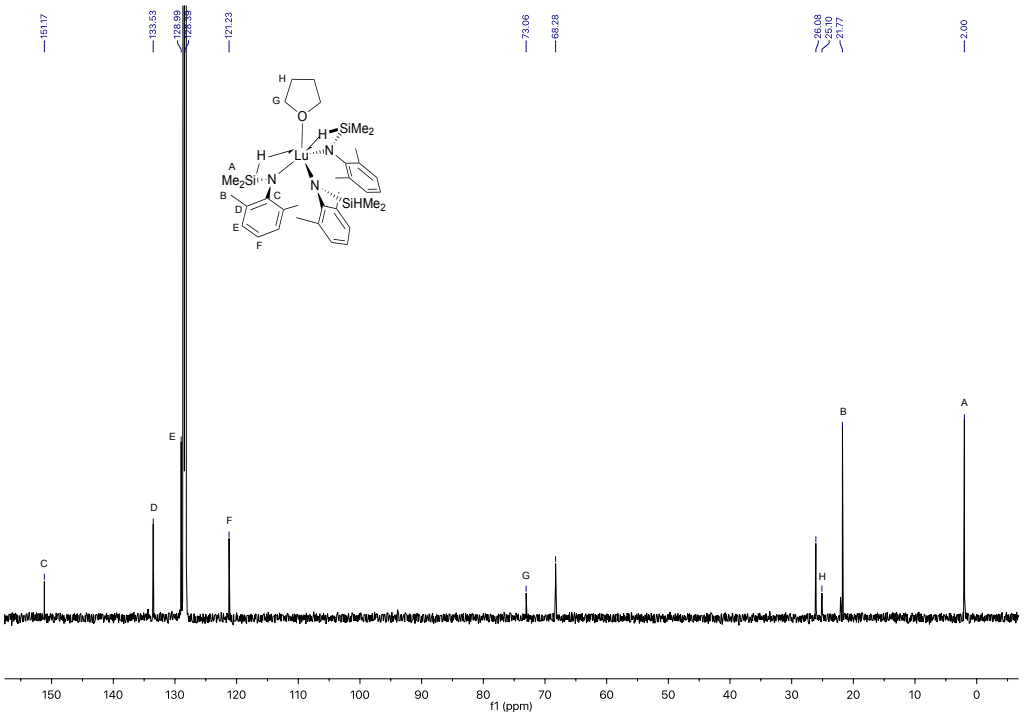

Figure S26. $^{13}C\{^{1}H\}$ NMR spectrum of Lu{N(SiHMe$_2$)dmp}$_3$(THF) (**5b**) acquired in benzene-d_6 at room temperature.

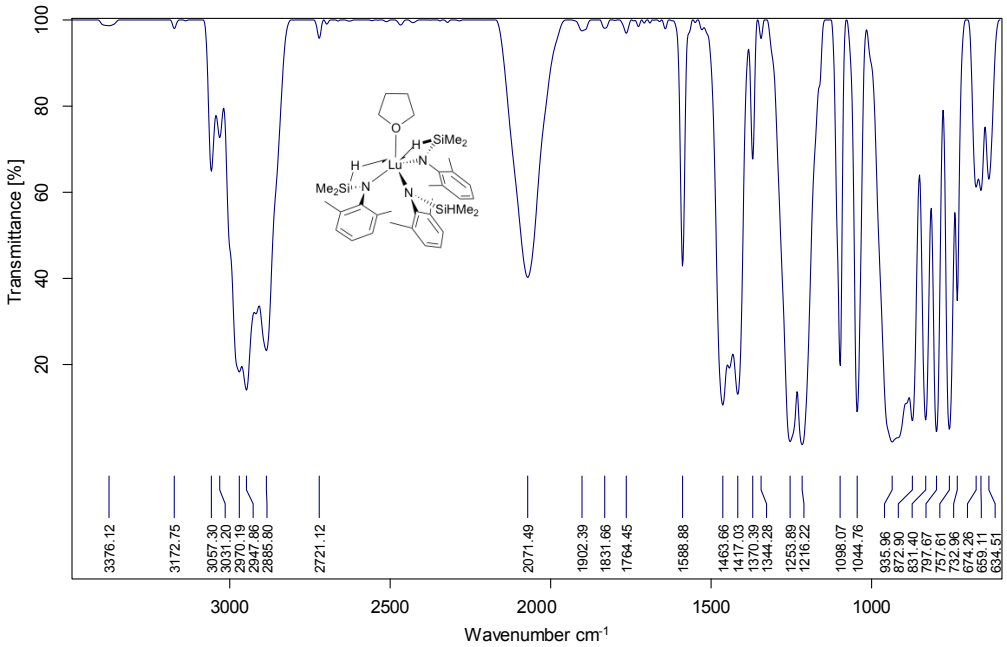

Figure S27. Infrared spectrum of Lu{N(SiHMe$_2$)dmp}$_3$(THF) (**5b**) (KBr pellet).

www.manaraa.com

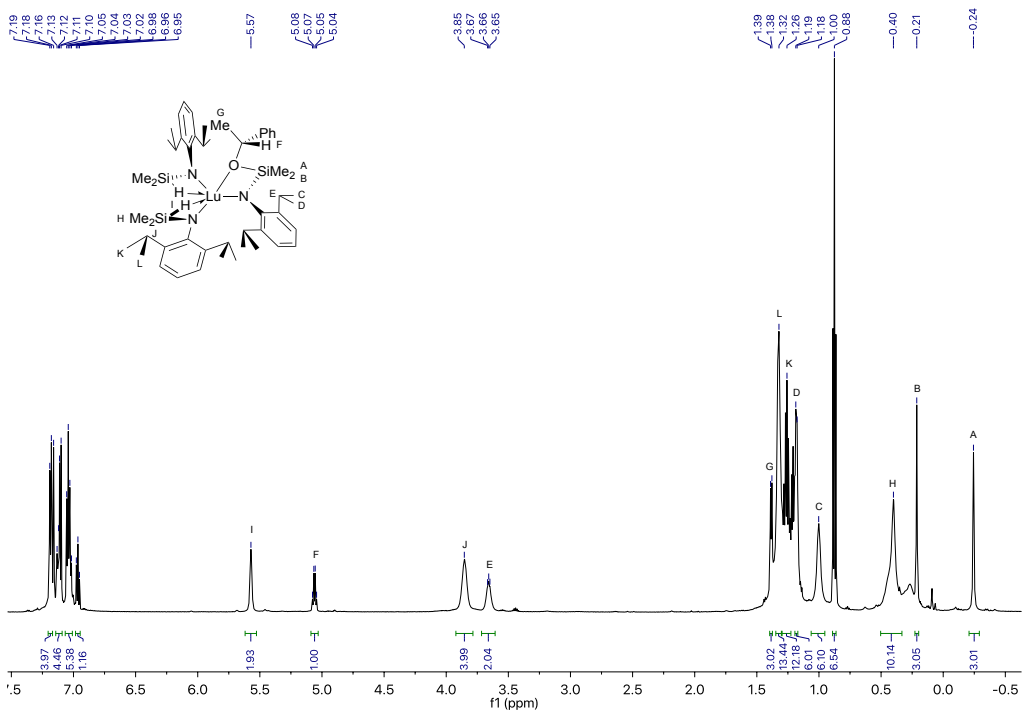

Figure S28. ^{1}H NMR spectrum of Lu{N(SiMe$_2$OCHMePh)dipp}{N(SiHMe$_2$)dipp}$_2$ (**5d**) acquired in benzene-d_6 at room temperature.

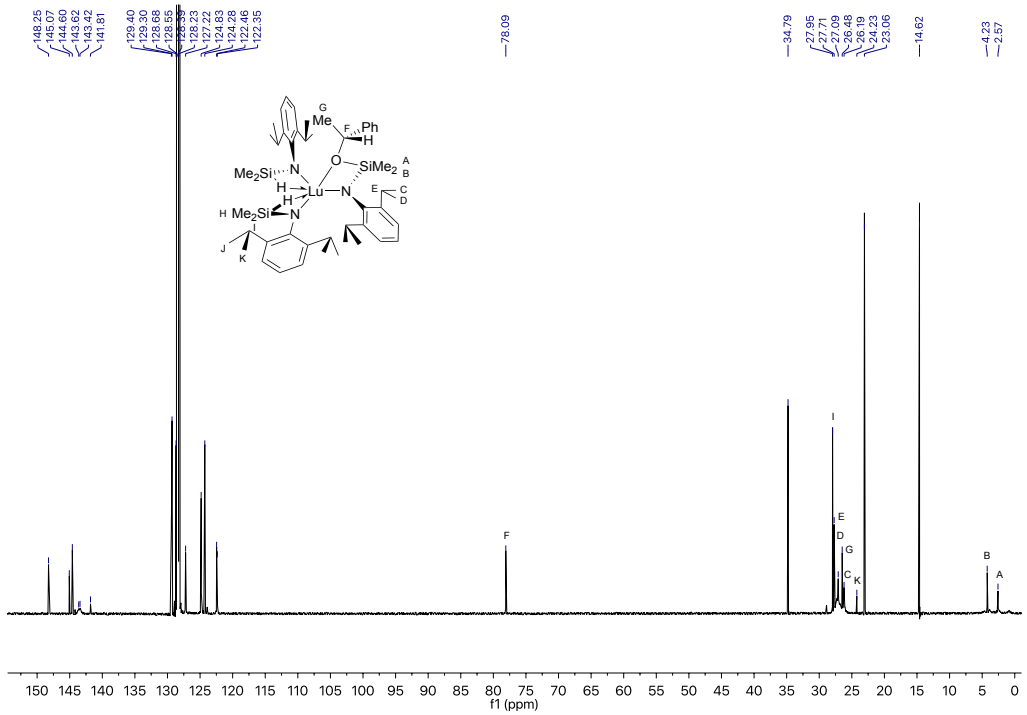

Figure S29. ^{13}C{^{1}H} NMR spectrum of Lu{N(SiMe$_2$OCHMePh)dipp}{N(SiHMe$_2$)dipp}$_2$ (**5d**) acquired in benzene-d_6 at room temperature.

www.manaraa.com

Peaks H; 3.91 ppm and J; 27.30 ppm were obtained only in ^{13}C HMQC

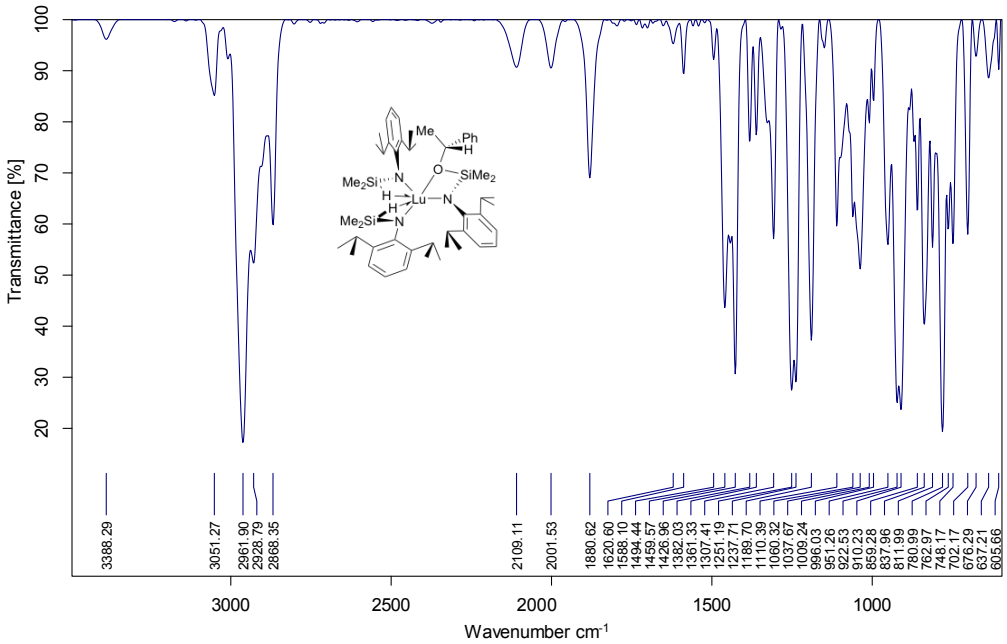

Figure S30. Infrared spectrum of Lu{N(SiMe$_2$OCHMePh)dipp}{N(SiHMe$_2$)dipp}$_2$ (**5d**) (KBr pellet).

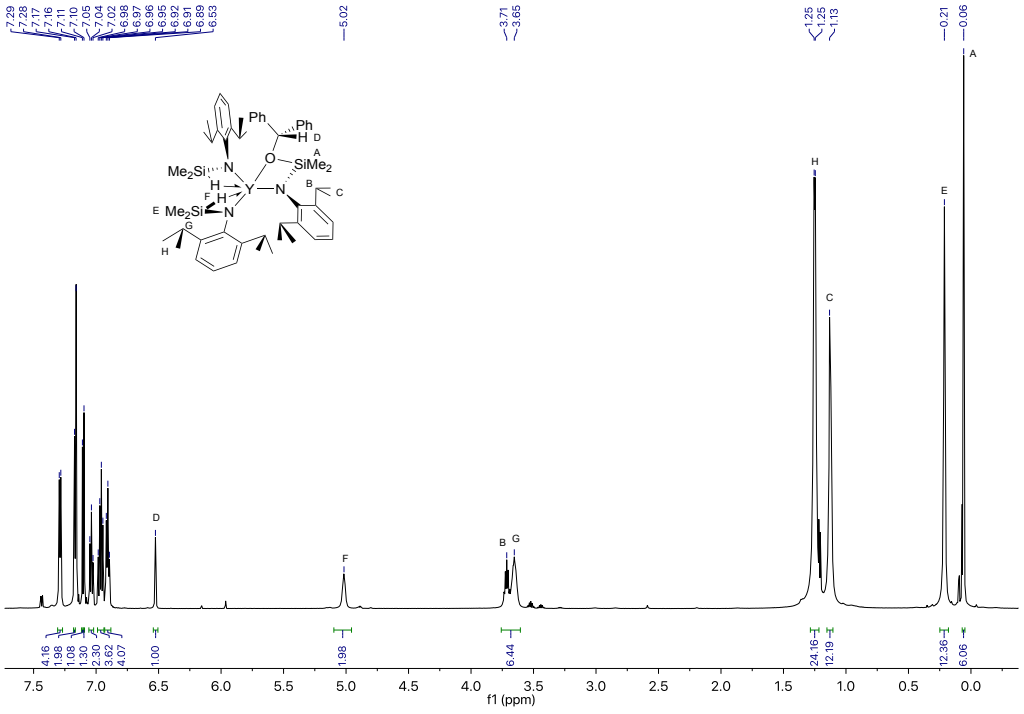

Figure S31. ^1H NMR spectrum of Y{N(SiMe$_2$OCHPh$_2$)dipp}{N(SiHMe$_2$)dipp}$_2$ (**4e**) acquired in benzene-d_6 at 308 K.

www.manaraa.com

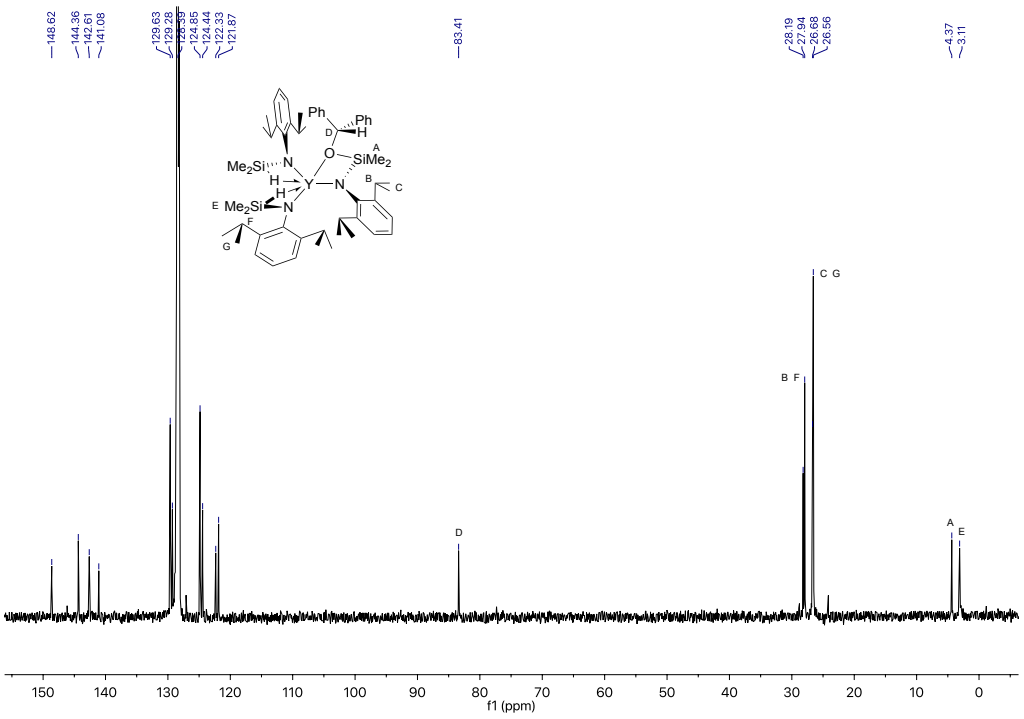

Figure S32. $^{13}C\{^{1}H\}$ NMR spectrum of Y{N(SiMe$_2$OCHPh$_2$)dipp}{N(SiHMe$_2$)dipp}$_2$ (**4e**) acquired in benzene-d_6 at 308 K.

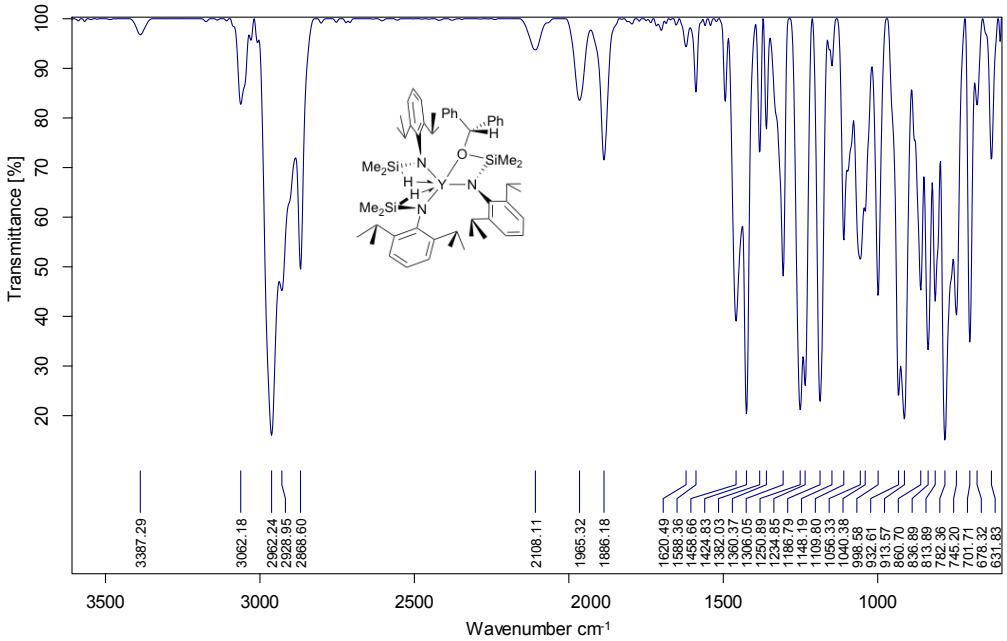

Figure S33. Infrared spectrum of Y{N(SiMe$_2$OCHPh$_2$)dipp}{N(SiHMe$_2$)dipp}$_2$ (**4e**) (KBr pellet).

www.manaraa.com

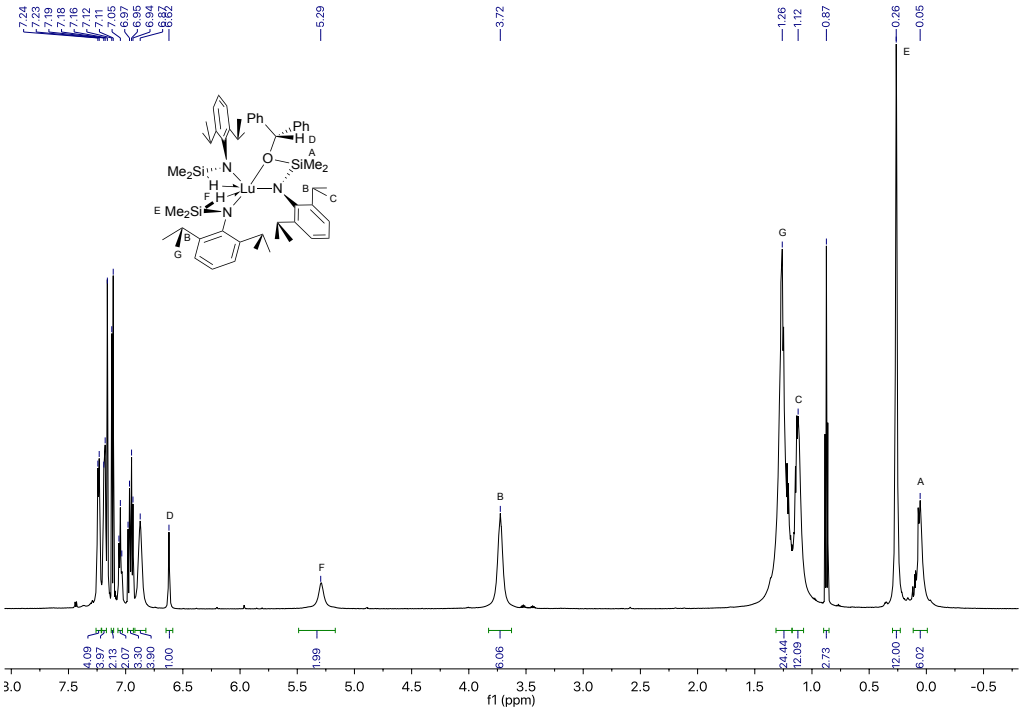

Figure S34. ^{1}H NMR spectrum of Lu{N(SiMe$_2$OCHPh$_2$)dipp}{N(SiHMe$_2$)dipp}$_2$ (**5e**) acquired in benzene-d_6 at room temperature.

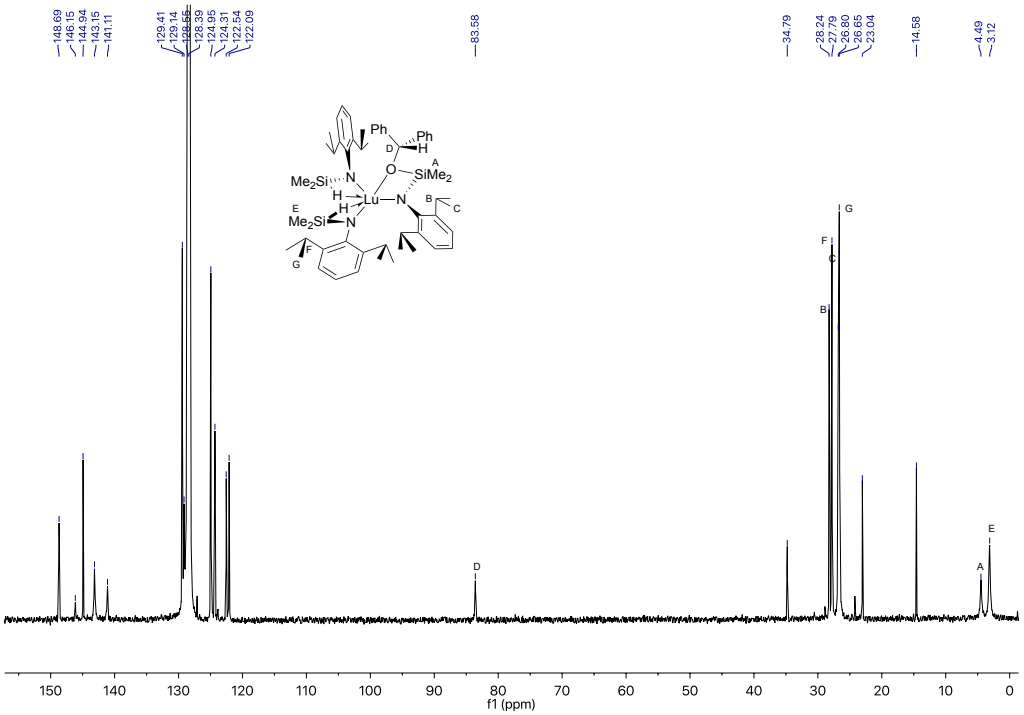

Figure S35. $^{13}C\{^{1}H\}$ NMR spectrum of Lu{N(SiMe$_2$OCHPh$_2$)dipp}{N(SiHMe$_2$)dipp}$_2$ (**5e**) acquired in benzene-d_6 at room temperature.

www.manaraa.com

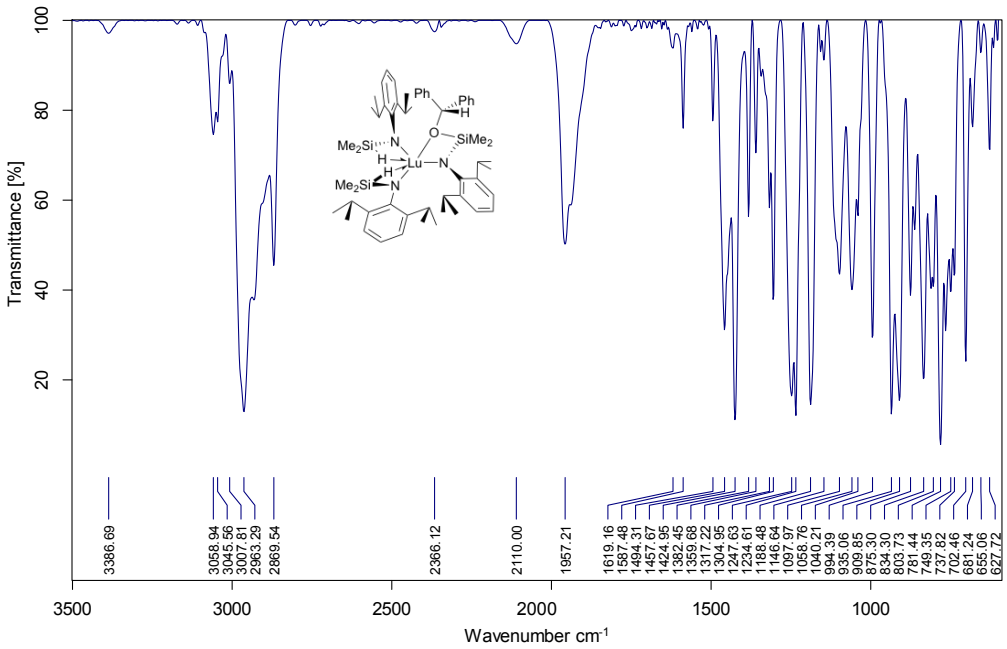

Figure S36. Infrared spectrum of Lu{N(SiMe$_2$OCHPh$_2$)dipp}{N(SiHMe$_2$)dipp}$_2$ (**5e**) (KBr pellet).

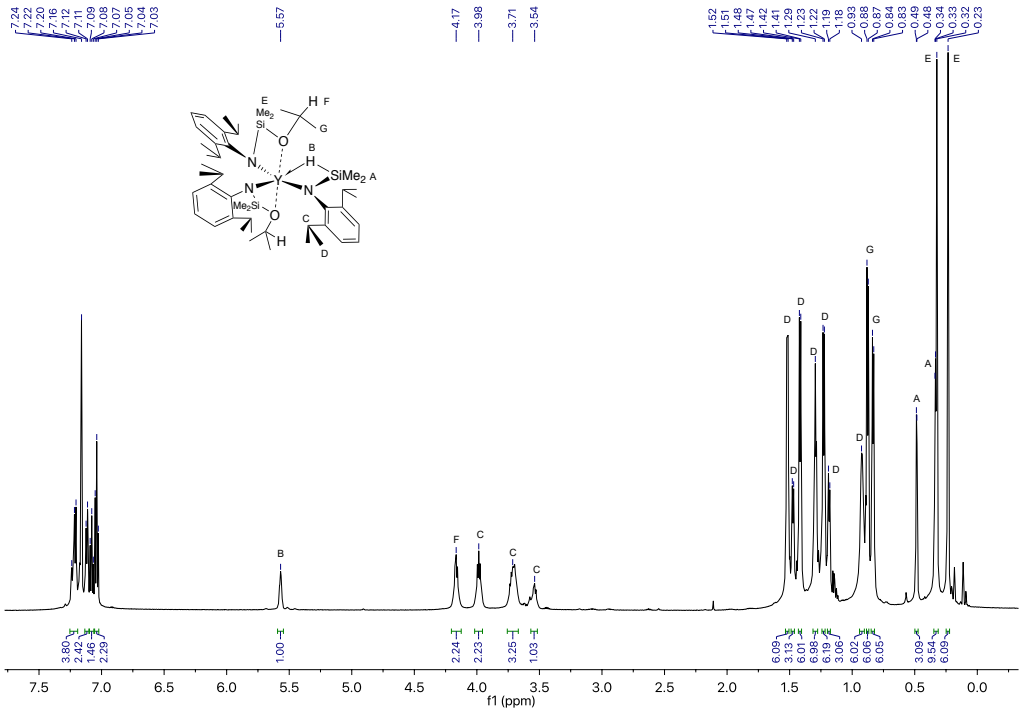

Figure S37. ^{1}H NMR spectrum of Y{N(SiMe$_2$OCHMe$_2$)dipp}$_2${N(SiHMe$_2$)dipp} (**4f**) acquired in benzene-d_6 at room temperature.

www.manaraa.com

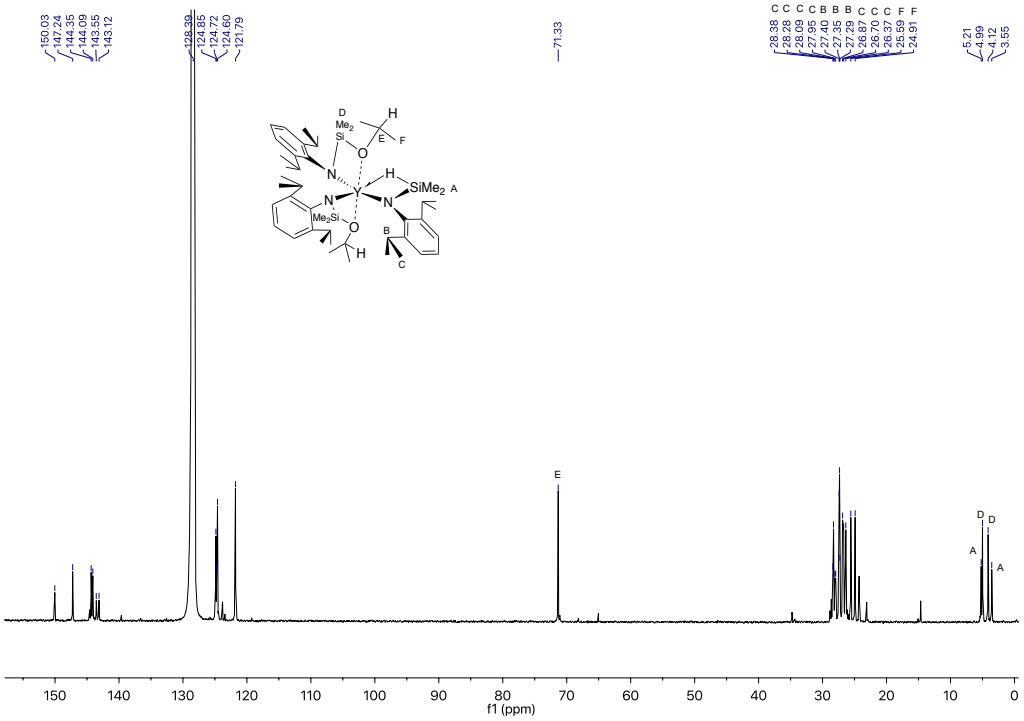

Figure S38. $^{13}C\{^{1}H\}$ NMR spectrum of $Y\{N(SiMe_2OCHMe_2)dipp\}_2\{N(SiHMe_2)dipp\}$ (**4f**) acquired in benzene-d_6 at room temperature.

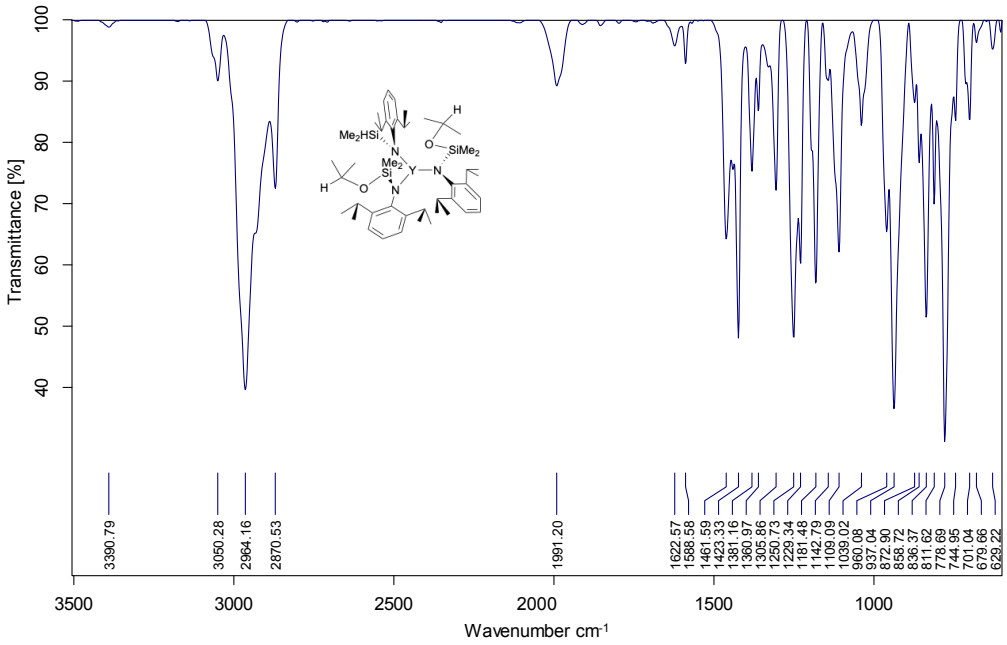

Figure S39. Infrared spectrum of $Y\{N(SiMe_2OCHMe_2)dipp\}_2\{N(SiHMe_2)dipp\}$ (**4f**) (KBr pellet).

www.manaraa.com

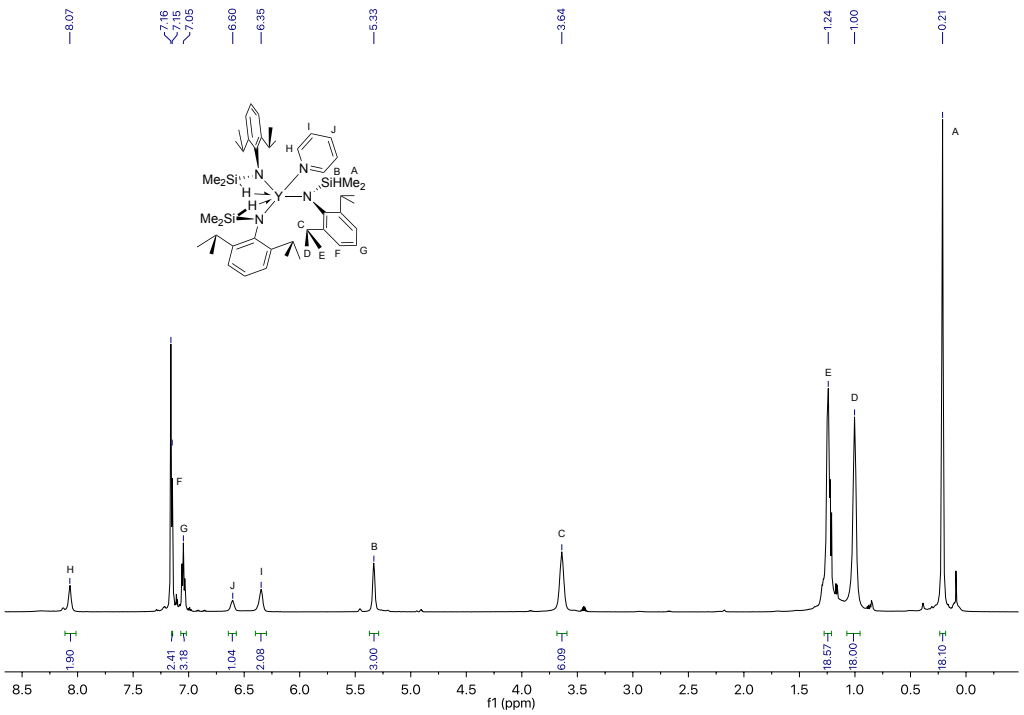

Figure S40. ^{1}H NMR spectrum of Y{N(SiHMe$_2$)dipp}$_3${pyridine} (**4c·py**) acquired in benzene-d_6 at room temperature.

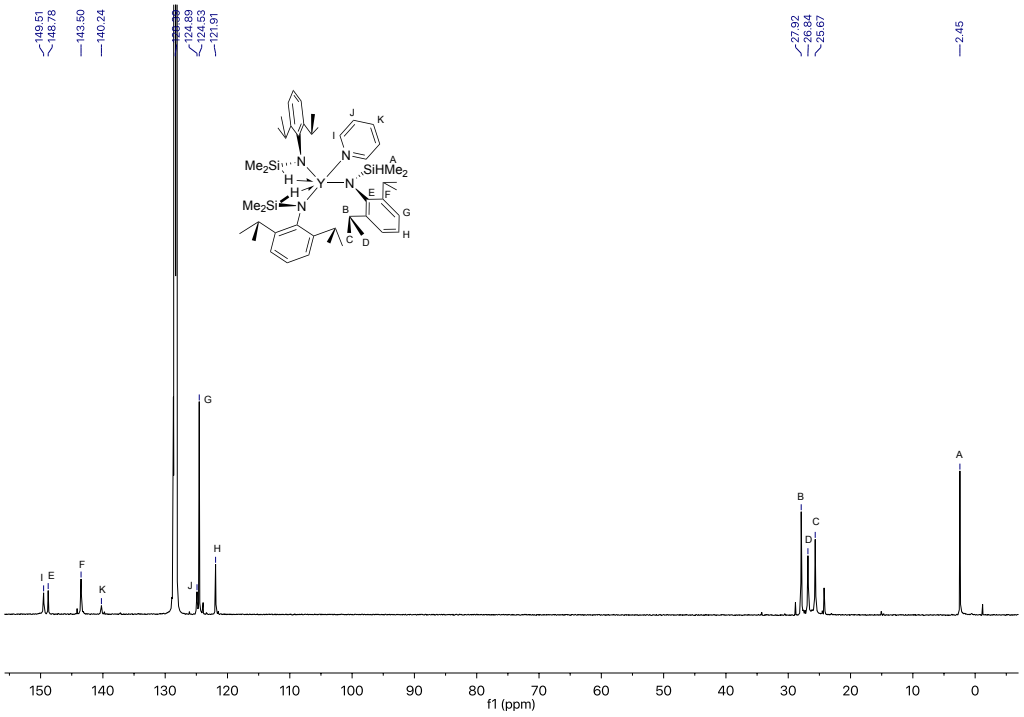

Figure S41. ^{13}C{^{1}H} NMR spectrum of Y{N(SiHMe$_2$)dipp}$_3${pyridine} (**4c·py**) acquired in benzene-d_6 at room temperature.

www.manaraa.com

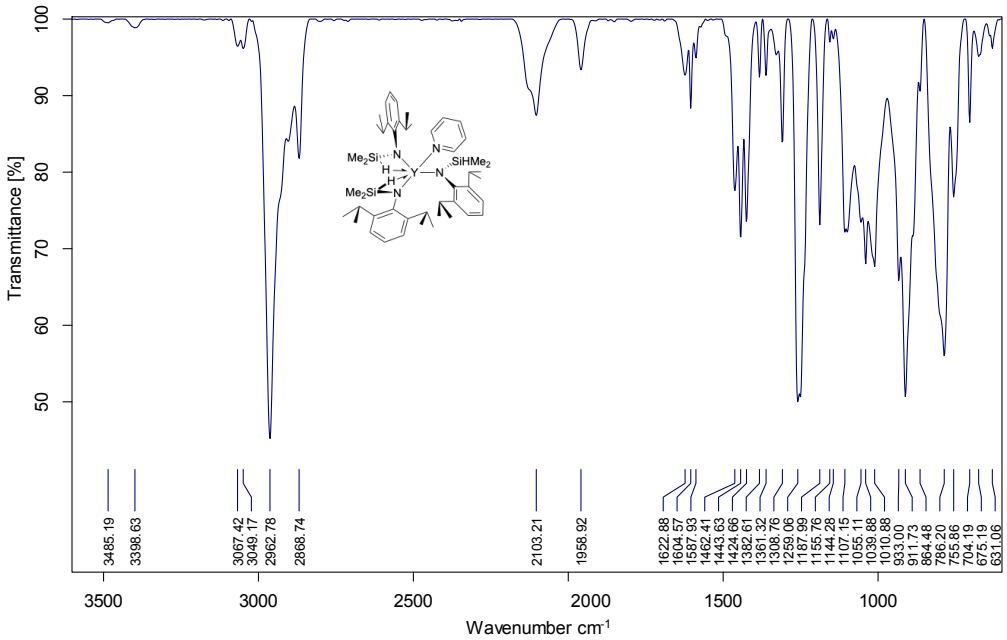

Figure S42. Infrared spectrum of Y{N(SiHMe$_2$)dipp}$_3${pyridine} (**4c·py**) (KBr pellet).

www.manaraa.com

CHAPTER 5. REACTIVITY OF RARE EARTH DIISOPROPYLSILAZIDO COMPOUNDS WITH $B(C_6F_5)_3$

Kasuni C. Boteju, Aaron D. Sadow*

US Department of Energy Ames Laboratory and Department of Chemistry, Iowa State University, Ames IA, 50011, USA

Modified from a manuscript to be submitted to Organometallics

Abstract

The reaction of $Ln\{N(SiHMe_2)dipp\}_3$ and one equivalent of $B(C_6F_5)_3$ provides the cationic species $Ln\{\kappa^2\text{-}N(dipp)SiMe_2N(SiHMe_2)dipp\}\{N(SiHMe_2)dipp\}HB(C_6F_5)_3$ by β-SiH abstraction. The decomposition of the cationic complex provides $(Me_2Si–Ndipp)_2$ and a rare earth adduct. Further, this elimination reaction follows a second order rate law.

Introduction

A metal complex which contains β hydrogens and at least one empty orbital in an open cis coordination site has the possibility for an elimination reaction, for example; isobutylene is released from $Cp_2ErCMe_3(THF)$ to open a coordination site.[1] In addition, unsaturated organolanthanides are known for β methyl elimination as they are highly reactive to cleave C–C bond.[2,3] The metal complexes containing bridging interactions between the metal center and β-SiH are considered not to undergo elimination reactions[4]; however, β-SiH abstraction reactions facilitated by Lewis acids of such complexes are reported in literature.

The reactivity of silazides with Lewis acids is known for tetramethyldisilazide $N(SiHMe_2)_2$ ligand containing compounds. $Cp_2Zr\{N(SiHMe_2)_2\}H$ and $B(C_6F_5)_3$ provides cationic $[Cp_2Zr\{N(SiHMe_2)_2]^+$ by abstracting the hydride. The reaction of $Cp_2Zr\{N(SiHMe_2)_2\}R$ (R = Me,

www.manaraa.com

Et, *n*-C_3H_7, CH=CHSiMe$_3$) and $B(C_6F_5)_3$ gives a mixture of $[Cp_2Zr\{N(SiHMe_2)_2]^+$ and $[Cp_2ZrN(SiHMe_2)(SiRMe_2)]^+$ indicating the abstraction of β-SiH and migration of R group to the β Si center in the latter compound.[5] A few examples of β-SiH abstraction in metal alkyl complexes by Lewis acids are also reported. The reaction between the $M\{C(SiHMe_2)_3\}_2THF_2$ (M = Ca, Yb) and $B(C_6F_5)_3$ provides a zwitterionic hydroborate species.[6] Similarly, $La\{C(SiHMe_2)_3\}_3$ and one equivalent of $B(C_6F_5)_3$ provides $La\{C(SiHMe_2)_3\}_2$ and 0.5 equiv. of cyclosilabutane.[7] In contrast to the above reaction, yttrium and lutetium analogs give only $Ln\{C(SiHMe_2)_3\}_2\{C(SiHMe_2)_2SiMe_2\}$ and dicyclosilabutane was not observed. These examples show that β-SiH bridging interactions provide ground state stabilization against β hydride elimination.[8]

As I mentioned in my chapter 3 and 4, the insertion of ketones into $Ln\{N(SiHMe_2)dipp\}_3$ provides the hydrosilylated product. Some ketones provided not only the insertion product mentioned above but also an elimination product of the silazido ligand $(Me_2Si–Ndipp)_2$. The latter product is also possible from a reaction between a rare earth silazido compound and a Lewis acid. Therefore, in this chapter we were motivated to study how β-SiH of $Ln\{N(SiHMe_2)dipp\}_3$ reacts with a Lewis acid. Further, explore the reactivity of β-SiHs in catalyst precursors is important to build new reaction mechanisms for catalytic conversions.

Results and Discussion

$Y\{N(SiHMe_2)dipp\}_3$ (dipp = diisopropylphenyl) reacts rapidly with one equivalent of fluorenone to give silylether-containing $Y\{\kappa^2\text{-}N(SiOCHFlu)dipp\}\{N(SiHMe_2)dipp\}_2$ (**YFlu**) while 2-5 equivalents of 3-pentanone provides $Y\{\kappa^2\text{-}N(SiOCHEt_2)dipp\}_2\{N(SiHMe_2)dipp\}$ (**YPent$_2$**). In both reactions, $(Me_2Si–Ndipp)_2$ was observed as a side product by elimination of a

www.manaraa.com

silazido ligand. The decomposition product, $(Me_2Si–Ndipp)_2$ was isolated as X-ray quality crystals from both reaction mixtures. We propose that once the ketone is coordinated to the yttrium center, instead of oxygen transfers to the silicon, Y–N bond cleaves followed by SiH transfer to the carbonyl carbon to provide $(Me_2Si–Ndipp)_2$ and the metal alkoxide.

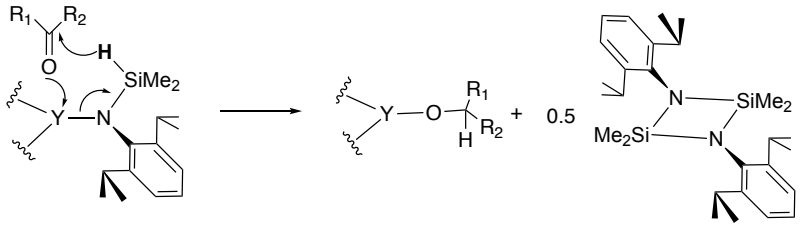

Scheme 1. Proposed reaction pathway for the formation of $(Me_2Si–Ndipp)_2$ by the reaction of $Y\{N(SiHMe_2)dipp\}_3$ and ketone.

Therefore, we were curious if the elimination of a silazido ligand occurs in the presence of a Lewis acid to form $(Me_2Si–Ndipp)_2$. $Ln\{N(SiHMe_2)dipp\}_3$ react with $B(C_6F_5)_3$ instantaneously in benzene at room temperature to give the species $Ln\{\kappa^2$-$N(dipp)SiMe_2N(SiHMe_2)dipp\}\{N(SiHMe_2)dipp\}HB(C_6F_5)_3$ (Ln = Y, **1**; Lu, **2**) as oily products. Further pentane washings of the oily residue provide light yellow solids for both yttrium **1** and lutetium **2** analogues (Eq 1). Interestingly, $(Me_2Si–Ndipp)_2$ was not observed indicating that a silazido ligand was not eliminated by the Lewis acid, although a SiH is abstracted from one ligand to give the borohydride cationic species.

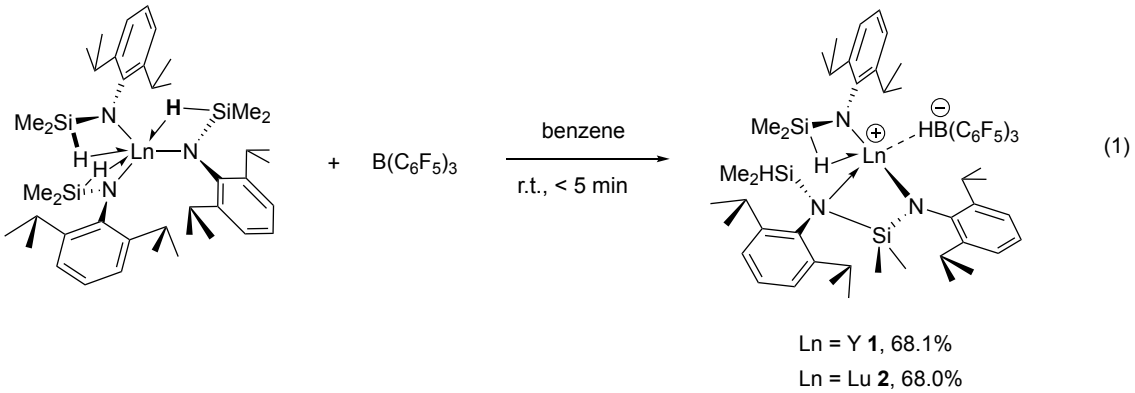

www.manaraa.com

The silicon atom of the ligand which lost the hydride, forms a bond with the nitrogen atom of one of the unreacted ligands by breaking the Ln–N bond. The ^{1}H NMR spectrum of **1** revealed that the three silazido ligands of Y{N(SiHMe$_2$)dipp}$_3$ became inequivalent, as evidenced by three sets of dipp signals and three sets of SiMe signals. Two of the SiMe signals were doublets at 0.11 ppm ($^{3}J_{HH}$ = 3.4 Hz) and 0.07 ppm ($^{3}J_{HH}$ = 2.6 Hz), which correlated in a COSY to SiH at 4.42 ppm ($^{1}J_{SiH}$ = 204.0 Hz) and 3.88 ppm respectively, indicating intact SiHMe$_2$ groups. The other SiMe was a singlet at –0.13 ppm, which suggested that H in SiHMe$_2$ was removed in Y{N(SiHMe$_2$)dipp}$_3$. The three sets of dipp signals included three peaks at 3.68 ppm, 2.78 ppm, and 2.54 ppm assigned to methine groups, indicating the three aryl groups freely rotate around the N–C bonds at room temperature. Three ^{29}Si NMR signals, observed as cross peaks in a ^{1}H-^{29}Si HMBC experiment, at –15.44, –3.60, and 17.56 ppm were correlated to the doublet and singlet signals. The high frequency signal correlated to the singlet in the ^{1}H NMR dimension. ^{15}N HMBC NMR showed only one peak at –325.49 ppm (out of three nitrogen atoms) which correlate with 0.11 ppm and –0.13 ppm ^{1}H NMR chemical shifts. These two correlations from one nitrogen with two SiMe groups provides strong support for formation of a new Si–N bond in **1**. In addition, ^{11}B NMR spectrum contain a signal at –24.28 ppm corresponding to the formed borohydride. ^{1}H-^{89}Y HSQC experiment showed a signal at 361.47 ppm in the yttrium dimension which correlated with the SiH peak at 3.88 ppm in the proton dimension. This observation suggests that **1** contains β SiH bridging interactions with the metal center.

The same pattern of the peaks was observed in the ^{1}H NMR spectrum of **2** as described for **1** above, suggesting their structures are very similar. The chemical shifts at 4.50 ppm and 4.42 ppm obtained for the unreacted SiHs. ^{29}Si HMBC NMR showed three correlations for the SiMe groups. The SiMe moieties of the unreacted ligands contained peaks at 0.18 ppm and 0.12 ppm in

www.manaraa.com

^{1}H NMR which correlated with peaks at –6.61 ppm and –3.50 ppm in silicon NMR respectively. The chemical shift of the reacted SiMe group appeared at –0.11 ppm and 19.38 ppm in ^{1}H and ^{29}Si NMR respectively. The most significant contrast to the yttrium analogue is found in ^{1}H-^{15}N HMBC experiment. Two chemical resonances appeared at –325.1 ppm and –199.32 ppm in ^{15}N hmbc NMR for two nitrogen atoms. The peak at –325.1 ppm again correlates with two SiMe peaks appeared at 0.12 ppm and –0.11 ppm in ^{1}H NMR suggesting that formation of Me_2HSi–N–$SiMe_2$ bond. In addition, a correlation between the nitrogen peak at –199.32 ppm and the proton peak at –0.11 ppm is observed suggesting a formation of N–$SiMe_2$–N moiety. This data is evidence to prove that the silicon atom of the reacted ligand forms a bond with the nitrogen atom of an unreacted ligand by breaking it's Ln–N bond.

The IR spectrum of **1** contains bands at 2382, 2138 and 1856 cm^{-1} assigned to B–H, non-bridging SiH and bridging SiH stretching respectively. Similarly, to **1**, **2** also contains bands at 2384 (BH), 2138 (non-bridging SiH) and 1833 (bridging SiH) cm^{-1} in the IR spectrum. In both compounds the observation of B–H stretching in IR spectra is consistent with the observation of a borate in the ^{11}B NMR spectrum.

The compounds **1** and **2** decompose to $(Me_2Si–Ndipp)_2$ and a rare earth adduct in less than one hour at 60 °C in a sealed NMR tube (Eq 2).

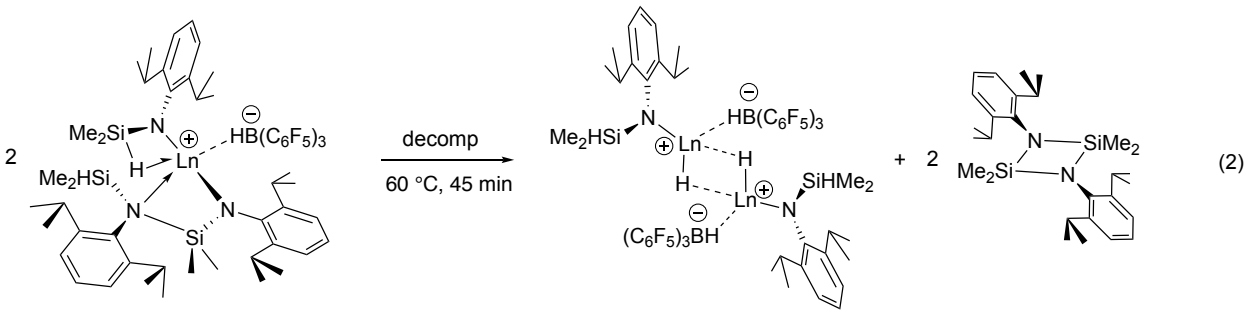

(2)

The silylamine cycle contained resonances at 3.94 ppm and 1.27 ppm for the dipp group and 0.35 ppm for the SiMe group in the ^{1}H NMR spectrum. In the ^{1}H-^{29}Si HMBC and ^{1}H-^{15}N HMBC NMR

www.manaraa.com

spectra of $(Me_2Si–Ndipp)_2$ contained signals at 5.03 ppm and 331.3 ppm respectively. The rare earth adduct obtained from the decomposition of the zwitterion is tentatively identified as $LnH\{NSiHMe_2dipp\}\{H(BC_6F_5)_3\}$ species by ^1H NMR spectroscopy. The yttrium analog of the adduct $YH\{NSiHMe_2dipp\}\{H(BC_6F_5)_3\}$ contains resonances at 5.12 ppm, 3.22 ppm, 0.94 ppm and 0.24 ppm assigned for SiH, methine of dipp, methyl of dipp and SiMe respectively in the ^1H NMR spectrum. Interestingly, the ^1H chemical shift obtained for the SiH at 5.12 ppm correlated with a peak at 398.45 ppm in the yttrium dimension in ^1H-^{89}Y HSQC NMR spectrum. This observation indicates that the remaining SiH of the yttrium adduct forms bridging interactions. Similarly, to **1**, the ^1H NMR spectrum of lutetium adduct $LuH\{NSiHMe_2dipp\}\{H(BC_6F_5)_3\}$ also contained resonances at 5.46 ppm, 3.25 ppm, 0.90 ppm and 0.30 ppm assigned for SiH, methine of dipp, methyl of dipp and SiMe respectively. The attempts to isolate the $LnH\{NSiHMe_2dipp\}\{H(BC_6F_5)_3\}$ species failed due to decomposition of the adduct in to unknown multiple species.

The elimination reaction of **1** was monitored by NMR kinetic studies at 60 °C. The reaction provided a second order rate law (Fig 1). The initial concentration of **1** and the final concentration of $(Me_2Si–Ndipp)_2$ provided similar values indicating 1:1 stoichiometry between **1** and $(Me_2Si–Ndipp)_2$. Together these observations suggest that two molecules of **1** provide two molecules of $(Me_2Si–Ndipp)_2$ and a dimeric species of the rare earth adduct in order to follow the mass balance (Eq 2).

www.manaraa.com

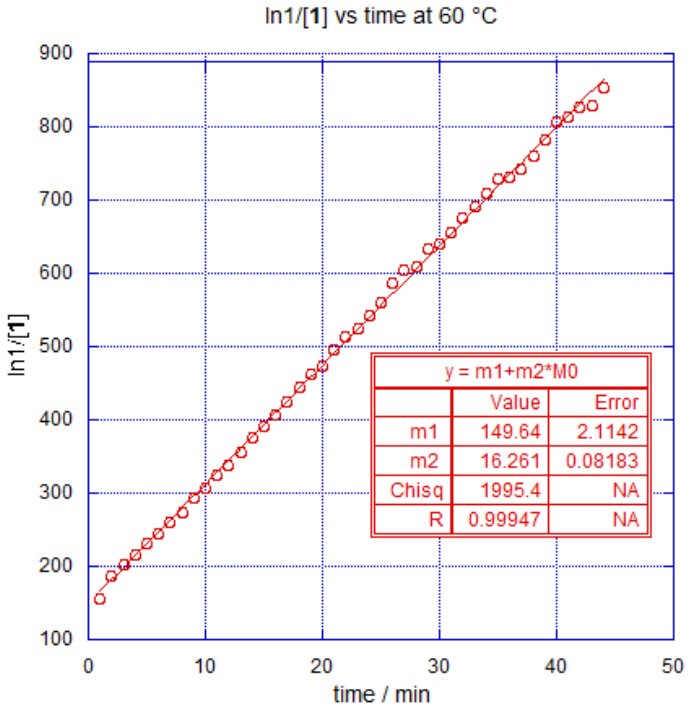

Figure 1. Second-order plot of ln1/[**1**] vs. time for the elimination of **1**. The curve represents non-weighted linear least squares best fits of the data to the equation: $\ln 1/[\mathbf{1}]_t = \ln[\mathbf{1}]_0 + kt$.

Conclusion

The β-SiH of Ln{N(SiHMe$_2$)dipp}$_3$is abstracted by the Lewis acid to provide only the zwitterionic species. Thus, the hydride of β-SiH moiety is the most nucleophilic site in the pre-catalyst. The kinetic studies of decomposition of the zwitterionic species provided a bimolecular rate law indicating that two molecules of the zwitterion involve in the rate determining step.

Experimental

General. All manipulations were performed under a dry argon atmosphere using standard Schlenk techniques or under a nitrogen atmosphere in a glovebox unless otherwise indicated.

www.manaraa.com

Water and oxygen were removed from benzene, pentane, and ether solvents using an IT PureSolv system. Benzene-d_6, was heated to reflux over Na/K alloy and vacuum-transferred. Ln{N(SiHMe$_2$)dipp}$_3$[9] and B(C$_6$F$_5$)$_3$[10] were prepared according to the literature procedures. Fluorenone was purchased from Sigma-Aldrich and used as received. ^{1}H, ^{11}B ^{13}C, ^{15}N and ^{29}Si HMBC NMR spectra were collected on a Bruker DRX-400 spectrometer or a Bruker Avance III-600 spectrometer. Infrared spectra were measured on a Bruker Vertex 80, using KBr pellet (transmission mode). Elemental analyses were performed using a Perkin-Elmer 2400 Series II CHN/S. X-ray diffraction data was collected on a Bruker APEX II diffractometer.

Y{N(SiMe$_2$OCHFlu)dipp}{N(SiHMe$_2$)dipp}$_2$ (YFlu). Y{N(SiHMe$_2$)dipp}$_3$ (0.0763 g, 0.0963 mmol) was dissolved in benzene (3 mL), and fluorenone (0.0174 g, 0.0963 mmol) was added to the solution. The reaction mixture was stirred for 15 min., and the solvent was evaporated under vacuum. The resulting oily residue was extracted with pentane (3 × 5 mL), concentrated, and cooled to –30 °C to provide the desired product as a white crystalline solid (0.0481 g, 0.0495 mmol, 51.3%). ^{1}H NMR (benzene-d_6, 600 MHz, 25 °C): δ 7.35 – 6.92 (19 H, aromatic region), 6.28 (s, 1 H, OC*H*Flu), 5.33 (br s, 2 H, $^1J_{SiH}$ = 130.0 Hz, Si*H*Me$_2$), 3.65 (br, 6 H, C*H*Me$_2$), 1.21 (br, 24 H, CH*Me*$_2$), 1.10 (d, 12 H, $^3J_{HH}$ = 6.6 Hz CH*Me*$_2$), 0.33 (br s, 12 H, SiH*Me*$_2$), –0.12 (s, 6 H, Si*Me*$_2$). ^{13}C NMR (benzene-d_6, 150 MHz, 25 °C): δ 148.49, 143.74, 142.66, 142.26, 140.96, 130.59, 127.24, 124.68, 122.04, 121.61, 120.90 (aromatic region), 80.09 (O*C*HFlu), 27.95 (*C*HMe$_2$), 26.72 (CH*Me*$_2$), 26.40 (CH*Me*$_2$), 4.67 (Si*Me*$_2$). ^{29}Si NMR (benzene-d_6, 119.3 MHz, 40 °C): δ 6.46 (*Si*Me$_2$). IR (KBr, cm^{-1}): 3386 w, 3067 w, 3051 w, 2961 s, 2868 m, 2108 w (SiH, from hydrolysis), 1945 w (SiH), 1881 w (SiH), 1614 w, 1589 w, 1456 s, 1427 s, 1382 w, 1360 w, 1328 w, 1307 s, 1250 s, 1237 s, 1190 s, 1152 w, 1110 m, 1072 m, 1054 m, 1041 m, 1017 m, 988 m, 963

www.manaraa.com

m, 934 s, 856 m, 835 m, 813 m, 781 s, 768 s, 743 s, 698 w, 678 w, 609 w. Anal. Calcd for $C_{55}H_{80}N_3OSi_3Y$: C, 67.93; H, 8.29; N, 4.32. Found: C, 67.47; H, 8.10; N, 4.10. mp 181 – 183 °C.

Y{N(SiMe$_2$OCHEt$_2$)dipp}$_2${N(SiHMe$_2$)dipp} (YPent$_2$). This compound was able to prepare only in NMR scale. ^{1}H NMR (benzene-d_6, 600 MHz, 25 °C): δ 7.20 – 6.99 (9 H, aromatic region), 5.65 (septet 1H, $^1J_{SiH}$ = 138.2 Hz, Si*H*Me$_2$), 4.00 (br s, 2 H, C*H*Me$_2$), 3.86 (v septet, 2 H, $^3J_{HH}$ = 3.9 Hz OC*H*Et), 3.69 (br s, 4 H, C*H*Me$_2$), 1.56 (br, 8 H, OCHC*H*$_2$Me), 1.48 (br s, 6 H, CH*Me*$_2$), 1.41 (br s, 6 H, CH*Me*$_2$), 1.30 (br s, 12 H, CH*Me*$_2$), 1.25 (br s, 6 H, CH*Me*$_2$), 0.91(br s, 6 H, CH*Me*$_2$), 0.63 (br s, 6 H, OCHCH$_2$*Me*), 0.53 (br s, 3 H, SiH*Me*$_2$), 0.48 (br s, 6 H, OCHCH$_2$*Me*), 0.32 (br s, 12 H, Si*Me*$_2$), 0.27 (br s, 3 H, SiH*Me*$_2$).

Y{κ^2-N(dipp)SiMe$_2$N(SiHMe$_2$)dipp}{N(SiHMe$_2$)dipp}HB(C$_6$F$_5$)$_3$ (1). Y{N(SiHMe$_2$)dipp}$_3$ (0.0778 g, 0.0982 mmol) was dissolved in benzene (2 mL), and B(C$_6$F$_5$)$_3$ (0.0503 g, 0.0982 mmol) dissolved in benzene (2 mL) was added to the solution. The reaction mixture was stirred for 5 min., and the solvent was evaporated under vacuum. The resulting oily residue was washed with pentane (3 × 5 mL), to provide the desired product as a pale yellow solid (0.0872 g, 0.0667 mmol, 68.1%). ^{1}H NMR (benzene-d_6, 600 MHz, 25 °C): δ 7.90 – 6.87 (9 H, aromatic region), 4.42 (v pentet, 1 H, $^1J_{SiH}$ = 204.0 Hz, Si*H*Me$_2$), 3.88 (two v pentets, 1 H, Si*H*Me$_2$), 3.68 (septet, 2 H, $^3J_{HH}$ = 6.9 Hz C*H*Me$_2$), 2.78 (septet, 2 H, $^3J_{HH}$ = 6.9 Hz C*H*Me$_2$), 2.54 (septet, 2 H, $^3J_{HH}$ = 6.7 Hz C*H*Me$_2$), 1.12 (d, 6 H, $^3J_{HH}$ = 7.0 Hz CH*Me*$_2$), 1.06 (d, 6 H, $^3J_{HH}$ = 7.0 Hz CH*Me*$_2$), 1.01 (d, 6 H, $^3J_{HH}$ = 7.0 Hz CH*Me*$_2$), 0.87 (br s, 12 H, CH*Me*$_2$), 0.64 (d, 6 H, $^3J_{HH}$ = 7.1 Hz CH*Me*$_2$), 0.11 (d, 6 H, $^3J_{HH}$ = 3.4 Hz, SiH*Me*$_2$), 0.07 (d, 6 H, $^3J_{HH}$ = 2.6 Hz, SiH*Me*$_2$), –0.13 (s, 6 H, Si*Me*$_2$). ^{13}C NMR (benzene-d_6, 150 MHz, 25 °C): δ 157.53, 156.82, 150.29, 148.71,

www.manaraa.com

144.27, 143.71, 141.82, 138.95, 138.60, 126.33, 125.24, 124.01 (aromatic region), 30.40 (CH*Me*$_2$), 29.91 (*C*HMe$_2$), 28.53 (*C*HMe$_2$), 28.09 (*C*HMe$_2$), 25.63 (CH*Me*$_2$), 25.13 (CH*Me*$_2$), 22.64 (CH*Me*$_2$), 21.56 (CH*Me*$_2$), 4.35 (Si*Me*$_2$), 1.23 (SiH*Me*$_2$), 0.30 (SiH*Me*$_2$). ^{11}B NMR (benzene-d_6, 192 MHz): δ –24.28 (br s). ^{15}N NMR (benzene-d_6, 60.8 MHz, 25 °C): δ –325.49 (Me$_2$HSi*N*SiMe$_2$). ^{29}Si NMR (benzene-d_6, 119.3 MHz, 40 °C): δ –15.44 (*Si*HMe$_2$), –3.60 (*Si*HMe$_2$), 17.56 (*Si*Me$_2$). IR (KBr, cm^{-1}): 3058 w, 2968 s, 2873 w, 2382 w (BH), 2138 w (SiH), 1856 w (SiH), 1643 w, 1581 w, 1512 s, 1466 s, 1423 m, 1369 w, 1325 w, 1310 w, 1258 m, 1192 w, 1106 m, 1043 w, 970 s, 913 s, 834 m, 768 m, 660 w. Anal. Calcd for $C_{60}H_{72}BF_{15}N_3Si_3Y$: C, 55.26; H, 5.56; N, 3.22. Found: C, 55.13; H, 5.60; N, 3.13. mp 94 – 96 °C.

Lu{κ^2-N(dipp)SiMe$_2$N(SiHMe$_2$)dipp}{N(SiHMe$_2$)dipp}HB(C$_6$F$_5$)$_3$ (2). Lu{N(SiHMe$_2$)dipp}$_3$ (0.0518 g, 0.0590 mmol) was dissolved in benzene (2 mL), and B(C$_6$F$_5$)$_3$ (0.0302 g, 0.0590 mmol) dissolved in benzene (2 mL) was added to the solution. The reaction mixture was stirred for 5 min., and the solvent was evaporated under vacuum. The resulting oily residue was washed with pentane (3 × 5 mL), to provide the desired product as a pale yellow solid (0.0558 g, 0.0401 mmol, 68.0%). ^{1}H NMR (benzene-d_6, 600 MHz, 25 °C): δ 8.00 – 6.85 (9 H, aromatic region), 4.50 (v pentet, 1 H, Si*H*Me$_2$), 4.42 (v pentet, 1 H, Si*H*Me$_2$), 3.71 (septet, 2 H, $^3J_{HH}$ = 7.0 Hz C*H*Me$_2$), 2.87 (septet, 2 H, $^3J_{HH}$ = 6.9 Hz C*H*Me$_2$), 2.62 (septet, 2 H, $^3J_{HH}$ = 6.9 Hz C*H*Me$_2$), 1.14 (d, 6 H, $^3J_{HH}$ = 6.8 Hz CH*Me*$_2$), 1.06 (d, 6 H, $^3J_{HH}$ = 7.1 Hz CH*Me*$_2$), 1.02 (d, 6 H, $^3J_{HH}$ = 6.9 Hz CH*Me*$_2$), 0.86 (br s, 12 H, CH*Me*$_2$), 0.68 (d, 6 H, $^3J_{HH}$ = 7.0 Hz CH*Me*$_2$), 0.18 (d, 6 H, $^3J_{HH}$ = 2.5 Hz, SiH*Me*$_2$), 0.12 (d, 6 H, $^3J_{HH}$ = 3.4 Hz, SiH*Me*$_2$), –0.11 (s, 6 H, Si*Me*$_2$). ^{13}C NMR (benzene-d_6, 150 MHz, 25 °C): δ 157.48, 156.87, 150.24, 148.66, 144.32, 143.59, 142.41, 140.03, 138.54, 126.01, 124.77, 124.44, 124.20 (aromatic region), 30.29 (CH*Me*$_2$), 29.98 (*C*HMe$_2$), 28.33

www.manaraa.com

(*C*HMe$_2$), 28.29 (*C*HMe$_2$), 25.47 (CH*Me*$_2$), 25.28 (CH*Me*$_2$), 22.41 (CH*Me*$_2$), 21.01 (CH*Me*$_2$), 4.51 (Si*Me*$_2$), 1.65 (SiH*Me*$_2$), 0.31 (SiH*Me*$_2$). ^{11}B NMR (benzene-d_6, 192 MHz): δ -24.40 (br s). ^{15}N NMR (benzene-d_6, 60.8 MHz, 25 °C): δ –325.1 (Me$_2$HSi*N*SiMe$_2$N), –199.32 (Me$_2$HSiNSiMe$_2$*N*). ^{29}Si NMR (benzene-d_6, 119.3 MHz, 40 °C): δ –6.61 (*Si*HMe$_2$), –3.50 (*Si*HMe$_2$), 19.38 (*Si*Me$_2$). IR (KBr, cm^{-1}): 3059 w, 2968 s, 2872 w, 2384 w (BH), 2138 w (SiH), 1833 w (SiH), 1643 m, 1587 w, 1512 s, 1465 s, 1369 w, 1326 w, 1311 m, 1256 s, 1192 m, 1163 w, 1106 s, 1042 m, 970 s, 911 s, 837 s, 788 s, 684 w, 659 w. Anal. Calcd for $C_{60}H_{72}BF_{15}N_3Si_3Lu$: C, 51.84; H, 5.22; N, 3.02. Found: C, 51.80; H, 5.10; N, 2.65. mp 86 – 88 °C.

Procedure for kinetic measurements of decomposition of Y{κ^2-N(dipp)SiMe$_2$N(SiHMe$_2$)dipp}{N(SiHMe$_2$)dipp}HB(C$_6$F$_5$)$_3$ (1). Reactant concentration was monitored by ^{1}H NMR spectroscopy using a Bruker Avance III-600 spectrometer. Concentration of the reactant was determined by integration of resonances corresponding to species of interest and integration of a hexamethybenzene standard of known concentration. A stock solution of hexamethybenzene (10 mM) in benzene-d_6 was prepared and used for the experiment. In a typical experiment, 0.0092 mmol of the reactant was dissolved in 0.5 mL of the stock solution, and the solution was placed in NMR tube and a ^{1}H NMR spectrum was acquired at room temperature. The NMR tube was removed from the spectrometer and the NMR probe was heated to 60 °C. The probe temperature was calibrated using a thermocouple. Once the temperature is equilibrated the NMR tube was injected to the spectrometer. The decomposition reaction was monitored by taking a single scan ^{1}H NMR spectra at regular preset intervals. The rate constant was obtained by a non-weighted linear least-squares regression analysis of the integrated second-order rate law: ln[**(1)**] = ln[**(1)**]$_0$ + kt.

www.manaraa.com

References

1. Evans, W. J.; Meadows, J. H.; Wayda, A. L.; Hunter, W. E.; Atwood, J. L. *J. Am. Chem. Soc*. **1982**, *104*, 2015-2017.

2. Watson, P. L.; Roe, D. C. *J. Am. Chem. Soc*. **1982**, *104*, 6471-6473

3. Watson, P. L.; Parshall, G. W. *Acc. Chem. Res*.**1985**, *18,* 51-56

4. Dawoodi, Z.; Green, M. L. H.; Mtetwa, V. S. B.; Prout, K. J. *Chem. Soc., Chem. Commun*.**1982**, 802-803.

5. Yan, K.; Duchimaza Heredia, J. J.; Ellern, A.; Gordon, M. S.; Sadow, A. D. *J. Am. Chem. Soc*. **2013**, *135*, 40, 15225-15237.

6. Yan, K.; Upton, B. M.; Ellern, A.; Sadow, A. D. *J. Am. Chem. Soc*. **2009**, *131*, 42, 15110-15111.

7. Schmidt, B. M.; Pindwal, A.; Venkatesh, A,; Ellern, A.; Rossini, A. J.; Sadow, A. D. *ACS Catal*. **2019**, *9*, *2*, 827-838.

8. Burger, B. J.; Thompson, M. E.; Cotter, W. D.; Bercaw, J. E. *J. Am. Chem. Soc*. **1990**, *112*, 1566-1577.

9. Boteju, K. C.; Wan, S.; Venkatesh, A.; Ellern, A.; Rossini, A. J.; Sadow, A. D. **2018**, *54*, 7318-7321.

10. Massey, A. G.; Park, A. J., *J. Organomet. Chem*. **1964**, *2*, 245-250

www.manaraa.com

Appendix

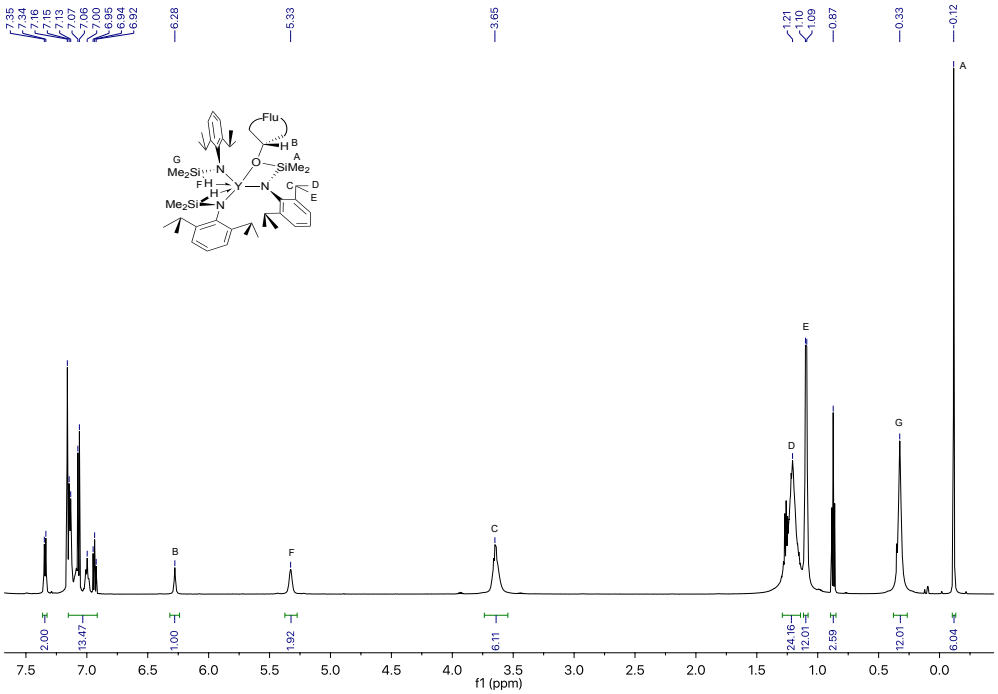

Figure S1. ^{1}H NMR spectrum of Y{N(SiMe$_2$OCHFlu)dipp}{N(SiHMe$_2$)dipp}$_2$ (**YFlu**) acquired in benzene-d_6 at room temperature.

www.manaraa.com

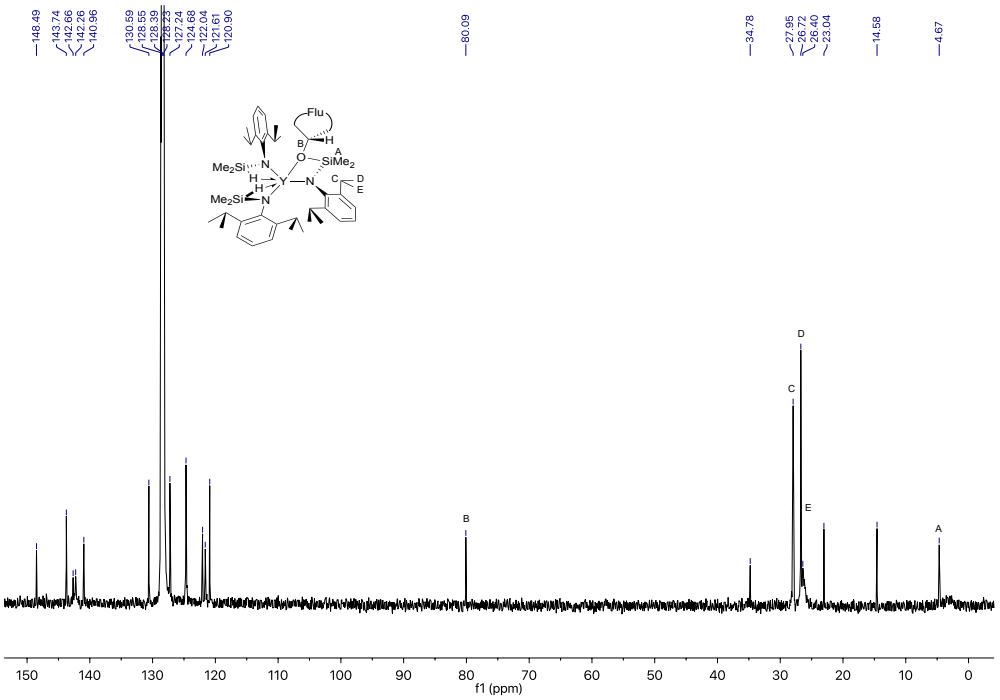

Figure S2. ^{13}C NMR spectrum of Y{N(SiMe$_2$OCHFlu)dipp}{N(SiHMe$_2$)dipp}$_2$ (**YFlu**) acquired in benzene-d_6 at room temperature.

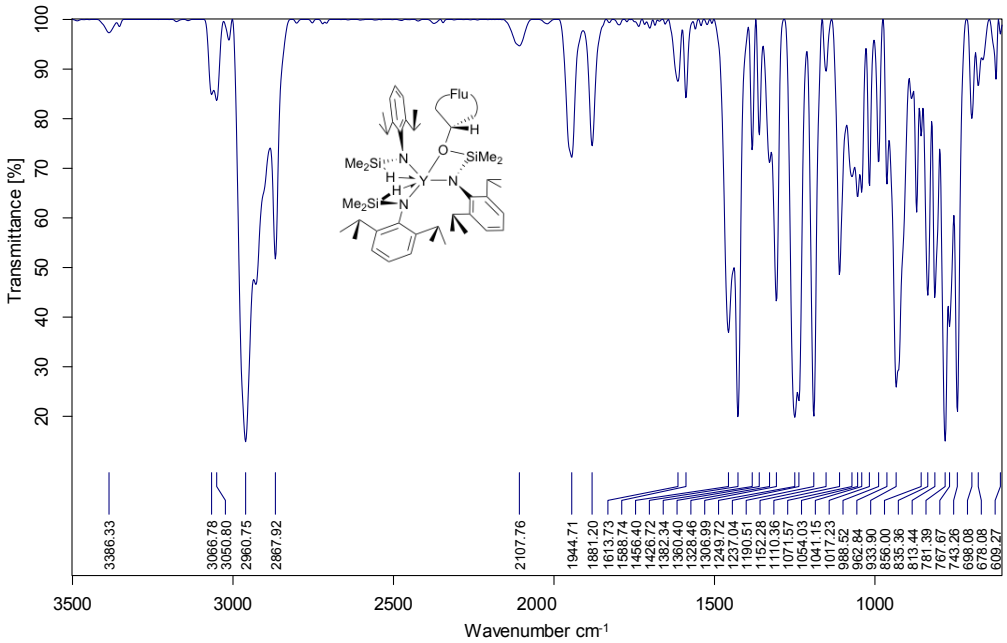

Figure S3. Infrared spectrum of Y{N(SiMe$_2$OCHFlu)dipp}{N(SiHMe$_2$)dipp}$_2$ (**YFlu**) (KBr pellet).

www.manaraa.com

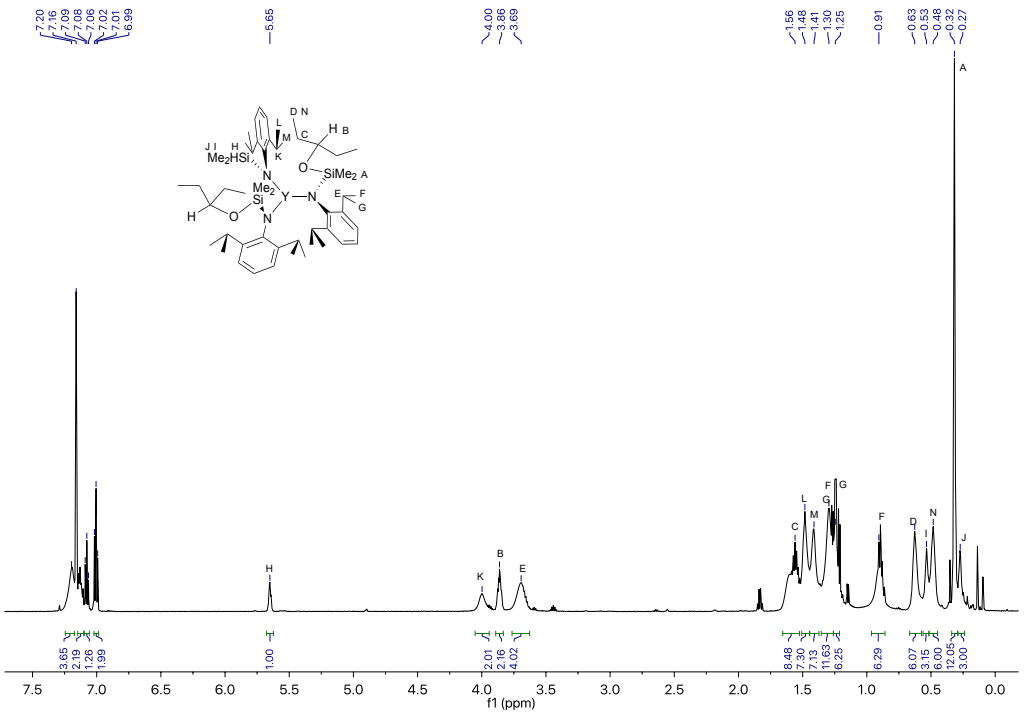

Figure S4. ^{1}H NMR spectrum of Y{N(SiMe$_2$OCHEt$_2$)dipp}{N(SiHMe$_2$)dipp}$_2$ (**YPent$_2$**) acquired in benzene-d_6 at room temperature.

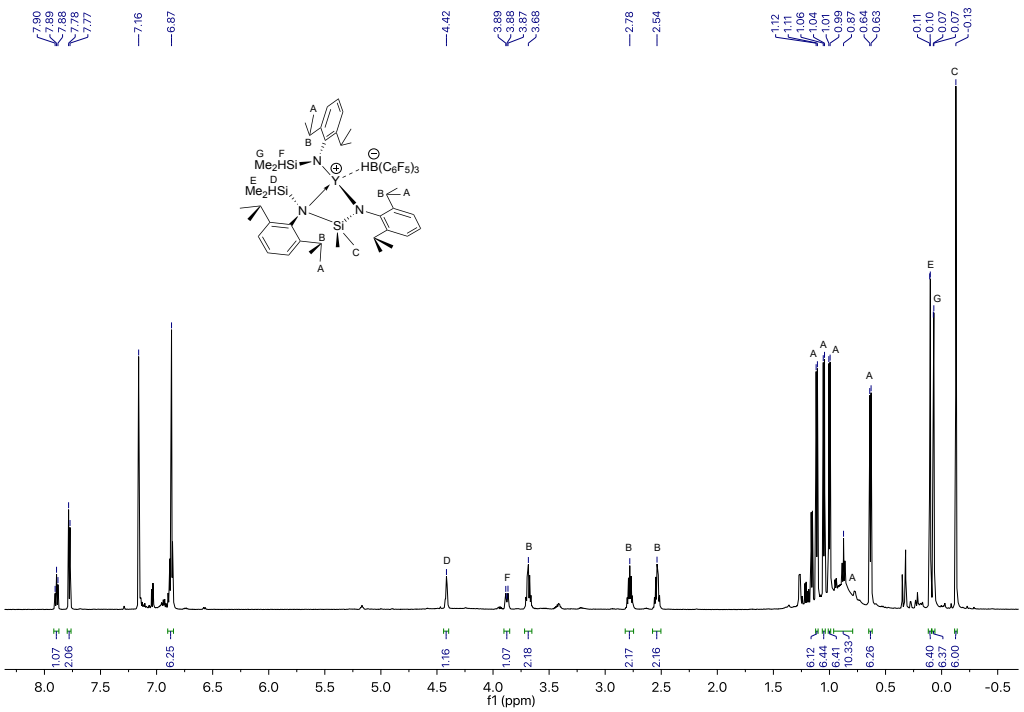

Figure S5. ^{1}H NMR of Y{κ^2N(dipp)SiMe$_2$N(SiHMe$_2$)dipp}{N(SiHMe$_2$)dipp}HB(C$_6$F$_5$)$_3$ (**1**) acquired in benzene-d_6 at room temperature.

www.manaraa.com

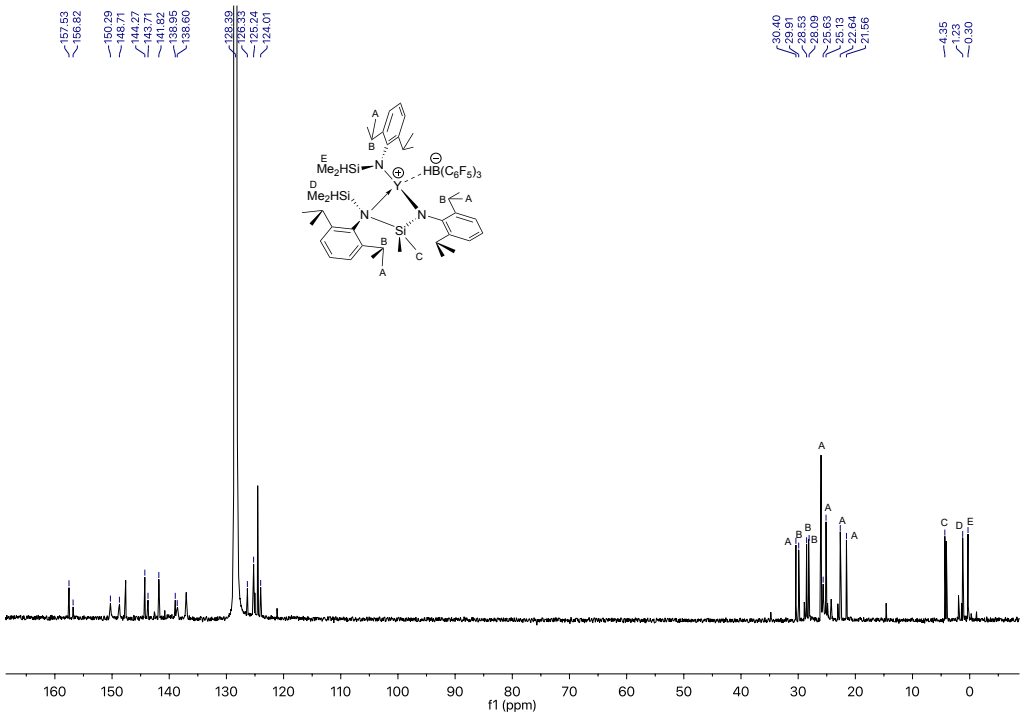

Figure S6. ^{13}C NMR of $Y\{\kappa^2N(dipp)SiMe_2N(SiHMe_2)dipp\}\{N(SiHMe_2)dipp\}HB(C_6F_5)_3$ (**1**) acquired in benzene-d_6 at room temperature.

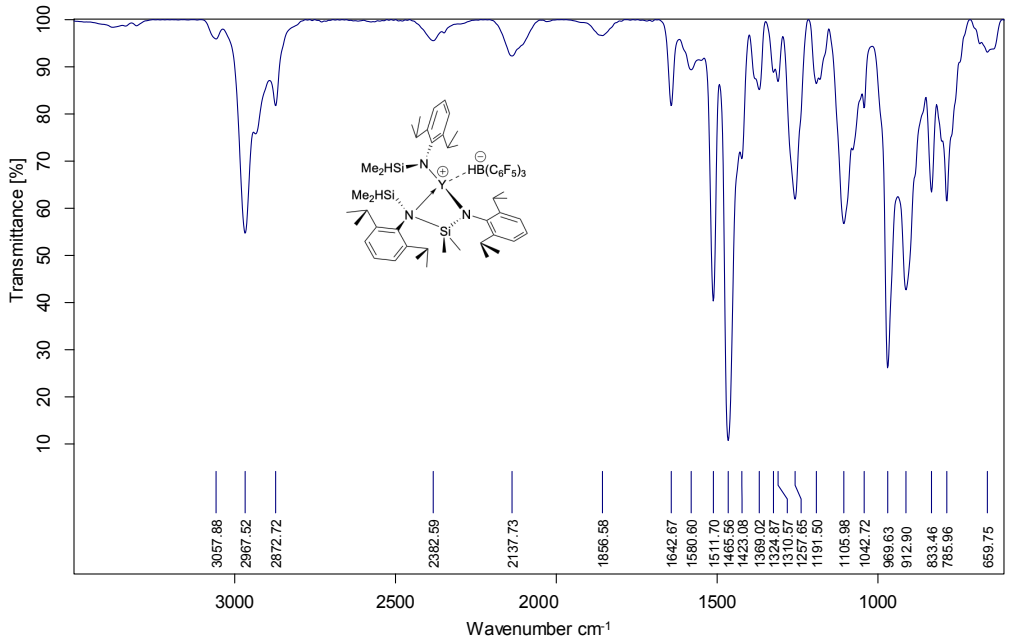

Figure S7. IR spectrum of $Y\{\kappa^2N(dipp)SiMe_2N(SiHMe_2)dipp\}\{N(SiHMe_2)dipp\}HB(C_6F_5)_3$ (**1**) (KBr pellet).

www.manaraa.com

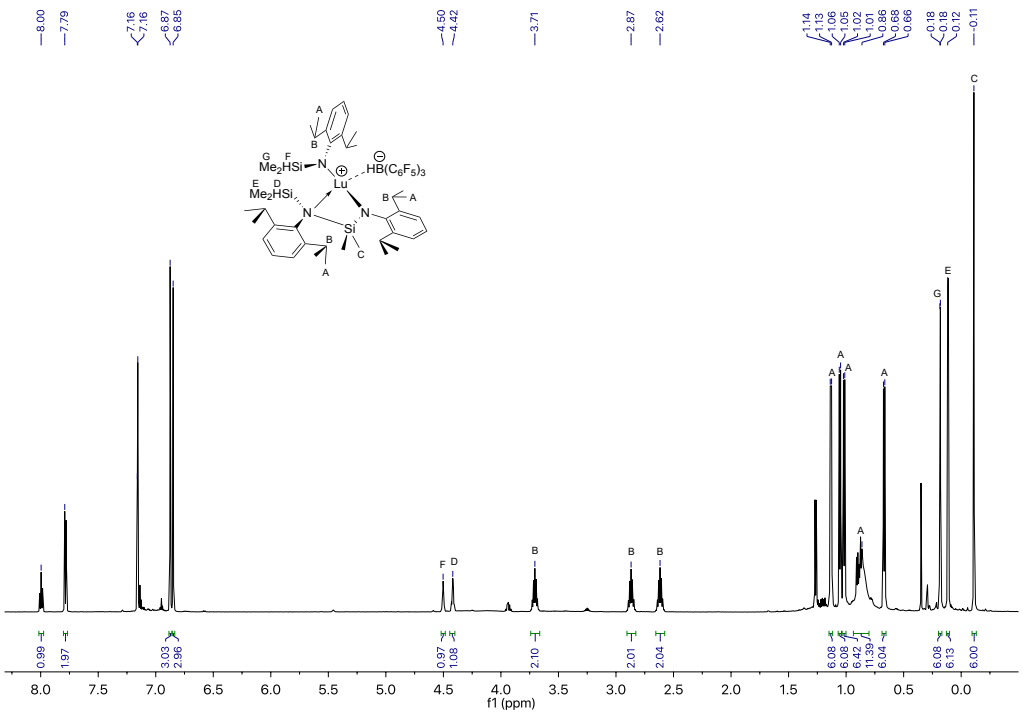

Figure S8. ^{1}H NMR of Lu{κ^{2}N(dipp)SiMe$_2$N(SiHMe$_2$)dipp}{N(SiHMe$_2$)dipp}HB(C$_6$F$_5$)$_3$ (**2**) acquired in benzene-d_6 at room temperature.

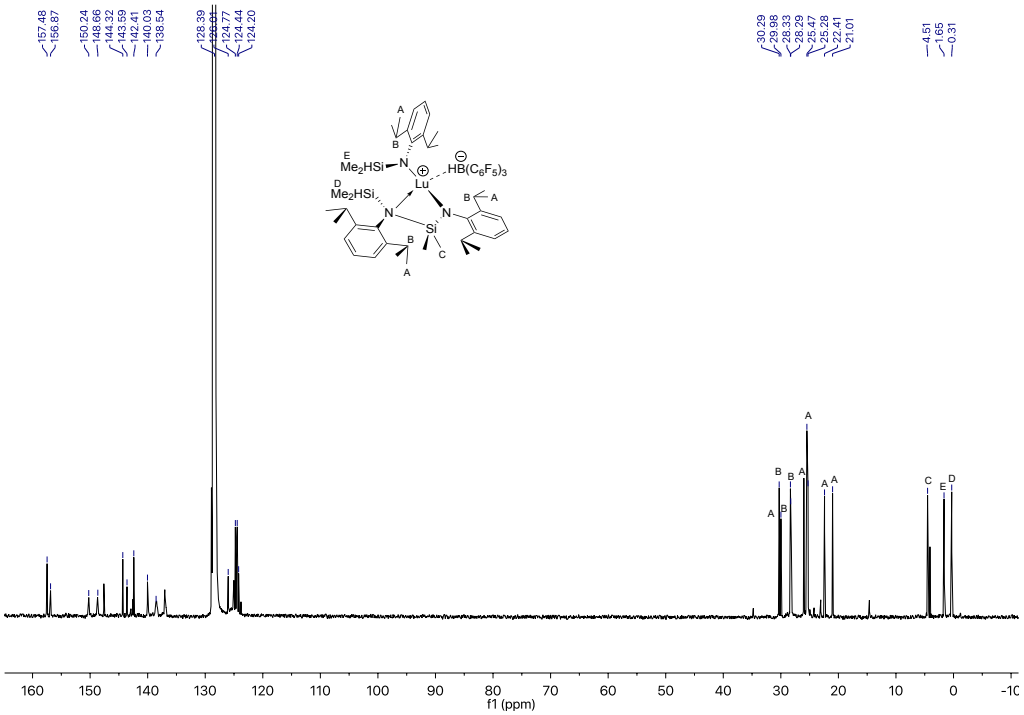

Figure S9. ^{13}C NMR of Lu{κ^{2}N(dipp)SiMe$_2$N(SiHMe$_2$)dipp}{N(SiHMe$_2$)dipp}HB(C$_6$F$_5$)$_3$ (**2**) acquired in benzene-d_6 at room temperature.

www.manaraa.com

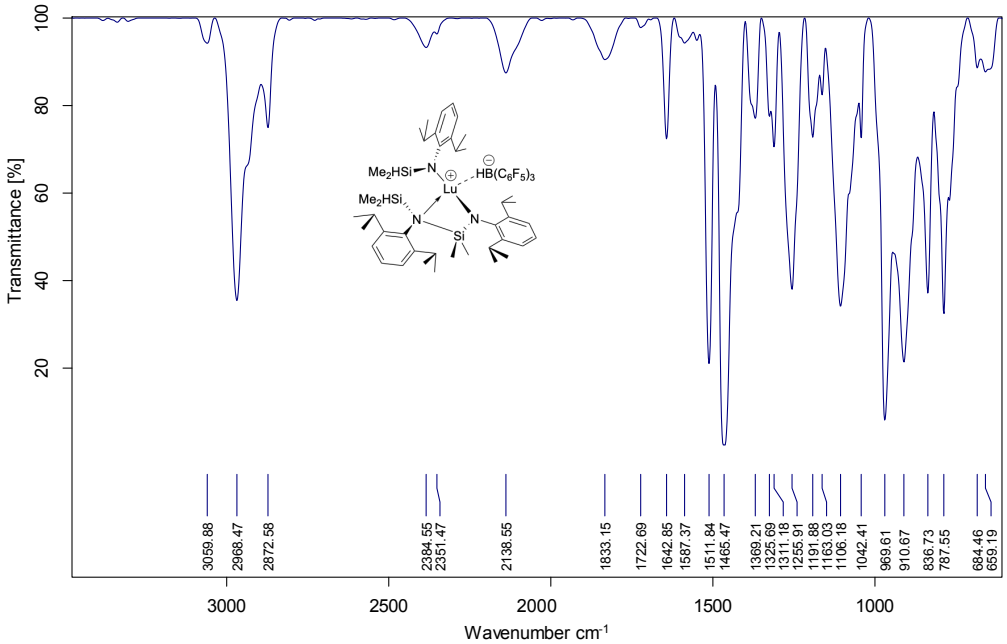

Figure S10. IR spectrum of Lu{κ^{2}N(dipp)SiMe$_2$N(SiHMe$_2$)dipp}{N(SiHMe$_2$)dipp}HB(C$_6$F$_5$)$_3$ (**2**) (KBr pellet).

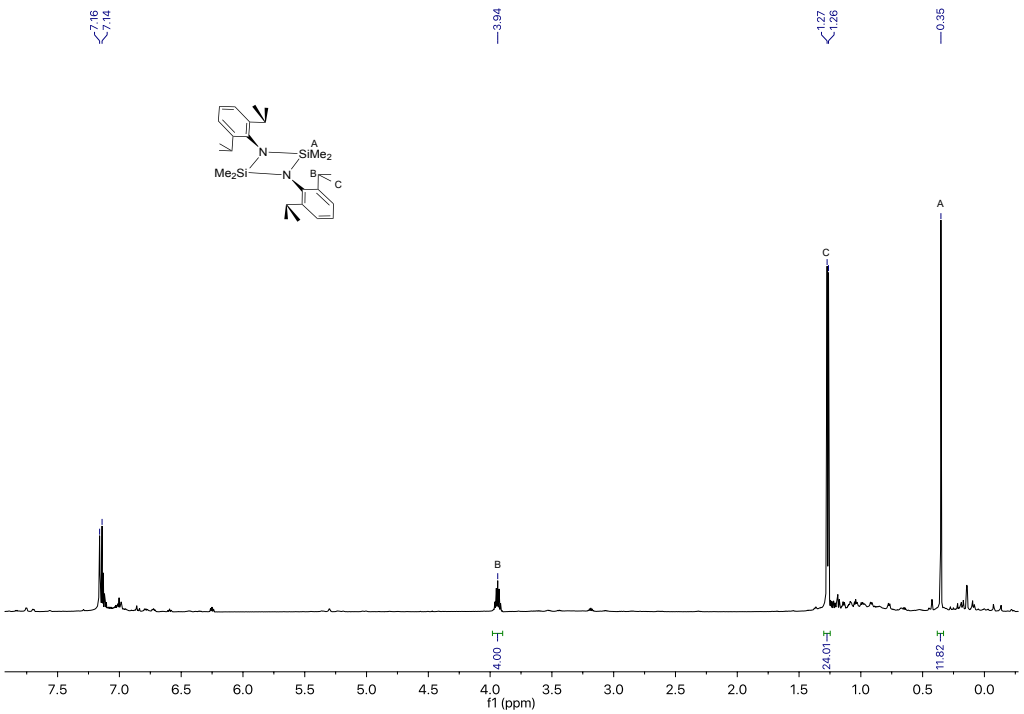

Figure S11. ^{1}H NMR spectrum of (Me$_2$Si–Ndipp)$_2$ acquired in benzene-d_6 at room temperature.

www.manaraa.com

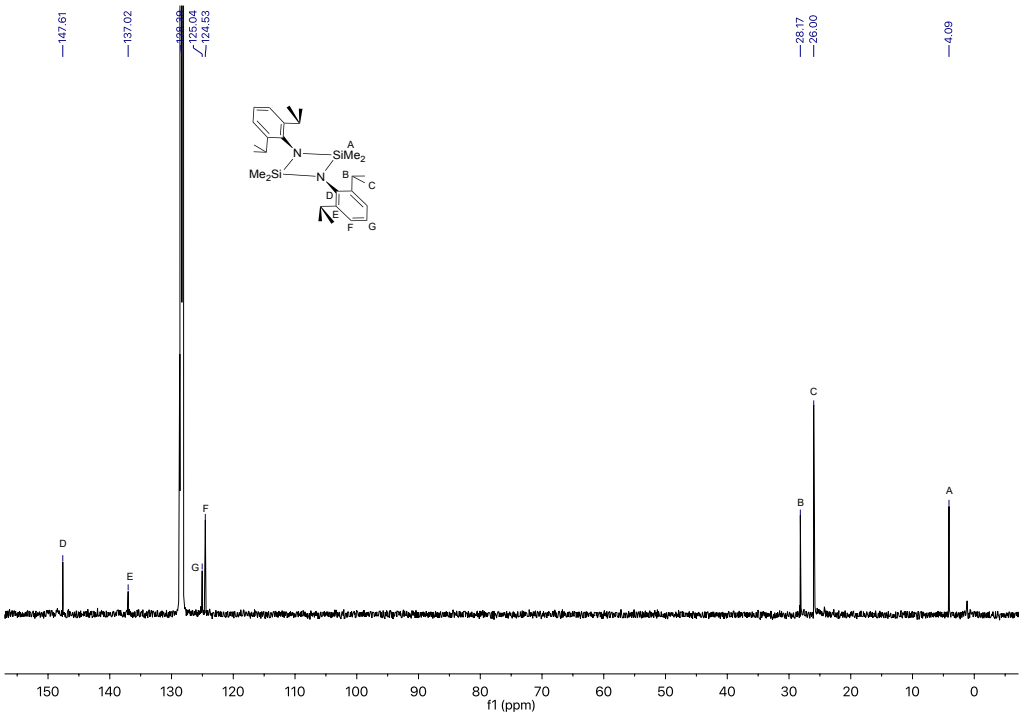

Figure S12. ^{13}C NMR spectrum of $(Me_2Si–Ndipp)_2$ acquired in benzene-d_6 at room temperature.

www.manaraa.com

CHAPTER 6. MECHANISTIC INVESTIGATIONS OF THE REACTION OF TRIS(OXAZOLINYL)BORATO MAGNESIUM ALKYL COMPLEXES AND A HYDRIDE SOURCE

Kasuni C. Boteju, Aaron D. Sadow*

US Department of Energy Ames Laboratory and Department of Chemistry, Iowa State University, Ames IA, 50011, USA

Modified from a manuscript to be submitted to Organometallics

Abstract

Kinetic studies of reactions between tris(oxazolinyl)boratomagnesium alkyl ($To^{M}MgR$) complexes and HBpin were performed for comparison with other sigma bond metathesis type reactions. The reaction of $To^{M}MgMe$ or $To^{M}Mg^{n}Pr$ with HBpin was too fast even at –78 °C to measure using NMR methods. In contrast, $To^{M}MgBn$ reacts with HBpin or DBpin more slowly at room temperature, and studies revealed a second order rate law. Activation parameters obtained from the Eyring plot are $\Delta H^{\ddagger}$ = 13.08(0.02) kcal mol^{-1} and $\Delta S^{\ddagger}$ = –29.09(0.05) cal mol^{-1} K^{-1} for HBpin, whereas the values for the reaction with DBpin are $\Delta H^{\ddagger}$ 11.86(0.05) kcal mol^{-1} and $\Delta S^{\ddagger}$ = –33.44(0.15) cal mol^{-1} K^{-1}. This study shows a kinetic isotope effect of 1.35 at 55 °C and it appears to be increased with increasing the temperature. Thus, B-H/B-D bond cleavage is involved in the rate-determining step.

Introduction

B–E bond formation is important in catalysis (hydroborations, dearomatization, reductions etc.). Some of those reactions involve M–E species interacting with H–B to form B–E bond. Mechanistic understanding of B-E bond formation step or the activation step of a catalytic reaction is important when new selective catalytic sites are designed.

www.manaraa.com

Sometimes B–E bond formation type reactions are postulated to involve concerted four-center transition states identified as σ-bond metathesis and these are generally invoked when redox (oxidative addition/reductive elimination) reactions are unlikely. The hydroboration reactions of pyridine derivatives, aldehydes, ketones, aldemines and ketimines with HBpin using (^{Dipp}Nacnac)Mg*n*Bu (^{Dipp}Nacnac = [(2,6-diisopropyl-phenyl)NC-Me]$_2$CH) as the catalyst are proposed to occur through the concerted σ-bond metathesis mechanism.[1-3] The stoichiometric reaction of (^{Dipp}Nacnac)Mg*n*Bu and HBpin provided [(^{Dipp}Nacnac)Mg(μ-H)$_2$Mg-(^{Dipp}Nacnac)] and *n*BuBin. The Mg–H species was detected by ^{1}H NMR spectroscopy in the above reaction. Addition of 1 equivalent of PhHC=NPh to a reaction mixture of (^{Dipp}Nacnac)Mg*n*Bu and HBpin provided [(^{Dipp}Nacnac)MgNPhCH$_2$Ph indicating that the aldimine inserted into the Mg–H bond.[3] Further, the stoichiometric reaction of (^{Dipp}Nacnac)Mg*n*Bu, HBpin and benzophenone provided (^{Dipp}Nacnac)MgOCHPh$_2$ compound which was identified by ^{1}H NMR spectroscopy.[2] The reaction between (^{Dipp}Nacnac)Mg*n*Bu.pyridine and PhSiH$_3$ gave (^{Dipp}Nacnac)Mg-1,4-dihydropyridine.[4] All these examples of stoichiometric reactions are also proposed to go through concerted σ-bond metathesis mechanism.

Further, B–E formation type reactions using lanthanide or transition metal catalysts are proposed to occur through σ-bond metathesis mechanism. The hydroboration of pyridine derivatives using Cp*$_2$LaH and hydrosilyation of alkenes using Cp*$_2$SmCH(SiMe$_3$)$_2$ are two relevant examples.[5, 6] The stoichiometric reaction between Cp*$_2$ScCH$_2$CMe$_3$ and CH$_4$ to provide Cp*$_2$ScCH$_3$ and CMe$_4$ is proposed to go through concerted σ-bond metathesis mechanism via a transfer of hydrogen from methane to neopentyl ligand.[7] Further methane dehydrosilation with Ph$_2$SiH$_2$ catalyzed by Cp*$_2$ScCH$_3$ is proposed to occur through the same type of mechanism by either Cp*$_2$ScCH$_3$ reacts with Ph$_2$SiH$_2$ (methyl transfer) or Cp*$_2$ScSiHPh$_2$ reacts with CH$_4$ (silyl

www.manaraa.com

transfer) in the transition state.[8] The drehydropolymerization of silanes to polysilanes is also proposed to go through concerted σ-bond metathesis mechanism. Further stochiometric studies of Cp*CpHf(SiH_2Ph)Cl and $PhSiH_3$ provides Cp*CpHfHCl and Ph_2SiSiH_2Ph by coupling of the metal silyl complex with the hydrosilane to produce Si–Si bond via σ-bond metathesis mechanism.[9]

In addition, B–E bond formation type reactions are postulated to involve pathways avoiding σ-bond metathesis. The hydroboration of pyridine derivatives catalyzed by $(^{Dipp}Nacnac)_2Mg_2H_2$ is proposed to occur through a hydride transfer from borane to pyridine to give 1,2 and 1,4 dihydro pyridine derivatives.[10] A zwitterionic mechanism is proposed for the hydroboration of esters catalyzed by To^MMgMe. The addition of HBpin to To^MMgOCH_2R to form the B–O bond is occurred via $To^MMg\{(RCH_2O)_2Bpin\}$ zwittorionic intermediate.[11] The proposed mechanism for the dehydrocoupling of primary amines and silanes using $To^MMgNHtBu$ as the catalyst is a nucleophilic attack on the silane to form the Si–N bond.[12] The stoichiometric reaction between $To^MMgNHtBu$ and $PhMeSiH_2$ is also proposed to occur through a nucleophilic attack by the magnesium amide.[12] Hydrosilylation of alkenes catalyzed by $KCH(SiMe_3)(o\text{-}NMe_2Ph)$ is postulated to occur through a pathway of which KH (active catalyst) reacts with $PhSiH_3$ to give $K^+[PhSiH_4]^-$ followed by alkene reaction to provide the hydrosilylated product. The extra hydride from the silyl anion is eliminated to react with another $PhSiH_3$ to provide the anion $[PhSiH_4]^-$ in the catalytic cycle.[13]

Examples of transition and rare earth metal complexes involved in non σ-bond metathesis reaction pathways are also available in literature. The α-phenyl elimination of Cp*CpHf($SnPh_3$)Cl complex is proposed to occur through a phenonium ion via nucleophilic attack of the migrating aryl group onto the electrophilic metal center.[14] The hydroboration of carbonyls catalyzed by

www.manaraa.com

$Cp_2Ti(HBcat)_2$ is proposed to go through an intermediate formed by the reaction of $Cp_2Ti(Hpin)$ and the carbonyl compound in the catalytic cycle which is a resonance structure between a Ti(II) η_2 carbonyl complex and a Ti(IV) metallacycle.[15] The hydrosilylation of CO_2 catalyzed by a cationic scandium anilido bypyridyl complex is postulated to occur through a nucleophilic attack of $(C_6F_5)_3B–OCHO$ on $SiEt_3$, thus forming silylformate ($Et_3SiOCHO$) and regenerating the cationic Sc complex.[16]

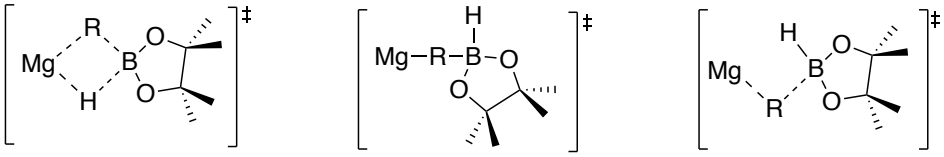

Figure 1. Proposed mechanisms for B–E bond formation

Attempts to trap Mg–H or the active species of the catalytic cycle can be found in literature. The compound (^{Dipp}Nacnac)Mg*n*Bu was reacted with HBpin to provide [(^{Dipp}Nacnac)Mg(μ-H) (μ-H_2Bpin)Mg-(^{Dipp}Nacnac)][1] and the reaction of To^{M}MgMe with excess HBpin provided To^{M}MgH_2Bpin.[11] Similarly to the HBpin reactions, $PhSiH_3$ also used as a hydride source to isolate MgH species. The compound [(^{Dipp}Nacnac)Mg–Mg[(^{Dipp}Nacnac)] was reacted with $PhSiH_3$ to obtain [(^{Dipp}Nacnac)Mg(μ-H)$_2$Mg-(^{Dipp}Nacnac)] complex.[17] The tertbutyl version of the same type of compound (^{tBu}Nacnac)Mg*n*Bu was treated with $PhSiH_3$ to give [(^{tBu}Nacnac)Mg(μ-H)$_2$Mg-(^{tBu}Nacnac)] and addition of DMAP to that provided (^{tBu}Nacnac)MgH.DMAP compound.[18] All of these Mg–H adducts are characterized by X-ray diffraction studies.

The stoichiometric kinetic studies between Mg alkyl complexes & HBpin has not been studied in literature. The kinetic features of reactions of magnesium alkyls with a borane (HBpin)

www.manaraa.com

was investigated to identify parameters associated with σ-bond metathesis type reactions which leads to find the mechanism of the activation step of the catalytic cycle in hydroboration.

Results

The reaction of To^{M}MgMe (To^{M} = tris(4,4-dimethyl-2-oxazolinyl)phenylborate) and 1 equivalent of HBpin provides MeBpin quantitively. A black precipitate is also observed at the end of the reaction, and this material is insoluble and poorly characterized (Eq 1).[11] The reaction is instantaneous at room temperature or at –78 °C.

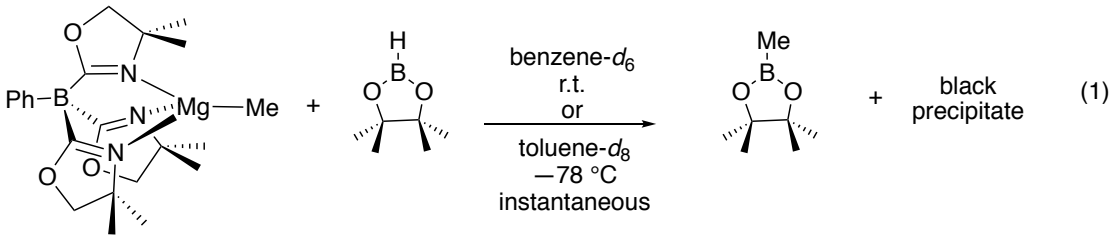

(1)

As the reaction of To^{M}MgMe with HBpin failed to monitor through NMR or IR kinetic studies, two other To^{M}MgR compounds (To^{M}Mg*n*Pr and To^{M}MgBn) were tested for the reactivity with HBpin. The reaction of To^{M}Mg*n*Pr with 1 equivalent of HBpin provides To^{M}MgH$_2$Bpin and *n*PrBpin (Eq 2). In contrast to the To^{M}MgMe reaction, a black precipitate is not observed. The To^{M}Mg*n*Pr reaction is also instantaneous at –78 °C. Similarly, to the To^{M}Mg*n*Pr reaction, 1:1 equivalent reaction of To^{M}MgBn and HBpin provides To^{M}MgH$_2$Bpin and BnBpin (Eq 3). The latter reaction is slow enough at room temperature to monitor by NMR kinetics.

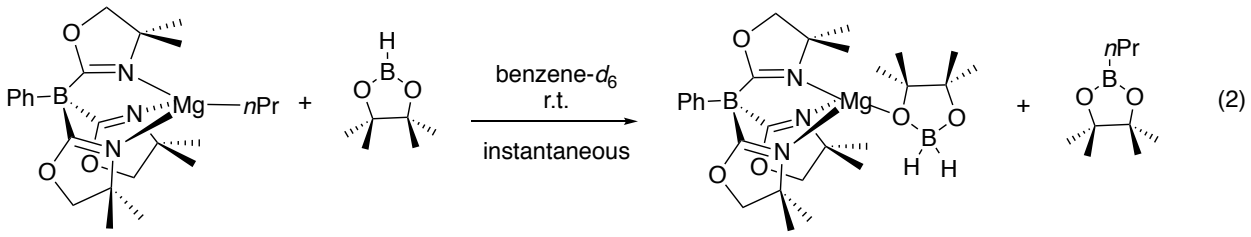

(2)

www.manaraa.com

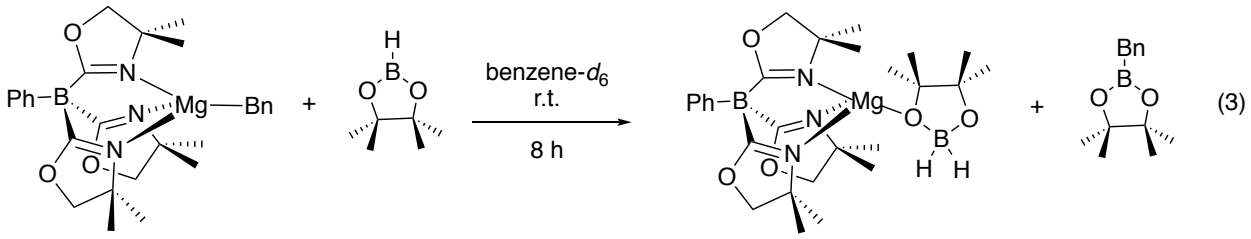

The reaction of To^{M}MgBn and HBpin was monitored by ^{1}H NMR spectroscopy and the concentrations of reactants (To^{M}MgBn) were determined by integration and comparison to a standard of known concentration. Pseudo first order kinetics experiments of To^{M}MgBn with excess HBpin concentrations at room temperature provided first order dependence on both To^{M}MgBn and HBpin (Figure 2 and 3).

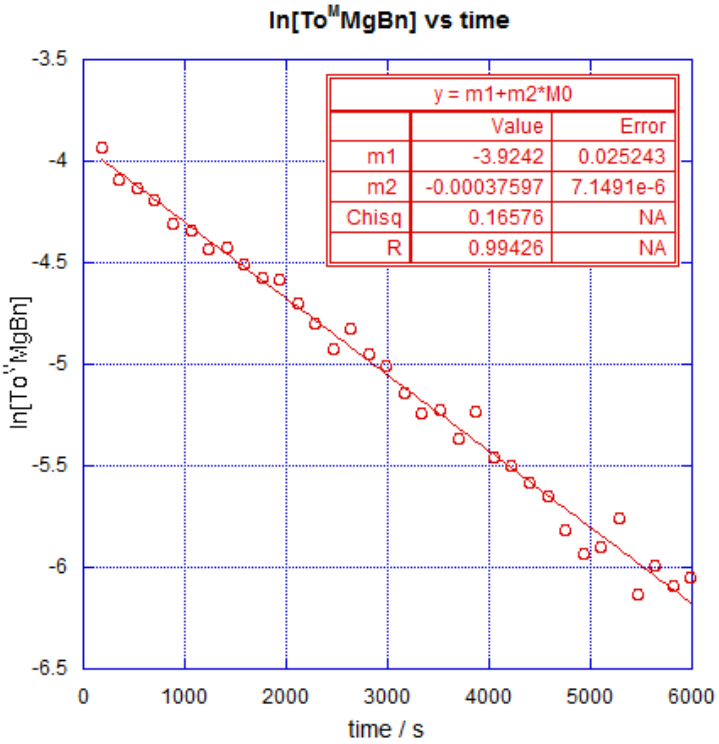

Figure 2. Pseudo first order plot of ln([To^{M}MgBn]) vs. time for the reaction of To^{M}MgBn:HBPin = 1:10. The curve represents non-weighted linear least squares best fit of the data to the equation: $\ln([To^{M}MgBn]_t) = \ln([To^{M}MgBn]_0) - k_{obs}t$.

www.manaraa.com

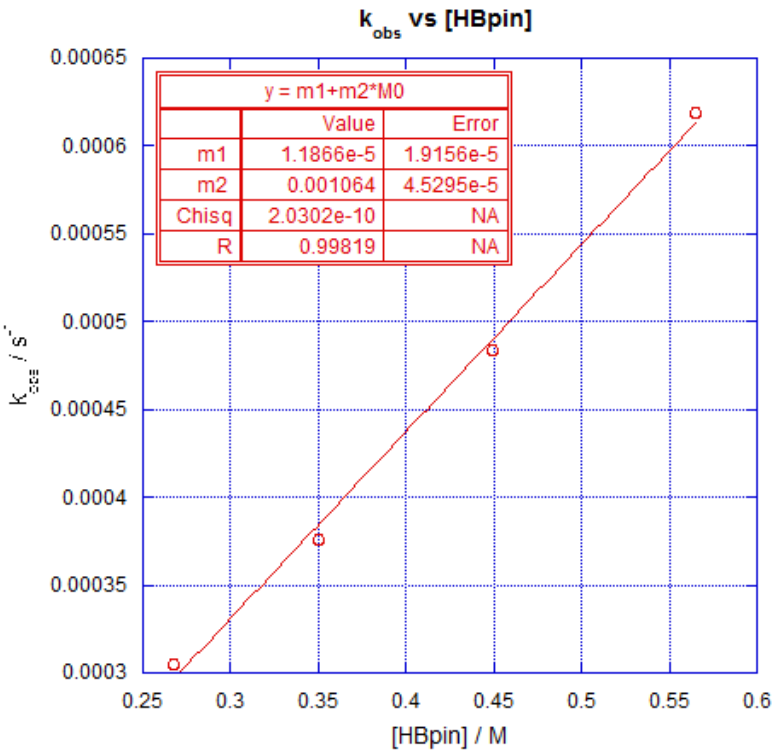

Figure 3. Plot of k_{obs} vs. [HBpin] for the reaction of To^{M}MgBn and HBPin; To^{M}MgBn:HBPin = 1:10, 1:15, 1:20, 1:25. The curve represents non-weighted linear least squares best fit of the data to the equation: $k_{obs} = k[HBpin]$.

Second order kinetics experiments were run with little excess of HBpin and the results confirmed that it is an overall second order reaction in the rate determining step with a rate constant of 7.013×10^{-4} $M^{-1}s^{-1}$obtained at 298 K (Figure 4).

$$-\frac{d[To^{M}MgBn]}{dt} = k[To^{M}MgBn][HBpin]$$

www.manaraa.com

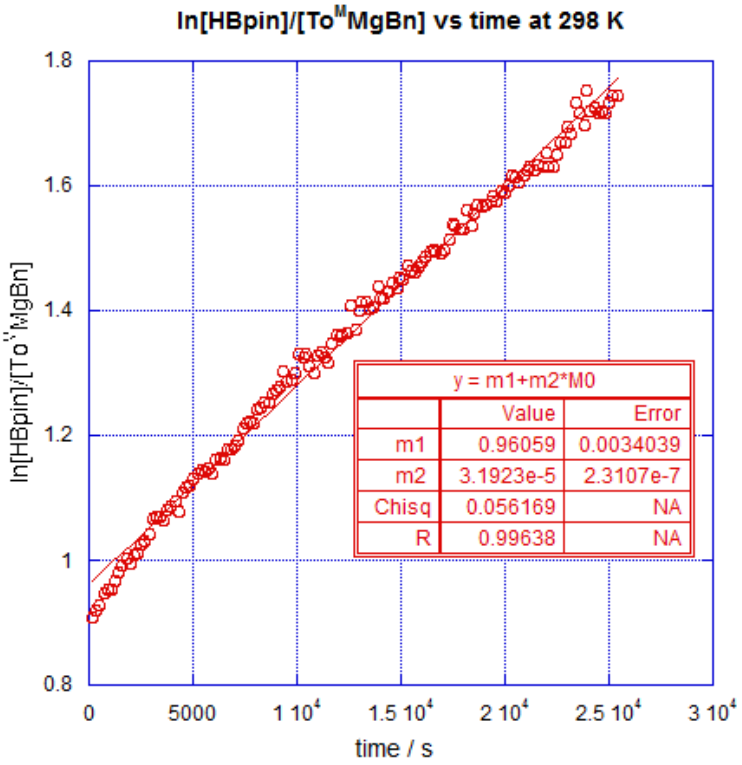

Figure 4. Second-order plots of ln([HBPin]/[To^{M}MgBn]) vs. time for the stoichiometric reaction of To^{M}MgBn and HBPin. The curves represent non-weighted linear least squares best fits of the data to the equation: $\ln([HBPin]_t/[To^{M}MgBn]_t) = \ln([HBPin]_0/[To^{M}MgBn]_0) + k\Delta_0 t$. Δ_0(298 K) = 0.0455 M; Δ_0(308 K) = 0.0482 M; Δ_0(318 K) = 0.0485 M; Δ_0(328 K) = 0.0521 M; Δ_0(338 K) = 0.0485 M.

Second order kinetics experiments between To^{M}MgBn and HBpin were run from 298 K to 338 K at every 10 K intervals to find the activation parameters. The Eyring plot provided $\Delta H^{\ddagger}$ = 13.08(0.02) kcal mol^{-1} and $\Delta S^{\ddagger}$ = –29.09(0.05) cal mol^{-1} K^{-1} as the parameters (Figure 5).

The rate law of the B-C bond formation reaction indicates the rate-limiting step involves both To^{M}MgR and HBpin. Further kinetic investigations were needed at this point to make the determination between σ-bond metathesis or other type of mechanism.

www.manaraa.com

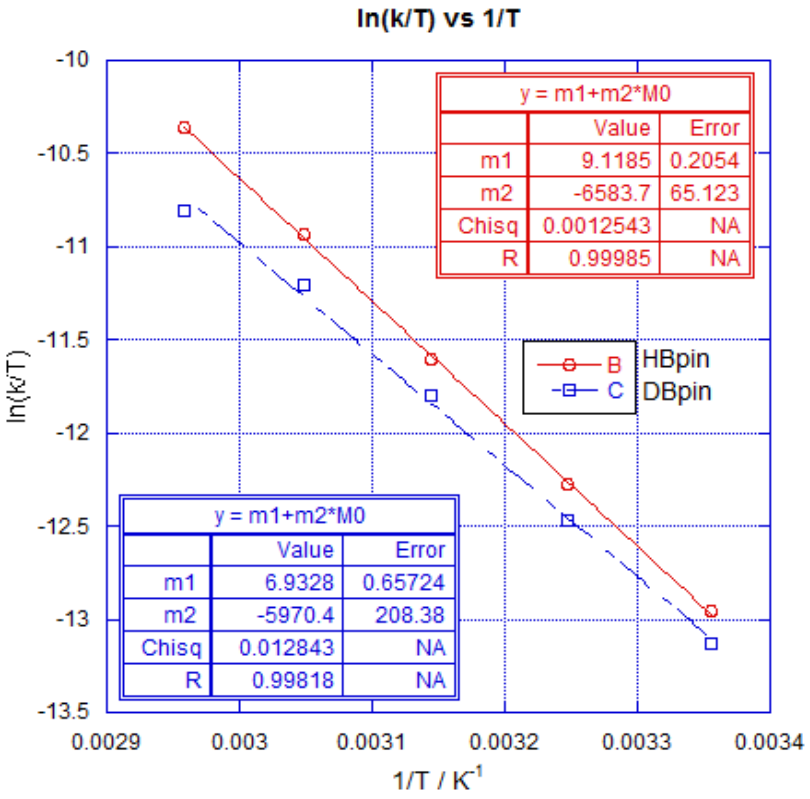

Figure 5. Plot showing the temperature dependence for the reaction of To^{M}MgBn and HBpin (Blue) and To^{M}MgBn and DBpin (Red) from 298 K to 338 K. Each ln(k/T) value is obtained from a linear-least-squares fit of ln([H(D)Bpin]/[To^{M}MgBn]) vs. time.

In order to study the kinetic isotope effect, second order kinetics experiments were run for the reaction of To^{M}MgBn and little excess of DBpin. The results showed an overall second order dependence of this reaction similarly to HBpin. The rate constant for the reaction at room temperature was 5.924×10^{-4} $M^{-1}s^{-1}$. The activation parameter values obtained from the Eyring plot were $\Delta H^{\ddagger}$ 11.86(0.05) kcal mol^{-1} and $\Delta S^{\ddagger}$ = –33.44(0.15) cal mol^{-1} K^{-1}. The results showed a kinetic isotope effect of 1.35 and 1.55 at 55 °C and 65 °C respectively. Despite a measurable kinetic isotope effect was not observed in the temperature range of 25 – 45 °C.

www.manaraa.com

Discussion

Here we compare the kinetic parameters obtained from To^{M}MgBn and HBpin reaction with other B–E bond formation type reactions in literature.

Although the stoichiometric reaction of To^{M}MgBn and HBpin provided a bimolecular rate law, the catalytic reaction of hydroboration of aldemines and ketimines with HBpin using (^{Dipp}Nacnac)Mg*n*Bu catalyst provided an overall third order rate law; rate = –k'[(^{Dipp}Nacnac)Mg*n*Bu][Imine]^{2}/[HBpin]^{0}.[3] Marks and co-workers obtained a rate law of, rate = k[Cp*$_2$LaH][pyridine]^{x}[HBpin]$^{-1}$ (x = 0-1) for the hydroboration of pyridine derivatives catalyzed by Cp*$_2$LaH.[5] As a combination of above two B–N formation reactions, B–O formation reaction by Sadow and co-workers obtained a rate law with a half order dependence on the substrate and zero order dependence on borane; rate = –k'[ToMMgMe][ester]$^{0.5}$[HBpin]^{0} for the hydroboration of esters.[11] The hydroboration of pyridine derivatives (B–N formation) catalyzed by Cp*$_2$LaH provided activation parameters of $\Delta H^{\ddagger}$ = 15.7(0.5) kcal mol^{-1} and $\Delta S^{\ddagger}$ = –27.2(0.3) cal mol^{-1} K^{-1}.[5] These values are comparable with current investigations of B–C formation using To^{M}MgBn and HBpin which provided the activation parameters of $\Delta H^{\ddagger}$ = 13.08(0.02) kcal mol^{-1} and $\Delta S^{\ddagger}$ = –29.09(0.05) cal mol^{-1} K^{-1}. In addition, both reaction pathways occur through an associative mechanism.

Similarly, to the To^{M}MgBn and HBpin reaction, both stoichiometric reactions of To^{M}MgNH*t*Bu with PhMeSiH$_2$ and To^{M}MgMe with PhSiH$_3$ provided bimolecular rate laws; rate = k[Mg][silane].[12] The catalytic reaction of hydrosilylation of alkenes using Cp*$_2$SmCH(SiMe$_3$)$_2$ by Mark's group also obtained an overall second order rate law, with first order in both catalyst and silane.[6] The activation parameters are calculated for the Si–N and Si–C formation reactions performed by Sadow and co-workers. In the reaction of To^{M}MgNH*t*Bu and PhMeSiH$_2$, the activation parameters were $\Delta H^{\ddagger H}$ = 5.9(2) kcal mol^{-1} and $\Delta S^{\ddagger H}$ = –46.5(8) cal mol^{-1} K^{-1}.[12] The

www.manaraa.com

reaction of To^{M}MgMe and *p*-MeC$_6$H$_4$SiH$_3$ provided $\Delta H^{\ddagger}$ = 15(1) kcal mol^{-1} and $\Delta S^{\ddagger}$ = –30(3) cal mol^{-1} K^{-1} as the activation parameters. The values obtained for the reaction of To^{M}MgBn and HBpin ($\Delta H^{\ddagger}$ = 13.08(0.02) kcal mol^{-1} and $\Delta S^{\ddagger}$ = –29.09(0.05) cal mol^{-1} K^{-1}) are in a similar range to the values obtained for Si–C formation rather than Si–N formation reaction. The same trend in the activation parameters was observed for the reactions with deuterated silanes and borane. Further, the negative entropy of activation implies that all three reactions have highly ordered transitions states. In contrast to the reaction of To^{M}MgBn with H(D)Bpin, a primary kinetic isotope effect was not observed for the reactions of To^{M}MgNH^{t}Bu with PhMeSiH(D)$_2$ and To^{M}MgMe with *p*-MeC$_6$H$_4$SiH(D)$_3$. Therefore, breaking of Si–H bond does not involve in the rate-determining step in the latter two reactions. Furthermore, the aryl substituent showed a significant effect on the rate of reactions between To^{M}MgNH^{t}Bu or To^{M}MgMe and substituted Ph(aryl)SiH$_2$ (aryl = Ph, *p*-C$_6$H$_4$F, *p*-C$_6$H$_4$Me, *p*-C$_6$H$_4$OMe, *p*-C$_6$H$_4$CF$_3$) where the organosilanes with electron-withdrawing groups reacted more rapidly than those with electron-donating groups. Hammett plots of log(k_X/k_H) versus σ_p^i provided a straight line with a positive slope and a ρ value of 1.4 ($\rho_{MgNHtBu}$) and 1.5(2) (ρ_{MgMe}). Therefore, a nucleophilic attack by Mg–E on silicon to give a five coordinate Si species (To^{M}MgH$_3$C–Si(aryl)H$_3$) in the rate determining step followed by a rapid hydride transfer on the [Mg] and loss of organosilane is proposed as the mechanism for the Si–N and Si–C bond formation reaction.

Similarly, to the B–C formation reaction of To^{M}MgBn and HBpin, the stoichiometric reaction of Cp*$_2$ScCH$_2$CMe$_3$ and CH$_4$ provided a bimolecular rate law; rate = k[Cp*$_2$ScCH$_2$CMe$_3$][CH$_4$] for the C–H formation.[7] In addition, the stoichiometric reaction between Cp*CpHf(SiH$_2$Ph)Cl and PhSiH$_3$ also provided a similar rate law as above for the Si–Si formation reaction.[9] The activation parameters obtained for the reactions of Cp*$_2$ScCH$_2$CMe$_3$ with

www.manaraa.com

CH_4 and Cp*CpHf(SiH_2Ph)Cl with $PhSiH_3$ were $\Delta H^{\ddagger}$ = 11.4(1) kcal mol^{-1}, $\Delta S^{\ddagger}$ = –36(1) cal mol^{-1} K^{-1} and $\Delta H^{\ddagger}$ = 18.5(5) kcal mol^{-1} and $\Delta S^{\ddagger}$ = –21(2) cal mol^{-1} K^{-1} respectively.[7, 9] The enthalpy and entropy of activation values obtained for the alpha phenyl elimination of Cp*CpHf($SnPh_3$)Cl (Sn–Sn formation) were $\Delta H^{\ddagger}$ = 24(1) kcal mol^{-1} and $\Delta S^{\ddagger}$ = –15(1) cal mol^{-1} K^{-1} respectively.[14] All these values are close to the activation parameters obtained for the reaction of To^{M}MgBn and HBpin ($\Delta H^{\ddagger}$ = 13.08(0.02) kcal mol^{-1} and $\Delta S^{\ddagger}$ = –29.09(0.05) cal mol^{-1} K^{-1}). Similarly, to the To^{M}MgBn and HBpin reaction, above three reactions (C–H, Si–Si, Sn–Sn formation) have highly ordered transition states. A kinetic isotope effect was observed for both the reactions of Cp*$_2$ScCH_2CMe_3 vs CH_4 and Cp*CpHf(SiH_2Ph)Cl vs $PhSiH_3$ as the k_H/k_D were 10.2 and 2.7 respectively.[7, 9] The results indicate that transfer of hydrogen from CH_4 in Cp*CpHf(SiH_2Ph)Cl and $PhSiH_3$ reaction and transfer of hydride from silane in Cp*CpHf(SiH_2Ph)Cl and $PhSiH_3$ reaction involve in the rate determining step. Therefore, σ-bond metathesis mechanism is postulated for these two reactions. The rate of the reaction of alpha phenyl elimination of Cp*CpHf($SnPh_3$)Cl to provide Cp*CpHfPhCl and $(Ph_2Sn)_n$ showed a significant effect on aryl substituent (*p*-C_6H_4OMe, *p*-C_6H_4F, *p*-$C_6H_4CF_3$) where the aryl with electron-donating groups reacted more rapidly than those with electron-withdrawing groups. Hammett plot provided a straight line with a negative slope and a ρ value of –2.13. Therefore, the mechanism of the reaction is proposed to involve an interaction of the electrophilic hafnium center with the nucleophilic migrating group.[14]

After comparing the kinetic parameters obtained for the stoichiometric reaction between To^{M}MgBn and HBpin with literature examples, the current investigations of B–C bond formation are concluded below.

www.manaraa.com

Conclusion

The negative entropy of activation implies that B–C bond formation reaction performs through an ordered transition state. A primary kinetic isotope effect is observed for the B–C bond formation, showing that breaking of the B–H bond involves in the rate-determining step. Thus, the reaction can be occurred via a concerted σ-bond metathesis mechanism or a nucleophilic attack by the benzyl carbon on boron followed by the hydride transfer on the [Mg] in the rate-determining step to give [Mg]–H and BnBpin via an associative mechanism.

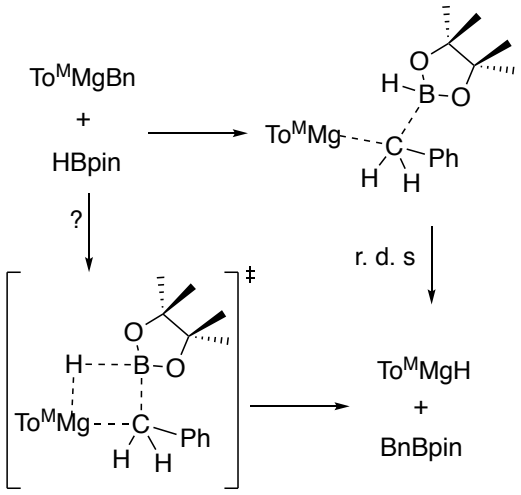

Scheme 1. Plausible reaction pathways for the stoichiometric reaction between To^{M}MgBn and HBpin

Experimental

General. All manipulations were performed under a dry argon atmosphere using standard Schlenk techniques or under a nitrogen atmosphere in a glovebox unless otherwise indicated. Water and oxygen were removed from benzene, toluene, pentane, diethyl ether, and tetrahydrofuran solvents using an IT PureSolv system. Benzene-d_6 and toluene-d_8 were heated to reflux over Na/K alloy and vacuum-transferred. HBpin was purchased Sigma-Aldrich and used as

www.manaraa.com

received. $To^{M}MgMe$[19] and DBpin[20] were prepared according to literature procedures. Mg*n*Pr$_2$(O$_2$C$_4$H$_8$)$_2$ and MgBn$_2$(O$_2$C$_4$H$_8$)$_2$ were prepared according to the same procedure which involves the preparation of MgMe$_2$(O$_2$C$_4$H$_8$)$_2$.[21] ^{1}H, ^{13}C, and ^{15}N HMBC NMR spectra were collected on a Bruker DRX-400 spectrometer or a Bruker Avance III-600 spectrometer. Infrared spectra were measured on a Bruker Vertex 80, using KBr pellet (transmission mode). Elemental analyses were performed using a Perkin-Elmer 2400 Series II CHN/S. X-ray diffraction data was collected on a Bruker APEX II diffractometer.

To^{M}Mg*n*Pr. Solid Mg(*n*-C$_3$H$_7$)$_2$(O$_2$C$_4$H$_8$)$_2$ (0.209 g, 0.730 mmol) was added to a benzene solution of H[To^{M}] (0.233 g, 0.608 mmol, 10 mL), and the reaction mixture was stirred for 2 h. The solvent was evaporated under reduced pressure to provide a white solid, which was washed with pentane (3 × 3 mL) to provide spectroscopically pure material in moderate yield (0.146 g, 0.297 mmol, 48.8%). Recrystallization of 0.102 g of the crude product from diethyl ether at –30 °C gave an analytically pure product (0.0176 g, 0.0357 mmol, 17.9%). ^{1}H NMR (benzene-d_6, 600 MHz): δ 8.30 (d, $^3J_{HH}$ = 6.0 Hz, 2 H, *ortho*-C$_6$H$_5$), 7.54 (t, $^3J_{HH}$ = 6.6 Hz, 2 H, *meta*-C$_6$H$_5$), 7.36 (t, $^3J_{HH}$ = 6.6 Hz, 1 H, *para*-C$_6$H$_5$), 3.40 (s, 6 H, CNCMe$_2$C*H*$_2$O), 2.24 (m, $^3J_{HH}$ = 6.6 Hz 2 H, MgCH$_2$C*H*$_2$CH$_3$), 1.55 (t, $^3J_{HH}$ = 6.6 Hz 3 H, MgCH$_2$CH$_2$C*H*$_3$), 1.02 (s, 18 H, CNC*Me*$_2$CH$_2$O), 0.27 (t, $^3J_{HH}$ = 7.8 Hz 2 H, MgC*H*$_2$CH$_2$CH$_3$), ^{13}C NMR (benzene-d_6, 150 MHz): δ 191.59 (br, *C*NCMe$_2$CH$_2$O), 142.85 (*ipso*-C$_6$H$_5$), 136.48 (*ortho*-C$_6$H$_5$), 127.20 (*meta*-C$_6$H$_5$), 126.24 (*para*-C$_6$H$_5$), 80.37 (CNCMe$_2$*C*H$_2$O), 65.61 (CN*C*Me$_2$CH$_2$O), 28.51 (CNC*Me*$_2$CH$_2$O), 24.81 (Mg-CH$_2$CH$_2$*C*H$_3$), 24.72 (Mg-CH$_2$*C*H$_2$CH$_3$), 10.74 (Mg-*C*H$_2$CH$_2$CH$_3$), ^{11}B NMR (benzene-d_6, 192 MHz): δ –18.1 (br s). ^{15}N NMR (benzene-d_6, 60.8 MHz): δ –157.0. IR (KBr, cm^{-1}): 3074 s, 3044 s, 2964 s, 2930 s, 2885 s, 1593 s (ν_{CN}), 1493 s, 1463 s, 1433 m, 1383 m, 1365 s, 1269 s, 1194 s,

www.manaraa.com

1153 s, 989 m, 968 s, 932 s, 893 s, 839 s, 809 s, 745 s, 703 s, 660 m, 595 s, 494 m, 473 m. Anal. Calc. for $C_{25}H_{39}BN_3O_3Mg$: C, 64.61; H, 8.46; N, 9.04. Found: C, 64.20; H, 8.22; N, 9.02. Mp 135-137 °C (dec).

To^{M}MgBn. Solid $Mg(Bn)_2(O_2C_4H_8)_2$ (0.296 g, 0.773 mmol) was added to a benzene solution of H[To^{M}] (0.247 g, 0.644 mmol, 10 mL), and it was stirred for 5 h. The reaction mixture was filtered, and the solvent was evaporated under reduced pressure to provide a pale yellow solid, which was washed with pentane (3 × 3 mL) to provide the desired product (0.205 g, 0.400 mmol, 62.0%). Recrystallization of product from diethyl ether at –30 °C gave x-ray quality crystals. ^{1}H NMR (benzene-d_6, 600 MHz): δ 8.25 (d, $^{3}J_{HH}$ = 7.4 Hz, 2 H, *ortho*-C_6H_5), 7.51 (t, $^{3}J_{HH}$ = 7.7 Hz, 2 H, *meta*-C_6H_5), 7.34 (t, $^{3}J_{HH}$ = 7.4 Hz, 1 H, *para*- C_6H_5), 7.30 (d, $^{3}J_{HH}$ = 7.6 Hz, 2 H, *ortho*-$CH_2C_6H_5$), 7.25 (t, $^{3}J_{HH}$ = 7.6 Hz, 2 H, *meta*-$CH_2C_6H_5$), 6.85 (t, $^{3}J_{HH}$ = 7.2 Hz, 1 H, *para*-$CH_2C_6H_5$), 3.36 (s, 6 H, $CNCMe_2CH_2O$), 2.02 (s, 2 H, $CH_2C_6H_5$), 0.92 (s, 18 H, $CNCMe_2CH_2O$). ^{13}C NMR (benzene-d_6, 150 MHz): δ 191.78 (br, $CNCMe_2CH_2O$), 155.83 (*ipso*- $CH_2C_6H_5$), 142.51 (*ipso*- C_6H_5), 136.42 (*ortho*-C_6H_5), 129.18 (*meta*-$CH_2C_6H_5$), 127.20 (*meta*-C_6H_5), 126.30 (*para*-C_6H_5), 124.72 (*ortho*-$CH_2C_6H_5$), 118.36 (*para*-$CH_2C_6H_5$), 80.49 ($CNCMe_2CH_2O$), 65.56 ($CNCMe_2CH_2O$), 28.37 ($CNCMe_2CH_2O$), 21.72 ($CH_2C_6H_5$), ^{11}B NMR (benzene-d_6, 192 MHz): δ -18.28 (s). ^{15}N NMR (benzene-d_6, 60.8 MHz): δ -158.1. IR (KBr, cm^{-1}): 3068 w, 3046 w, 2966 s, 2929 m, 2894 m, 2873 m, 1589 s (ν_{CN}), 1493 m, 1461 s, 1433 w, 1386 w, 1367 s, 1273 s, 1196 s, 1156 s, 1099 w, 1060 w, 1025 w, 1002 m, 965 s, 934 m, 895 w, 872 w, 842 w, 812 w, 799 w 745 s, 702 s, 677 w, 658 w, 639 w, 618 w. Anal. Calc. for $C_{29}H_{39}BN_3O_3Mg$: C, 67.93; H, 7.67; N, 8.19. Found: C, 67.51; H, 7.88; N, 7.82. Mp 205-207 °C.

www.manaraa.com

Procedure for kinetic measurements of To^{M}MgBn and HBpin. Reactants (To^{M}MgBn and HBpin) concentrations were monitored by ^{1}H NMR spectroscopy using a Bruker DRX-400 MHz spectrometer. Concentrations of the reactants were determined by integration of resonances corresponding to species of interest and integration of a 1,1,1,3,3,3-hexamethyl-2,2-bis(trimethylsilyl)trisilane (TMSS) standard of known concentration. Stock solutions of TMSS (10 mM) in benzene-d_6 were prepared and used for a series of experiments; rate constants were obtained reproducibly through several batches of stock solutions. The NMR probe was preheated or pre-cooled to the desired temperature, and the probe temperature was calibrated using an 80% ethylene glycol sample in 20% DMSO-d_6. The temperature was monitored during the kinetic measurements using a thermocouple. In a typical experiment, 0.022 mmol of To^{M}MgBn was dissolved in 0.5 mL of the stock solution, and the solution was placed in NMR tube and a ^{1}H NMR spectrum was acquired. 0.050 mmol of HBpin was injected into the NMR tube. The reaction was monitored by taking a single scan ^{1}H NMR spectra at regular preset intervals. Rate constants were obtained by a non-weighted linear least-squares regression analysis of the integrated second-order rate law: $\ln = \ln\{[\text{HBpin}]_0/[\text{To}^{M}\text{MgBn}]_0\} + k\Delta_o t$.

References

1. Arrowsmith, M.; Hill, M. S.; Hadlington, T.; Kociok-Köhn, G.; Weetman, C., *Organometallics* **2011,** *30* (21), 5556-5559.

2. Arrowsmith, M.; Hadlington, T. J.; Hill, M. S.; Kociok-Köhn, G., *Chemical Communications* **2012,** *48* (38), 4567-4569.

3. Arrowsmith, M.; Hill, M. S.; Kociok-Köhn, G., *Chemistry – A European Journal* **2013,** *19* (8), 2776-2783.

4. Hill, M. S.; MacDougall, D. J.; Mahon, M. F., *Dalton Transactions* **2010,** *39* (46), 11129-11131.

www.manaraa.com

5. Dudnik, A. S.; Weidner, V. L.; Motta, A.; Delferro, M.; Marks, T. J., *Nature Chemistry* **2014,** *6*, 1100.

6. Fu, P.-F.; Brard, L.; Li, Y.; Marks, T. J., *Journal of the American Chemical Society* **1995,** *117* (27), 7157-7168.

7. Sadow, A. D.; Tilley, T. D., *Journal of the American Chemical Society* **2003,** *125* (26), 7971-7977.

8. Sadow, A. D.; Tilley, T. D., *Angewandte Chemie International Edition* **2003,** *42* (7), 803-805.

9. Woo, H. G.; Walzer, J. F.; Tilley, T. D., *Journal of the American Chemical Society* **1992,** *114* (18), 7047-7055.

10. Intemann, J.; Lutz, M.; Harder, S., *Organometallics* **2014,** *33* (20), 5722-5729.

11. Mukherjee, D.; Ellern, A.; Sadow, A. D., *Chemical Science* **2014,** *5* (3), 959-964.

12. Dunne, J. F.; Neal, S. R.; Engelkemier, J.; Ellern, A.; Sadow, A. D., *Journal of the American Chemical Society* **2011,** *133* (42), 16782-16785.

13. Buch, F.; Brettar, J.; Harder, S., *Angewandte Chemie International Edition* **2006,** *45* (17), 2741-2745.

14. Neale, N. R.; Tilley, T. D., *Journal of the American Chemical Society* **2005,** *127* (42), 14745-14755.

15. Oluyadi, A. A.; Ma, S.; Muhoro, C. N., *Organometallics* **2013,** *32* (1), 70-78.

16. LeBlanc, F. A.; Piers, W. E.; Parvez, M., *Angewandte Chemie International Edition* **2014,** *53* (3), 789-792.

17. Green, S. P.; Jones, C.; Stasch, A., *Angewandte Chemie International Edition* **2008,** *47* (47), 9079-9083.

18. Bonyhady, S. J.; Jones, C.; Nembenna, S.; Stasch, A.; Edwards, A. J.; McIntyre, G. J., *Chemistry – A European Journal* **2010,** *16* (3), 938-955.

19. Dunne, J. F.; Fulton, D. B.; Ellern, A.; Sadow, A. D. *J. Am. Chem. Soc*. **2010,** *132* (50), 17680-17683.

20. Hleba, Y. B., *D. Phil. Thesis*. Queen's University, Kingston, Ontario, Canada (2007).

21. Tobia, D.; Baranski, J.; Rickborn, B. *J. Org. Chem*. **1989**, *54*, 4253.

www.manaraa.com

Appendix

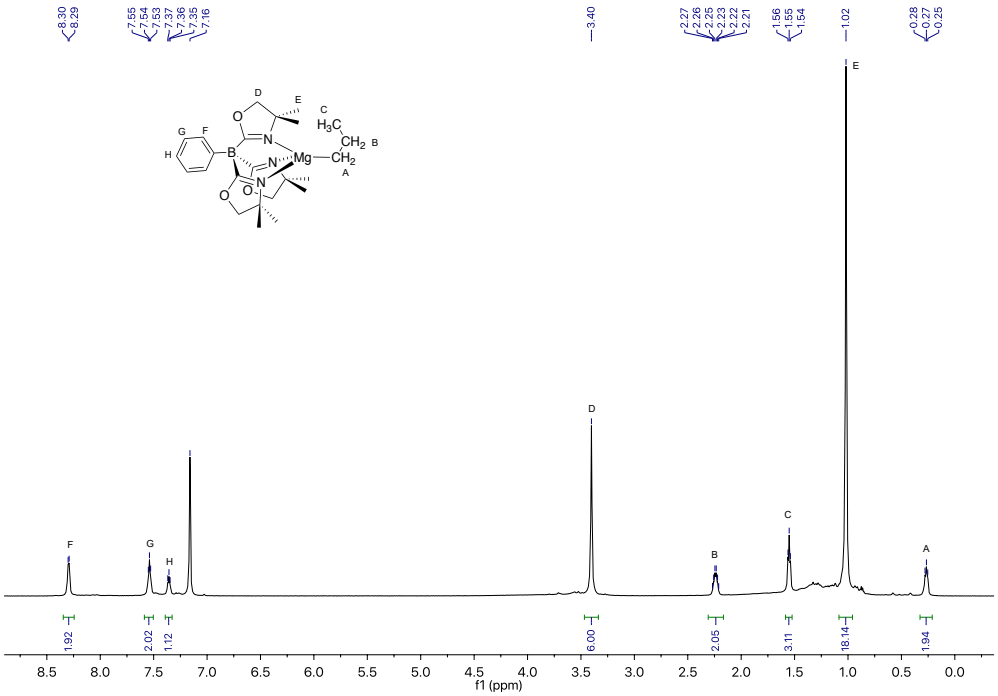

Figure S1. ^{1}H NMR spectrum of **To^{M}Mg*n*Pr** acquired in benzene-d_6 at room temperature.

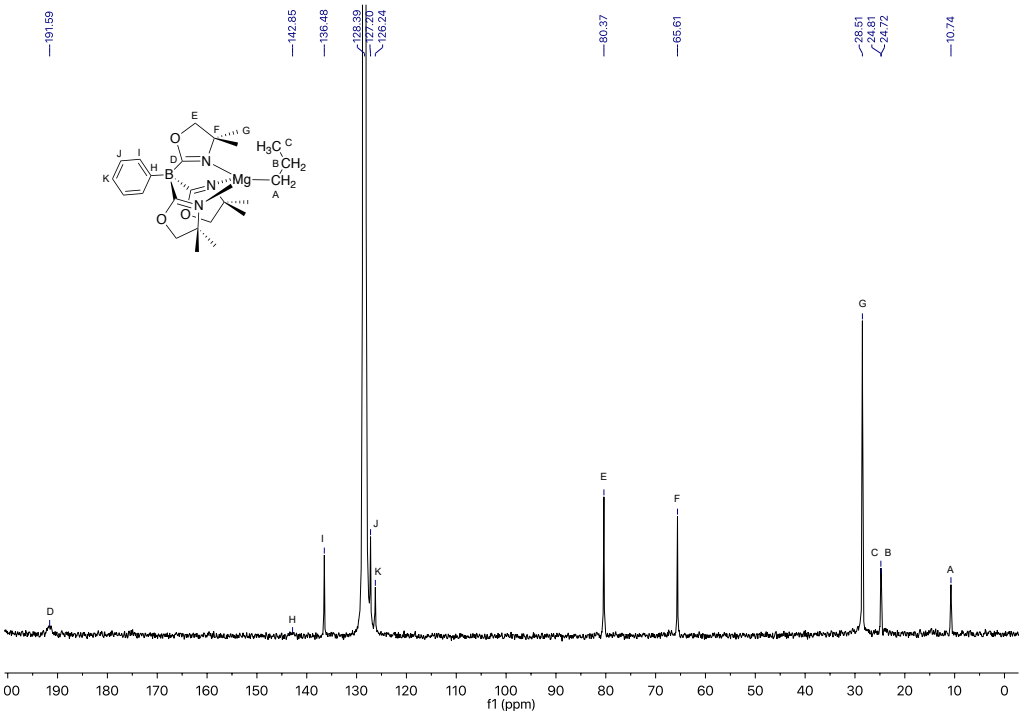

Figure S2. ^{13}C NMR spectrum of **To^{M}Mg*n*Pr** acquired in benzene-d_6 at room temperature.

www.manaraa.com

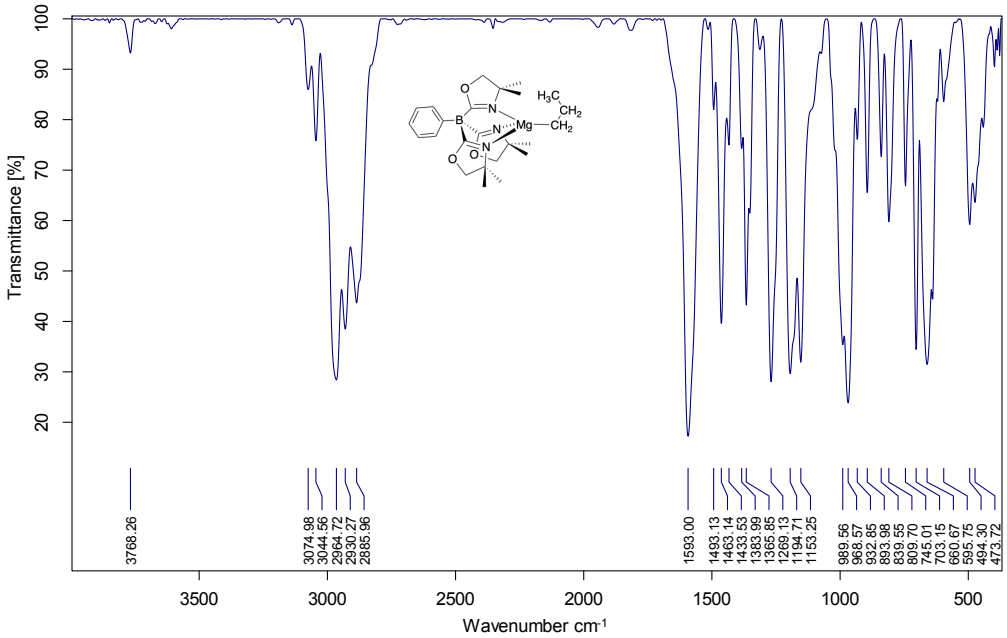

Figure S3. Infrared spectrum of **To^{M}Mg*n*Pr** (KBr pellet).

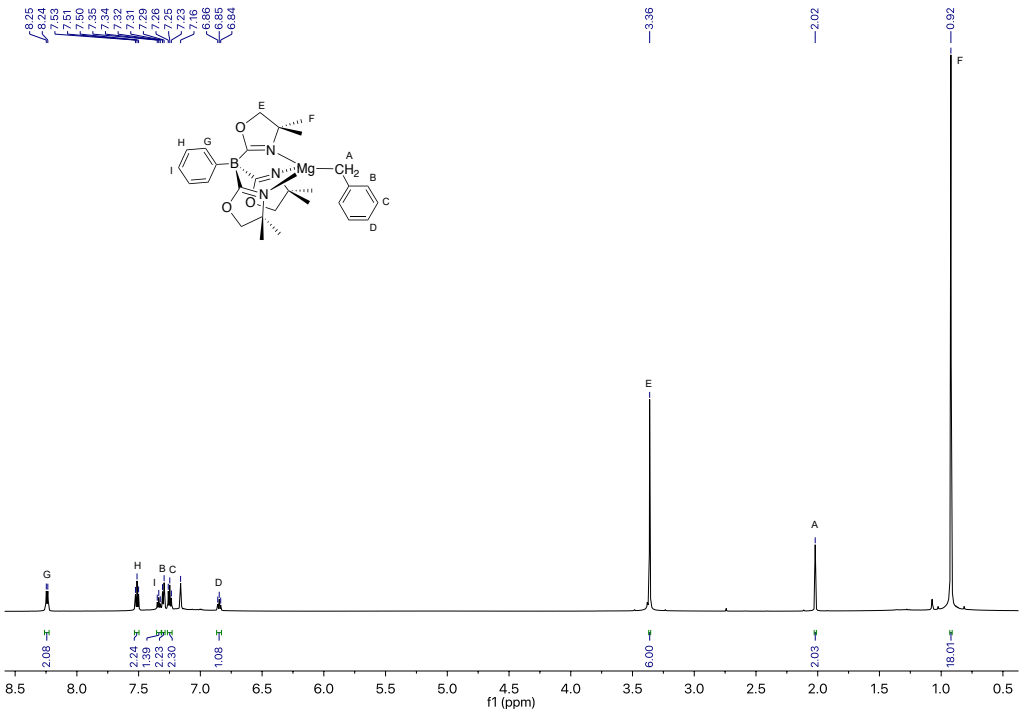

Figure S4. ^{1}H NMR spectrum of **To^{M}MgBn** acquired in benzene-d_6 at room temperature.

www.manaraa.com

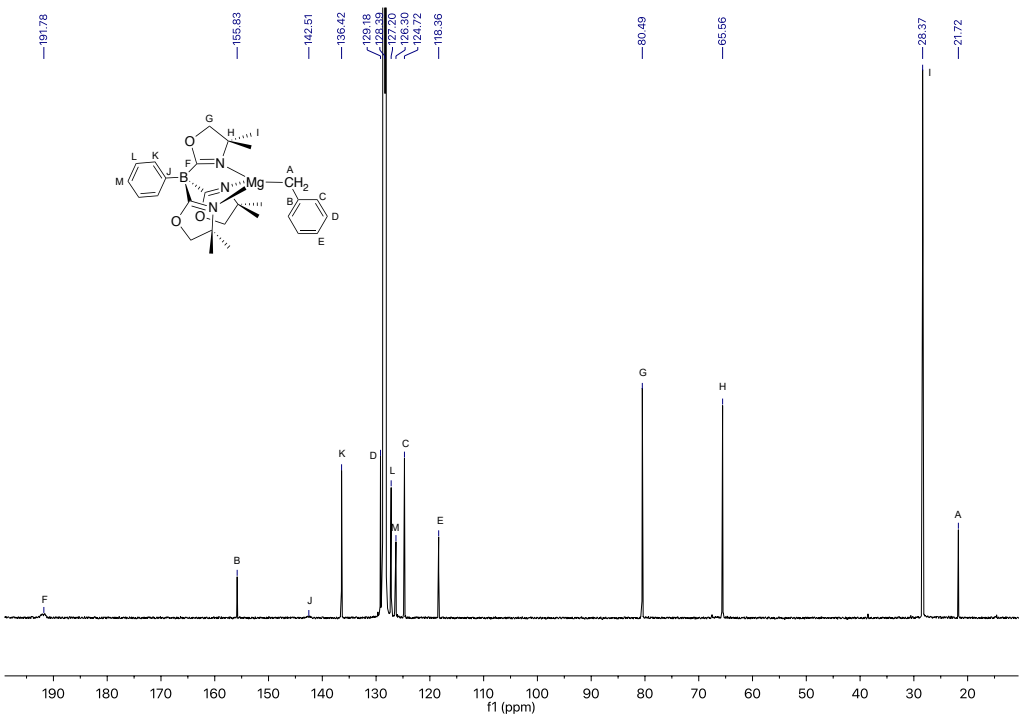

Figure S5. ^{13}C NMR spectrum of **To^{M}MgBn** acquired in benzene-d_6 at room temperature.

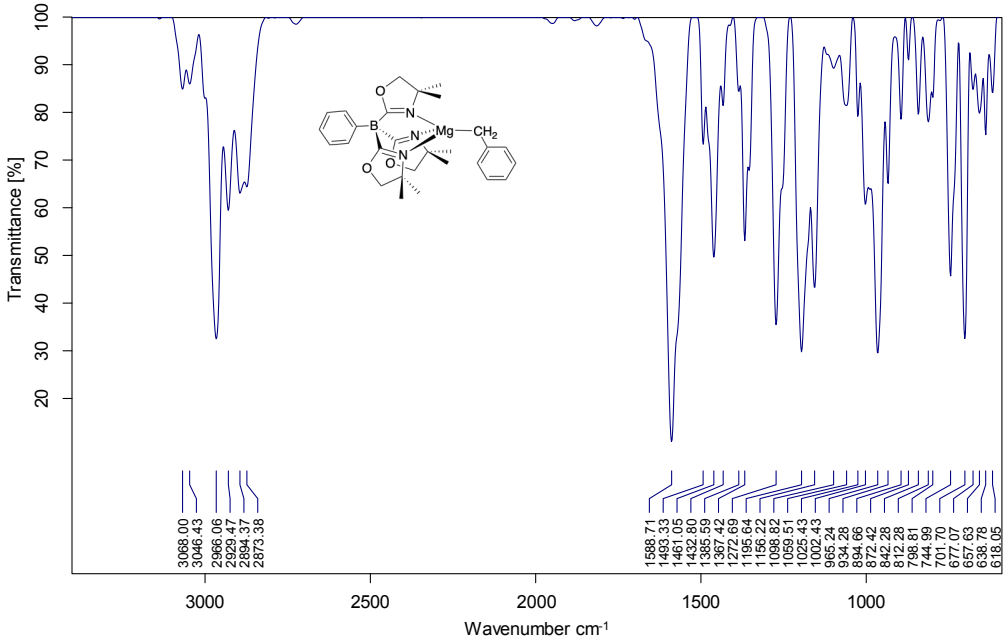

Figure S6. Infrared spectrum of **To^{M}MgBn** (KBr pellet).

www.manaraa.com

CHAPTER 7. GENERAL CONCLUSIONS

In this thesis we have described the synthesis and reactivity of new β-SiH functionalized alkyl and amide ligands and their rare earth complexes. Further, mechanistic investigations of a stoichiometric reaction between a magnesium alkyl complex and a borane source have included in the thesis.

The idea that β-SiH groups support large, coordinatively unsaturated rare earth centers in homoleptic, solvent-free compounds has been extended to a new benzyl dimethylsilyl ligand. The alkane, $HC(SiHMe_2)_2Ph$ of particular ligand is synthesized by the reaction of $HCPhBr_2$ and $SiHMe_2Cl$. The deprotonation of $HC(SiHMe_2)_2Ph$ with KBn provides a mixture of $KC(SiHMe_2)_2Ph$, Me_2SiBn_2 and other side products. This suggested a competing reaction involving nucleophilic attack on a Si center to cleave the C–Si bond. Therefore we developed an alternative route to $KC(SiHMe_2)_2Ph$ by reacting $PhC(SiHMe_2)_3$ with KO*t*Bu that affords the desired product in excellent yield. The synthesis of a series of solvent free tris(alkyl) lanthanides $Ln\{C(SiHMe_2)_2Ph\}_3$ {Ln = La, Ce, Pr, Nd} is described in the thesis. The structural parameters of the compounds (Ln–C, Ln–H, Si–C, Si–H distances) obtained by X-ray diffraction studies, for moieties involved in secondary Ln←H–Si interactions are different than those with nonbridging SiH groups. One Ln←H–Si interaction is observed per ligand and total three bridging interactions are observed for all the complexes. The secondary interactions involving β-SiH and aryl moieties are likely important to the facile isolation of these compounds.

The development of three new silazido ligands are described in this thesis. The reaction of aniline derivatives H_2NAryl (Aryl = Ph, 2,6-$C_6Me_2H_3$ (dmp), 2,6-$C_6iPr_2H_3$ (dipp)) with *n*BuLi, followed by the reaction with $ClSiHMe_2$ provides the silazanes $HN(SiHMe_2)Aryl$. The deprotonation of silazanes with *n*BuLi gives the desired lithium silazido compounds

www.manaraa.com

LiN(SiHMe$_2$)Aryl. Three sets of homoleptic rare earth amide complexes are obtained from the new silazido ligands and described in the thesis. All the compounds are characterized by NMR, IR and X-ray diffraction techniques. –N(SiHMe$_2$)Ph ligand provides five coordinated compounds Ln{N(SiHMe$_2$)Ph}$_3$(THF)$_2$ {Ln = Sc, Y, Lu} while –N(SiHMe$_2$)dmp provides four coordinated compounds Ln{N(SiHMe$_2$)dmp}$_3$(THF) {Ln = Y, Lu}. Solvent free compounds Ln{N(SiHMe$_2$)dipp}$_3$ {Ln = Sc, Y, Lu} are obtained for the –N(SiHMe$_2$)dipp ligand. Thus, the number of solvent molecules coordinated to the metal center is varied upon the steric properties of the ligand. Further, the overall symmetry of the complexes is affected by the symmetry of the ligands. Ln{N(SiHMe$_2$)Ph}$_3$(THF)$_2$ show distorted trigonal bipyramidal geometry while Ln{N(SiHMe$_2$)dmp}$_3$(THF) show distorted tetrahedral geometry. Interestingly Ln{N(SiHMe$_2$)dipp}$_3$ compounds are trigonal planar around the metal center.

Ln{N(SiHMe$_2$)Ph}$_3$(THF)$_2$ contain only classical β-SiH interactions with the metal center. Ln{N(SiHMe$_2$)dmp}$_3$(THF) contain three and two non-classical β-SiH interactions for yttrium and lutetium analogs respectively. Ln{N(SiHMe$_2$)dipp}$_3$ contain one bridging interaction per ligand. Thus, a greater number of bridging interactions between β-SiH and the metal center are observed for the complexes which has fewer number of coordinated solvent molecules. The SiH moieties of Ln{N(SiHMe$_2$)dipp}$_3$ undergo fast exchange on NMR time scale at room temperature to give one signal assigned to SiH moiety, however the exchange process slows down at low temperature to give resolved signals assigned to SiH groups on NMR time scale. In addition, we have noticed that the Y←HSi moiety with the lowest δ_{SiH} and smallest $^1J_{SiH}$ also shows the greatest ^{1}H-^{89}Y HSQC peak intensity in Y{N(SiHMe$_2$)dipp}$_3$. The latter measurement probes through-bond interactions (*J*) and it is tempting to assign that this group contains the most activated SiH. In comparison with literature compounds, the spectroscopic and structural features of Ln{(N(SiHMe$_2$)*t*Bu}$_3$(THF) and

www.manaraa.com

Ln{N(SiHMe$_2$)*t*Bu}$_3$ {Ln = Sc, Y, Lu} suggest that their SiH are more activated compared to Ln{(N(SiHMe$_2$)dmp}$_3$(THF) and Ln{N(SiHMe$_2$)dipp}$_3$ respectively. For example, the Ln{N(SiHMe$_2$)*t*Bu}$_3$ compounds contain lower $^1J_{SiH}$ and lower ν_{SiH} compared to the diisopropylsilazido-supported compounds.

The attempts to react Ln{N(SiHMe$_2$)Ph}$_3$(THF)$_2$ or Ln{N(SiHMe$_2$)dmp}$_3$THF with ketones did not provide any clean isolable product. In contrast, the reaction between Ln{N(SiHMe$_2$)dipp}$_3$ and ketones occurs via hydrosilylation, rather than forming an enolate. The reaction between Ln{N(SiHMe$_2$)dipp}$_3$ {Ln= Y, Lu} and acetophenone or benzophenone provides one ketone inserted product while acetone gives two ketones inserted product. Thus, three Ln⇽HSi secondary interactions reacts inequivalently from each other. In addition, the insertion of C=O into SiH occurs even in the presence of a donor, for example the reaction undergoes with the pyridine coordinated diisopropylsilazido compounds. The attempts to monitor the hydrosilylation reaction failed as the reaction is instantaneous even at –78 °C. To study if this reaction pathway is associative or dissociative, EXSY NMR experiments were performed with Y{N(SiHMe$_2$)dipp}$_3$ in the presence of excess pyridine. As the exchange of coordinated and free pyridine with Y{N(SiHMe$_2$)dipp}$_3$ is an associative mechanism, we propose that the ketone coordinates to the metal center first followed by the oxygen atom attacks the silicon center while the hydride transferrers to the carbonyl carbon to give the product. The pyridine molecule can be either dissociated from the complex prior to Si–O and C–H bond formation or it can stay coordinated until that is completed.

The isolation of the cationic complex of Ln{N(SiHMe$_2$)dipp}$_3$ {Ln = Y, Lu} with B(C$_6$F$_5$)$_3$ is described in this thesis. The compounds are characterized by NMR and IR techniques. Interestingly the most nucleophilic site in the complexes is the hydride of SiH moiety. Thus, a β-

www.manaraa.com

SiH is abstracted by the Lewis acid to provide only the zwitterionic species. The decomposition of that provides $(Me_2Si–Ndipp)_2$ and a rare earth adduct. The kinetic studies show that two molecules of the zwitterionic species involve in the rate determining step to provide one molecule of decomposition product.

The kinetic studies of $To^{M}MgBn$ and HBpin provided a negative entropy of activation which implies that B–C bond formation reaction performs through an ordered transition state. A primary kinetic isotope effect is observed for the B–C bond formation. Therefore, breaking of the B–H bond involves in the rate-determining step. One of the mechanisms proposed for the reaction is that it can be occurred via a concerted σ-bond metathesis. The other postulated mechanism is that nucleophilic attack by the benzyl carbon on boron followed by the hydride transfer on the [Mg] in the rate- determining step to give [Mg]–H and BnBpin. The latter mechanism is similar to the one proposed for Si–N and Si–C bond formation by [Mg] and silane which is previously reported by our research group.

I have developed new ligands, metal complexes and have studied kinetic parameters of stoichiometric reactions. Thus, findings of my research can be extended towards catalytic applications and their mechanistic investigations.

www.manaraa.com